DRAFT

NOAA OAR Special Report

PMEL Tsunami Forecast Series: Vol. 10
A Tsunami Forecast Model for Unalaska, Alaska

Yong Wei[1,2]

[1]Joint Institute for the Study of the Atmosphere and Ocean (JISAO), University of Washington, Seattle, WA
[2]NOAA/Pacific Marine Environmental Laboratory (PMEL), Seattle, WA

September 2011

UNITED STATES DEPARTMENT OF COMMERCE

Gary Locke
Secretary

NATIONAL OCEANIC AND ATMOSPHERIC ADMINISTRATION

Jane Lubchenco
Under Secretary for Oceans and Atmosphere/Administrator

Office of Oceanic and Atmospheric Research

Craig McLean
Assistant Administrator

Contribution No. 3357 from NOAA/Pacific Marine Environmental Laboratory
Contribution No. 1778 from Joint Institute for the Study of the Atmosphere and Ocean (JISAO)

Also available from the National Technical Information Service (NTIS)
(http://www.ntis.gov)

Contents

List of Figures

List of Tables

Foreword

Tsunamis have been recognized as a potential hazard to United States coastal communities since the mid-twentieth century, when multiple destructive tsunamis caused damage to the states of Hawaii, Alaska, California, Oregon, and Washington. In response to these events, the United States, under the auspices of the National Oceanic and Atmospheric Administration (NOAA), established the Pacific and Alaska Tsunami Warning Centers, dedicated to protecting United States interests from the threat posed by tsunamis. NOAA also created a tsunami research program at the Pacific Marine Environmental Laboratory (PMEL) to develop improved warning products.

The scale of destruction and unprecedented loss of life following the December 2004 Sumatra tsunami served as the catalyst to refocus efforts in the United States on reducing tsunami vulnerability of coastal communities, and on 20 December 2006, the United States Congress passed the "Tsunami Warning and Education Act" under which education and warning activities were thereafter specified and mandated. A "tsunami forecasting capability based on models and measurements, including tsunami inundation models and maps…" is a central component for the protection of United States coastlines from the threat posed by tsunamis. The forecasting capability for each community described in the *PMEL Tsunami Forecast Series* is the result of collaboration between the National Oceanic and Atmospheric Administration office of Oceanic and Atmospheric Research, National Weather Service, National Ocean Service, National Environmental Satellite, Data, and Information Service, the University of Washington's Joint Institute for the Study of the Atmosphere and Ocean, National Science Foundation, and United States Geological Survey.

NOAA Center for Tsunami Research

PMEL Tsunami Forecast Series: Vol. 10
A Tsunami Forecast Model for Unalaska, Alaska

Y. Wei[1,2]

Abstract. NOAA's tsunami forecast system relies on a series of community forecast models constructed to provide inundation and current velocities following tsunami generation. This report addresses the development, validation, and stability testing of the tsunami forecast model for Unalaska, Alaska, the nation's most productive fishing ground and home to 4,000 residents. Development of the Unalaska tsunami forecast model employed the optimized version of the Method of Splitting Tsunamis (MOST) model constructed at a spatial resolution of 50–60 m in the finest grid to accomplish 4-hr simulation of tsunami inundation within 10 min. A reference inundation model was developed in parallel with the optimized model using grids of higher resolution, up to 9 m, to provide forecast model reference. Observations during 14 historical tsunami events were compared with their modeled counterparts and provide quantitative estimation of the tsunami time series, inundation, and runup at Unalaska. The forecast model stability was evaluated using 43 synthetic scenarios generated from all predetermined subduction zones of the Pacific Basin at the magnitude level Mw 9.3. By virtue of this forecast model, this work also provided the opportunity to conduct model assessment of tsunami impact along the Unalaska coast. A total of 4,289 distant and local synthetic tsunami scenarios in the Pacific Basin at the magnitude levels Mw 7.5, 7.8, 8.2, 8.7, and 9.3 were modeled. In addition, synthetic tsunamis from the two seismic gaps in Alaska, the Unalaska and Shumagin gaps, at magnitude levels Mw 7.5, 8.0, 8.5, and 9.0 were investigated in detail. Model computations show that large-magnitude events may generate maximum tsunami wave amplitudes of 3 m at the location of the Unalaska tide station, and a maximum tsunami wave runup of 7 m along the Unalaska coastline.

1. Background and Objectives

The National Oceanic and Atmospheric Administration (NOAA) Center for Tsunami Research (NCTR) at the NOAA Pacific Marine Environmental Laboratory (PMEL) has developed a tsunami forecasting capability for operational use by NOAA's two Tsunami Warning Centers located in Hawaii and Alaska (Titov *et al.*, 2005). The system is designed to quickly and accurately provide basin-wide warning of approaching tsunami waves. The system, termed Short-term Inundation Forecast of Tsunamis (SIFT), combines real-time tsunami event data with numerical models to produce estimates of tsunami wave arrival times and amplitudes at a coastal community of interest. The SIFT system integrates several key components: deep-ocean observations of tsunamis in real time, a basin-wide precomputed propagation database of water level and flow velocities based on potential seismic unit sources, an inversion algorithm to refine the tsunami source based on deep-ocean observations during an event, and high-resolution tsunami forecast models.

The city of Unalaska is the eleventh largest city in the U.S. state of Alaska and encompasses Unalaska Island, on which the town center and industrial docks are located, and the smaller Amaknak Island, home to the International Port of Dutch Harbor and the regional Dutch Harbor airport. The two islands

[1]Joint Institute for the Study of the Atmosphere and Ocean (JISAO), University of Washington, Seattle, WA

[2]NOAA/Pacific Marine Environmental Laboratory (PMEL), Seattle, WA

are connected by the low-lying South Channel Bridge, locally referred to as the "Bridge to the Other Side" in contrasting reference to the infamous Alaska "Bridge to nowhere" (`http://www.alaskaroads.com/photos-Unalaska.htm`). A regional map of the two islands of Unalaska and connecting South Channel Bridge are shown in **Figure 1**. Unalaska Bay opens toward the Bering Sea to the north. A higher-resolution aerial view of the southern portion of Amaknak Island, connected to Unalaska Island by the low-lying South Channel Bridge across the channel south of Captains Bay, is also shown.

In terms of population, Unalaska is home to 4,000 permanent residents. Its population is known to seasonally increase to as large as 10,000 at the height of the fishing season when fishing and crab boats descend upon the Port of Dutch Harbor and processing facilities are fully staffed and operational. So important is the fishing industry to the local economy that the name Dutch Harbor is often used interchangeably with Unalaska to refer to the community. The strategic position near the center of the nation's most productive fishing grounds makes Dutch Harbor the number one fishing port in the nation with commercial fishing, fish processing plants, fleet services, and shipping activities responsible for the region's employment and economy. Again, due to strategic location, the harbor is the hub of the transshipment of cargo between Pacific Rim trading partners (`http://unalaska-ak.us/`).

Alaska has a greater earthquake and tsunami potential than any other state because of its proximity to one of the most seismically active regions in the world. The Aleutian-Alaska-Cascadia Subduction Zone, where the Pacific Plate is subducting under the North American Plate, has the potential to generate both local and basin-wide tsunamis that threaten coastal communities in Alaska and the Pacific Basin. Distant and local earthquakes along the subduction zones in the Pacific account for 80% of the origins of tsunamis that have impacted Alaskan coastlines. Historically, local tsunamis such as the 1946 Unimak and 1957 Andreanov events have caused higher risks at Unalaska than distant tsunamis. In addition, potential tsunamis generated in the two major seismic gaps of Alaska, the Shumagin and Unalaska gaps, need special attention. The Shumagin Gap is a segment of the Alaska-Aleutian arc that has not ruptured in a great earthquake since at least 1899–1903 (Davies *et al.*, 1981), and accordingly may have a high seismic potential. To the west of the location of the 1946 rupture area is the 200-km-long Unalaska seismic gap (House *et al.*, 1981), which has not generated a large earthquake in about as long and holds a similar risk. Boyd and Jacob (1986) suggested that a major seismicity gap exists for events of magnitudes greater than 4.6 in the forearc region near Unalaska Island. Davies *et al.* (1981) described as a "worst scenario" that an earthquake nucleated in the Shumagin Gap could also rupture the possible Unalaska Gap with resultant magnitude up to Mw 9.0. A tsunami induced by such an earthquake could be devastating for many communities, not only on the Alaska-Aleutian coasts, including Unalaska, but also in the far field along Hawaiian Island coasts and the U.S. west coast.

In tsunami hazard mapping of Alaskan coastal communities, Unalaska is located in a zone of highest tsunami potential (Suleimani *et al.*, 2002). The Tsunami Hazard Map of Unalaska, developed by Data Directions Consulting Group and shown in **Figure 2**, defines the Tsunami Safe Zone as areas above

50 ft (~15 m) in elevation. This map also shows the tsunami evacuation routes developed and reviewed by local emergency management officials.

The main objective of this work is to develop a tsunami forecast model for Unalaska to maximize the length of time that the community has to react to a tsunami threat by quickly providing accurate information to emergency managers and other officials responsible for the community and infrastructure. An additional goal is minimization of false alarms that ultimately erode system credibility with the resident and fishing populations. Discussion of the details of the individual components of the Unalaska forecast model, including the development of grids using bathymetry and topography, model validation using historical tsunami cases, model stability and robustness, sensitivity testing using synthetic tsunami events, the basic model setup, and model parameters are provided in this report.

2. Forecast Methodology

A high-resolution inundation model was used as the basis for development of a tsunami forecast model to operationally provide an estimate of wave arrival time, height, and inundation at Unalaska, Alaska, following tsunami generation. All tsunami forecast models are run in real time while a tsunami is propagating across the open ocean. The Unalaska model was designed and tested to perform under stringent time constraints, given that time is generally the single limiting factor in saving lives and property.

The general tsunami forecast model, based on the Method of Splitting Tsunamis (MOST), is used in the tsunami inundation and forecasting system to provide real-time tsunami forecasts at selected coastal communities. The model runs in minutes while employing high-resolution grids based on the digital elevation model (DEM) from the National Geophysical Data Center (NGDC). MOST is a suite of numerical simulation codes capable of simulating three processes of tsunami evolution: earthquake, transoceanic propagation, and inundation of dry land. The MOST model has been extensively tested against a number of laboratory experiments and benchmarks, and was successfully used for simulations of many historical tsunami events (Synolakis *et al.*, 2008). The main objective of a forecast model is to provide an accurate and rapid estimate of wave arrival time, wave height, and inundation in the minutes after a tsunami is generated. Titov and González (1997) describe the technical aspects of forecast model development, stability, testing, and robustness, and Tang *et al.* (2009) provide detailed forecast methodology.

A basin-wide database of precomputed water elevations and flow velocities for unit sources covering worldwide subduction zones has been generated to expedite forecasts (Gica *et al.*, 2008). As the tsunami wave propagates across the ocean and successively reaches tsunameter observation sites, recorded sea level is ingested into the tsunami forecast application in near real time and incorporated into an inversion algorithm to produce an improved estimate of the tsunami source. A linear combination of the precomputed database is then performed based on this tsunami source, now reflecting the transfer of energy to the fluid body, to produce synthetic boundary conditions of water elevation and flow velocities to initiate the forecast model computation.

Accurate forecasting of the tsunami impact on a coastal community largely relies on the accuracies of bathymetry and topography and the numerical computation. The high spatial and temporal grid resolution necessary for modeling accuracy poses a challenge in the run-time requirement for real-time forecasts. Each forecast model consists of three telescoped grids with increasing spatial resolution into the finest grid, and temporal resolution for simulation of wave inundation onto dry land. The forecast model uses the most recent bathymetry and topography available to reproduce more accurate wave dynamics during the inundation computation. Forecast models, including the Unalaska model, are constructed for at-risk populous coastal communities in the Pacific

and Atlantic oceans. Past and present development of forecast models in the Pacific have validated the accuracy and efficiency of each forecast model currently implemented in the real-time tsunami forecast system (Titov *et al.*, 2005; Wei *et al.*, 2008; Titov, 2009; Tang *et al.*, 2009). Models are tested when the opportunity arises and are used for scientific research.

3. Model Development

The general methodology for modeling at-risk coastal communities such as Unalaska, Alaska, is to develop a set of three nested grids, referred to as A, B, and C grids, each of which becomes successively finer in resolution as they telescope into the population and economic center of the community of interest. The offshore area is covered by the largest and lowest-resolution A grid, while the near-shore details are resolved within the finest-scale C grid to the point that tide gauge observations recorded during historical tsunamis are resolved within expected accuracy limits. The grids are then optimized by sub-sampling to coarsen the resolution and shrink the overall grid dimensions to achieve a 4- to 10-hr simulation of modeled tsunami waves within the required time period of 10 min of wall-clock time. The basis for these grids is a high-resolution DEM constructed by NGDC and NCTR using all available bathymetric, topographic, and shoreline data to reproduce the wave dynamics during the inundation computation for an at-risk community. For each community, data are compiled from a variety of sources to produce a DEM referenced to Mean High Water in the vertical and to the World Geodetic System 1984 in the horizontal (`http://ngdc.noaa.gov/mgg/inundation/tsunami/inundation.html`). From these DEMs, a set of three high-resolution "reference" elevation grids are constructed for development of a high-resolution reference model from which an "optimized" model is constructed to run in an operationally specified period of time. The operationally developed model is referred to as the optimized tsunami forecast model, or forecast model for brevity. The procedure begins with development of a large spatial extent merged with bathymetric/topographic grids at high resolution.

3.1 Forecast area

The city of Unalaska, Alaska, is located along the seismically active Aleutian Chain, approximately 1300 km southwest of Anchorage. The Port of Dutch Harbor on Amaknak Island is located along a sheltered cove on the northwest side of Iliuliuk Bay. Unalaska lies approximately 170 km from the Alaska-Aleutian Trench, where the Pacific Plate is subducting under the North America Plate. As a result, there is great potential for the generation of both local and basin-wide tsunamis that threaten the coastal communities along Pacific Basin and Alaska coastlines, including those of Unalaska. Moreover, the harbor of Unalaska is exposed to the open water of the Bering Sea, making Unalaska coastlines vulnerable to tsunamis from the Kamchatka-Kuril-Japan Subduction Zone.

Tsunami forecast models coupled with deep-ocean observations play an important role in protecting vulnerable communities, including Unalaska, by providing timely forecasts of tsunami impacts on Alaska's seismically active, populated coastlines. **Figure 3** shows the locations of 15 historical tsunamigenic earthquakes in the Pacific and the proximity of the Deep-ocean Assess-

ment and Reporting of Tsunamis (DART) systems along with the location of the 100-km by 50-km unit sources as defined in the PMEL tsunami propagation database. (Gica *et al.*, 2008)

3.2 Historical tsunamis in Unalaska and water level at tide station

Historical tsunamis have had a devastating impact on the Alaskan coastline. Lander (1996) documented 100 tsunami events that affected Alaskan coastlines between 1737 and 1996, including 43 from distant sources, 31 from local sources, 14 landslide-generated, 10 volcanic-generated, and 2 meteorologically induced tsunamis. The source locations, subduction zones, and magnitudes of the 14 significant events shown in **Figure 3** are provided in **Table 1**. These 14 events were used to validate the Unalaska tsunami forecast model as discussed later in this report. Note that for events of unknown source, locations are not provided in **Figure 3**.

There have been 122 fatalities due to tsunamis in Alaska since 1900. Between 1940 and 1970, the five destructive tsunamis, 1946 Unimak, 1952 Kamchatka, 1957 Andreanov, 1960 Chile, and 1964 Alaska, represented an era of tsunami hazards and led to intensive efforts in tsunami monitoring and modeling. These events were recorded by tide gauges throughout the Pacific and have since provided valuable datasets for tsunami research (U.S. Coast and Geodetic Survey, 1953; Berkman and Symons, 1964; Spaeth, 1964). The 1946 Unimak tsunami caused five fatalities and the 1964 Prince William Sound event resulted in 106 fatalities and $84 million in damages. Since 1996, 12 distant and 2 local tsunamis have been observed at tide stations in Alaska, including the devastating 26 December 2004 Sumatra tsunami (National Geophysical Data Center / World Data Center (NGDC/WDC) Historical Tsunami Database). No tsunami-related damages or fatalities have been reported in Alaska since 1996. However, 10 Pacific events since 2006 provided rich water-level data at both deep-ocean tsunameters and coastal tide gauges for model validation.

Unalaska has documented nearly every major historical tsunami that has reached its tide station, a detail of which is evident in **Figure 4 THIS IS NOT TRUE**. The Unalaska tide station was established in 1955 and moved to its present installation in 1989. The tide station, shown in both **Figures 1 and 4**, is located at the head of Iliuliuk Bay on the Unalaska Island-side of the channel. The mean tidal range in the vicinity is approximately 0.9 m and the diurnal range is 1.1 m. The mean sea level has been continuously dropping at a rate of 6.44 mm/yr since 1957.

The 10 November 1938 Alaska Peninsula tsunami of magnitude Mw 8.3 is the earliest documented event with a maximum wave amplitude of 5 cm. **Table 2** shows the observed maximum wave amplitude at the Unalaska tide station for 29 tsunami events since 1938. The maximum wave amplitude is approximately 0.7 m, recorded during the 1957 Andreanov and 1960 Chilean tsunamis. None of the tsunamis listed caused serious damage or flooding in Unalaska. In contrast, the 1946 Unimak event generated a tsunami in Dutch Harbor that damaged several small boat landings and pilings, although, inter-

Table 1: Fourteen historical events of significance used to validate tsunami reference and forecast models for Unalaska, Alaska.

Earthquake/Seismic				Model		
Event	USGS Date Time (UTC) Epicenter	CMT Date Time (UTC) Centroid	Magnitude Mw	Tsunami Magnitude[1]	Subduction Zone	Tsunami Source
1946 Unimak	01 Apr 12:28:56 52.75°N 163.50°W	01 Apr 12:28:56 53.32°N 163.19°W	[2]8.5	8.5	Aleutian-Alaska-Cascadia (ACSZ)	7.5 × b23 + 19.7 × b24 + 3.7 × b25
1960 Chile	22 May 19:11:14 [3]38.29°S 73.05°W	22 May 19:11:14 39.50°S 74.50°W	[3]9.5		Central and South America (CSSZ)	Kanamori and Ciper (1974)
1964 Alaska	28 Mar 03:36:00 [3]61.02°N 147.65°W	28 Mar 03:36:14 61.10°N 147.50°W	[3]9.2	9.0	Aleutian-Alaska-Cascadia (ACSZ)	Tang *et al.* (2006)
1994 East Kuril	04 Oct 13:22:58 43.73°N 147.321°E	04 Oct 13:23:28.5 43.60°N 147.63°E	[4]8.3	8.1	Kamchatka-Kuril-Japan-Izu-Mariana-Yap (KISZ)	9.0 × a20
1996 Andreanov	10 Jun 04:03:35 51.56°N 175.39°W	10 Jun 04:04:03.4 51.10°N 177.410°W	[4]7.9	7.8	Aleutian-Alaska-Cascadia (ACSZ)	2.40 × a15 + 0.80 × b16
2001 Peru	23 Jun 20:33:14 16.265°S 73.641°W	23 Jun 20:34:23.3 17.28°S 72.71°W	[4]8.4	8.2	Central and South America (CSSZ)	5.7 × a15 + 2.9 × b16 + 1.98 × a16
2003 Rat Island	17 Nov 06:43:07 51.13°N 178.74°E	17 Nov 06:43:31.0 51.14°N 177.86°E	[4]7.7	7.8	Aleutian-Alaska-Cascadia (ACSZ)	[5]2.81 × b11
2006 Tonga	03 May 15:26:39 20.13°S 174.164°W	03 May 15:27:03.7 20.39°S 173.47°W	[4]8.0	8.0	New Zealand-Kermadec-Tonga (NTSZ)	6.6 × b29
2006 Kuril	15 Nov 11:14:16 46.607°N 153.230°E	15 Nov 11:15:08 46.71°N 154.33°E	[4]8.3	8.1	Kamchatka-Kuril-Japan-Izu-Mariana-Yap (KISZ)	[5]4 × a12 + 0.5 × b12 + 2 × a13 + 1.5 × b13
2007 Kuril	13 Jan 04:23:20 46.272°N 154.455°E	13 Jan 04:23:48.1 46.17°N 154.80°E	[4]8.1	7.9	Kamchatka-Kuril-Japan-Izu-Mariana-Yap (KISZ)	–3.82 × b13
2007 Solomon	01 Apr 20:39:56 8.481°S 156.978°E	01 Apr 20:40:38.9 7.79°S 156.34°E	[6]8.1	8.2	New Britain-Solomons-Vanuatu (NVSZ)	12.0 × b10
2007 Peru	15 Aug 23:40:57 13.354°S 76.509°W	15 Aug 23:41:57.9 13.73°S 77.04°W	[4]8.0	8.1	Central and South America (CSSZ)	.9 × a61 + 1.25 × b61 + 5.6 × a62 + 6.97 × b62 + 3.5 × z62
2007 Chile	14 Nov 15:40:50 22.204°S 69.869°W	14 Nov 15:41:11.2 22.64°S 70.62°W	[6]7.7	7.6	Central and South America (CSSZ)	z75 × 1.65
2010 Chile	27 Feb 06:34:14 35.909°S 72.733°W	27 Feb 06:35:15.4 35.95°S 73.15°W	[4]8.8	8.8	Central and South America (CSSZ)	[1]a88 × 17.24 + a90 × 8.82 + b88 × 11.86 + b89 × 18.39 + b90 × 16.75 + z88 × 20.78 + z90 × 7.06

[1]Preliminary source—Derived from source and deep-ocean observations
[2]López and Okal (2006)
[3]Kanamori and Ciper (1974)
[4]Centroid Moment Tensor
[5]Tsunami source was obtained in real time and applied to the forecast
[6]United States Geological Survey (USGS)

Table 2: Observed maximum wave amplitude at Unalaska tide station for historical tsunami events.

Tsunami Event	Time	Mw	Source of Mw	Max Amp. (cm)
Alaska	1938.11.10	8.2	USGS	~5
Unimak	1946.04.01	8.5	Inversion	—
Hokkaido	1952.03.04	8.1	Lander, 1996	~5
Kamchatka	1952.11.04	9.0	USGS	~60
Kamchatka	1956.03.30	7.4	Lander, 1996	~10
Andreanov	1957.03.09	8.6	USGS	~70
Chile	1960.05.22	9.5	USGS	~70
Alaska	1964.03.28	9.0	Inversion	~40
Rat Island	1965.02.04	8.7	USGS	~24
Unimak	1965.07.02	7.0	Lander, 1996	~8
Honshu	1968.05.16	7.9	Lander, 1996	~5
Kamchatka	1971.12.15	7.8	Lander, 1996	~4
Aleutian	1986.05.07	7.9	USGS	~12
Bering	1991.02.21	6.5	Lander, 1996	~30
Kuril	1994.10.04	8.2	Lander, 1996	~8
Chile	1995.07.30	7.8	Lander, 1996	~8
Aleutian	1996.06.10	7.9	USGS	~5
Kamchatka	1997.12.05	7.8	USGS	~8
Peru	2001.06.23	8.2	Inversion	~12
Hokkaido	2003.09.25	8.0	Inversion	~4
Rat Island	2003.11.17	8.0	Inversion	~3
Sumatra	2004.12.26	9.1	USGS	~14
Tonga	2006.05.03	8.1	Inversion	~4
Kuril	2006.11.15	8.1	Inversion	~4
Kuril	2007.01.13	7.9	Inversion	~6
Solomon	2007.04.01	8.2	Inversion	~5
Peru	2007.08.15	8.0	Inversion	~10
Samoa	2009.09.29	8.0	Inversion	—
Chile	2010.02.27	8.8	USGS	~19

estingly, this tsunami was not recorded at the Unalaska tide station (Lander, 1996).

3.3 Digital elevation models in Alaska

Accurate bathymetry and topography in offshore and coastal regions play the key role, globally and locally, in tsunami generation, propagation, and inundation. A number of global bathymetric and topographic datasets are available for public-domain research. Marks and Smith (2006) conducted an evaluation on six publicly available global bathymetry grids: DBDB2 (Digital Bathymetric Data Base by Naval Research Laboratory), ETOPO2 (Earth Topography by NGDC), GEBCO (General Bathymetric Chart of the Oceans by British Oceanographic Data Centre), GINA (Geographic Information Network of Alaska), Smith and Sandwell (1997), and S2004. They concluded that the original Smith and Sandwell grid might be the best source among these global bathymetric grids. Subsequently, they developed a new 1-min global topography grid S2004 that combines the Smith and Sandwell below 1000 m depth and equatorward of 72°

and GEBCO grids in shallow water and the polar region. NCTR developed a Pacific Basin 30-sec grid, derived primarily from the Smith and Sandwell grid and the SRTM30_PLUS grid, with amendments in areas where NCTR has better bathymetry. This comprehensive dataset covers the entire Pacific Ocean and part of the Arctic Ocean from 120°E to 68°W, and 80°S to 80°N.

While developing bathymetric and topographic grids for a few coastal sites, NCTR has been collaborating with NGDC in the Tsunami Inundation Gridding Project since 2005 to build high-resolution DEMs for additional U.S. coastal regions, and to anticipate forecast model development in the near future.

Figure 5 shows the extent of the bathymetric and topographic grids compiled by NGDC and NCTR/PMEL for the Alaska region. The coverage, resolution, and developer of each grid are described in **Table 3**. In the coarsest grid (A) of each forecast model, which covers large offshore regions and extends its boundary to deep water, a 2-min resolution is commonly used to compute the dynamics of tsunami waves. The 2-min grids produced in this work primarily use the 30-sec Pacific Basin dataset as the parental data sources, and possibly other datasets wherever they cover the domain with a grid finer than 30-sec resolution. The bathymetry and topography of the finer grids (B and C) in each forecast model make use of the DEMs developed by NGDC as the best source, and those developed by PMEL if NGDC has not developed a grid for the area.

Historical tsunamis have devastated the Alaskan coastline. Forecast models in Alaska play an important role in the forecast system to provide a timely estimate of the tsunami impact in populous Alaskan coastlines and to better prepare local communities for potential risks. **Figure 3** shows the epicenters of significant tsunami events of the last century in the Pacific, along with the layout of the 100 km × 50 km unit sources in SIFT. The orange circles label the outstanding tsunami events that were recorded by tide gauges in the Pacific, which are useful for model validation of the forecast model in this study.

The main objective of a forecast model is to provide an estimate of wave arrival time, height, and inundation immediately after the generation of a tsunami. Forecast models are run in real time while a tsunami is propagating in the open ocean, and consequently they are designed to perform under very stringent time limitations. Given the time constraints of this type of study, the process of computing the three stages of tsunami modeling, namely, wave generation, propagation, and inundation, has been expedited by generating a basin-wide database of precomputed water elevations and flow velocities for unit sources covering the entire subduction zones. As the tsunami wave propagates across the ocean and successively reaches the tsunameters, the recorded sea level information is reported back to SIFT and processed by the inversion algorithm to produce an improved forecast of the tsunami source. A linear combination of the precomputed database is then performed based on the tsunami source to produce synthetic boundary conditions of water elevation and flow velocities, to initiate the forecast model computation.

Each forecast model consists of three telescoped grids with increasing spatial (50–60 m in the finest grid) and temporal resolution for simulation of wave inundation onto dry land. The forecast model uses the most recent bathymetry

Table 3: Bathymetric and topographic grids in Alaska developed by the National Geophysical Data Center and the Pacific Marine Environmental Laboratory.

	Datasets	Coverage	Resolution	Developer
1	Pacific 30″	E120 – W68 S80 – N80	30″	NCTR/PMEL
2	AK SouthCentral 2′	W169 – W140 N52 – N62	2′	NCTR/PMEL
3	AK SouthCentral 24″	W156 – W147 N55 – N62	24″	NCTR/PMEL
4	Dutch Harbor 1’	W167.2001 – W165.9001 N53.4999 – N54.3499	1″	NGDC
5	Sand Point 3″	W161.0004 – W 159.7966 N54.6996 – N55.7004	3″	NGDC
6	Sand Point 1/3″	W161 – W159.8 N55.05 – N55.7	1/3″	NGDC
7	Kodiak 8″	W153.0023 – W152.0022 N56.9992 – N57.9993	8″	NCTR/PMEL
8	Kodiak 3″	W152.6518 – W152.2681 N57.5852 – N57.9267	3″	NCTR/PMEL
9	Kodiak 1″	W152.6247 – W152.31 N57.6545 – N57.8418	1″	NCTR/PMEL
10	Homer 1″	W151.5585 – W151.3666 N59.5837 – N59.6674	1″	NCTR/PMEL
11	Seward 8″	W150 – W149 N59.5 – N60.1667	8″	PMEL
12	Seward 3″	W149.5 – W149.2504 N59.9756 – N60.1667	3″	PMEL
13	Seward 1″	W149.4667 – W149.3083 N60.0748 – N60.1583	1″	PMEL
14	Yakutat 9″	W141.0 – W138.5 N59.0 – N60.5	9″	PMEL
15	Yakutat 3″	W140.0 – W139.5 N59.3333 – N59.7333	3″	PMEL
16	Yakutat 1″	W139.9333 – W139.6 N59.4333 – N59.5867	1″	PMEL
17	Sitka 9″	W136.3333 – W135.0008 N56.6667 – N57.3342	9″	PMEL
18	Sitka 3″	W135.6 – W135.1333 N56.9 – N57.1667	3″	PMEL
19	Sitka 1″	W135.4022 – W135.2267 N57.0 – N 57.1333	1″	PMEL

and topography developed by NGDC and NCTR in order to reproduce the correct wave dynamics during the inundation computation.

3.4 Model setup

Figure 6 shows the coverage of data sources available and used by NGDC to develop the high-resolution grids for Unalaska/Dutch Harbor. Taylor *et al.* (2006) describes the detailed procedure, data sources, and analysis of the DEM for Unalaska/Dutch Harbor. This DEM was delivered to NCTR in 2006 and has

been fully implemented for the Unalaska forecast model development in this study.

The computational domain of the outermost grid A has an extent of 4.5° (~300 km) in longitudinal and 5° (~555 km) in latitudinal direction. **Figure 7** shows the computational domain of the A grid for both the high-resolution and forecast model grids, for comparison of bathymetry resolution. **Figure 7 (left panel)** shows the bathymetry and topography of the A grid at the grid resolution of 2 arc min and **Figure 7 (right panel)** at a resolution of 36 arc sec. Both grids were interpolated from the Pacific 30-arc-sec dataset. The 36-arc-sec grid contains more details than the 2-arc-min grid in general and thus is chosen for the A grid for reference forecast model computation. The red frame in each plot indicates the coverage of the B grid, shown superimposed over the A-grid domain of the plot.

The southern part of the domain lies mainly in the Pacific, dominated by a water depth of thousands of meters. The relatively flat sea bottom of the south and southwest, with 5,000-m water depth, allows smooth transition of the linear boundary conditions from propagation run into grid A. The Aleutian Trench, alluded to by the dark band running parallel to the coast offshore in **Figure 7**, creates a steep gradient of water depth between 7,000 m and less than 100 m. In contrast, the water is about 2,000 m deep in the northwest of the domain where the Bering Sea is located, dropping only tens of meters to the east boundary. The exception is north of Unalaska Bay, where the water depth changes gradually from 2,000 to 1,000 m from west to east, while the waterway is rapidly narrowed. This feature makes Unalaska potentially more sensitive to tsunami waves from the west, such as Kamchatka, Kuril, and the Western Aleutians.

The computational extent of the middle B grid is 1.295° (~85 km) in longitudinal and 0.845° (~94 km) in latitudinal direction. **Figure 8** shows the computational domain of the B grid for both the high-resolution and forecast model grids for comparison of bathymetry resolution. **Figure 8 (upper panel)** shows the bathymetry and topography of grid B at the higher-grid resolution of 6 arc sec and **Figure 8 (lower panel)** at the Unalaska forecast model resolution of 18 arc sec for model runs covering the same domain. Both grids were interpolated from the Dutch Harbor 1-arc-sec dataset. The red frame in each plot indicates the coverage of the C grid shown superimposed over the B-grid domain of the plot.

The southern boundary of grid B is constrained to a water depth of 100 m, as no denser bathymetric data were available farther south at the time of grid development. After a gradual change from 100 to 50 m, the bathymetry becomes complicated by jagged coastlines, narrowed channels, and scattered islands as it approaches Unalaska Bay from the Pacific. While the surrounding water depth generally becomes shallower than 100 m from 1,000 m, Unalaska Bay connects to the Bering Sea by a 200-m-deep channel in the western part of the bay.

Figure 9 shows the computational domain of the finest grid C with an extent of 0.24° (~16 km) in longitudinal and 0.15° (~17 km) in latitudinal direction. The red cross symbol indicates the location of the National Ocean Service (NOS) tide gauge used as the forecast model warning point. **Figure 9 (lower**

Table 4: MOST setup parameters for reference and forecast models for Unalaska, Alaska.

		Reference Model				Forecast Model			
Grid	**Region**	**Coverage Lat. [°N] Lon. [°W]**	**Cell Size [″]**	**nx × ny**	**Time Step [sec]**	**Coverage Lat. [°N] Lon. [°W]**	**Cell Size [″]**	**nx × ny**	**Time Step [sec]**
A	Central Aleutians	50.5–55.5 169–164.5	36 × 36	451 × 501	2.4	50.5–55.5 169–164.5	120 × 120	136 × 151	8.0
B	Unalaska Island	53.5–54.34486 167.2–165.90514	6 × 6	780 × 510	0.8	53.5–54.34486 167.2–165.90514	18 × 18	260 × 170	2.0
C	City of Unalaska and Dutch Harbor	53.82–53.97 166.66–166.42	$\frac{1}{2} \times \frac{1}{3}$	1729 × 1621	0.2	53.82–53.97 166.66–166.42	3 × 2	289 × 271	1.0
Minimum offshore depth [m]			1				1		
Water depth for dry land [m]			0.1				0.1		
Friction coefficient (n^2)			0.001225				0.001225		
CPU time for a 4-hr simulation			10 min				40 hr		
Reference point at NOS tide gauge			193.459167° E, 53.879444° N (Row number I = 144, column number J = 164)						

Computations were performed on a single Intel Xeon processor at 3.6 GHz, Dell PowerEdge 1850.

panel) shows the bathymetry and topography of grid C with a grid resolution of 3 arc sec (~54 m) in x and 2 arc sec (~62 m) in y. **Figure 9 (upper panel)** is a plot of the same domain in higher-grid resolution for reference inundation model runs, 1/2 arc sec (~9 m) in longitudinal direction and 1/3 arc sec (~10 m) in latitudinal direction. Both high-resolution and forecast model grids were interpolated from the 1-arc-sec dataset, as no higher-resolution grid data were available for Dutch Harbor at the time of grid development.

The contour lines and color pattern in **Figure 9** indicate a complicated bathymetry and coastline inside Unalaska Bay. Transected by a deep channel, the western half of Unalaska Bay is generally deeper than the eastern half. The entire bay basically consists of three regional lobes: Nateekin Bay in the west, Captains Bay in the southwest, and Iliuliuk Bay in the easternmost regional lobe. While the deep channel ends at the two lobes in the west, Iliuliuk Bay lies atop the sloping bathymetry in the east, with water depth dredged to 30–35 m inside Dutch Harbor and its vicinity. Iliuliuk Bay is connected to Captains Bay through a narrow channel between Unalaska Island and Amaknak Island.

The model setup and input parameters for the Unalaska forecast and reference models are provided in **Table 4**. The three telescoping grids of the reference model cover exactly the same domain as the forecast model but with finer grids, to provide unbiased modeling references in terms of initial and boundary conditions. Grid C of the reference model employs a 10-m grid size, which results in a 36-times-larger spatial step and 5-times-larger temporal step, and is thus 180 times more intensive in computational efforts when compared to grid C of the forecast model, with an approximate grid size of 60 m. Considering the same situation in grids A and B, a single run of the reference model takes approximately 40 hr for a 4-hr simulation, while the forecast model runs in 10 min [**THIS CONTRADICTS TABLE 4, where ref = 10 min, forecast = 40 hr**].

4. Results and Discussion

4.1 Model validation

The 14 historical events listed in **Table 1** and shown in **Figure 3** were used for validation of the Unalaska, Alaska, tsunami forecast model. For each event, observations were compared with their modeled counterparts. The 1946 Unimak event generated a destructive transoceanic tsunami that became the milestone event for the United States to establish a Pacific-wide tsunami warning and forecast system. After 1946, four other destructive tsunamis, the 1952 Kamchatka, the 1957 Andreanov, the 1960 Chile, and the 1964 Alaska, led to intensive efforts for monitoring and modeling of tsunamis. These events were recorded by tide gauges throughout the Pacific and have since provided valuable datasets for tsunami research (U.S. Coast and Geodetic Survey, 1953; Berkman and Symons, 1964; Spaeth, 1964). In the early 1990s, the implementation of the high-quality bottom pressure recorder (BPR) in the deep ocean marked the beginning of the modern observation of tsunami waves. This was consolidated in 1998 by the project of Deep-ocean Assessment and Reporting of Tsunamis (DART) (González *et al.*, 1998).

The DART system of observations has played a critical role in defining the tsunami source and has provided accurate real-time tsunami forecasts for U.S. coastlines since the array was tested in the 1990s and modernized in 2001 (Eble and González, 1991; Titov *et al.*, 2003). Previous studies have shown successful applications of NOAA's experimental tsunami forecast system that constrain the tsunami source from the real-time tsunameter measurements, which is subsequently used to provide real-time propagation and coastal inundation forecasts (Titov *et al.*, 2003; Wei *et al.*, 2008; Tang *et al.*, 2009; Titov, 2009). These real-time inversions of the tsunami source have shown a forecast accuracy up to 90% of the tsunami waveforms at distant coastlines (Wei *et al.*, 2008). Seven of these events were used to validate the Unalaska forecast model, including 27 February 2010 Chile, 3 May 2006 Tonga, 15 November 2006 Kuril, 13 January 2007 Kuril, 1 April 2007 Solomon, and 15 August 2007 Peru.

Figures 10 to 23 are plots of the maximum water elevation and the maximum flow speed of the innermost C grid computed from both the forecast and reference models for 14 historical events. The complex bathymetry and jagged coastline inside Unalaska Bay result in areas with different features of wavefield. First, the higher water elevation in Iliuliuk Bay, Captains Bay, and Nakeetin Bay, more than any other areas, delineates the amplification of tsunami waves as they enter narrow or shallow water. With a wide and deep entrance, Nateekin Bay allows incoming waves to retreat easily back into Unalaska Bay during the rundown process. In contrast, Captains Bay is enclosed with narrow and shallow access that slows down the withdrawal of water exceptionally, which in turn leads to an increase of water elevation inside the bay. Iliuliuk Bay/Dutch Harbor, on the other hand, features a shallow entrance that induces

the same phenomenon as in Captains Bay. Second, there are essentially two major high-flow-speed zones in Unalaska Bay: one at the entrance of Iliuliuk Bay, and one located in the area surrounded by the entrance of Captains Bay, Amaknak Island, and the small islet to the west of Amaknak Island. The highest flow speed is seen at the entrance of Captains Bay. The third notable phenomenon is a tsunami entering Unalaska Bay from the west after crossing the Bering Sea, such as for the 2007 Kuril, 2006 Kuril, 2003 Hokkaido, 1996 Andreanov, and 1994 Kuril events, all of which caused higher water elevation in Captains Bay than in Iliuliuk Bay. This is probably a result of wave energy from the Bering Sea finding the easiest pathway into Captains Bay through the deep channel that connects Captains Bay with the Bering Sea, instead of traveling up and onto the slope of Iliuliuk Bay. However, for those tsunami waves coming in from the east of Unalaska, such as 2006 Tonga, 1960 Chile, and 1946 Unimak, a higher water elevation is induced in Iliuliuk Bay than in Captains Bay, implying that wave propagation follows its easiest and fastest path.

Also shown in **Figures 10 to 23** is the time series comparison with observations at the tide gauge within 12 hr of tsunami arrival at Unalaska. A cursory look shows excellent agreement between the modeling results and observations for most of the historical events, in spite of background noise. All events show good agreement up to 6 hr after the wave arrival, except for events for which the tsunami sources are still in debate, meaning the developed forecast model is accurate and valid in computing tsunami waves on the Unalaska coastline. The results computed by the reference model using high-resolution grids provide a more accurate computation of the wavefield, and, more importantly, provide reference for the computational accuracy of the forecast model.

The results computed by the reference model are similar to those computed by the forecast model, particularly for the first couple of waves. The right panel of **Figure 24** shows that the cross-correlation between the forecast model and the reference model is almost 1 without time delay for most of the historical events. This panel also shows evaluation of the cross-correlation between the forecast model and reference model, forecast model and observation, and reference model and observation. **Table 6** summarizes the error estimation of the computational results by forecast model and reference model compared to the signal-to-noise ratio of the tide-gauge observation. These results are plotted in **Figure 25**, showing that, for most of the historical events used in this work, the noise level is much more dominant than the estimated error computed by either forecast model or reference model, indicating a valid numerical simulation of the maximum wave height for most events. The two exceptions are the 1994 Kuril and 2001 Peru events, where the signal-to-noise ratio is slightly smaller than the estimated error. However, the cross-correlations of these two events are 0.64 and 0.81, respectively, suggesting the computational results are still highly correlated to the observations, although the models underestimate the maximum tsunami amplitude for both events. These results, overall, provide confidence that the forecast and reference models are producing highly comparable results. The difference of wave amplitude, wave period, and phase is nearly negligible for the first couple of tsunami waves in every case. The difference in wave amplitude and phase starts to show up in the following several later waves, which one can expect when the local effects become more

Table 5: Computed results of maximum runup height, maximum tsunami height, and maximum water elevation at the Unalaska tide station for historical events in Unalaska, Alaska.

Event	Time (UTC)	Mw	Max Comp. Runup (m)		Max Comp. Amp. (m)		Max Obs. Amp. (m)
Unimak	1946.04.01	8.5	2.82	1.50	1.41	1.01	Unknown
Chile	1960.05.22	9.5	1.33	1.34	0.71	0.59	0.80
Alaska	1964.03.28	9.0	0.51	0.51	0.36	0.30	0.36
Kuril	1994.10.04	8.1	—	—	0.05	0.05	0.15
Andreanov	1996.06.10	7.8	—	—	0.06	0.06	0.07
Peru	2001.06.23	8.2	—	—	0.04	0.04	0.08
Hokkaido	2003.09.25	8.0	—	—	0.04	0.05	0.04
Tonga	2006.05.03	8.1	—	—	0.01	0.01	0.04
Kuril	2006.11.15	8.1	—	—	0.05	0.05	0.10
Kuril	2007.01.13	7.9	—	—	0.02	0.03	0.04
Solomon	2007.04.01	8.2	—	—	0.02	0.02	0.05
Peru	2007.08.15	8.0	—	—	0.02	0.02	0.05
Chile	2010.02.27	8.8	0.44	0.40	0.14	0.08	0.19
Japan	2011.03.11	9.0	0.56	0.47	0.39	0.34	0.36

dominant as grids of the reference model contain more bathymetric and topographic features. However, bearing the expected error due to difference in grid resolution, it is recognized with confidence that forecast model results represent those of the reference model while saving 99.5% of the computing effort.

Table 5 lists the maximum tsunami runup and maximum water elevation at the tide station computed by both forecast and reference models. The computational results of three tsunami events, 1946 Unimak, 1960 Chile, and 1964 Alaska produce limited impact to the southern portion of Captains Bay but not in Dutch Harbor. A time series of observations 4 hr before and after the waves arrived at the Unalaska tide gauge (**Figure 24**) shows the level of tsunami interference from the background noise inherent in the location. Another noticeable computational result in **Table 5** is that the variation of maximum water elevation at the tide station demonstrates the same tendency, although of a smaller value, as that of the maximum tsunami height. This suggests that the forecast time series at the Unalaska tide station may be a good indication of the maximum tsunami height for the region.

4.2 Model stability testing using synthetic mega-tsunamis

Stability of the forecast model was verified using synthetic extreme events of Mw 9.3 generated in a representative region of every subduction zone in the Pacific Basin. Each scenario imitates an event equivalent to or greater than the 2004 Indian tsunami, which was the cause of tragedy and devastation never before seen on such a scale. Along the coastlines of the Indian Ocean, hundreds of thousands of people died, most of whom inhabited the low-lying island of Sumatra, Indonesia. Each synthetic tsunami source used for stability testing of the Unalaska forecast model consists of 20 unit sources, covering a rupture area

Table 6: Comparisons of error estimation of the modeling results with noise level at Unalaska tide gauge for historical events, where E is the model/data error computed by $(\eta_{\text{model}} - \eta_{\text{obs}})/\eta_{\text{obs}} \times 100\%$, C is the max cross-correlation between model and data. R_{noise} is the signal-to-noise ratio calculated from $A_{\text{noise}}/A_{\text{model}}$, where A_{noise} and A_{model} are, respectively, the root-mean-square amplitudes of 4-hr observation prior to tsunami arrival and first 4-hr tsunami signal of the model.

Event	Time (UTC)	Mw	Forecast Model E (%)	Forecast Model C	Reference Model E (%)	Reference Model C	R_{noise} (%)
Chile	1960.05.22	9.5	11.5	0.22	26.8	0.14	—
Alaska	1964.03.28	9.2	0.4	0.50	17.3	0.79	32
Kuril	1994.10.04	8.1	65.2	0.64	64.9	0.64	44
Andreanov	1996.06.10	7.9	18.1	0.59	18.8	0.45	39
Peru	2001.06.23	8.4	54.8	0.76	55.6	0.81	44
Hokkaido	2003.09.25	8.0	9.5	0.80	25.4	0.83	22
Tonga	2006.05.03	8.0	69.0	0.69	71.1	0.63	233
Kuril	2006.11.15	8.3	45.3	0.46	44.4	0.59	104
Kuril	2007.01.13	8.1	58.8	0.44	30.4	0.48	68
Solomon	2007.04.01	8.1	57.0	0.81	61.0	0.83	133
Peru	2007.08.15	8.1	61.0	0.77	58.0	0.47	88
Chile	2010.02.27	8.8	25.0	0.72	57.3	0.68	16.5

of 1000 km by 100 km, with an average 25.0-m slip for a Mw 9.3 event, as listed in **Table 7**. These scenarios are used to examine the stability of the developed forecast model under the impact of large waves generated by mega-tsunamis from all directions.

The computed maximum water elevation at the Unalaska tide station ranges from 0.06 m to 3 m. **Figures 26 to 46** show that the modeled wave amplitude and flow speed for all synthetic mega scenarios are stable without singularities or spreading instability. Thus, the Unalaska forecast model is robust and expected to provide operational warning center personnel and the City of Unalaska critical information during a tsunami event.

Among all synthetic scenarios, those originating from the Aleutians, ACSZ 6–15, ACSZ 16–25, and ACSZ 22–31 (scenarios 5, 6, and 7 in **Table 7**) cause the most severe impact on Unalaska. The same level of tsunami magnitude in the KISZ source regions can generate distant tsunamis striking Unalaska harder than those originating east of the Aleutian-Alaska-Cascadia Subduction Zone. The funneled bathymetry directs the waves, after crossing the Bering Sea from the west, to Unalaska Bay. It shows the important role of directionality in determining the tsunami impact at the destination. The maximum water elevation induced by tsunamis from the west of Unalaska is in general greater than that from the east. Other outstanding source regions in the east Pacific lie in the South America and South Chile subduction zones, which are also able to have a significant impact on Unalaska even though they are located the farthest away. As Titov *et al.* (1999) pointed out, the amplitude of the propagating tsunami varies significantly, not only by its source location and cylindrical spreading, but also by the directionality of the tsunami waves.

In the synthetic scenarios, tsunami inundation mainly occurs at two locations, Iliuliuk Bay/Dutch Harbor and the southern tip of Captains Bay. The

steep coastline of Iliuliuk Bay only allows high-amplitude waves to inundate this area, while the low land elevation, 0.1 to 0.2 m, at the southern tip of Captains Bay makes it the most vulnerable place when tsunamis strike Unalaska Bay. Most of the study cases show that the maximum water elevation at the tide station is a good indication of the maximum tsunami height and the maximum runup, as all three quantities follow the same tendency. The relationship between tsunami runup and tide gauge observations depends on multiple factors, including the complexity of the local bathymetry and topography, the wave characteristics, and the directionality of the tsunami.

4.3 Assessment of potential tsunami impact on Unalaska

The tsunami unit source is an important component of SIFT in defining the tsunami source through real-time data assimilation of a precomputed propagation database during an event in progress (Gica *et al.*, 2008). A combination of tsunami unit sources makes full use of the linearity of the tsunami wave in the deep ocean and the precomputed propagation database to provide offshore tsunami scenarios for modeling assessment of impact at identified sites. More than a thousand tsunami unit sources have been developed in NOAA's tsunami forecast system along the subduction zones to prepare for future events. A 1-m uplift on each tsunami source function represents a basic scenario of Mw 7.5. Varying combinations of uplift and source functions create synthetic tsunami scenarios with energy levels and equivalent magnitudes greater than the basic scenario. A suite of scenarios ranging from the basic Mw 7.5 to Mw 9.3 was used in this work to assess the potential tsunami impact on Unalaska. **Table 8** provides source and uplift information for a total of 4,289 scenarios investigated spanning five specific energy levels.

Figures 47–48 and **Figures 49–50**provide an overview of the maximum runup and wave amplitude caused by Mw 7.5 and Mw 7.8 events, respectively, showing that the most serious scenarios are due to tsunami sources closest to Unalaska. In general, tsunami sources in Alaska produce larger tsunami waves in Unalaska. The impact due to the tsunami sources at the east end of the Aleutian-Alaska-Cascadia Subduction Zone is relatively minor. **Figures 47 to 53** illustrate that the potential tsunami threats from the West Aleutians, the southern part of the Cascadia Subduction Zone, the South America Subduction Zone, and the Kamchatka-Kuril Subduction Zone could be more serious than those from eastern Alaska. The maximum observed wave amplitudes listed in **Table 2** show that the 1952 Kamchatka, 1957 Andreanov, and 1960 Chile tsunamis all resulted in higher wave amplitudes observed at the Unalaska tide gauge than the 1964 Alaska event. Therefore, the 1964 Alaska event should probably not be considered as the control scenario when assessing tsunami impact on Unalaska.

Table 9 summarizes the computed maximum values for scenarios of different magnitude thresholds generated in the major subduction zones in the Pacific. Distant tsunamis generated by earthquakes with a moment magnitude less than Mw 8.2 would only cause minor water surface rising, without damage to the Unalaska coastline. The maximum tsunami runup heights due to distant

Table 7: Unit source combinations used for synthetic tsunami scenarios.

No.	Scenario Name	Source Zone	Tsunami Source	α [m]
Mega-tsunami Scenario				
1	KISZ 1–10	Kamchatka-Yap-Mariana-Izu-Bonin	A1–A10, B1–B10	25
2	KISZ 22–31	Kamchatka-Yap-Mariana-Izu-Bonin	A22–A31, B22–B31	25
3	KISZ 32–41	Kamchatka-Yap-Mariana-Izu-Bonin	A32–A41, B32–B41	25
4	KISZ 56–65	Kamchatka-Yap-Mariana-Izu-Bonin	A56–A65, B56–B65	25
5	ACSZ 6–15	Aleutian-Alaska-Cascadia	A6–A15, B6–B15	25
6	ACSZ 16–25	Aleutian-Alaska-Cascadia	A16–A25, B16–B25	25
7	ACSZ 22–31	Aleutian-Alaska-Cascadia	A22–A31, B22–B31	25
8	ACSZ 50–59	Aleutian-Alaska-Cascadia	A50–A59, B50–B59	25
9	ACSZ 56–65	Aleutian-Alaska-Cascadia	A56–A65, B56–B65	25
10	CSSZ 1–10	Central and South America	A1–A10, B1–B10	25
11	CSSZ 37–46	Central and South America	A37–A46, B37–B46	25
12	CSSZ 89–98	Central and South America	A89–A98, B89–B98	25
13	CSSZ 102–111	Central and South America	A102–A111, B102–B111	25
14	NTSZ 30–39	New Zealand-Kermadec-Tonga	A30–A39, B30–B39	25
15	NVSZ 28–37	New Britain-Solomons-Vanuatu	A28–A37, B28–B37	25
16	MOSZ 1–10	Manus-OCB	A1–A10, B1–B10	25
17	NGSZ 3–12	North New Guinea	A3–A12, B3–B12	25
18	EPSZ 6–15	East Philippines	A6–A15, B6–B15	25
19	RNSZ 12–21	Ryukyu-Kyushu-Nankai	A12–A21, B12–B21	25
Mw 7.5 Scenario				
20	NTSZ B36	New Zealand-Kermadec-Tonga	B36	1
Micro-tsunami Scenario				
21	EPSZ B19	East Philippines	B19	0.01

Table 8: Maximum values computed from a set of synthetic tsunami scenarios in the Pacific.

Energy Level (Mw)	Source (km)	Uplift (m)	Number of Scenarios
7.5	100 km × 50 km	1.0	804 × 2
7.8	100 km × 50 km	3.2	804 × 2
8.2	100 km × 100 km	6.35	402
8.7	300 km × 100 km	12.0	378
9.3	1000 km × 100 km	28.4	293
			Total = 4289

tsunamis generated by Mw 8.7 earthquakes are all less than 1 m, meaning no significant damage to the coastline, but that a damaging current may develop inside the harbor [See Uslu *et al.* (2007) and Kowalik *et al.* (2008) for discussions of current-related damages at Crescent City from the 15 November 2006 Kuril tsunami]. The distant tsunamis of Mw 9.3 may induce damage to the coastline up to a land elevation of 3 m, while a local tsunami of this magnitude could reach 6.4 m.

Results summarized in **Table 9** show that the greatest threat to Unalaska is from tsunamis generated in the near field along the Aleutian-Alaska-Cascadia Subduction Zone (ACSZ). Excluding near-field generation, the Kamchatka-Kuril-Japan-Izu-Mariana-Yap Subduction Zone (KISZ) is the primary distant source

Table 9: The computed maximum runup height R_{max} in Unalaska and the computed maximum wave amplitude η_{max} at Unalaska tide station for scenarios Mw 7.5, Mw 7.8, Mw 8.2, Mw 8.7, and Mw 9.3 generated in major Pacific subduction zones. The notation SCSZ refers to the South Chile subduction zone but has been incorporated into the CSSZ.

	Mw 7.5	**Mw 7.8**	**Mw 8.2**	**Mw 8.7**	**Mw 9.3**
	R_{max} / η_{max}	R_{max} / η_{max}	R_{max} / η_{max}	R_{max} / η_{max}	R_{max} / η_{max}
ACSZ	0.15 / 0.11	0.44 / 0.33	1.18 / 0.77	3.75 / 3.08	6.35 / 5.04
CSSZ	0.01 / 0.00	0.02 / 0.01	0.04 / 0.03	0.11 / 0.08	0.28 / 0.15
CESZ	0.01 / 0.01	0.04 / 0.02	0.07 / 0.04	0.33 / 0.21	0.83 / 0.68
SASZ	0.02 / 0.02	0.07 / 0.06	0.12 / 0.10	0.51 / 0.45	1.62 / 1.31
SCSZ	0.02 / 0.02	0.08 / 0.07	0.12 / 0.12	0.53 / 0.48	1.66 / 1.47
NGSZ	0.01 / 0.00	0.04 / 0.02	0.09 / 0.05	0.43 / 0.26	0.96 / 0.77
KISZ	0.02 / 0.02	0.08 / 0.05	0.28 / 0.14	0.87 / 0.69	3.10 / 2.38
RNSZ	0.01 / 0.01	0.04 / 0.03	0.08 / 0.05	0.28 / 0.20	0.73 / 0.47
NVSZ	0.01 / 0.01	0.03 / 0.02	0.08 / 0.05	0.28 / 0.18	0.79 / 0.60
EPSZ	0.02 / 0.01	0.05 / 0.03	0.15 / 0.10	0.62 / 0.46	2.09 / 1.72
MOSZ	0.01 / 0.01	0.03 / 0.03	0.09 / 0.07	0.42 / 0.29	1.50 / 0.97
NTSZ	0.01 / 0.01	0.04 / 0.04	0.09 / 0.07	0.37 / 0.27	0.93 / 0.67
ECSZ	0.01 / 0.01	0.04 / 0.02	0.07 / 0.04	0.33 / 0.21	0.83 / 0.68

region in the Pacific along which tsunamis generated pose the greatest threat to Unalaska. The major threats come from the northern portion of KISZ, specifically the Kamchatka source region. The secondary distant source regions are EPSZ, the Peru and Chile segments of CSSZ (SCSZ in **Table 9**), and MOSZ, which may cause damage to the coastline of Unalaska if the earthquake magnitude is greater than Mw 8.7. On the other hand, the Central American segment of CSSZ is expected to cause the least impact on Unalaska, as a Mw 9.3 event generated there would only produce a 0.3-m rising of water.

Also shown in **Figures 47 to 53** is the comparison of the runup height and wave amplitude at the tide station for each scenario. Although smaller than the computed maximum runup height, the computed maximum wave amplitude at the tide station presents a similar tendency with the varying runup height. Therefore, the observations at the tide station can be considered as a good indication of the runup and inundation in Unalaska. The worst scenario of all the cases, Mw 9.3 in ACSZ, gives a computed maximum runup height of 6.4 m, which is smaller than the current definition of the inundation limit in Unalaska, the 15-m contour above the mean sea level. This implies that the Tsunami Safe Zone developed by Data Directions Consulting Group (**Figure 2**) may be too conservative, which is further confirmed by the study of the synthetic tsunami scenarios generated from the nearby seismic gaps in the next section.

Based on the numerical results of all scenarios, we could approximately categorize the tsunami sources in the Pacific specific to the resulting impact at Unalaska. The most severe tsunami source for Unalaska is certainly the Aleutian-Alaska-Cascadia Subduction Zone (ACSZ), especially to the west of the Aleutian-Alaska Subduction Zone and central-south of the Cascadia Subduction Zone. The secondary tsunami sources should include the Kamchatka-Kuril-Japan Trench Subduction Zone and the Izu-Bonin-Marianas-Yap Subduction Zone (KISZ), and the East Philippines Subduction Zone (EPSZ). Addition-

ally, the subduction zones in South America (the Peruvian and Chilean segments of CSSZ) and the Manus-OCB Subduction Zone (MOSZ) should be paid attention to, as they may also pose a risk to the Unalaska coastline. All other subduction zones can be categorized into the fourth most severe sources, only producing minor impact to Unalaska coastlines, including the weakest source, which is the Central American segment of CSSZ.

4.4 Potential tsunamis originating in seismic gaps in the Aleutians

4.4.1 Shumagin Seismic Gap and Unalaska Seismic Gap

Popof Island, along with 19 other volcanic islands in its eastern and southern region, make up the Shumagin Islands. Unga Island, the largest, is separated from Popof Island by Popof Strait. The Schumagins lie a distance of 40 to 120 km from the active Aleutian volcanic arc and are situated in the Shumagin Gap. This seismic gap is a segment of the Alaska-Aleutian arc that has not ruptured in a great earthquake since at least 1899–1903 and that accordingly may have a high seismic potential (Davies *et al.*, 1981). Previous studies have shown that the rupture zones of Aleutian earthquakes in 1938, 1946, and 1948 did not break the interplate boundary beneath the Shumagin Islands (Davies *et al.*, 1981; Johnson, 1999). Davies *et al.* (1981) and Beavan *et al.* (1983) suggested the possibility of the occurrence of a major earthquake within this gap in the next two decades. The 13 May 1993 Shumagin Islands earthquake of Mw 6.8 occurred at an expected location in the seismic gap, but the magnitude was too small to fill the gap (Tanioka *et al.*, 1994). This earthquake did not generate a tsunami large enough to be observed at Popof Island's Sand Point tide station or at the ocean bottom pressure gauges at a distance of 100 and 300 km away. Nishenko and Jacob (1990) and Nishenko (1991) suggested that a gap-filling event will have an expected magnitude of Mw 7.4, with conditional probabilities of 27%, 48%, and 75% of occurring during the 5-, 10-, and 20-yr periods that end in 1994, 1999, and 2009, respectively. Since a gap-filling event has yet to occur, a great event is due in two years, meaning that evaluation of the potential tsunami hazards induced by the failure of the seismic gaps is an important study.

To the west of the 1946 rupture area is the 200-km-long Unalaska seismic gap, which has not generated a large earthquake in a century (House *et al.*, 1981). A review of a historic record from 1770 by Boyd and Jacob (1986) reveals that the Unalaska region may have ruptured in great earthquakes in 1878 and 1902. They suggested that a major seismicity gap exists for events of magnitudes greater than Mw 4.6 in the forearc region near Unalaska Island. The study of the 1957 Aleutian tsunami by Johnson (1999) showed low moment release in the eastern half of the aftershock zone, which further confirmed the existence of the Unalaska Gap.

Davies *et al.* (1981) described a "worst scenario": that an earthquake nucleated in the Shumagin Gap could also possibly rupture the Unalaska Gap to the west, the 1938 aftershock zone to the east, or both, with resultant magnitude

up to Mw 9.0. A tsunami induced by such an earthquake would be devastating for many communities, not only along the Alaska-Aleutian coasts, but also as far away as Hawaii and the U.S. west coast.

A map showing Unalaska Island in relation to the approximate locations of the Unalaska and Shumagin seismic gaps along the Aleutian-Alaska-Cascadia Subduction Zone is shown in **Figure 54**. Also shown in **Figure 54** is a layout of the tsunami unit sources for the full extent of the subduction zone, with the relative size of each earthquake and the two seismic gaps in terms of unit sources as represented in the SIFT forecast system (Gica *et al.*, 2008). Based on the above analysis of potential earthquakes in the Unalaska and Shumagin seismic gaps, a full numerical modeling study was conducted to assess the tsunami impact on the community of Unalaska subject to all these possible scenarios at different levels of Mw = 7.5, 8.0, 8.5, 8.7, and 9.0.

4.4.2 Impact assessment of tsunamis originating in the seismic gaps

The Unalaska Gap covers an area composed of four unit sources (A and B rows of ACSZ 23–24), and the Shumagin Gap covers an area of six source functions (A and B rows of ACSZ 26–28) as shown in **Figure 54**. As both gaps are bounded by the earthquake source of the 1 April 1946 Unimak event of Mw 8.5, five synthetic scenarios imitating the 1946 tsunami, with an averaged 23-m slip applied on a pair of functions, are used to evaluate the tsunami impact (López and Okal, 2006). Three synthetic scenarios, one of Mw 8.7 and two of Mw 9.0, are also put forward, with an 18-m slip and a 34-m slip on four and six unit sources, respectively. The results of these scenarios are presented in **Figure 46 to 56**.

Figures 54 to 65 show that the computed maximum wave amplitude at the Unalaska tide station can reach as high as 3 m for a Mw 9.0 scenario initiated in the Unalaska Gap and 2 m for a Mw 9.0 scenario initiated in the Shumagin Gap. An event greater than Mw 8.5 originated from either seismic gap could cause coastal inundation in Unalaska. While the computed wave amplitude at the tide station is less than 1 m, a local event of Mw 8.0 may cause damage to the harbor facilities and boats by introducing high-speed currents in the harbor and waterway.

Figure 66 summarizes the computed tsunami impact on Unalaska subject to the synthetic scenarios originating in the seismic gaps, including the maximum computed runup and wave amplitude at the Unalaska tide station. **Figure 66** shows that

- Unalaska is more vulnerable to tsunamis originating in the Unalaska seismic gap than in the Shumagin seismic gap.

- Local tsunamis in the seismic gaps at the level Mw 9.0 can produce tsunami runup as high as 6.8 m in Unalaska.

- Mw ≥ 8.5 should be considered hazardous for Unalaska. Most of these scenarios create at least a 2-m tsunami runup height in Unalaska.

- Mw 8.0 scenarios in the Unalaska seismic gap induce moderate impact to both locations, with a maximum tsunami runup height of less than 1 m at both forecast model sites.
- Tsunami impact caused by Mw 7.5 scenarios in both gaps is minor, with maximum tsunami heights less than 0.1 m for all cases.
- The potential for tsunami impact to Unalaska from tsunami sources along the two seismic gaps is considerable. Unit sources 23 and 24 span the Unalaska Gap, and unit sources 26 through 28 span the larger Shumagin Gap. An earthquake occurring along the nearshore row A sources pose the greatest risk.

5. Summary and Conclusions

A tsunami forecast model was developed for the community of Unalaska, the most populous community in the Aleutian Islands of Alaska, for operational use in NOAA's Short-term Inundation Forecast of Tsunamis (SIFT) system to provide real-time modeling forecasts of water elevations, runup, and inundation along the Unalaska coastline. The forecast model employs grids as fine as 54 m and can accomplish a 4-hr simulation after tsunami arrival at a deep-ocean observation system in 10 min of CPU time. A high-resolution reference model was developed in parallel with the Unalaska tsunami forecast model to provide a basis for evaluation of forecast model performance.

Model validation was developed using 14 historical tsunami events. For each event, model results were compared with observations recorded at the Unalaska tide station. The modeling results at Unalaska showed excellent agreement with observations for most of the historical events modeled. Validation shows that, of all historical events modeled, only the 1946 Unimak tsunami caused significant damage to the Unalaska coastline. The error estimations of the modeling results are mostly within the range of the noise level, indicating that modeling results agree well with the observations for most events. Results of 43 Mw 9.3 synthetic mega-events, including events generating 6-m-high waves along Unalaska's coastline, lend confidence to the stability of the model.

Including local and distant scenarios, a total of 4,289 synthetic tsunamis at five magnitude levels, Mw 7.5, 7.8, 8.2, 8.7, and 9.3, were run to assess the potential tsunami impact on Unalaska. The Aleutian-Alaska-Cascadia Subduction Zone poses the most serious threat to Unalaska. The worst-case scenario of locally generated tsunamis, a Mw 9.3 event generated offshore of Unalaska, may cause runup to a land elevation of 6.8 m in Unalaska. The computation shows that, out of all distant tsunami scenarios, the Kamchatka source region may produce the highest tsunami runup in Unalaska. A tsunami generated in the Central American segment of the Central and South America Subduction Zone (CSSZ) has the least likely impact on Unalaska. The modeling results also show that a distant tsunami generated by an earthquake less than Mw 8.2 causes little to no damage to the Unalaska coastline.

Both the Unalaska and Shumagin seismic gaps, both of which have the potential to initiate Mw 9.0 earthquakes, pose a significant threat to the city of Unalaska. Of the 30 possible tsunami scenarios originating from these seismic gaps investigated, a Mw 9.0 scenario may generate a maximum tsunami runup of 6.8 m in Unalaska. Local events of Mw $\geq$ 8.0 are considered hazardous to Unalaska coastlines.

This work also addressed the relationship of the maximum water elevation at the tide station, maximum tsunami runup height, and maximum tsunami height for all cases. The observations at the Unalaska tide station can be considered good indicators of the tsunami runup height in Unalaska. The overall

maximum tsunami runup of 6.8 m suggests that the current definition of the Tsunami Safe Zone in Unalaska, areas above 50 ft (~15 m), is conservative.

6. Acknowledgments

The author wishes to thank Edison Gica and Jean Newman for their work on the propagation database, Burak Uslu for providing propagation database tabular unit source information and graphics, and the entire modeling group of NCTR for helpful suggestions and discussion. The author especially acknowledges and thanks Marie Eble and Ryan Layne Whitney for providing invaluable technical assistance and editorial review. Collaborative contributions of the National Weather Service, the National Geophysical Data Center, and the National Data Buoy Center were invaluable.

Funding for this publication and all work leading to development of a tsunami forecast model for Unalaska, Alaska, was provided by the National Oceanic and Atmospheric Administration. This publication is partially funded by the Joint Institute for the Study of the Atmosphere and Ocean (JISAO) under NOAA Cooperative Agreement No. NA17RJ1232, JISAO Contribution No. 1778. This is PMEL Contribution No. 3357.

7. References

Beavan, J.E., E. Hauksson, S.R. McNutt, R. Bilham, and K.H. Jacob (1983): Tilt and seismicity changes in the Shumagin seismic gap. *Science*, *222*, 322–325.

Berkman, S.C., and J.M. Symons (1964): The tsunami of May 22, 1960 as recorded at tide stations. Coastal and Geodetic Survey, U.S. Department of Commerce, 79 pp.

Boyd, T.M., and K. Jacob (1986): Seismicity of the Unalaska region, Alaska. *Bull. Seismol. Soc. Am.*, *76*, 463–481.

Davies, J., L. Sykes, L. House, and K. Jacob (1981): Schumagin seismic gap, Alaska Peninsula: history of great earthquakes, tectonic setting, and evidence for high seismic potential. *J. Geophys. Res.*, *86*(B5), 3821–3856.

Eble, M.C., and F.I. González (1991): Deep-ocean bottom pressure measurements in the northeast Pacific. *J. Atmos. Oceanic Technol.*, *8*, 221–223.

Gica, E., M.C. Spillane, V.V. Titov, C.D. Chamberlin, and J.C. Newman (2008): Development of the forecast propagation database for NOAA's Short-term Inundation Forecast for Tsunamis (SIFT). NOAA Tech. Memo. OAR PMEL-139, NTIS: PB2008-109391, NOAA/Pacific Marine Environmental Laboratory, Seattle, WA, 89 pp.

González, F.I., H.M. Milburn, E.N. Bernard, and J. Newman (1998): Deep-ocean assessment and reporting of tsunamis (DART): Brief overview and status report. In *Proceedings of the International Workshop on Tsunami Disaster Mitigation*, Tokyo, Japan, 19–22 January 1998, 118–129.

House, L.S., L.R. Sykes, J.N. Davis, K. H., and Jacob (1981): Identification of a possible seismic gap near Unalaska Island, eastern Aleutians, Alaska. Earthquake prediction—an international review. AGU, Washington D.C., 81–92.

Johnson, J.M. (1999): Heterogeneous coupling along Alaska-Aleutians as inferred from tsunami, seismic, and geodetic inversions. *Adv. Geophys.*, *39*, 1–116.

Kanamori, H., and J.J. Ciper (1974): Focal process of the great Chilean earthquake, May 22, 1960. *Phys. Earth Planet. In.*, *9*, 128–136.

Kowalik, Z., J. Horrillo, W. Knight, and T. Logan (2008): Kuril Islands tsunami of November 2006: 1. Impact at Crescent City by distant scattering. *J. Geophys. Res.*, *113*(C01020), 10.1029/2007JC004402.

Lander, J.F. (1996): Tsunamis affecting Alaska 1737–1996. NGDC Key to Geophysical Research Documentation No. 31, 205 pp.

López, A.M., and E.A. Okal (2006): A seismological reassessment of the source of the 1946 Aleutian "tsunami" earthquake. *Geophys. J. Int.*, *165*(3), 835–849, doi: 10.1111/j.1365-246x.2006.02899.x.

Marks, K.M., and W.H.F. Smith (2006): An evaluation of publicly available global bathymetry grids. *Mar. Geophys. Res.*, *27*, 19–34.

Nishenko, S.P. (1991): Circum-Pacific seismic potential 1989–1999. *Pure Appl. Geophys.*, *135*, 169–259.

Nishenko, S.P., and K.H. Jacob (1990): Seismic potential of the Queen-Charlotte-Alaska-Aleutian seismic zone. *J. Geophys. Res.*, *95*, 2511–2532.

Smith, W.H., and D. Sandwell (1997): Global sea floor topography from satellite altimetry and ship depth soundings. *Science*, *277*(5334), 1956–1962.

Spaeth, M.G. (1964): The tsunami of March 28, 1964, as recorded at tide stations. Coast and Geodetic Survey, U.S. Department of Commerce.

Suleimani, E.N., R.A. Combellick, R.A. Hansen, and G.A. Carver (2002): Tsunami hazard mapping of Alaska coastal communities. *Alaska GeoSurvey News*, *6*(2), 5 pp.

Synolakis, C.E., E.N. Bernard, V.V. Titov, U. Kânoğlu, and F.I. González (2008): Validation and verification of tsunami numerical models. *Pure Appl. Geophys.*, *165*(11–12), 2197–2228.

Tang, L., C. Chamberlin, E. Tolkova, M. Spillane, V.V. Titov, E.N. Bernard, and H.O. Mofjeld (2006): Assessment of potential tsunami impact for Pearl Harbor, Hawaii. NOAA Tech. Memo. OAR PMEL-131, NTIS: PB2007-100617, NOAA/Pacific Marine Environmental Laboratory, Seattle, WA, 36 pp.

Tang, L., V.V. Titov, and C.D. Chamberlin (2009): Development, testing, and applications of site-specific tsunami inundation models for real-time forecasting. *J. Geophys. Res.*, *114*, C12025, doi: 10.1029/2009JC005476.

Tanioka, Y., K. Satake, L. Ruff, and F. González (1994): Fault parameters and tsunami excitation of the May 13, 1993, Shumagin Islands earthquake. *Geophys. Res. Lett.*, *21*(11), 967–970.

Taylor, L.A., B.W. Eakins, R.R. Warnken, K.S. Carignan, G.F. Sharman, and P.W. Sloss (2006): Digital elevation models for San Juan and Mayagüez, Puerto Rico: Procedures, Data sources and analysis. Prepared for the NOAA Pacific Marine Environmental Laboratory (PMEL), Center for Tsunami Inundation Mapping Efforts (TIME) by the NOAA National Geophysical Data Center (NGDC).

Titov, V.V. (2009): Tsunami forecasting. In *The Sea*, Vol. 15, Chapter 12, Harvard University Press, Cambridge, MA, and London, England, 371–400.

Titov, V.V., and F.I. González (1997): Implementation and testing of the Method of Splitting Tsunami (MOST) model. NOAA Tech. Memo. ERL PMEL-112 (PB98-122773), NOAA/Pacific Marine Environmental Laboratory, Seattle, WA, 11 pp.

Titov, V.V., F.I. González, E.N. Bernard, M.C. Eble, H.O. Mofjeld, J.C. Newman, and A.J. Venturato (2005): Real-time tsunami forecasting: Challenges and solutions. *Nat. Hazards*, *35*(1), Special Issue, U.S. National Tsunami Hazard Mitigation Program, 41–58.

Titov, V.V., F.I. González, H.O. Mofjeld, and J.C. Newman (2003): Short-term inundation forecasting for tsunamis. In *Submarine Landslides and Tsunamis*, A.C. Yalciner, E. Pelinovsky, E. Okal, and C.E. Synolakis (eds.), Kluwer Academic Publishers, The Netherlands, 277–284.

Titov, V.V., H.O. Mofjeld, F.I. González, and J.C. Newman (1999): Offshore forecasting of Alaska-Aleutian Subduction Zone tsunamis in Hawaii. NOAA Tech. Memo. ERL PMEL-114, NTIS PB2002-101567, NOAA/Pacific Marine Environmental Laboratory, Seattle, WA, 22 pp.

U.S. Coast and Geodetic Survey (1953): The tsunami of November 4, 1952 as recorded at tide stations. U.S. Department of Commerce, 62 pp.

Uslu, B., J.C. Borrero, L.A. Dengler, and C.E. Synolakis (2007): Tsunami inundation at Crescent City, California generated by earthquake along the Cascadia Subduction Zone. *Geophys. Res. Lett.*, *34*, L20601, doi: 10.1029/2007GL030188.

Wei, Y., E. Bernard, L. Tang, R. Weiss, V. Titov, C. Moore, M. Spillane, M. Hopkins, and U. Kânoğlu (2008): Real-time experimental forecast of the Peruvian tsunami of August 2007 for U.S. coastlines. *Geophys. Res. Lett.*, *35*, L04609, doi: 10.1029/2007GL032250.

FIGURES

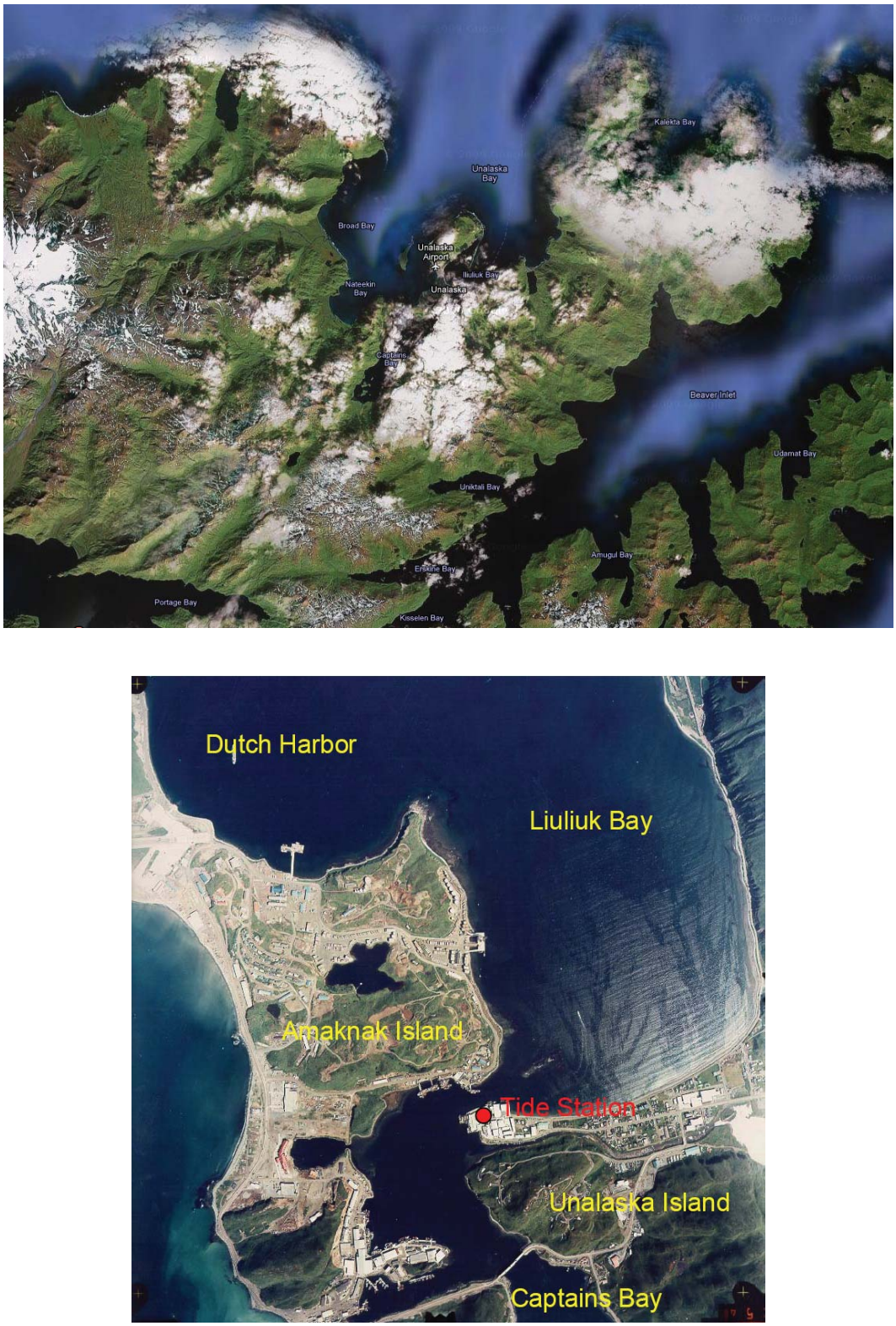

Figure 1: Unalaska, Alaska. (a) Google map of Unalaska and vicinity. (b) Aerial photo of Unalaska showing the infrastructure of Amaknak Island dominated by Dutch Harbor International Airport and the Port of Dutch Harbor. The South Channel Bridge linking Amaknak and Unalaska islands crosses Captains Bay in the lower right of the image. The location of the Unalaska tide station on Unalaska Island is marked in red. (Courtesy of City and County of Unalaska.)

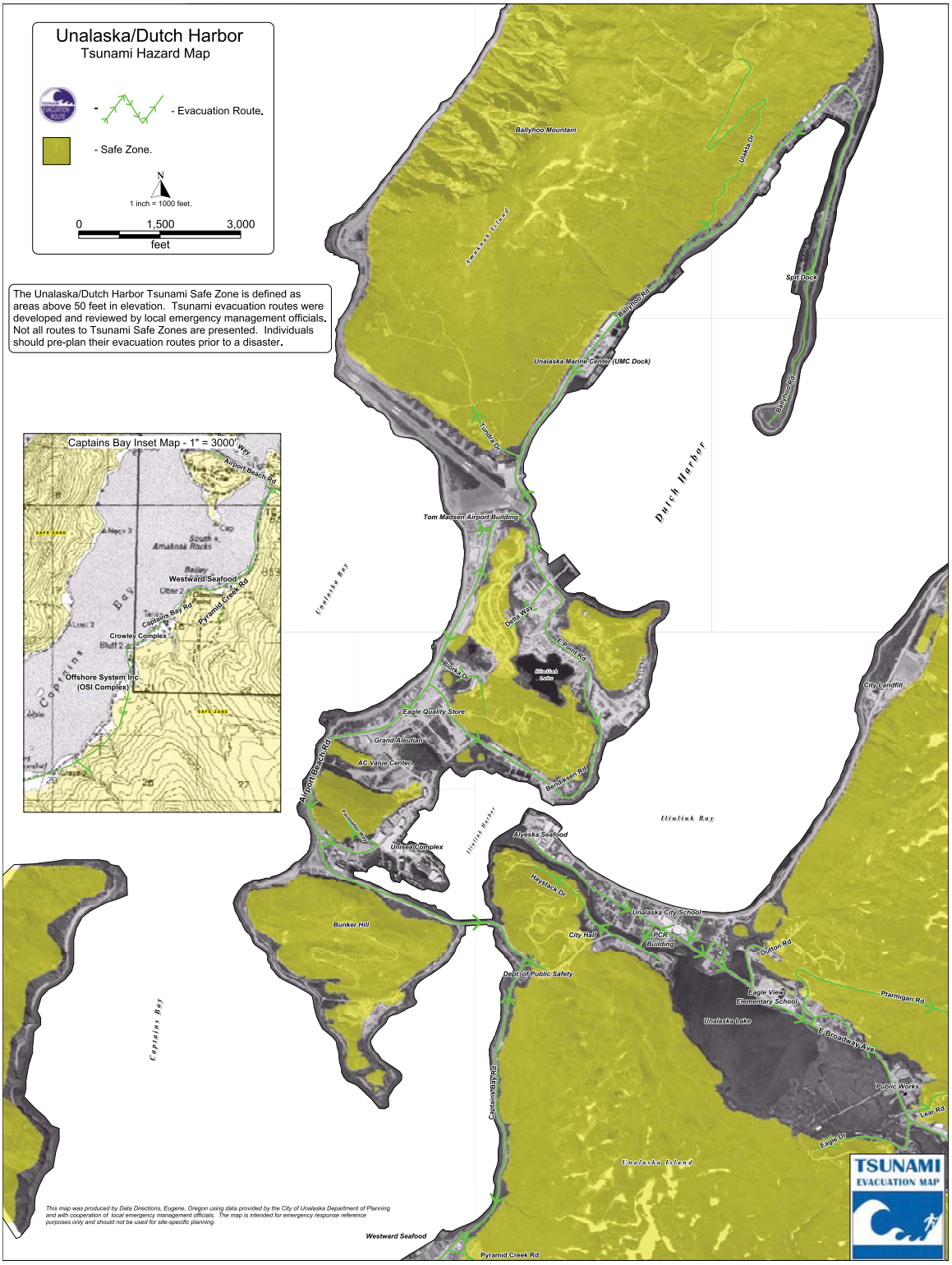

Figure 2: The tsunami hazard map with evacuation routes developed for Unalaska, Alaska, by Data Direction Consulting Group.

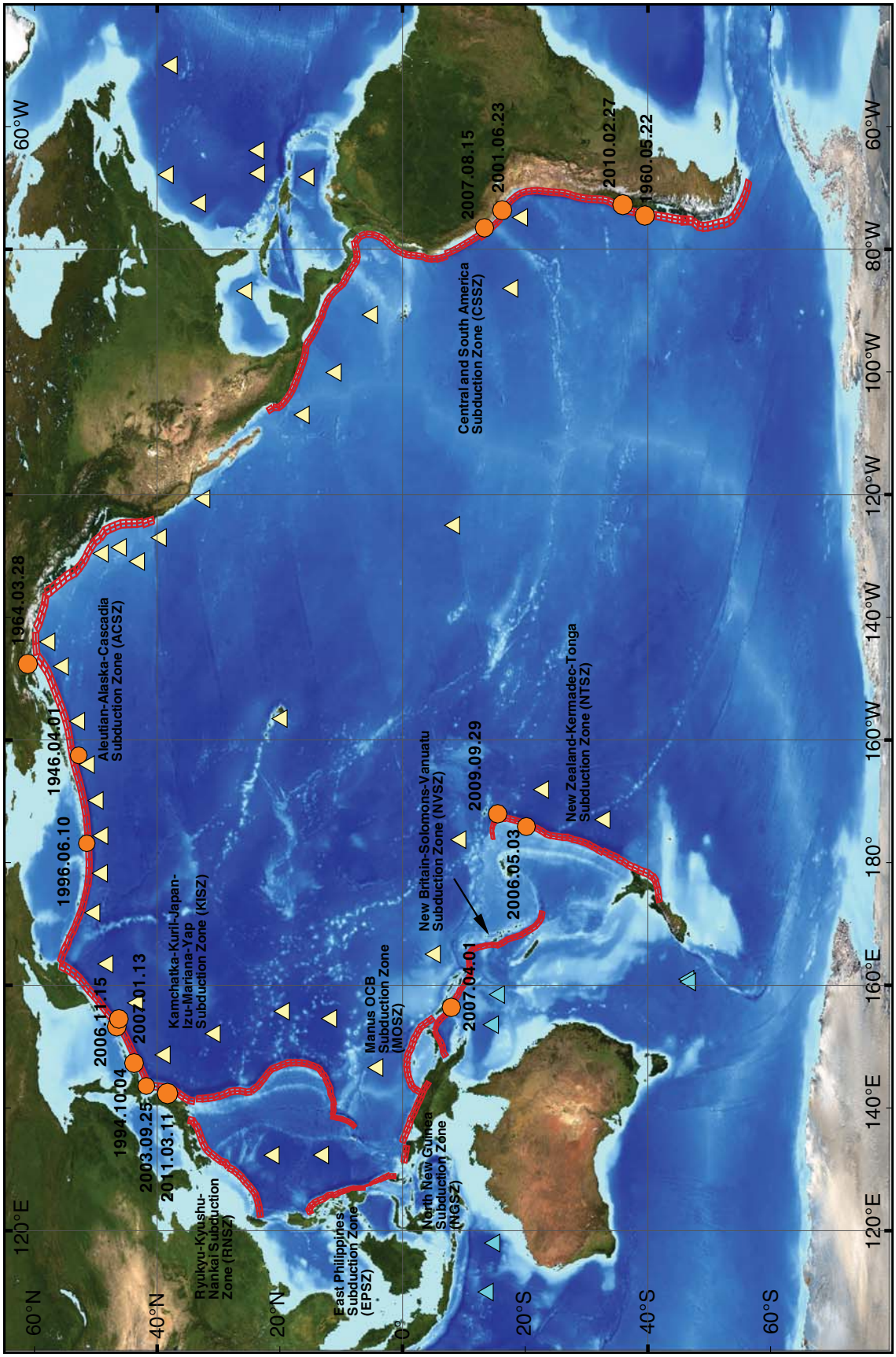

Figure 3: Map showing some of the historical tsunamis that occurred in the Pacific Basin. ● indicates epicenter location of the historical events; □ is the unit source; ▲ represents United States-operated deep-ocean tsunameter systems, and ▲ represents deep-ocean tsunameter systems operated by Australia. Note that due to recent unit source database updates, CASZ, CSSZ, and SCSZ are referred to singularly as CSSZ.

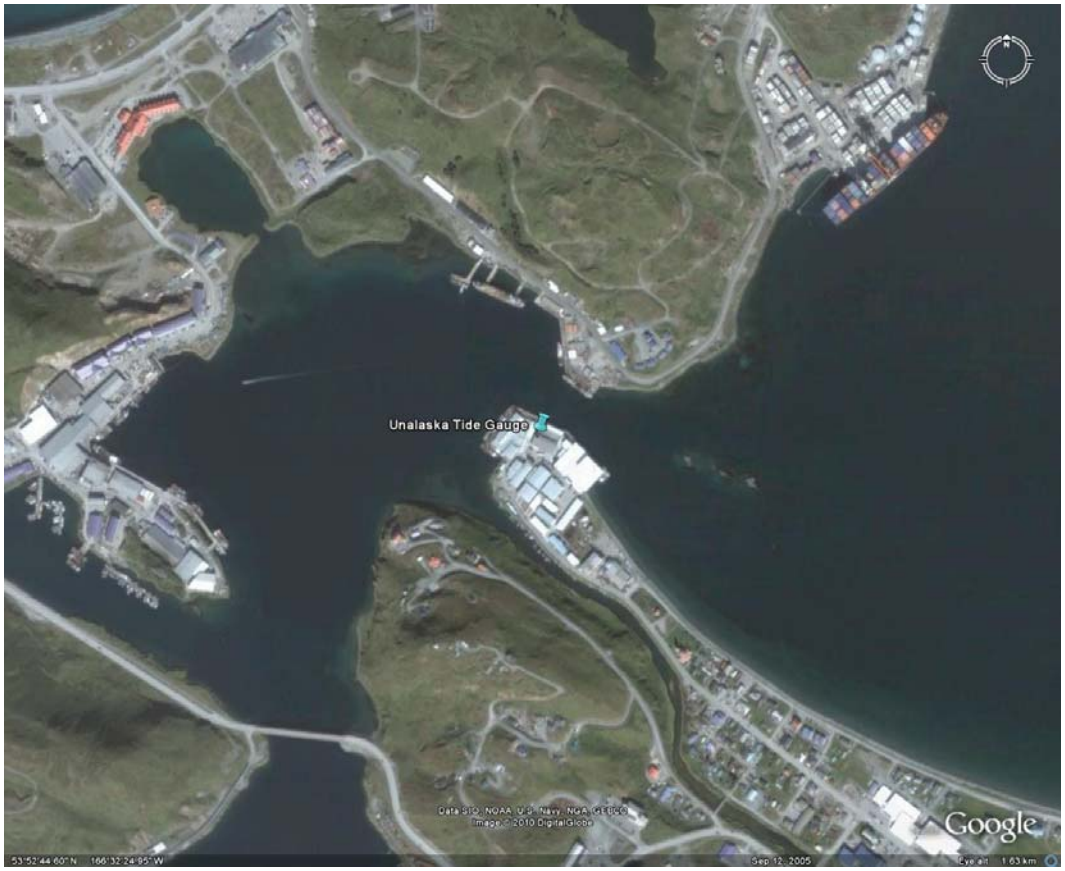

Figure 4: Location of the Unalaska tide gauge originally established in 1955 and installed at its current location in 1989.

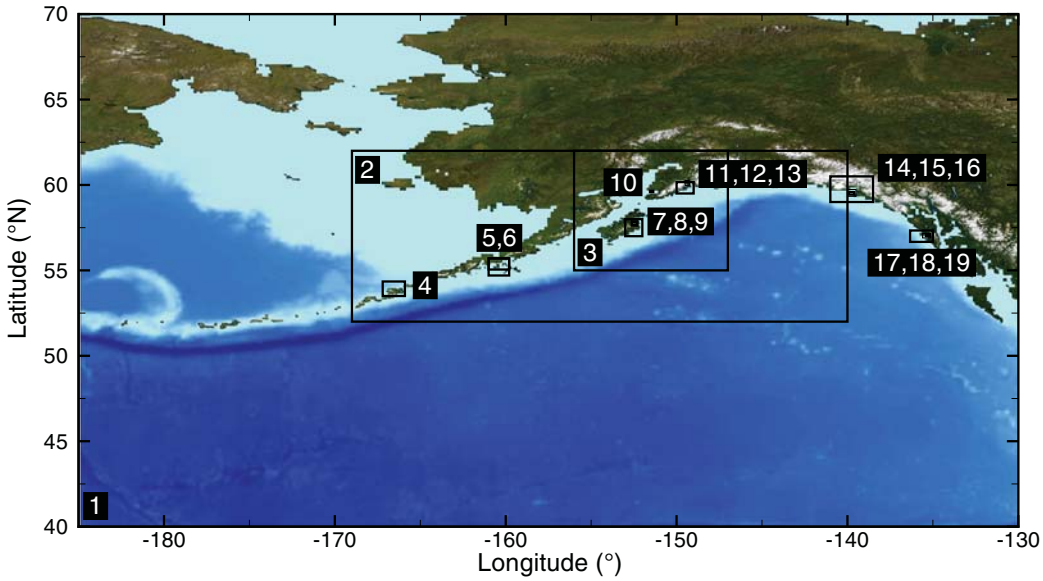

Figure 5: Extent of bathymetric and topographic grids in Alaska developed by National Geophysical Data Center and Pacific Marine Environmental Laboratory.

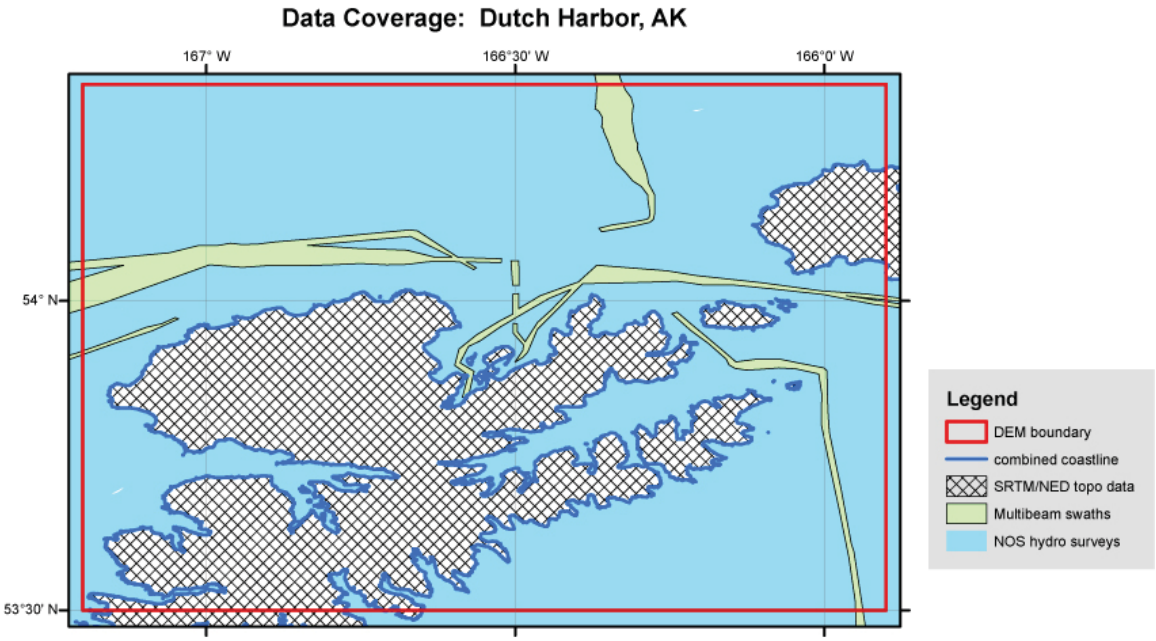

Figure 6: Coverage of data sources used to compile the Unalaska, Alaska, DEM (courtesy of Taylor *et al.*, 2006).

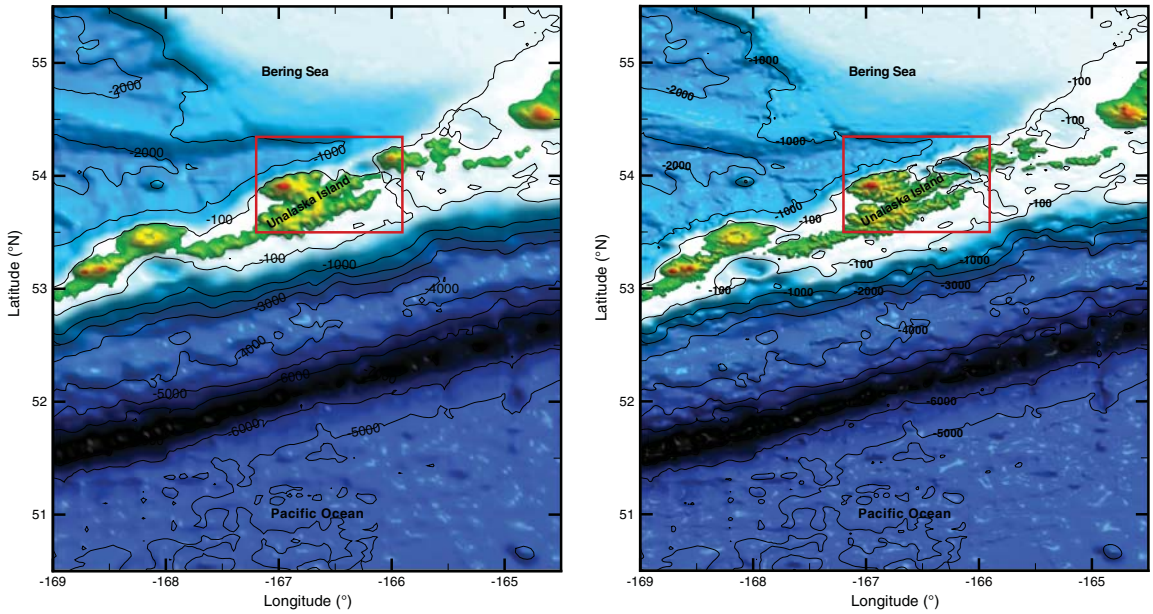

Figure 7: Bathymetry and topography of the A grid of the tsunami forecast model (left panel) and the reference model (right panel) of Unalaska, Alaska.

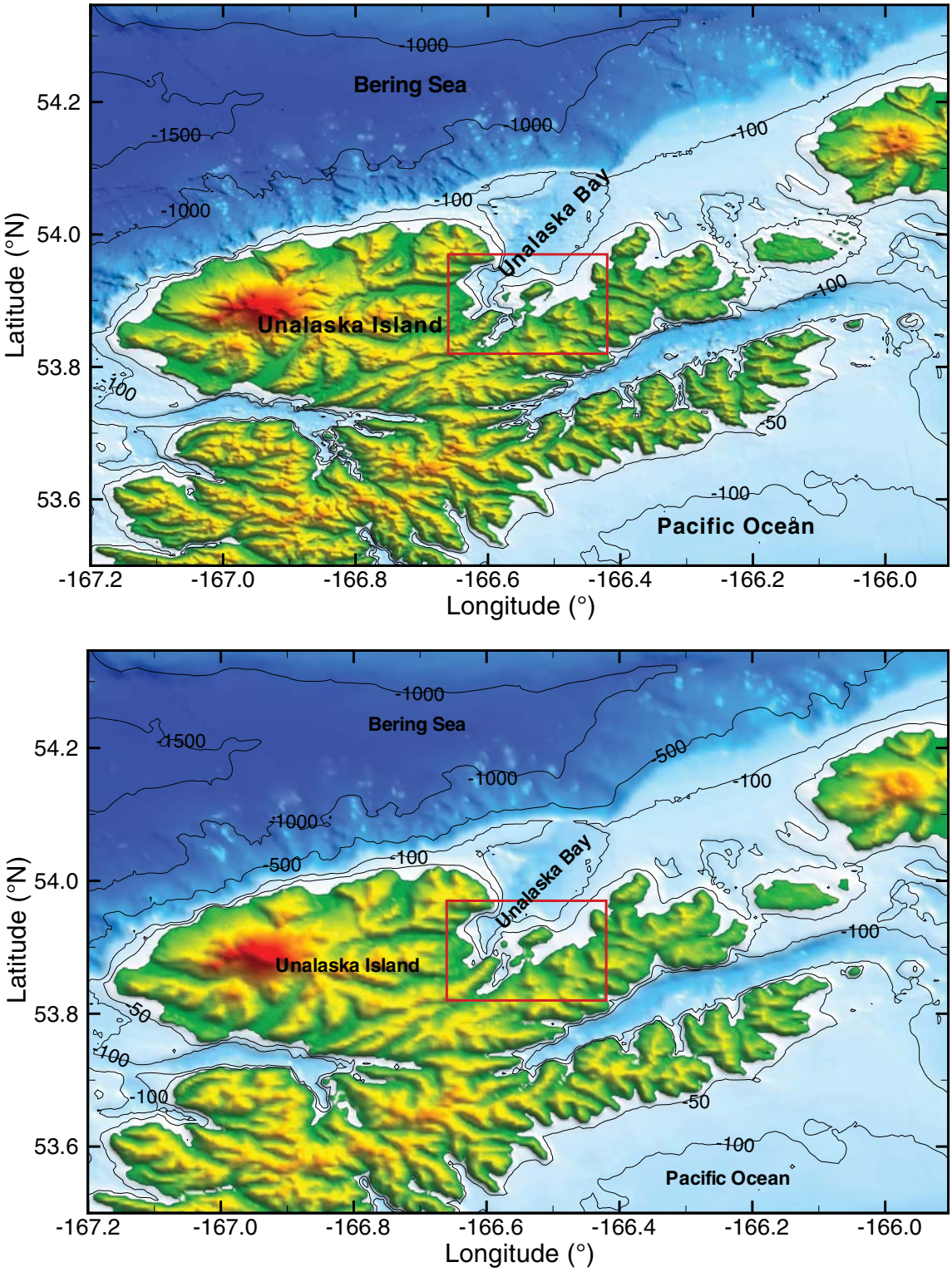

Figure 8: Bathymetry and topography of the B grid of the tsunami forecast model (top panel) and the reference model (bottom panel) of Unalaska, Alaska.

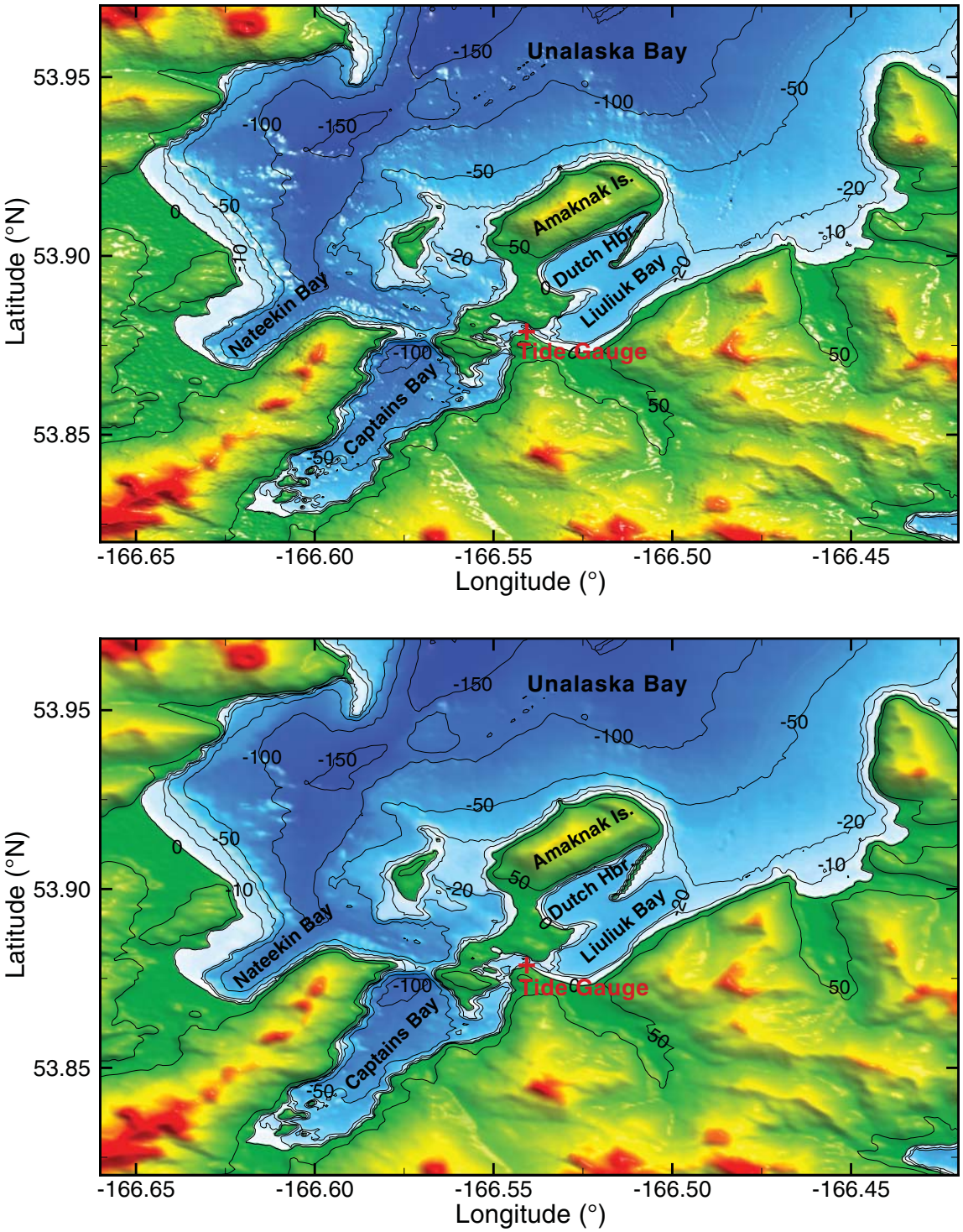

Figure 9: Bathymetry and topography of the C grid of the tsunami forecast model (top panel) and the reference model (bottom panel) of Unalaska, Alaska.

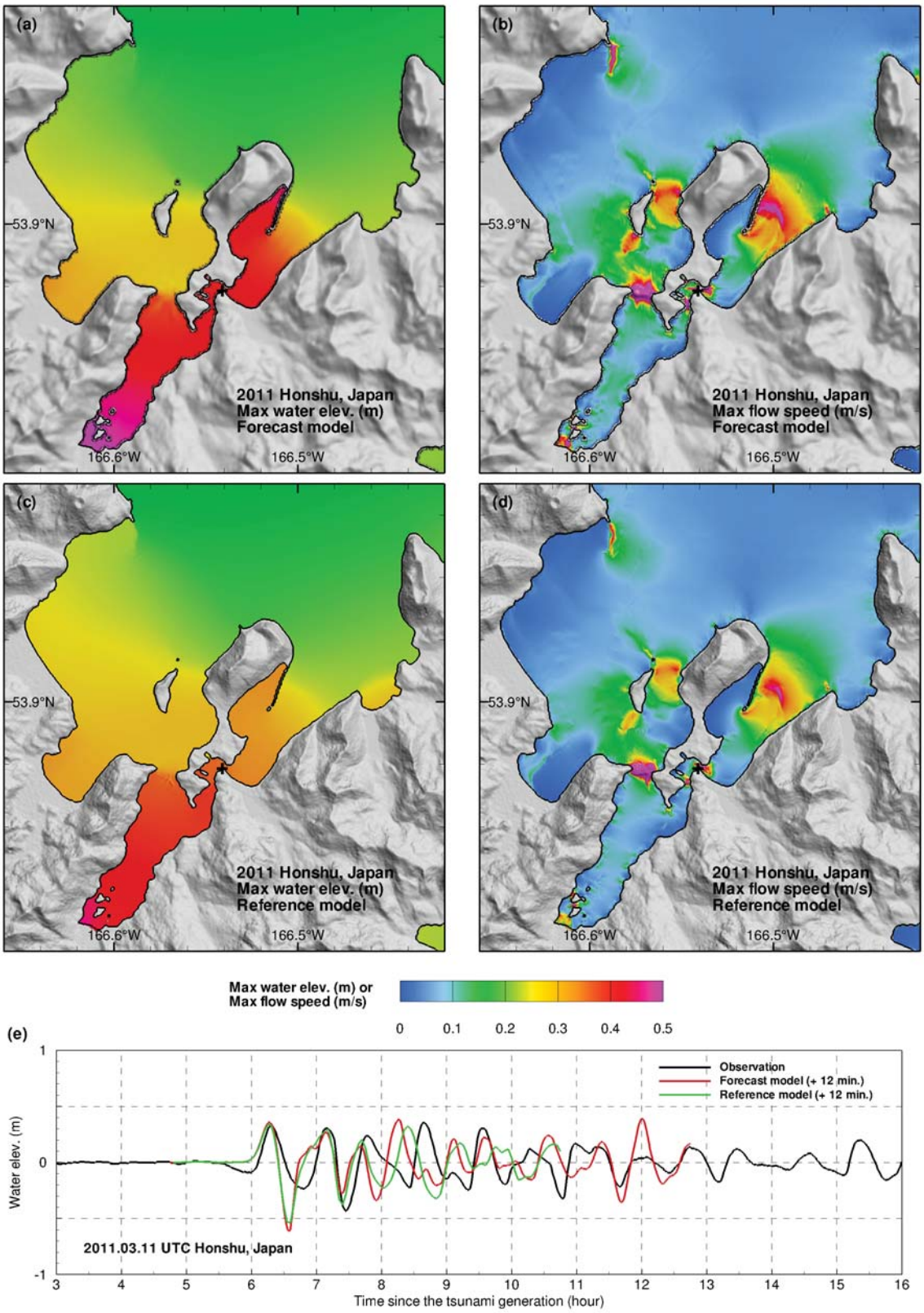

Figure 10: 11 March 2011 Honshu, Japan, tsunami. (a) and (b): maximum wave amplitude and flow speed computed from the forecast model; (c) and (d) maximum wave amplitude and flow speed computed from the reference model; (e) Model/data comparison at Unalaska tide gauge, which is noted as + in (a), (b), (c), and (d).

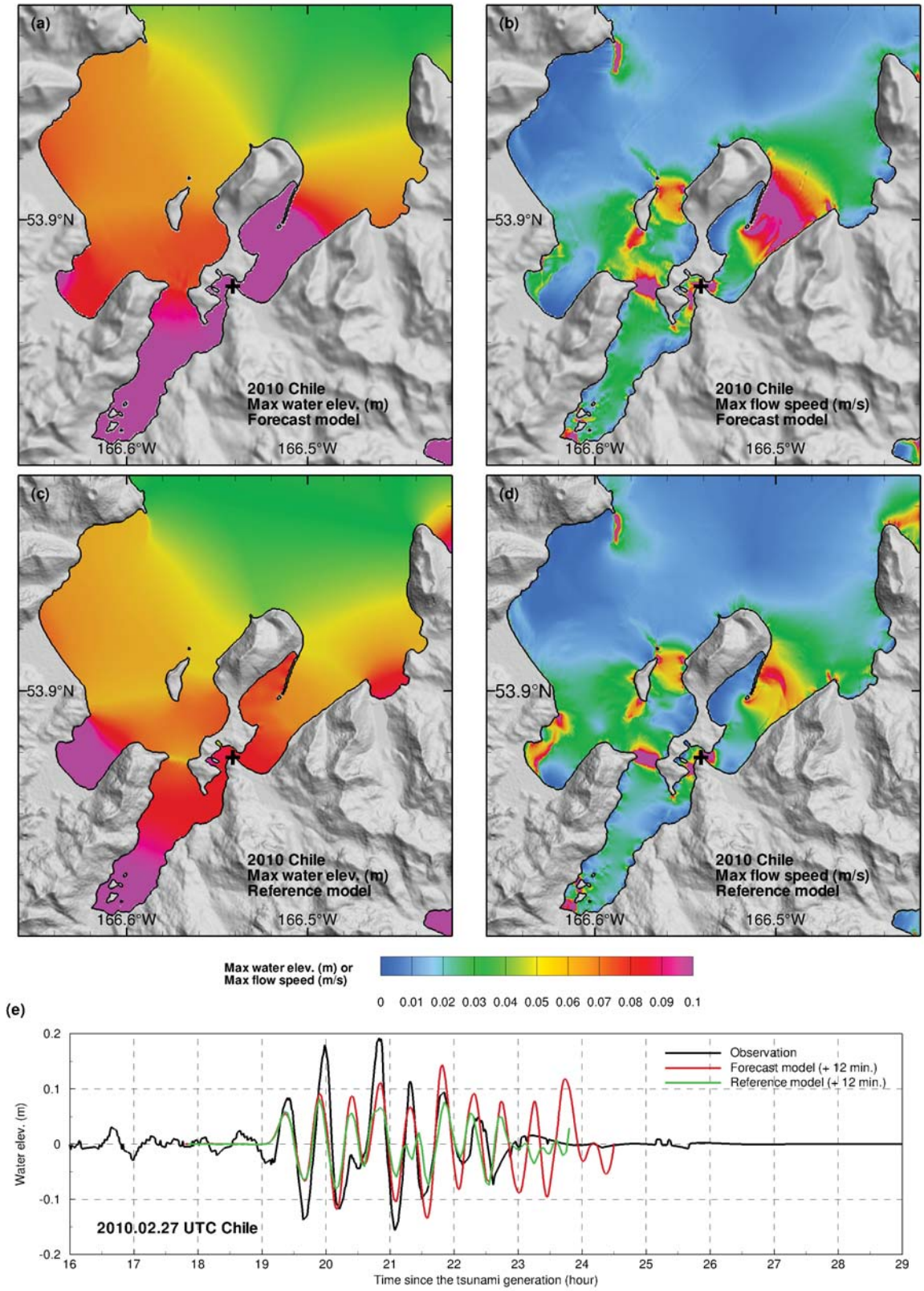

Figure 11: 27 February 2010 Chile tsunami. (a) and (b): maximum wave amplitude and flow speed computed from the forecast model; (c) and (d): maximum wave amplitude and flow speed computed from the reference model; (e): model/data comparison at Unalaska tide gauge, which is noted as + in (a), (b), (c), and (d).

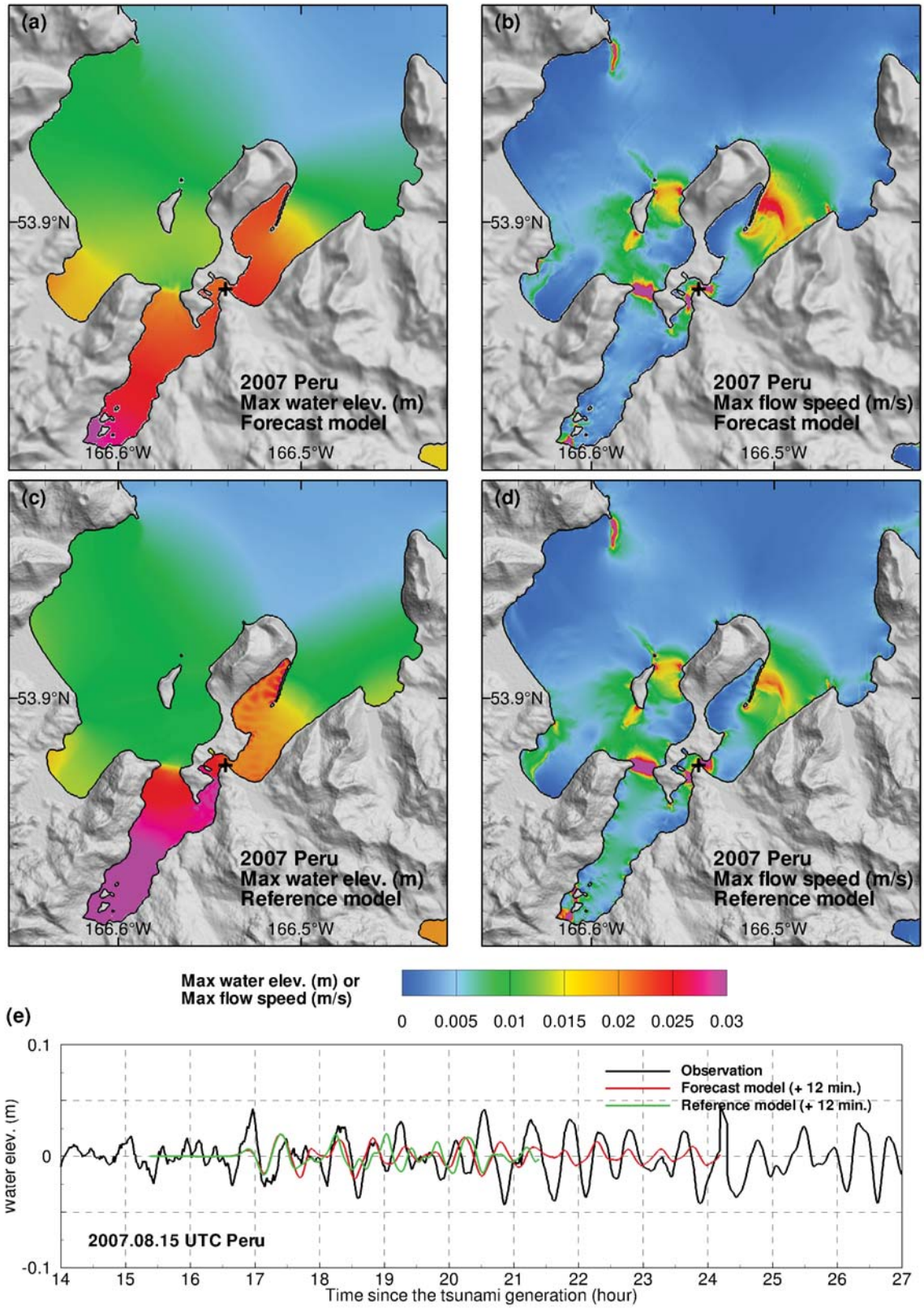

Figure 12: 15 August 2007 Peru tsunami. (a) and (b): maximum wave amplitude and flow speed computed from the forecast model; (c) and (d): maximum wave amplitude and flow speed computed from the reference model; (e): model/data comparison at Unalaska tide gauge, which is noted as + in (a), (b), (c), and (d).

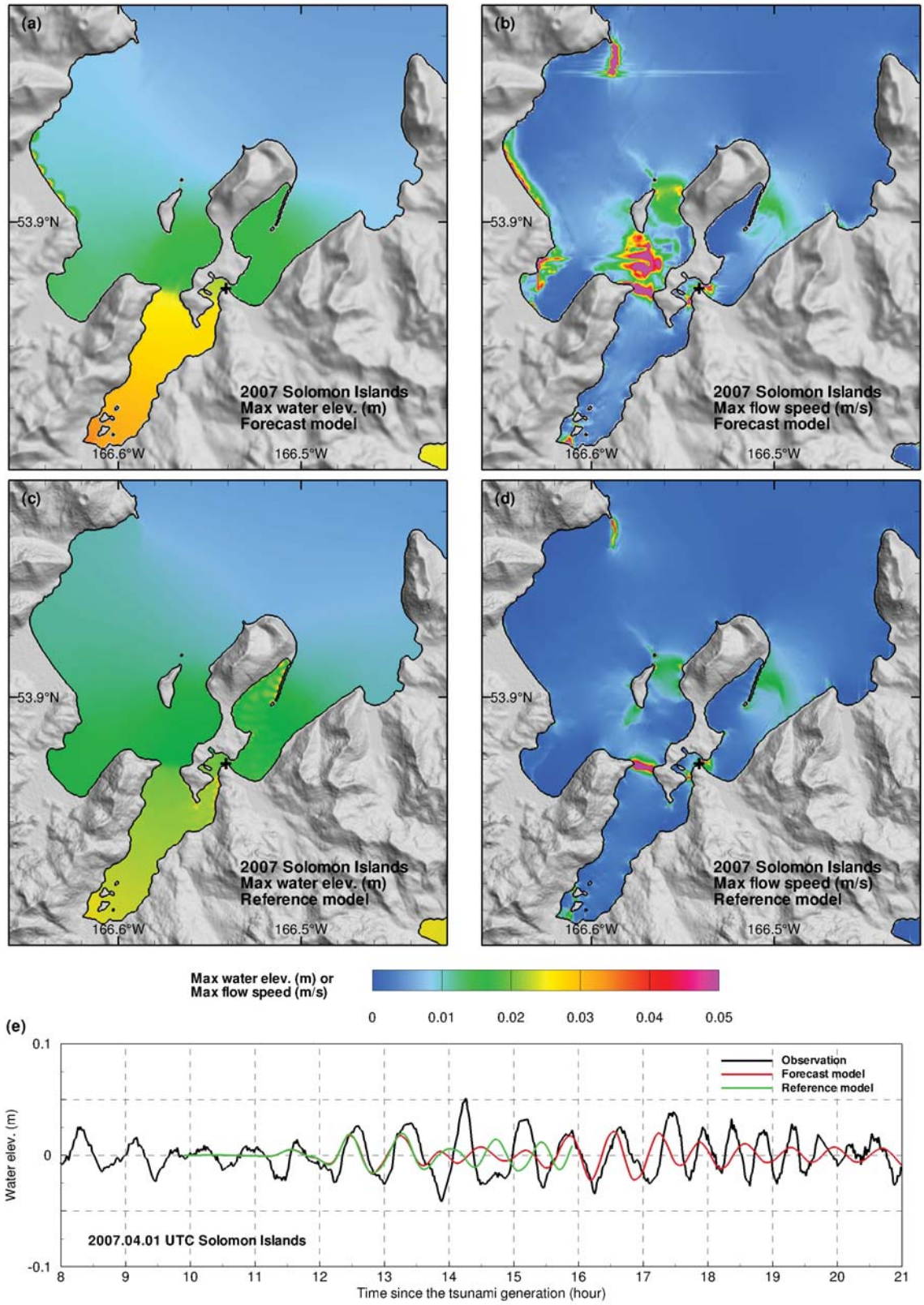

Figure 13: 1 April 2007 Solomon tsunami. (a) and (b): maximum wave amplitude and flow speed computed from the forecast model; (c) and (d): maximum wave amplitude and flow speed computed from the reference model; (e): model/data comparison at Unalaska tide gauge, which is noted as + in (a), (b), (c), and (d).

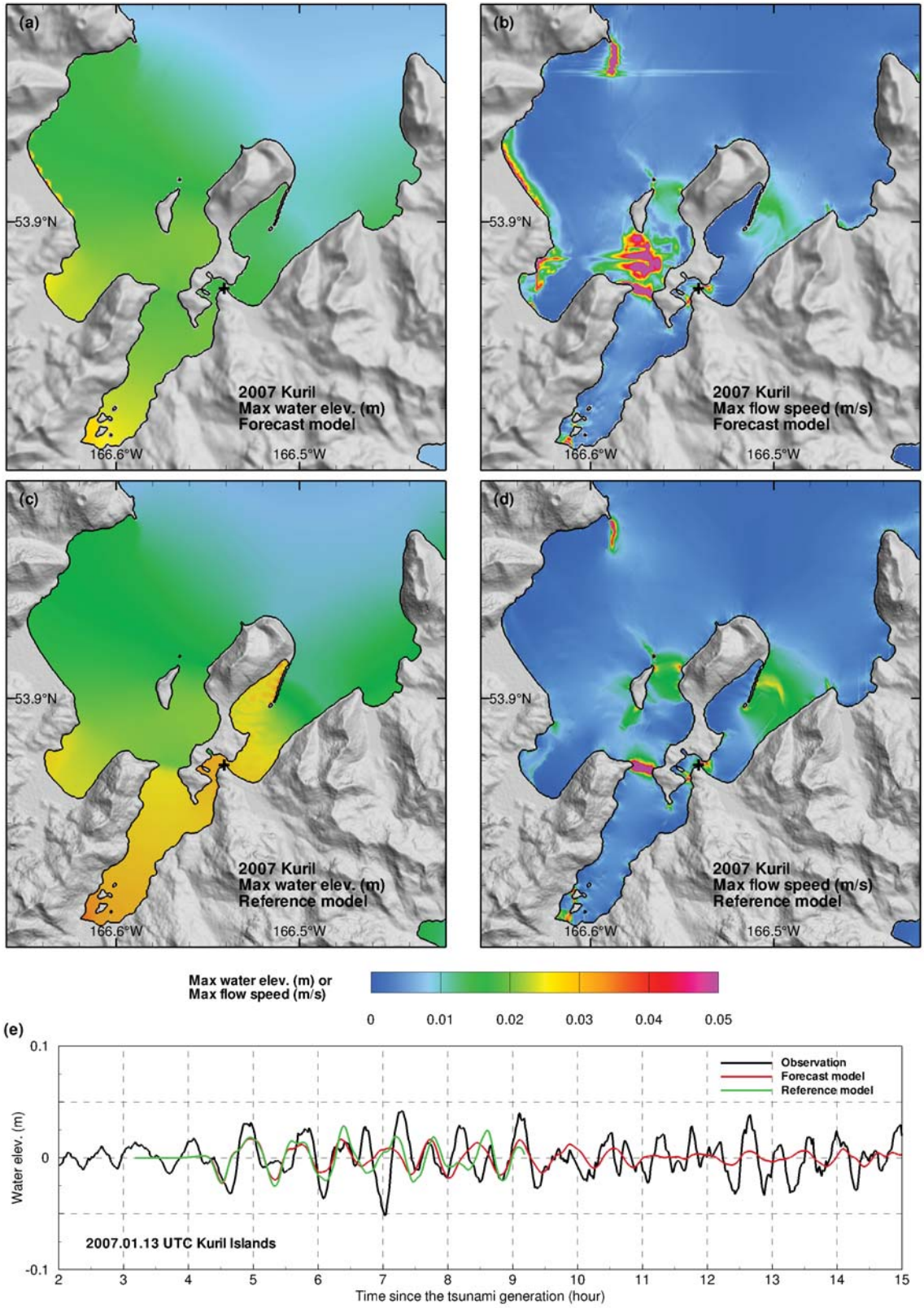

Figure 14: 13 January 2007 Kuril tsunami. (a) and (b): maximum wave amplitude and flow speed computed from the forecast model; (c) and (d): maximum wave amplitude and flow speed computed from the reference model; (e): model/data comparison at Unalaska tide gauge, which is noted as + in (a), (b), (c), and (d).

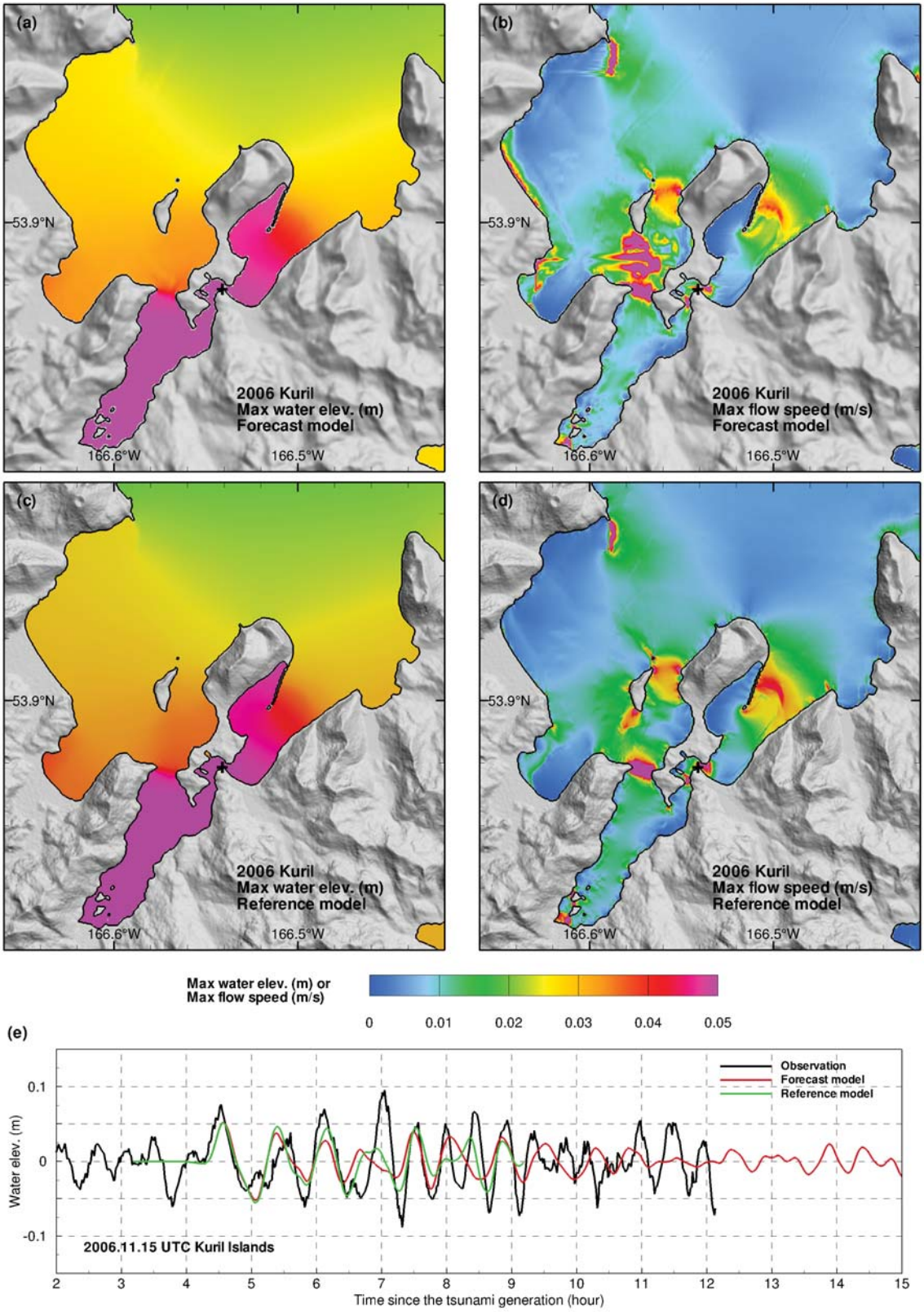

Figure 15: 15 November 2006 Kuril tsunami. (a) and (b): maximum wave amplitude and flow speed computed from the forecast model; (c) and (d): maximum wave amplitude and flow speed computed from the reference model; (e): model/data comparison at Unalaska tide gauge, which is noted as + in (a), (b), (c), and (d).

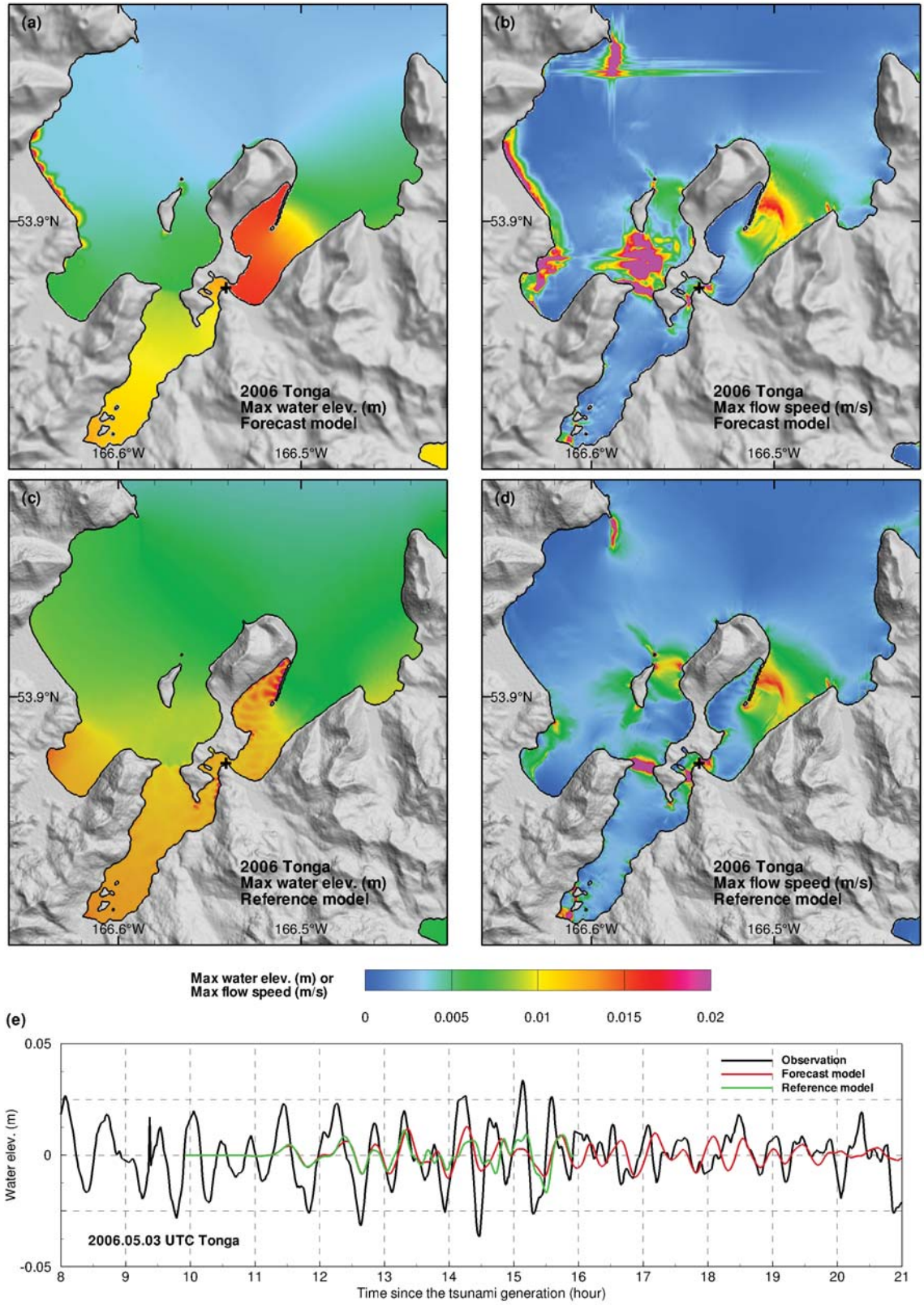

Figure 16: 3 May 2006 Tonga tsunami. (a) and (b): maximum wave amplitude and flow speed computed from the forecast model; (c) and (d): maximum wave amplitude and flow speed computed from the reference model; (e): model/data comparison at Unalaska tide gauge, which is noted as + in (a), (b), (c), and (d).

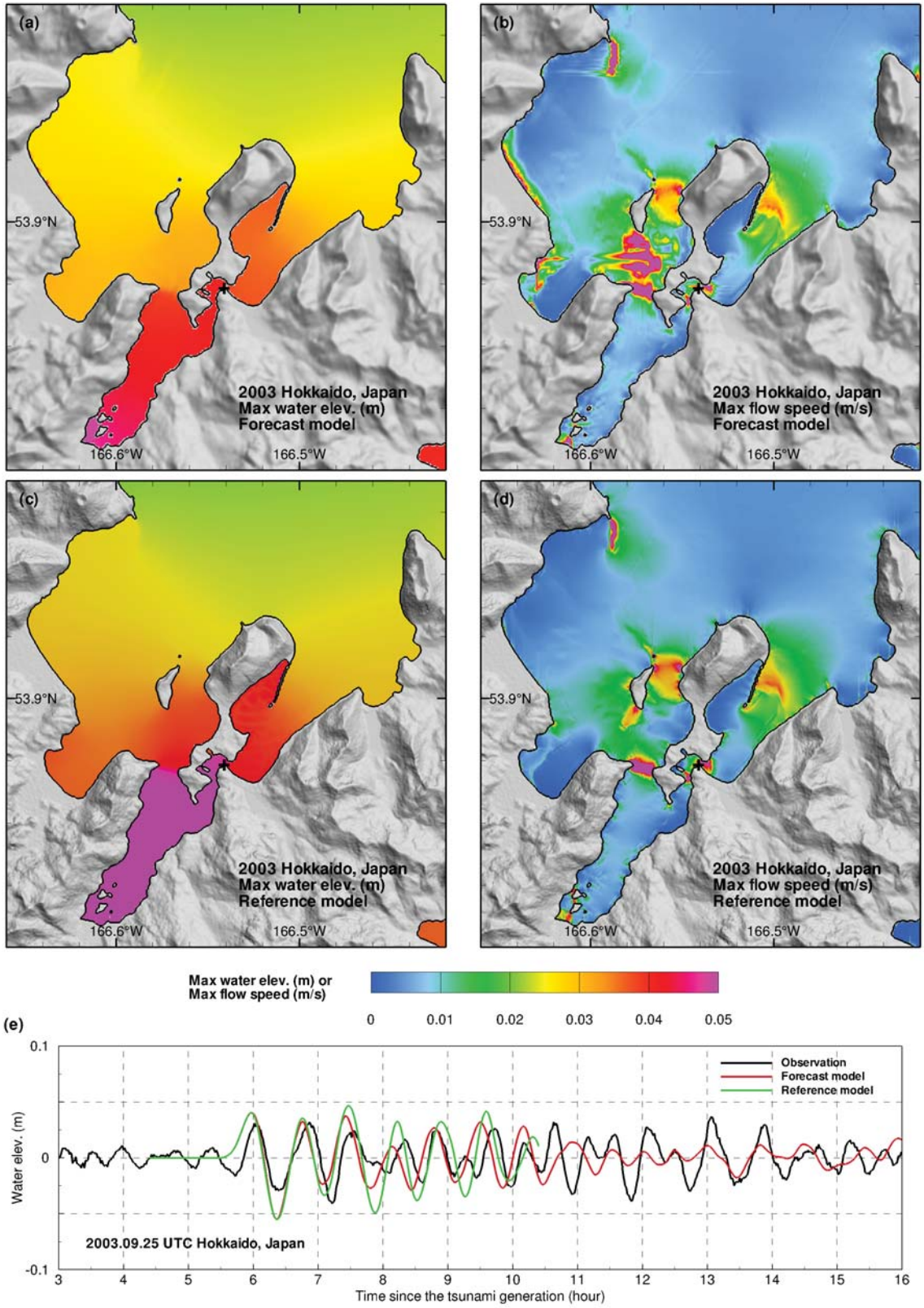

Figure 17: 25 September 2003 Hokkaido tsunami. (a) and (b): maximum wave amplitude and flow speed computed from the forecast model; (c) and (d): maximum wave amplitude and flow speed computed from the reference model; (e): model/data comparison at Unalaska tide gauge, which is noted as + in (a), (b), (c), and (d).

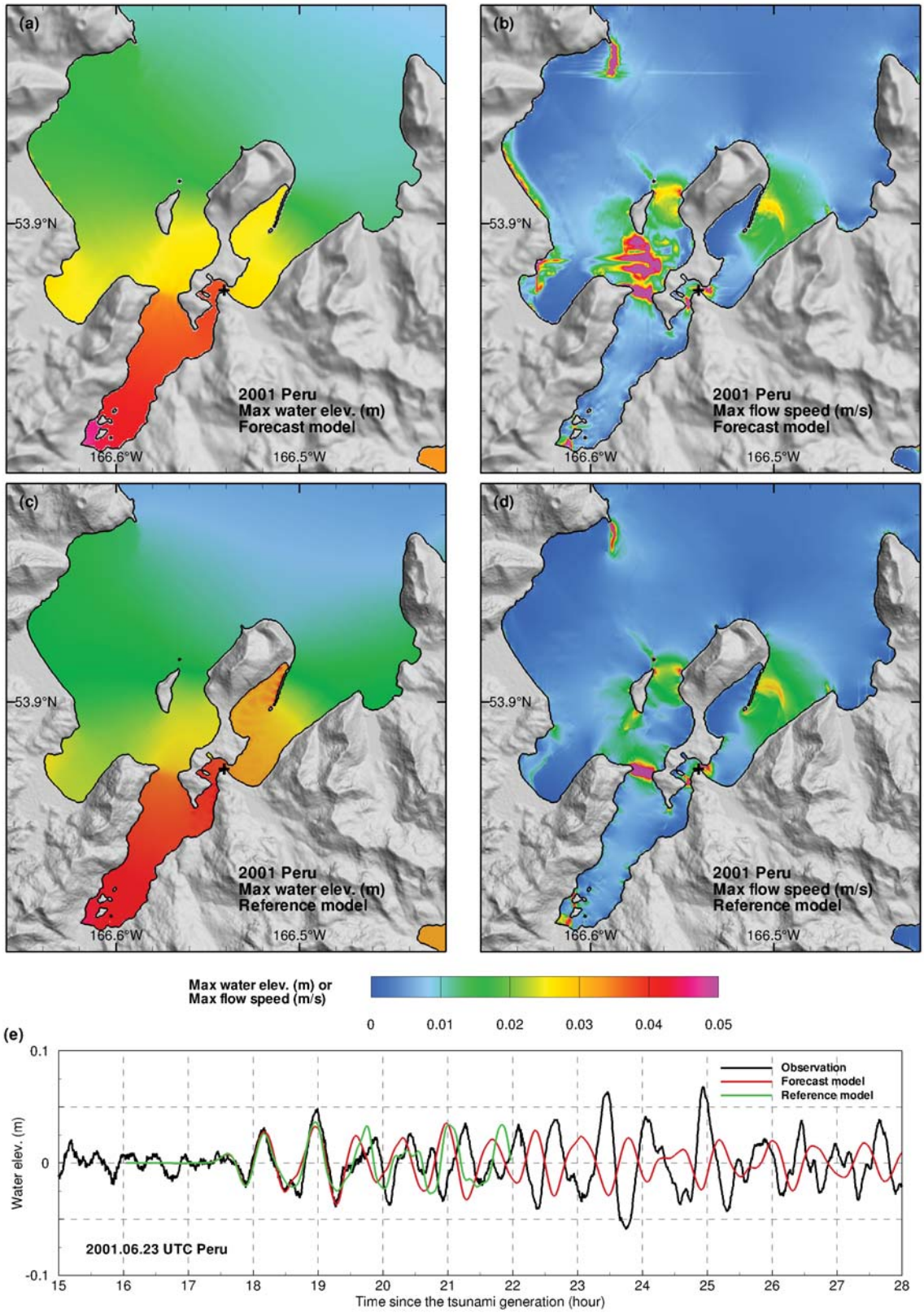

Figure 18: 23 June 2001 Peru tsunami. (a) and (b): maximum wave amplitude and flow speed computed from the forecast model; (c) and (d): maximum wave amplitude and flow speed computed from the reference model; (e): model/data comparison at Unalaska tide gauge, which is noted as + in (a), (b), (c), and (d).

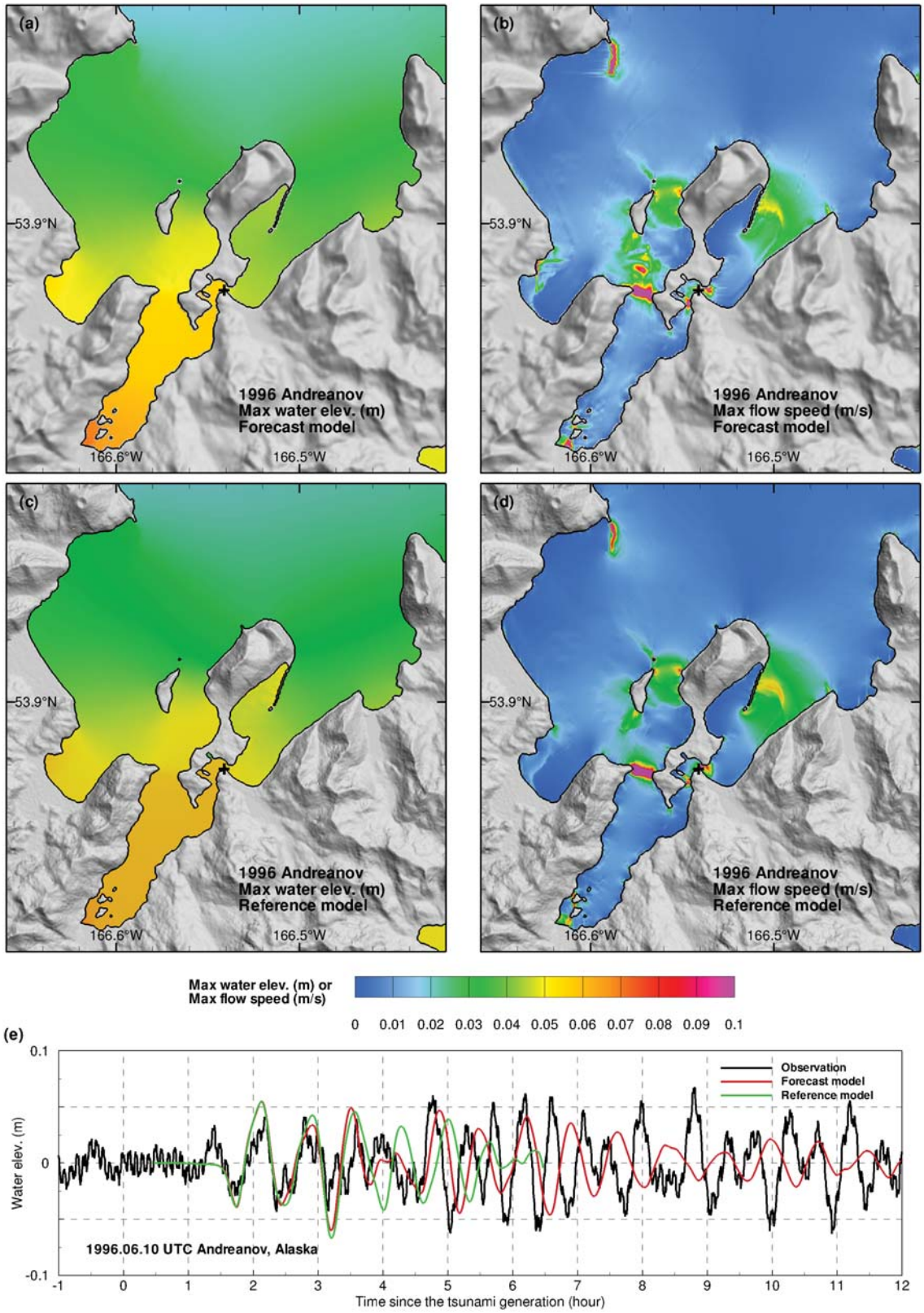

Figure 19: 10 June 1996 Andreanov tsunami. (a) and (b): maximum wave amplitude and flow speed computed from the forecast model; (c) and (d): maximum wave amplitude and flow speed computed from the reference model; (e): model/data comparison at Unalaska tide gauge, which is noted as + in (a), (b), (c), and (d).

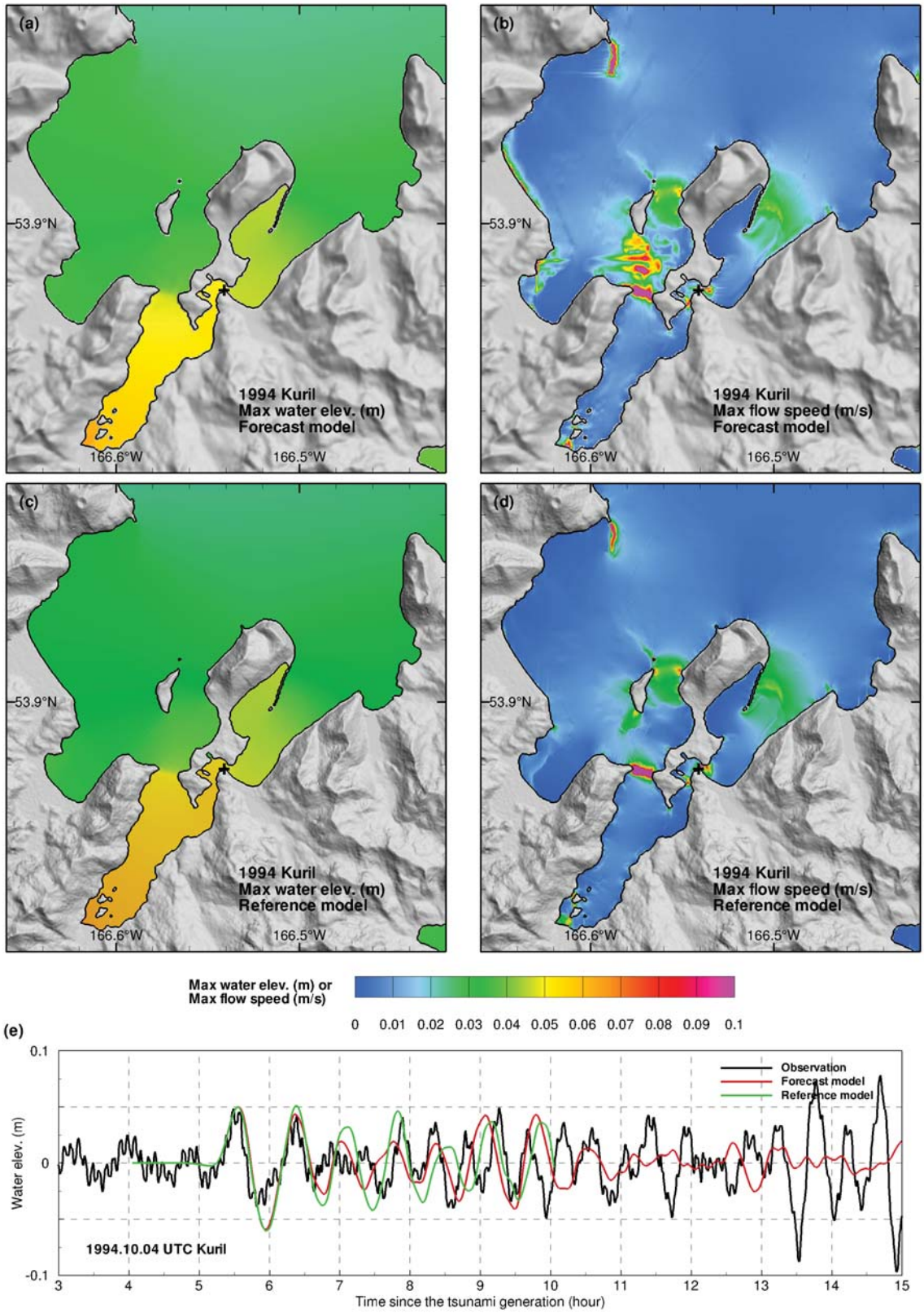

Figure 20: 4 October 1994 Kuril tsunami. (a) and (b): maximum wave amplitude and flow speed computed from the forecast model; (c) and (d): maximum wave amplitude and flow speed computed from the reference model; (e): model/data comparison at Unalaska tide gauge, which is noted as + in (a), (b), (c), and (d).

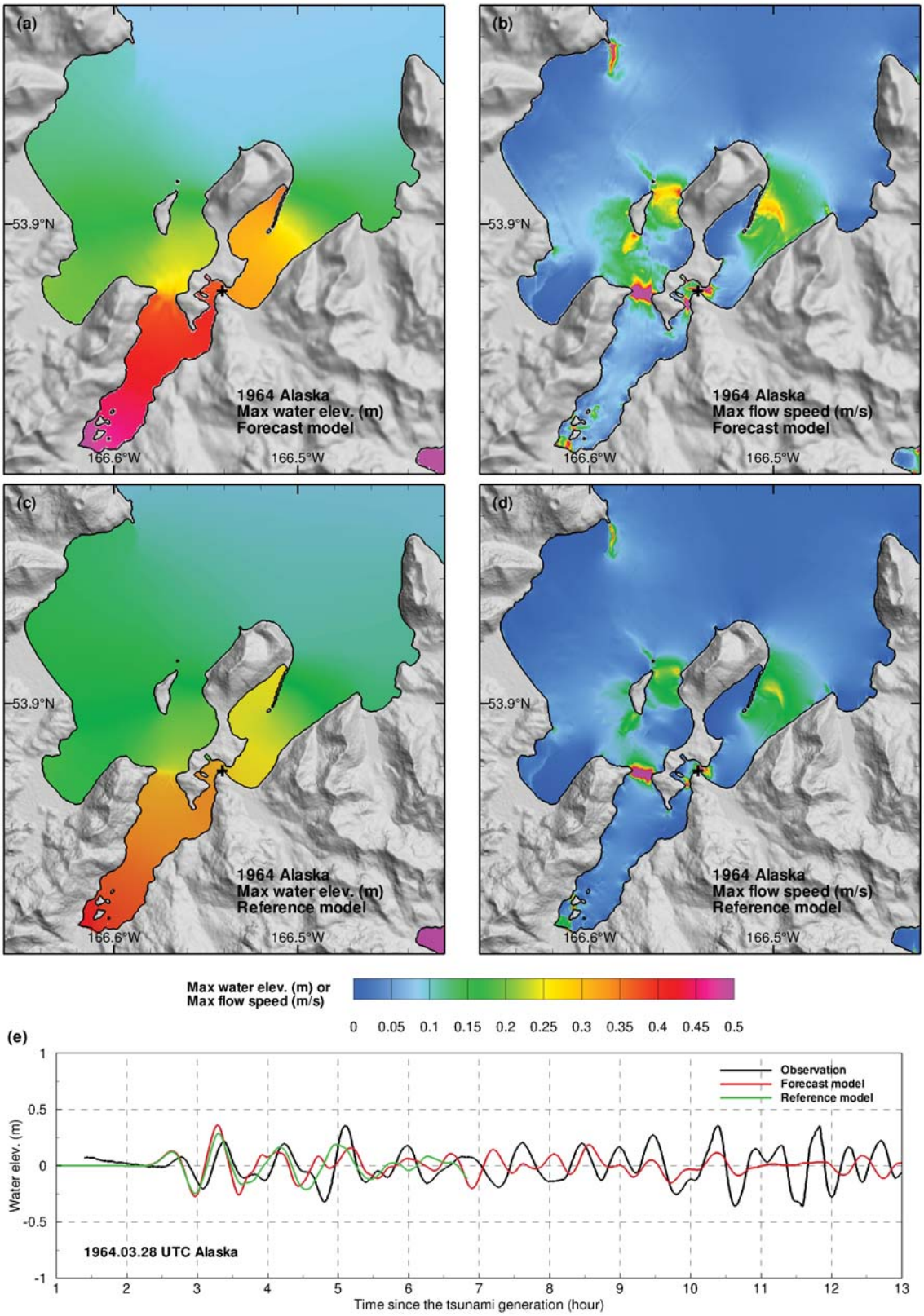

Figure 21: 28 May 1964 Alaska tsunami. (a) and (b): maximum wave amplitude and flow speed computed from the forecast model; (c) and (d): maximum wave amplitude and flow speed computed from the reference model; (e): model/data comparison at Unalaska tide gauge, which is noted as + in (a), (b), (c), and (d).

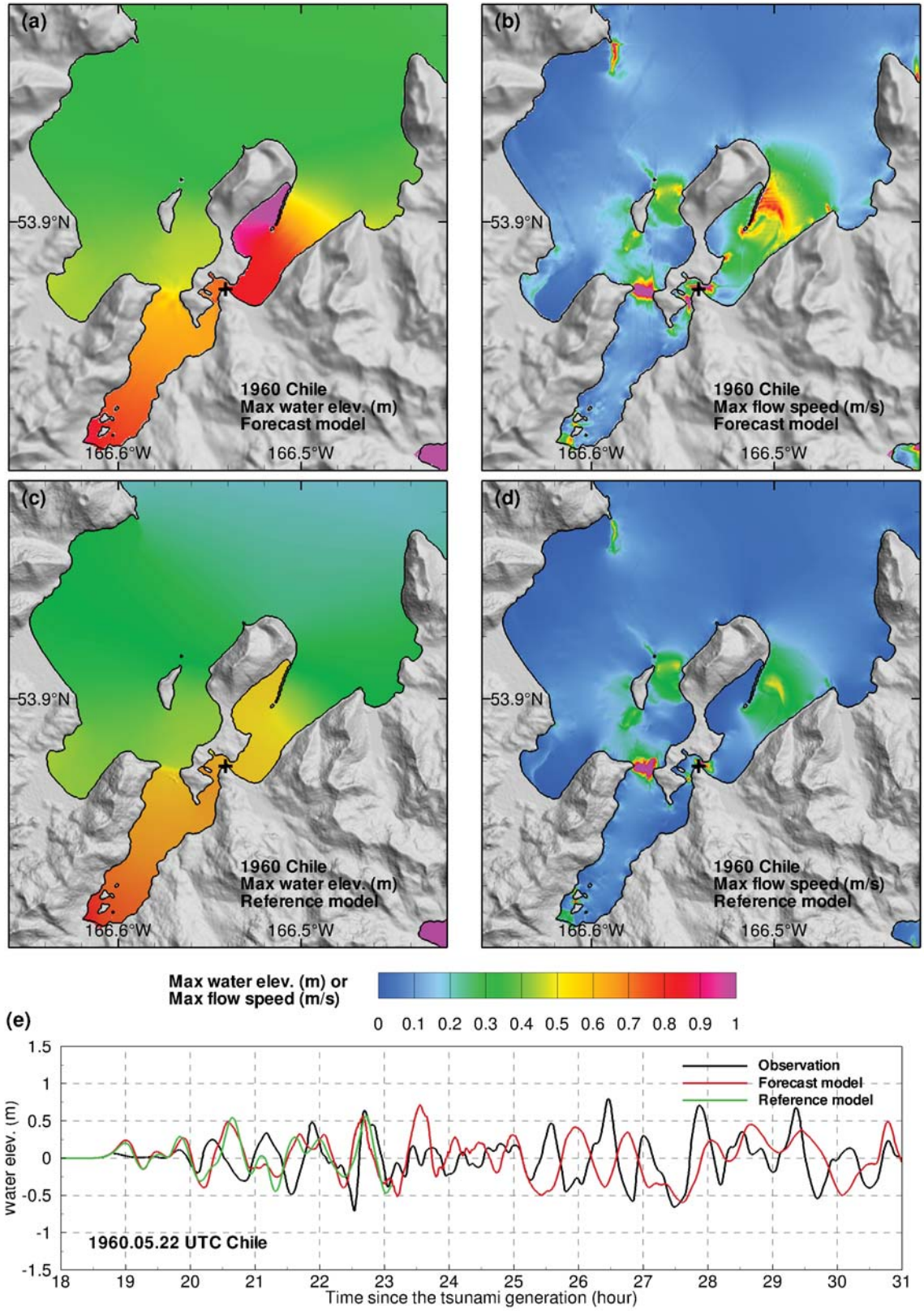

Figure 22: 22 May 1960 Chile tsunami. (a) and (b): maximum wave amplitude and flow speed computed from the forecast model; (c) and (d): maximum wave amplitude and flow speed computed from the reference model. (e): model/data comparison at Unalaska tide gauge, which is noted as + in (a), (b), (c), and (d); (e): model/data comparison at Unalaska tide gauge, which is noted as + in (a) (b) (c) and (d).

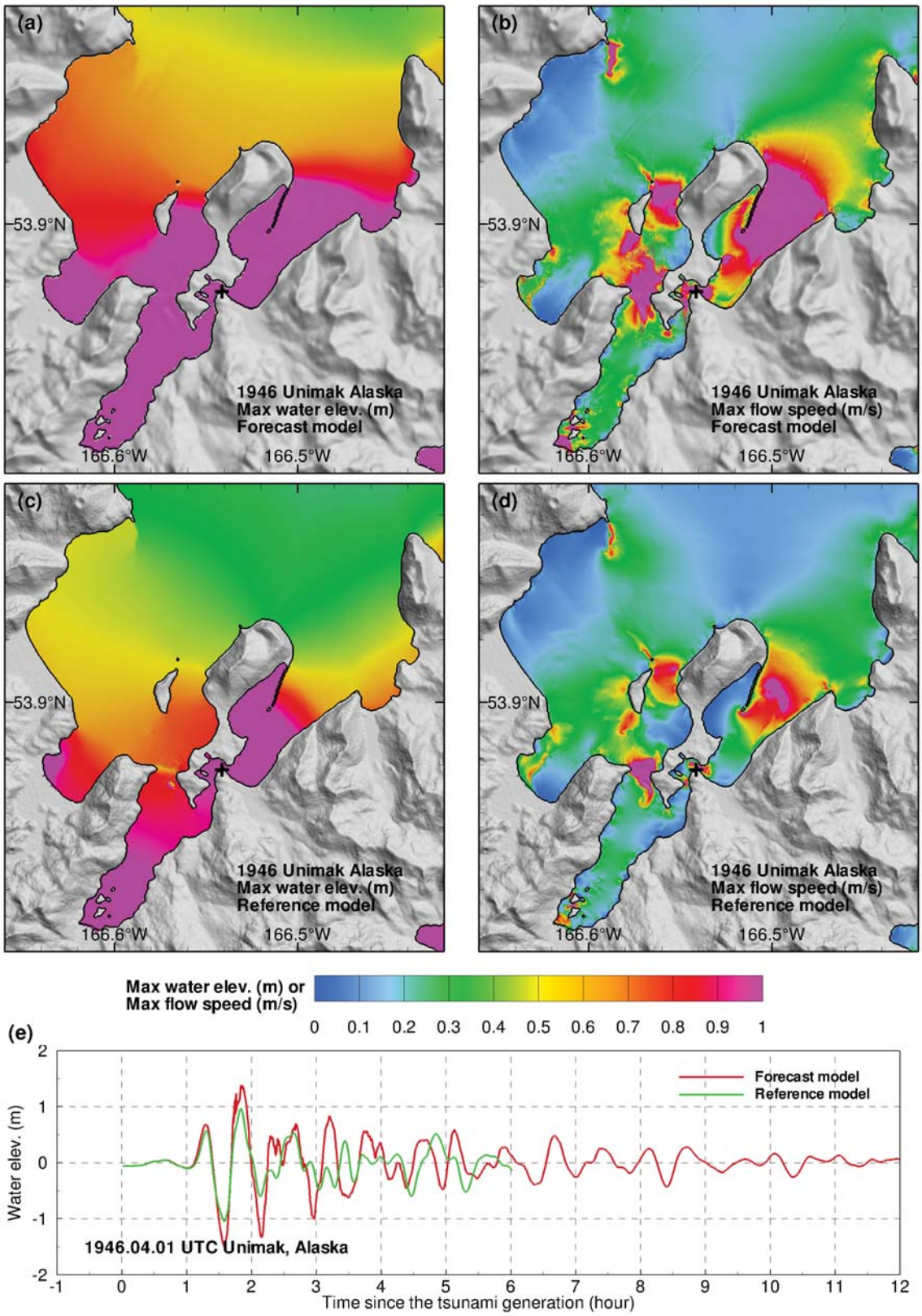

Figure 23: 1 April 1946 Unimak tsunami. (a) and (b): maximum wave amplitude and flow speed computed from the forecast model; (c) and (d): maximum wave amplitude and flow speed computed from the reference model; (e): model/data comparison at Unalaska tide gauge, which is noted as + in (a), (b), (c), and (d).

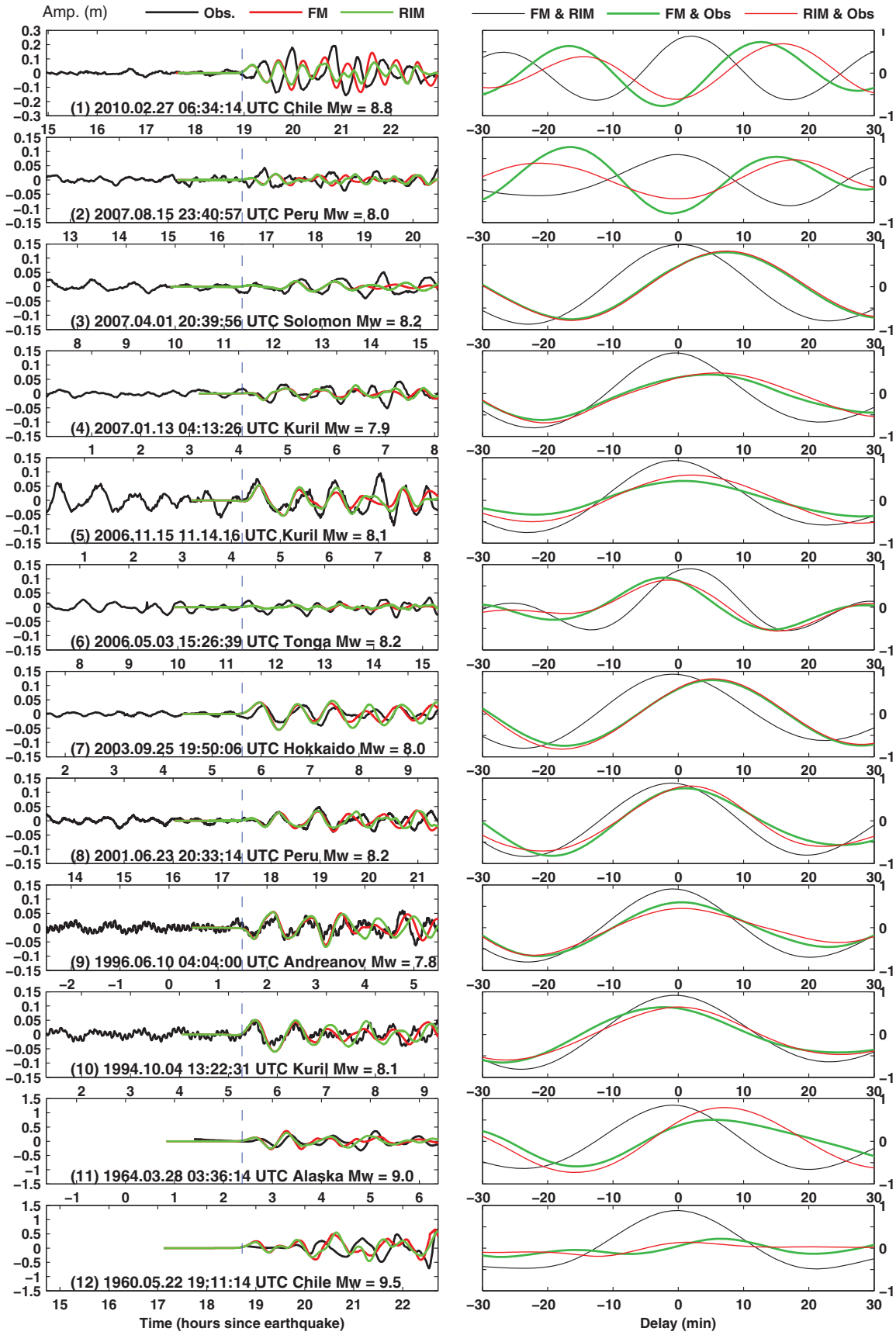

Figure 24: Model/observation cross-correlation for historical tsunami events at Unalaska tide gauge.

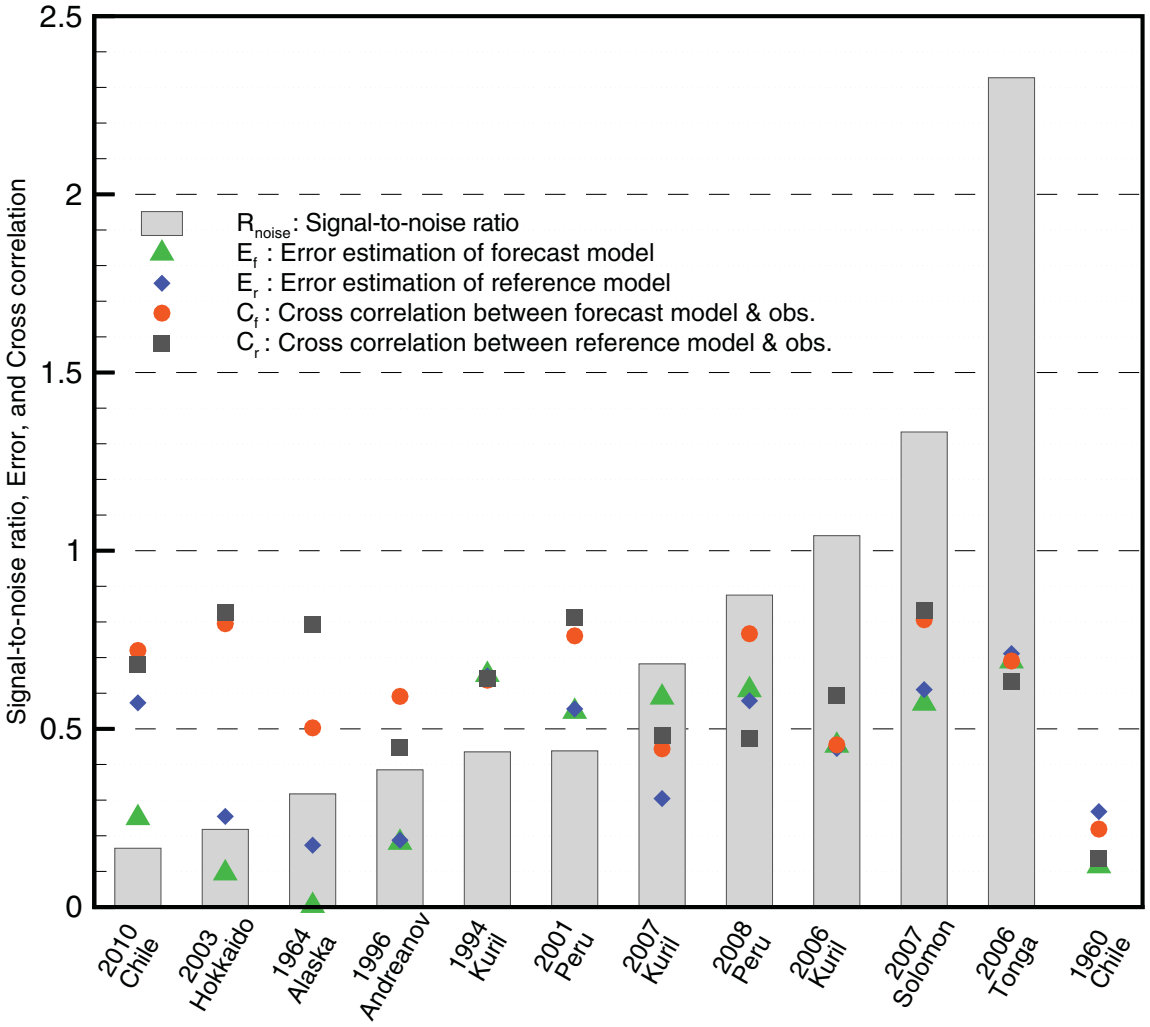

Figure 25: Comparisons of error estimation of modeling results with the noise level at Unalaska tide gauge for historical tsunami events, where E is the model/data error computed by $(\eta_{\text{model}} - \eta_{\text{obs}})$ / η_{obs} × 100%, C is the max cross-correlation between model and data. E_f and E_r indicate the errors of forecast model and reference model. C_f and C_r represent the cross-correlations between forecast model and obs, and between reference model and obs, respectively. R_{noise} is the signal-to-noise ratio calculated from A_{noise} / A_{model}, where A_{noise} and A_{model} are respectively the root-mean-square amplitudes of 4-hr observation prior to tsunami arrival and first 4-hr tsunami signal of the model.

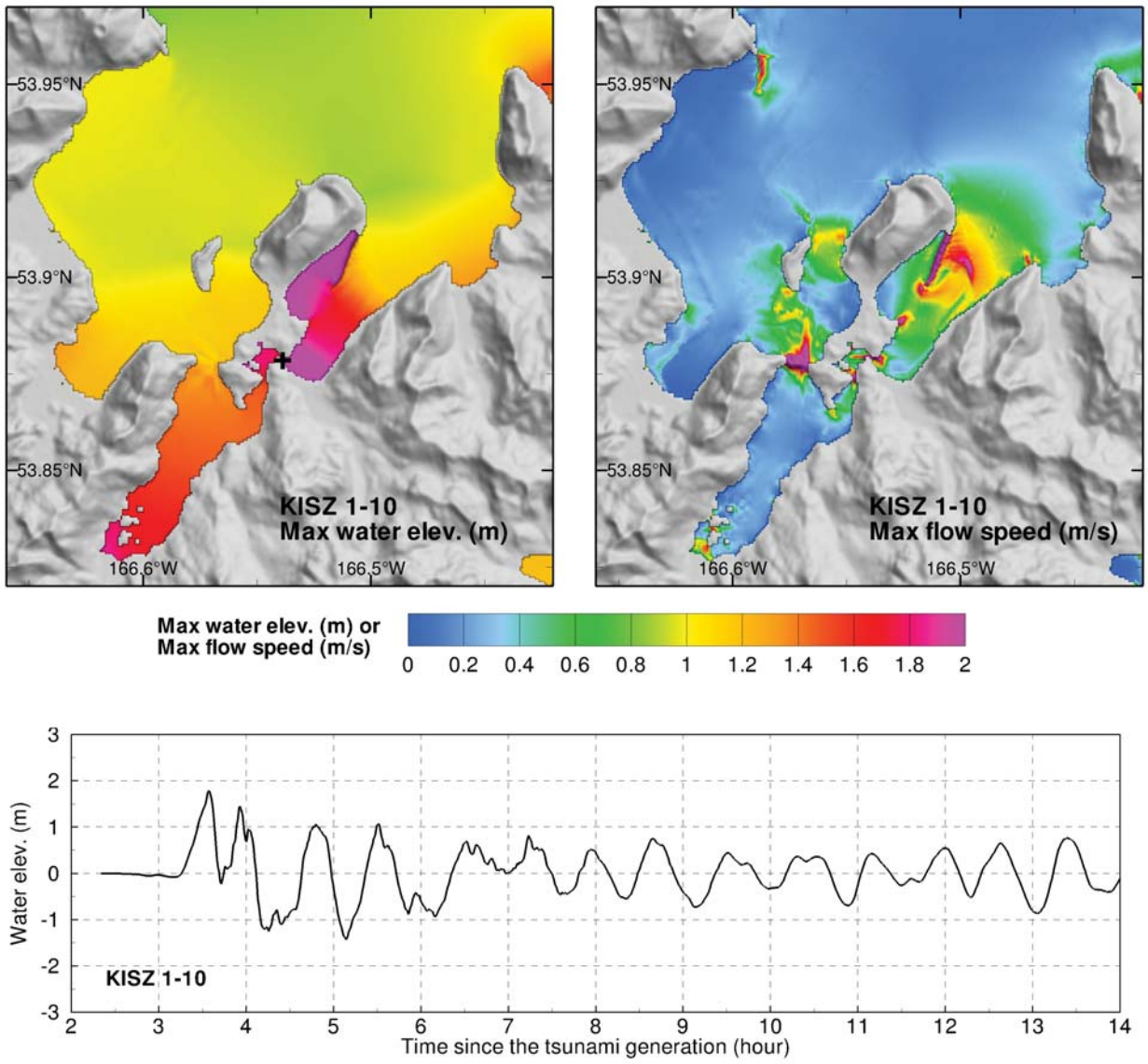

Figure 26: Maximum tsunami amplitude and maximum flow speed computed by the Unalaska forecast model for synthetic scenario KISZ AB 1–10 (Scenario 1 in Table 7): computed maximum water elevation (upper left panel); computed maximum flow speed (upper right panel); and computed time series at tide gauge (lower panel).

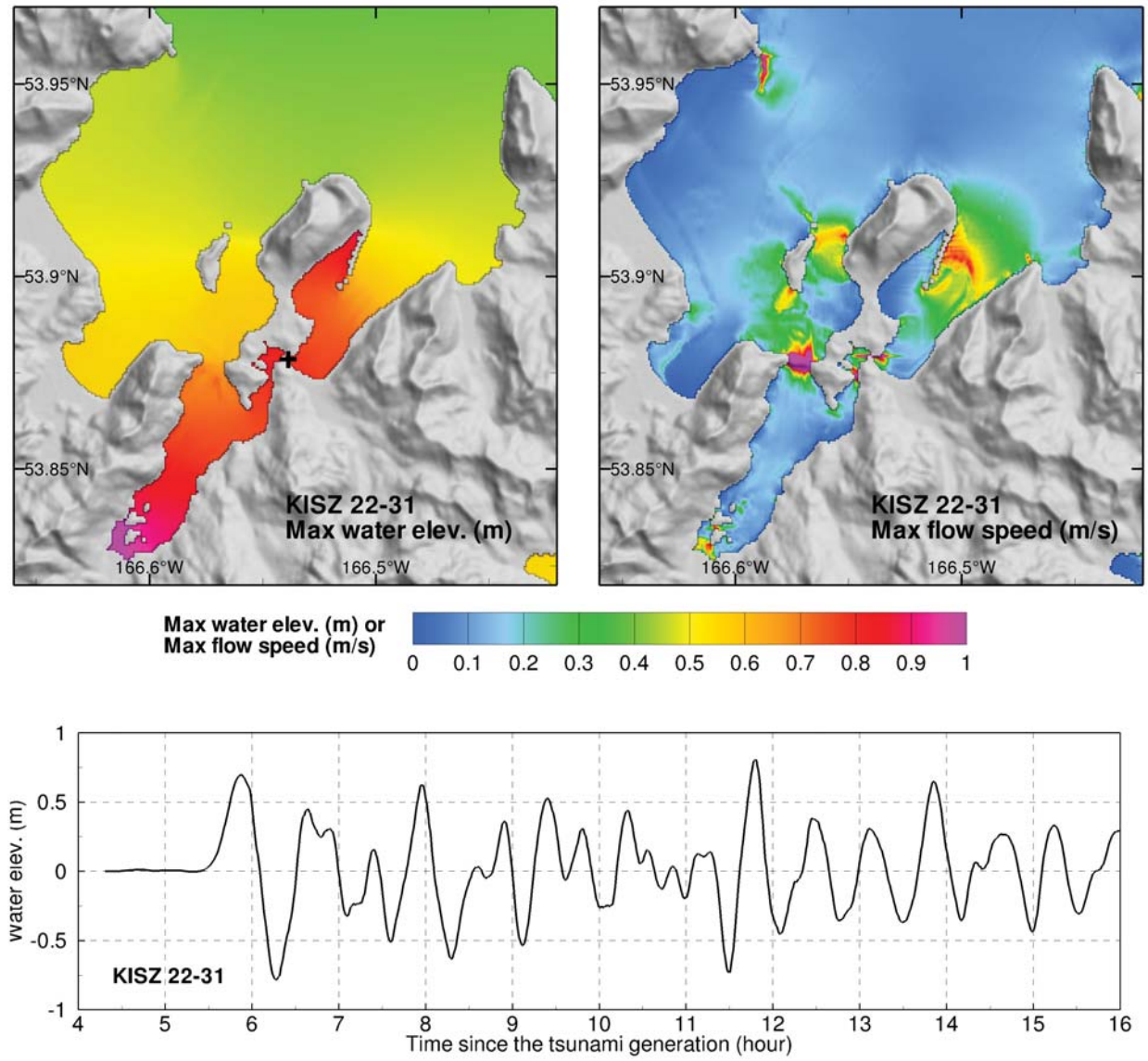

Figure 27: Maximum tsunami amplitude and maximum flow speed computed by the Unalaska forecast model for synthetic scenario KISZ AB 22–31 (Scenario 2 in Table 7): computed maximum water elevation (upper left panel); computed maximum flow speed (upper right panel); and computed time series at tide gauge (lower panel).

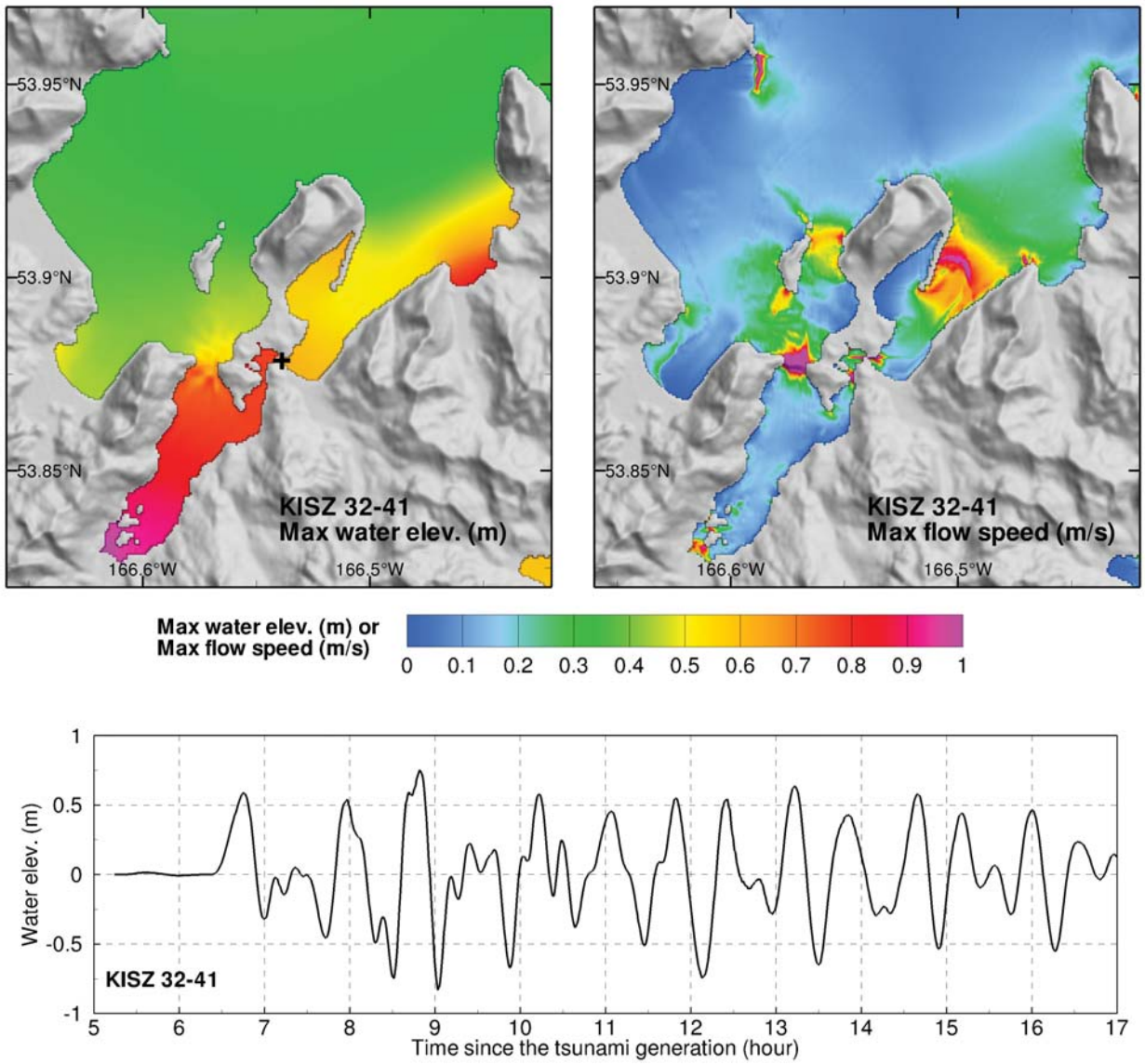

Figure 28: Maximum tsunami amplitude and maximum flow speed computed by the Unalaska forecast model for synthetic scenario KISZ AB 32–41 (Scenario 3 in Table 7): computed maximum water elevation (upper left panel); computed maximum flow speed (upper right panel); and computed time series at tide gauge (lower panel).

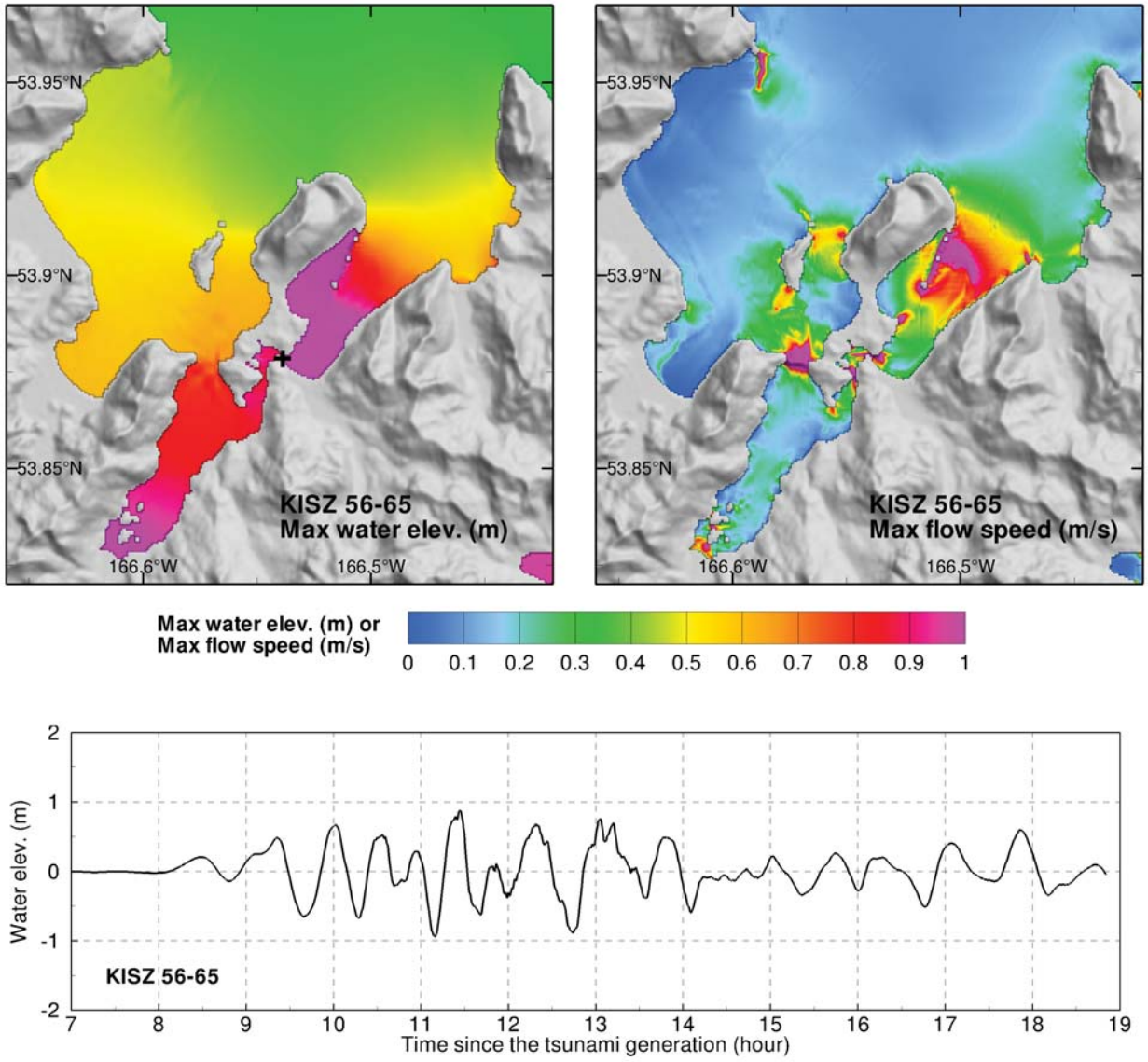

Figure 29: Maximum tsunami amplitude and maximum flow speed computed by the Unalaska forecast model for synthetic scenario KISZ AB 56–65 (Scenario 4 in Table 7): computed maximum water elevation (upper left panel); computed maximum flow speed (upper right panel); and computed time series at tide gauge (lower panel).

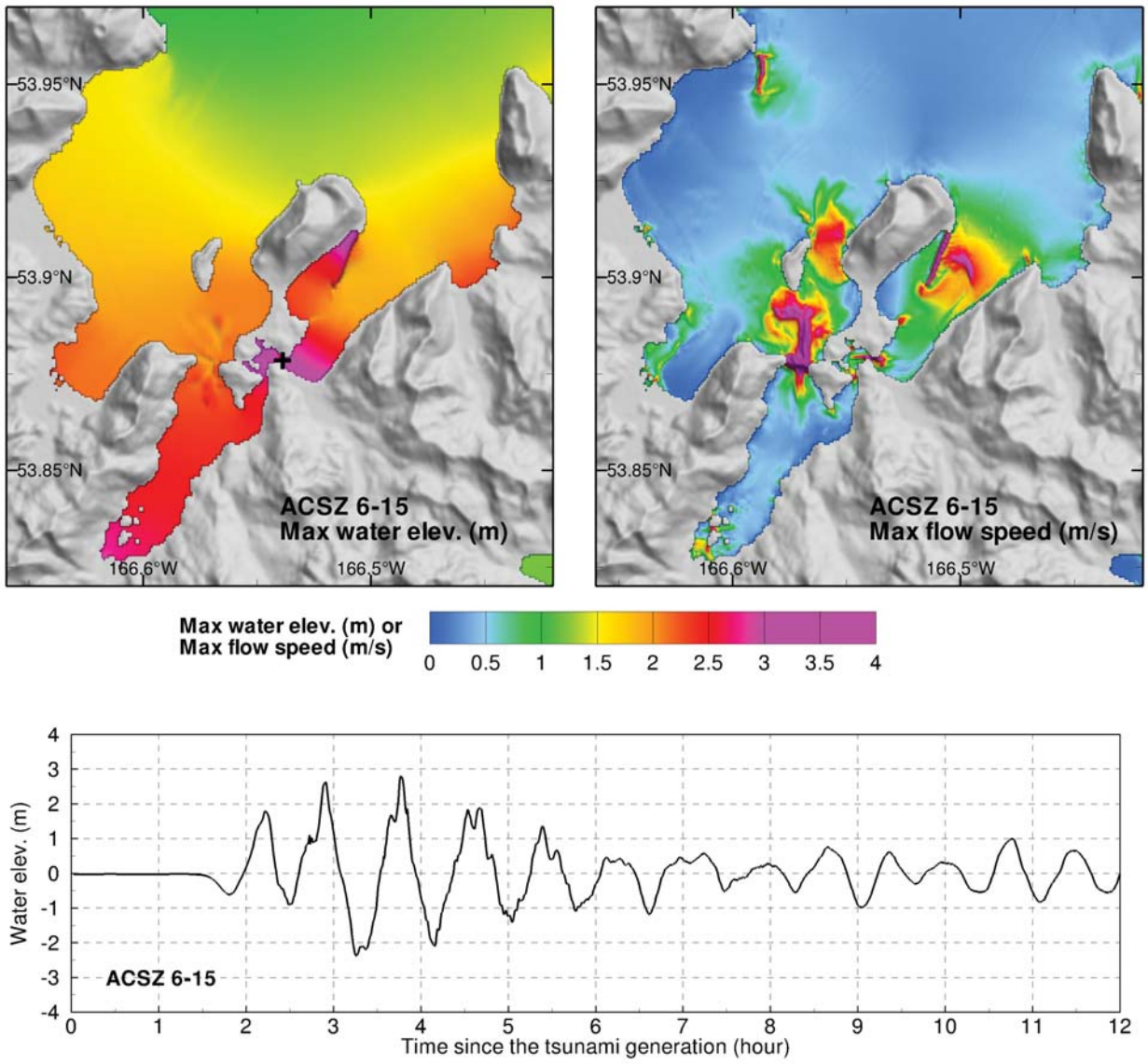

Figure 30: Maximum tsunami amplitude and maximum flow speed computed by the Unalaska forecast model for synthetic scenario ACSZ AB 6–15 (Scenario 5 in Table 7): computed maximum water elevation (upper left panel); computed maximum flow speed (upper right panel); and computed time series at tide gauge (lower panel).

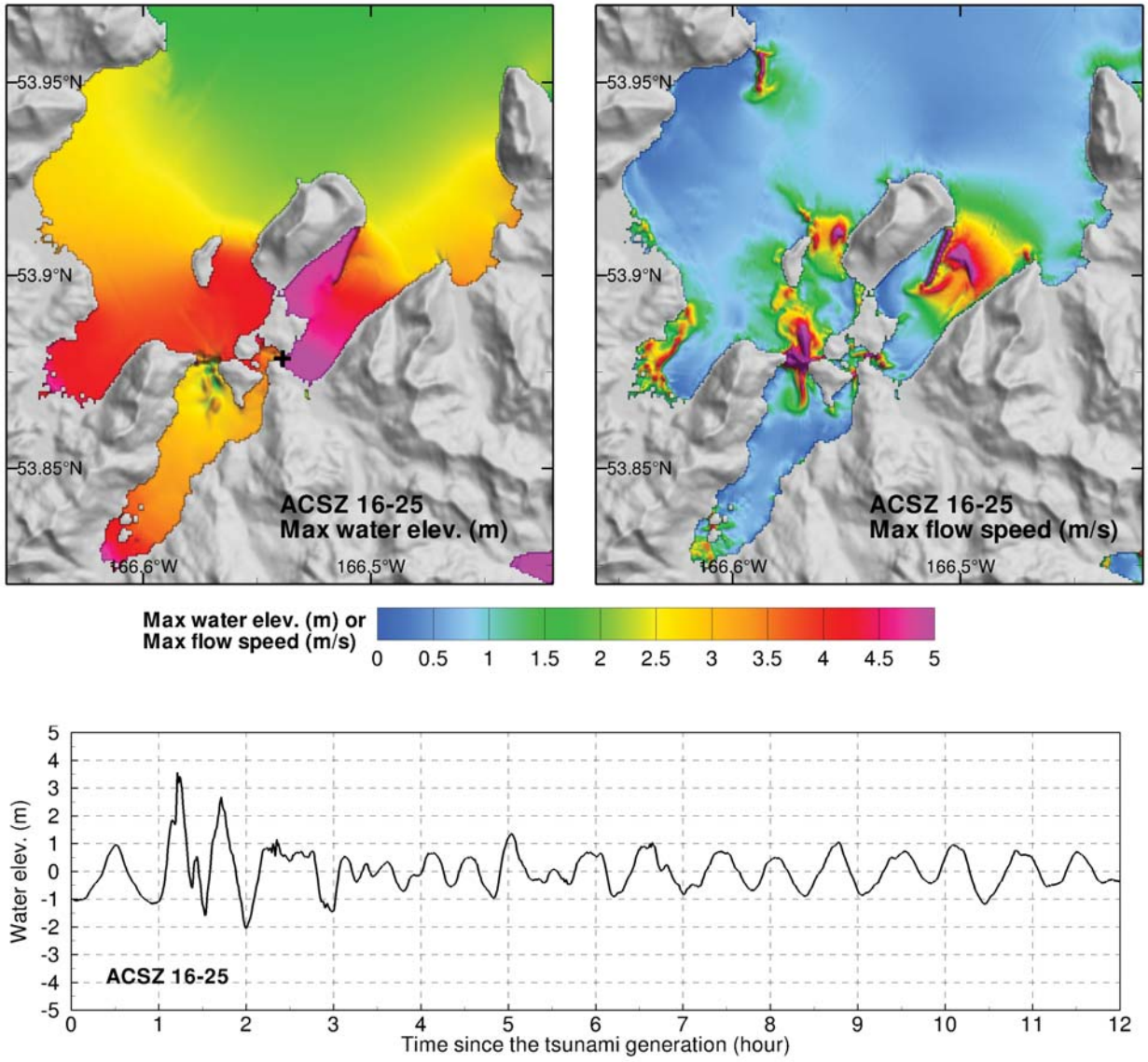

Figure 31: Maximum tsunami amplitude and maximum flow speed computed by the Unalaska forecast model for synthetic scenario ACSZ AB 16–25 (Scenario 6 in Table 7): computed maximum water elevation (upper left panel); computed maximum flow speed (upper right panel); and computed time series at tide gauge (lower panel).

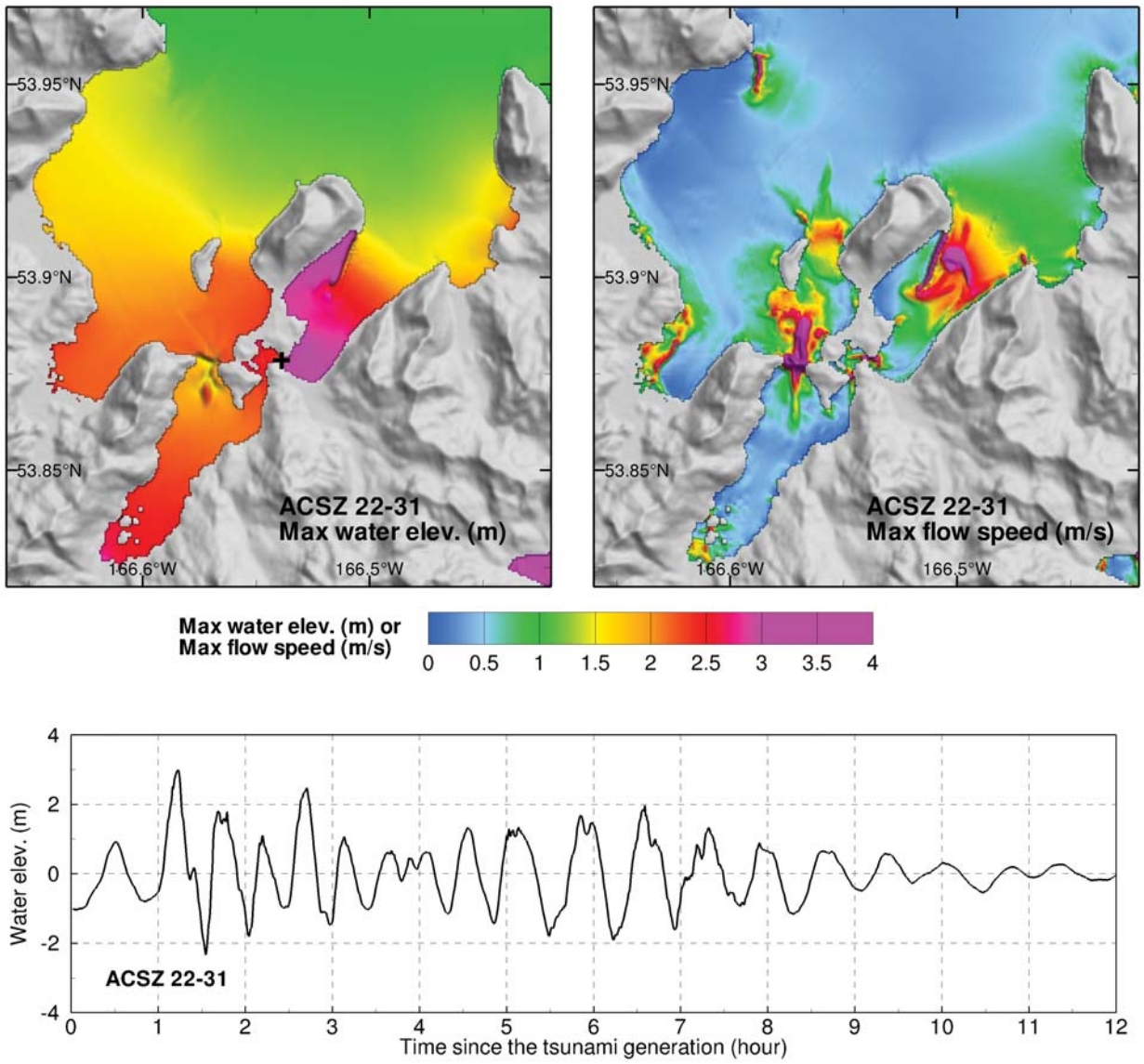

Figure 32: Maximum tsunami amplitude and maximum flow speed computed by the Unalaska forecast model for synthetic scenario ACSZ AB 22–31 (Scenario 7 in Table 7): computed maximum water elevation (upper left panel); computed maximum flow speed (upper right panel); and computed time series at tide gauge (lower panel).

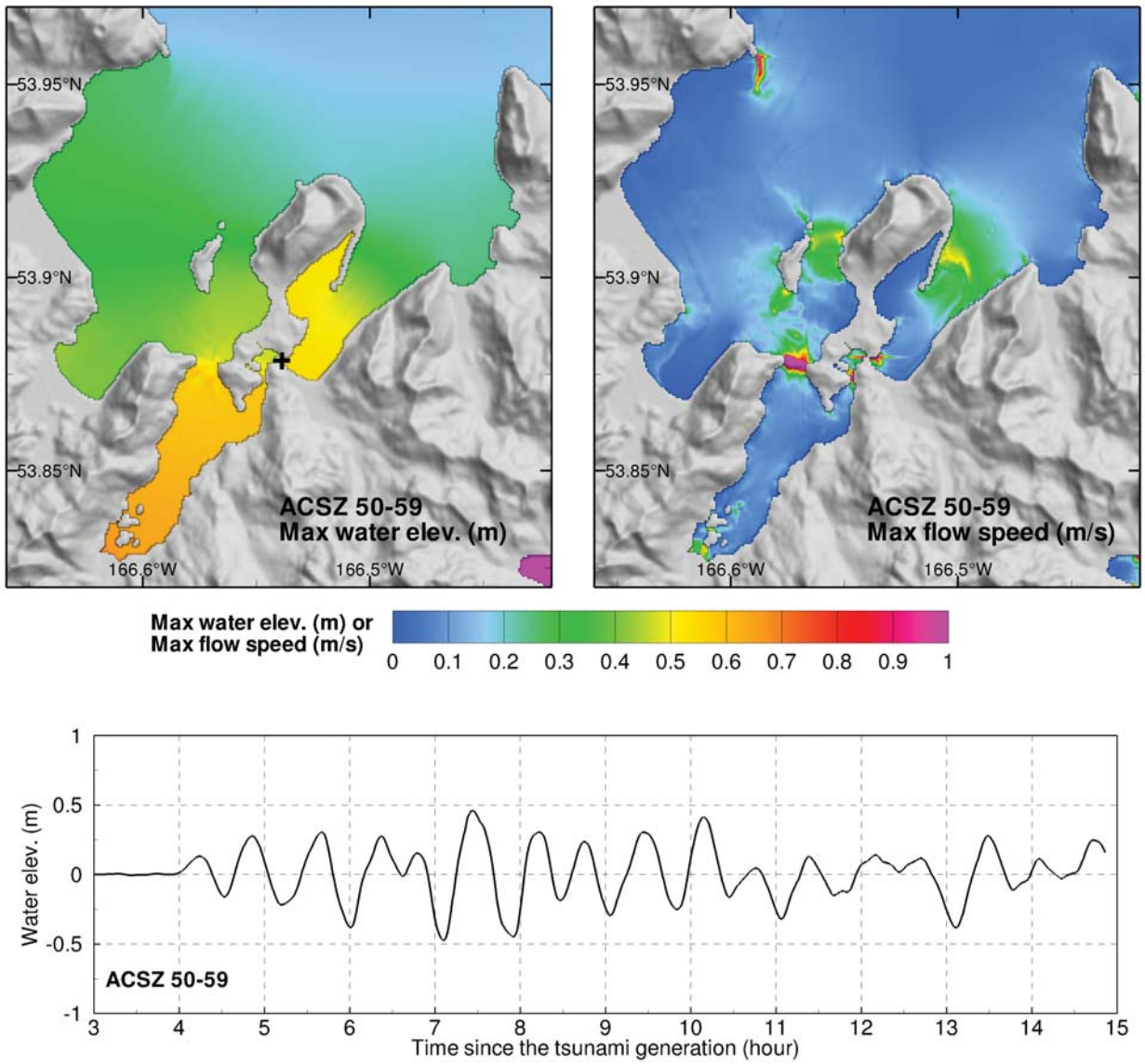

Figure 33: Maximum tsunami amplitude and maximum flow speed computed by the Unalaska forecast model for synthetic scenario ACSZ AB 50–59 (Scenario 8 in Table 7): computed maximum water elevation (upper left panel); computed maximum flow speed (upper right panel); and computed time series at tide gauge (lower panel).

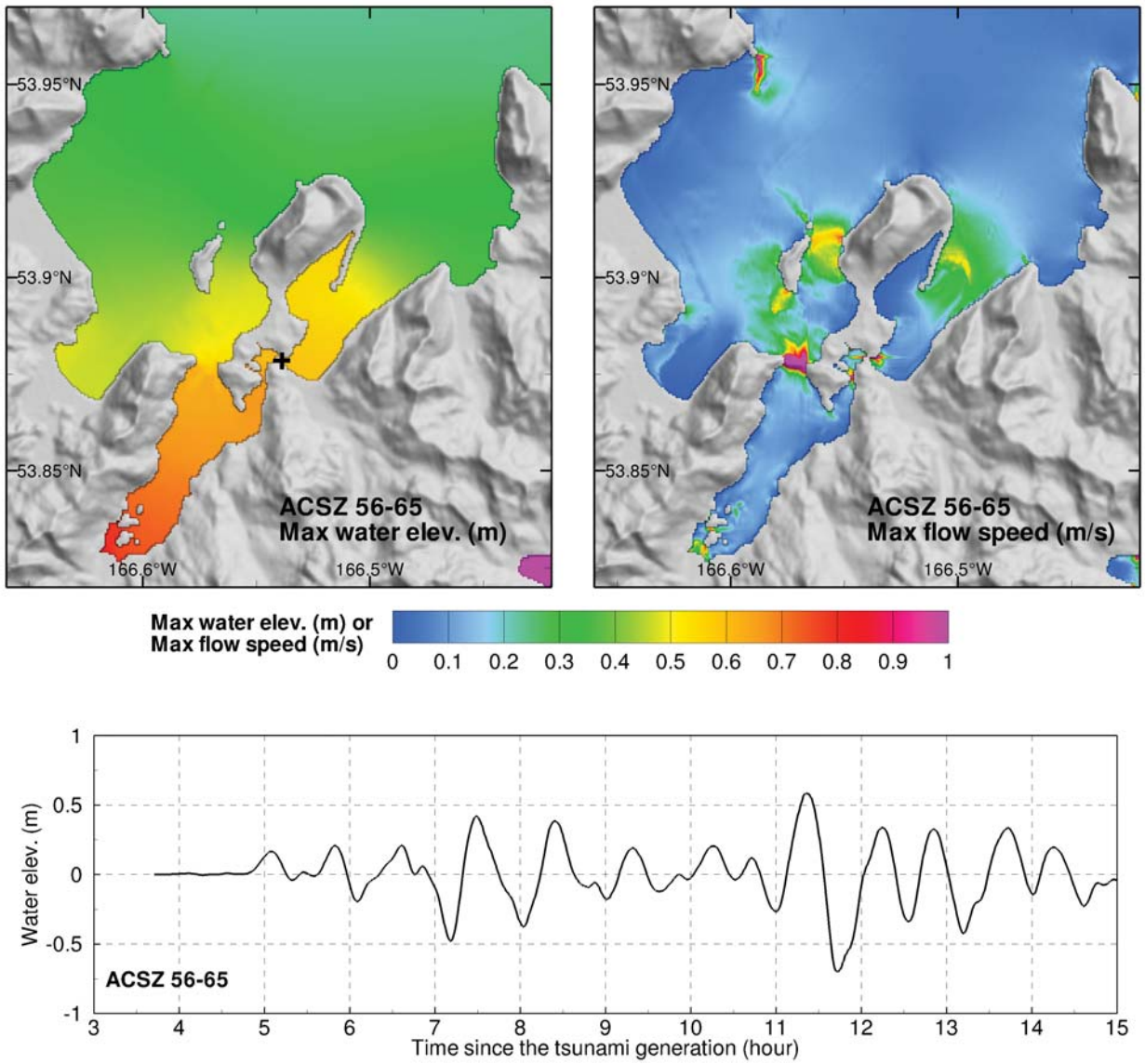

Figure 34: Maximum tsunami amplitude and maximum flow speed computed by the Unalaska forecast model for synthetic scenario ACSZ AB 56–65 (Scenario 9 in Table 7): computed maximum water elevation (upper left panel); computed maximum flow speed (upper right panel); and computed time series at tide gauge (lower panel).

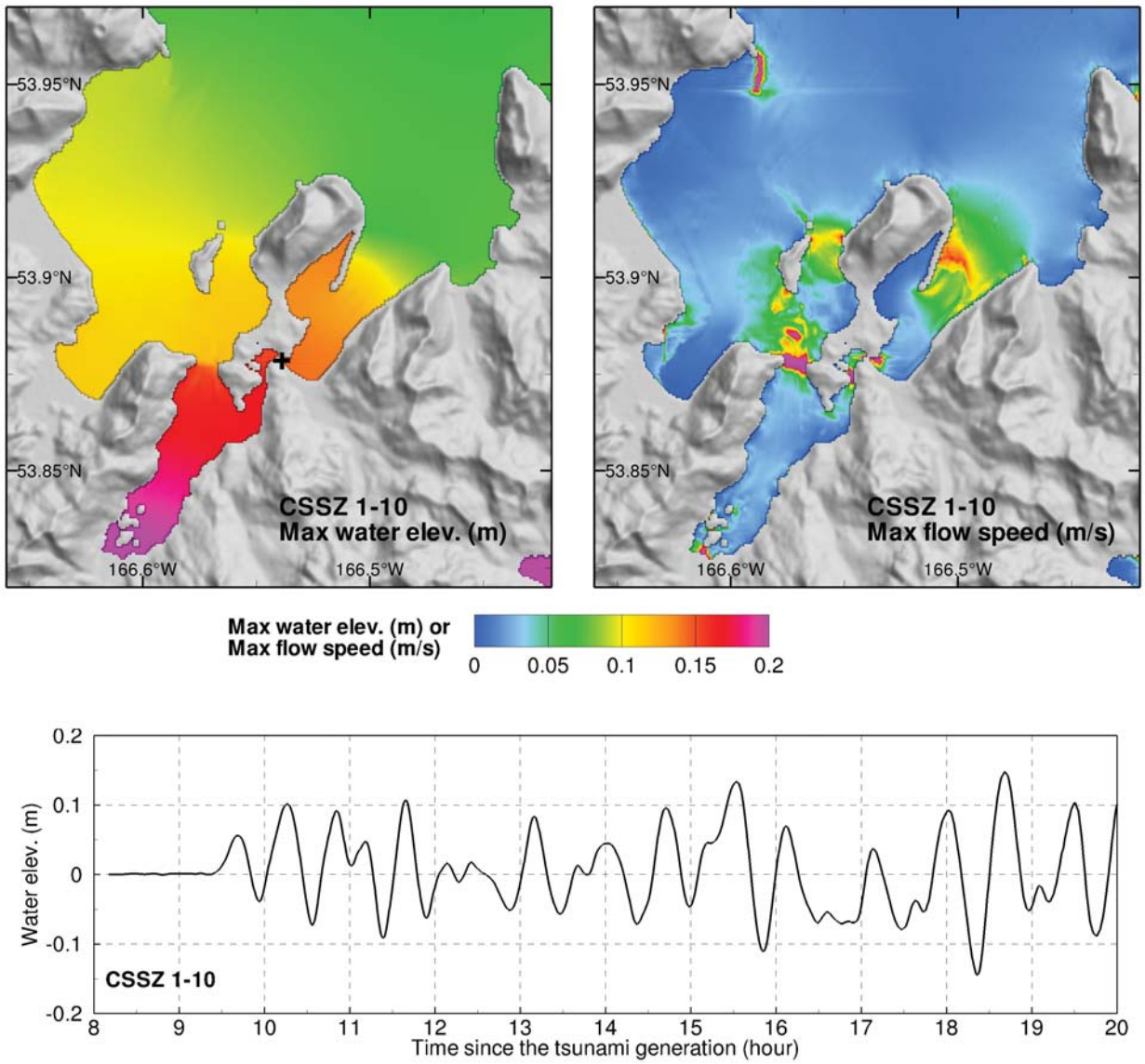

Figure 35: Maximum tsunami amplitude and maximum flow speed computed by the Unalaska forecast model for synthetic scenario CSSZ AB 1–10 (Scenario 10 in Table 7): computed maximum water elevation (upper left panel); computed maximum flow speed (upper right panel); and computed time series at tide gauge (lower panel).

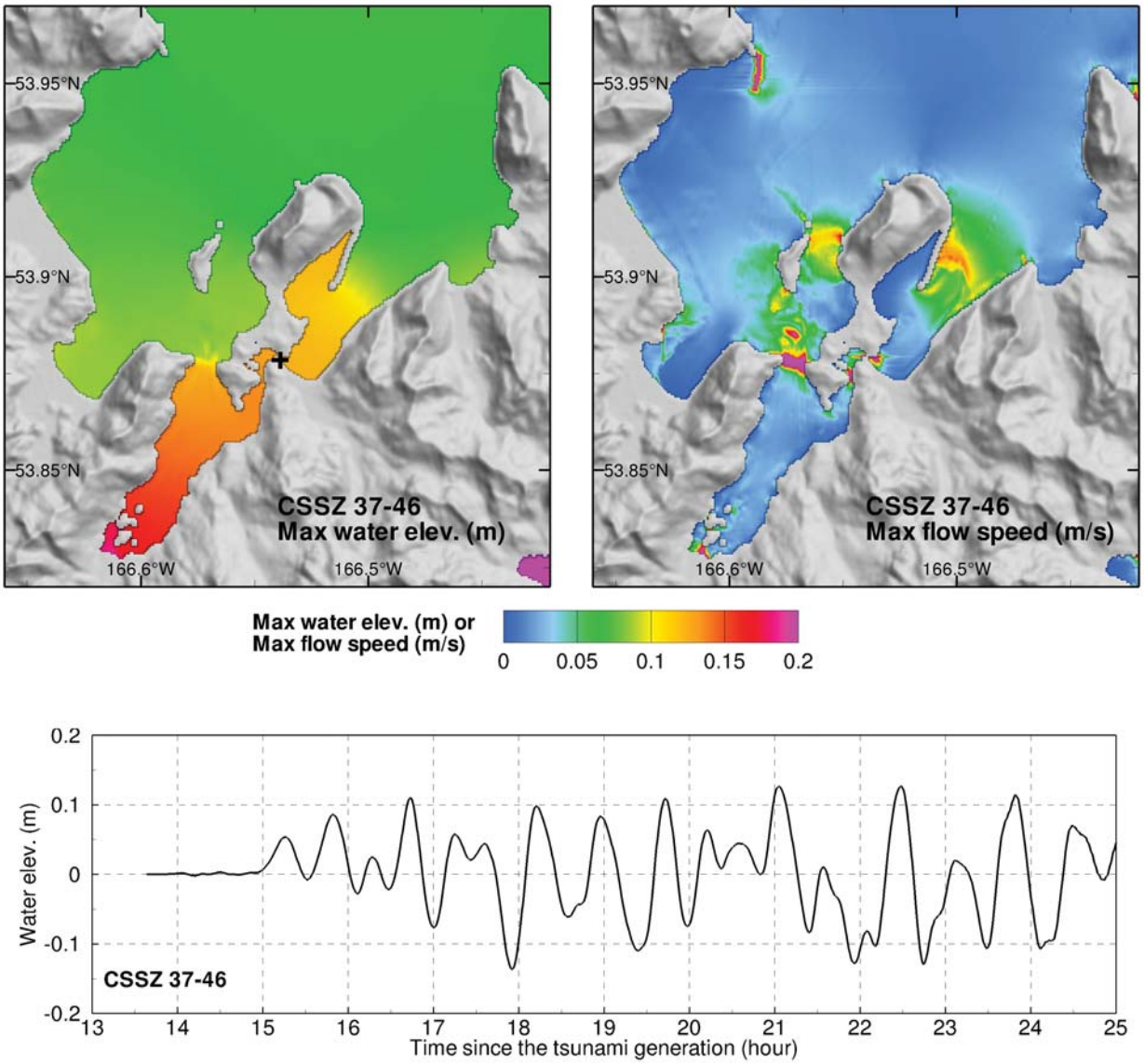

Figure 36: Maximum tsunami amplitude and maximum flow speed computed by the Unalaska forecast model for synthetic scenario CSSZ AB 37–46 (Scenario 11 in Table 7): computed maximum water elevation (upper left panel); computed maximum flow speed (upper right panel); and computed time series at tide gauge (lower panel).

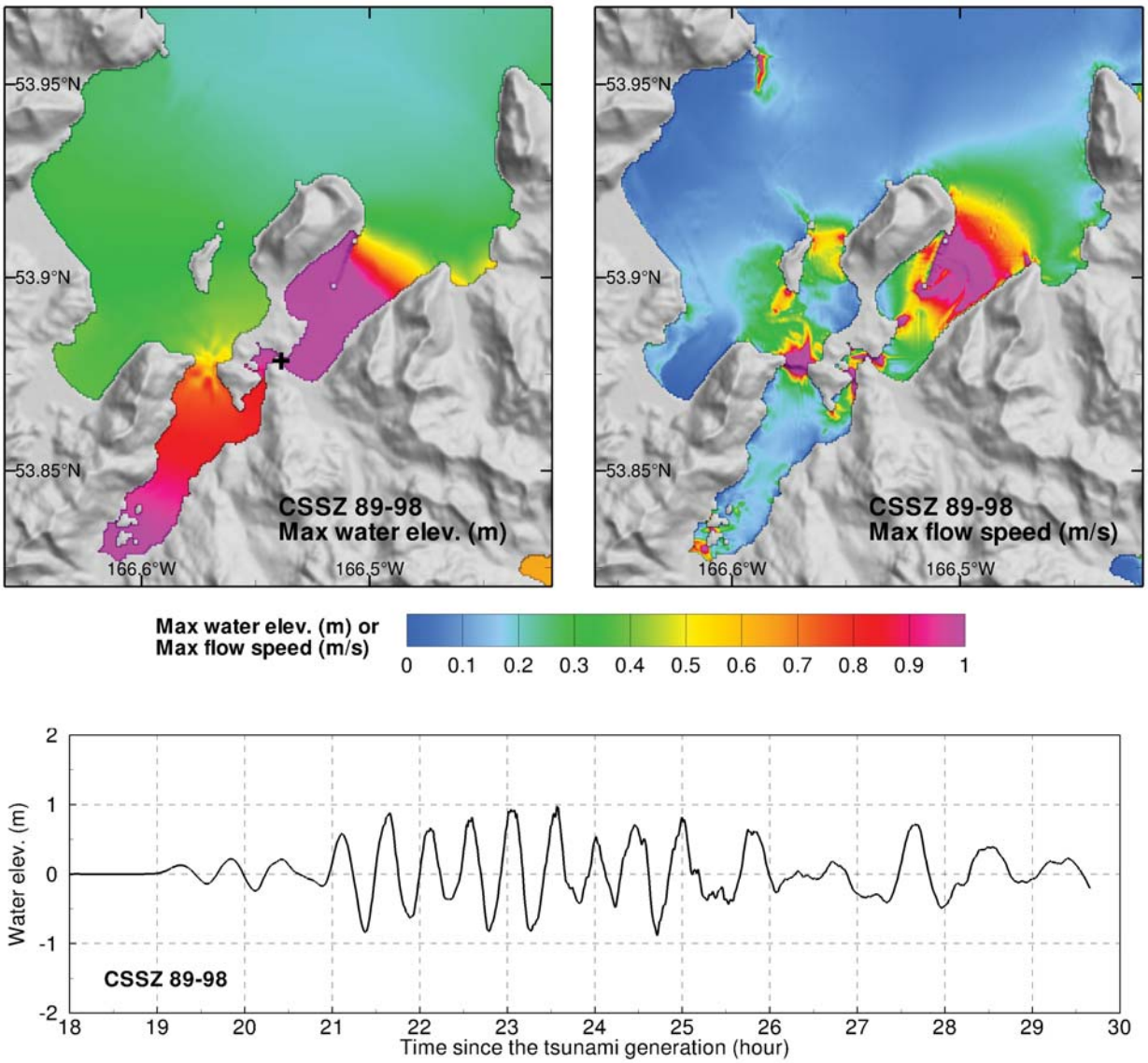

Figure 37: Maximum tsunami amplitude and maximum flow speed computed by the Unalaska forecast model for synthetic scenario CSSZ AB 89–98 (Scenario 12 in Table 7): computed maximum water elevation (upper left panel); computed maximum flow speed (upper right panel); and computed time series at tide gauge (lower panel).

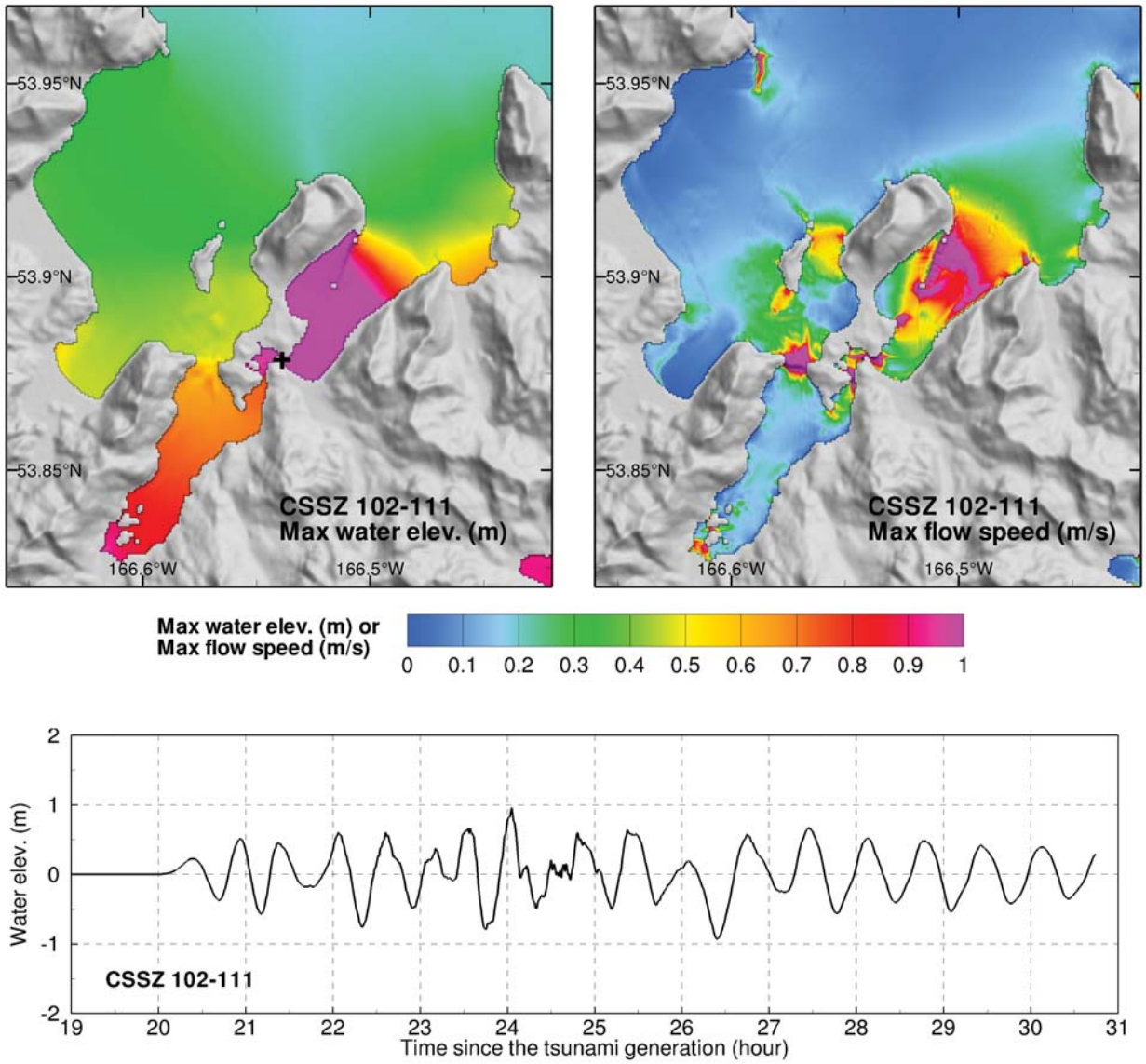

Figure 38: Maximum tsunami amplitude and maximum flow speed computed by the Unalaska forecast model for synthetic scenario CSSZ AB 102–111 (Scenario 13 in Table 7): computed maximum water elevation (upper left panel); computed maximum flow speed (upper right panel); and computed time series at tide gauge (lower panel).

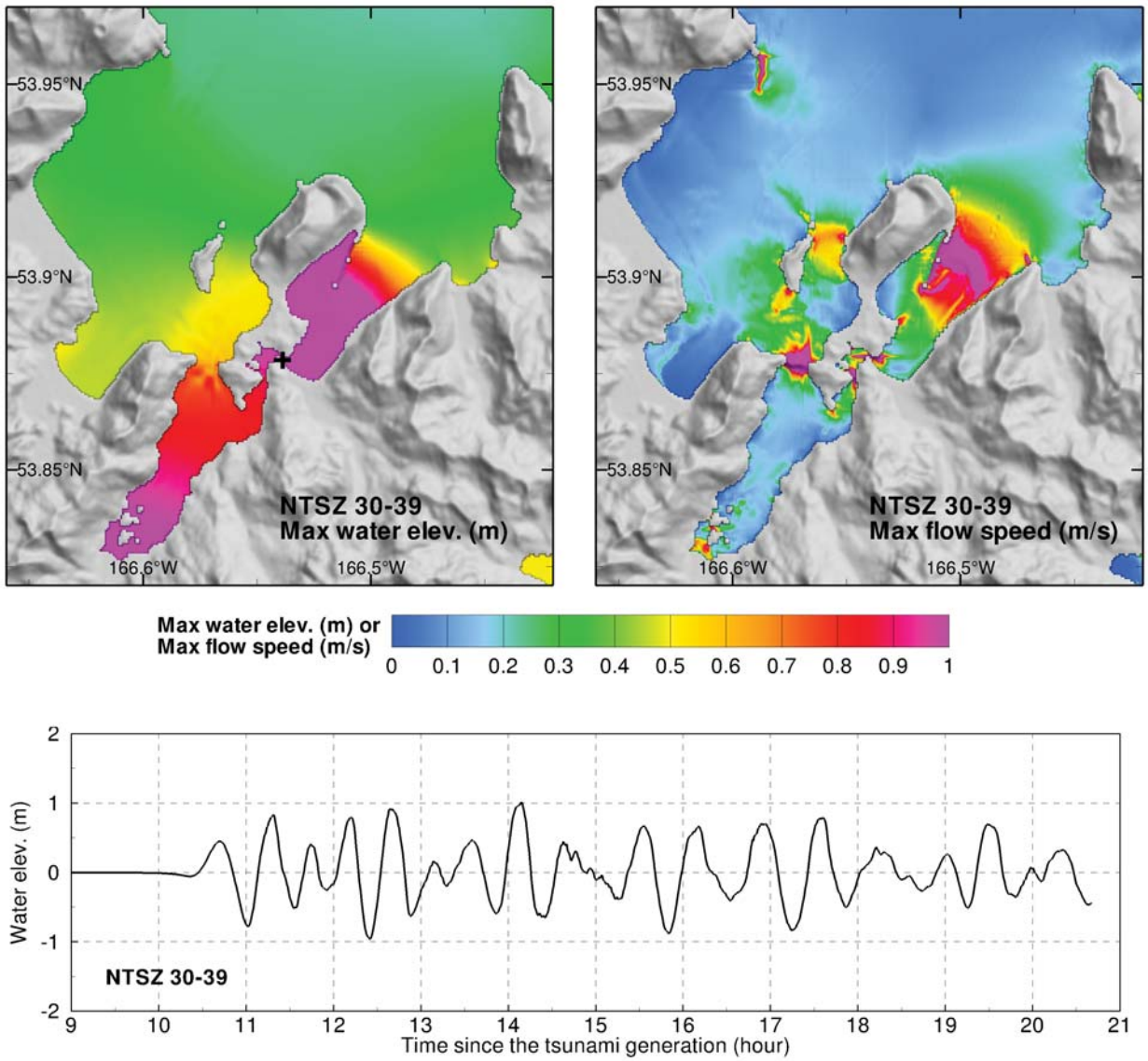

Figure 39: Maximum tsunami amplitude and maximum flow speed computed by the Unalaska forecast model for synthetic scenario NTSZ AB 30–39 (Scenario 14 in Table 7): computed maximum water elevation (upper left panel); computed maximum flow speed (upper right panel); and computed time series at tide gauge (lower panel).

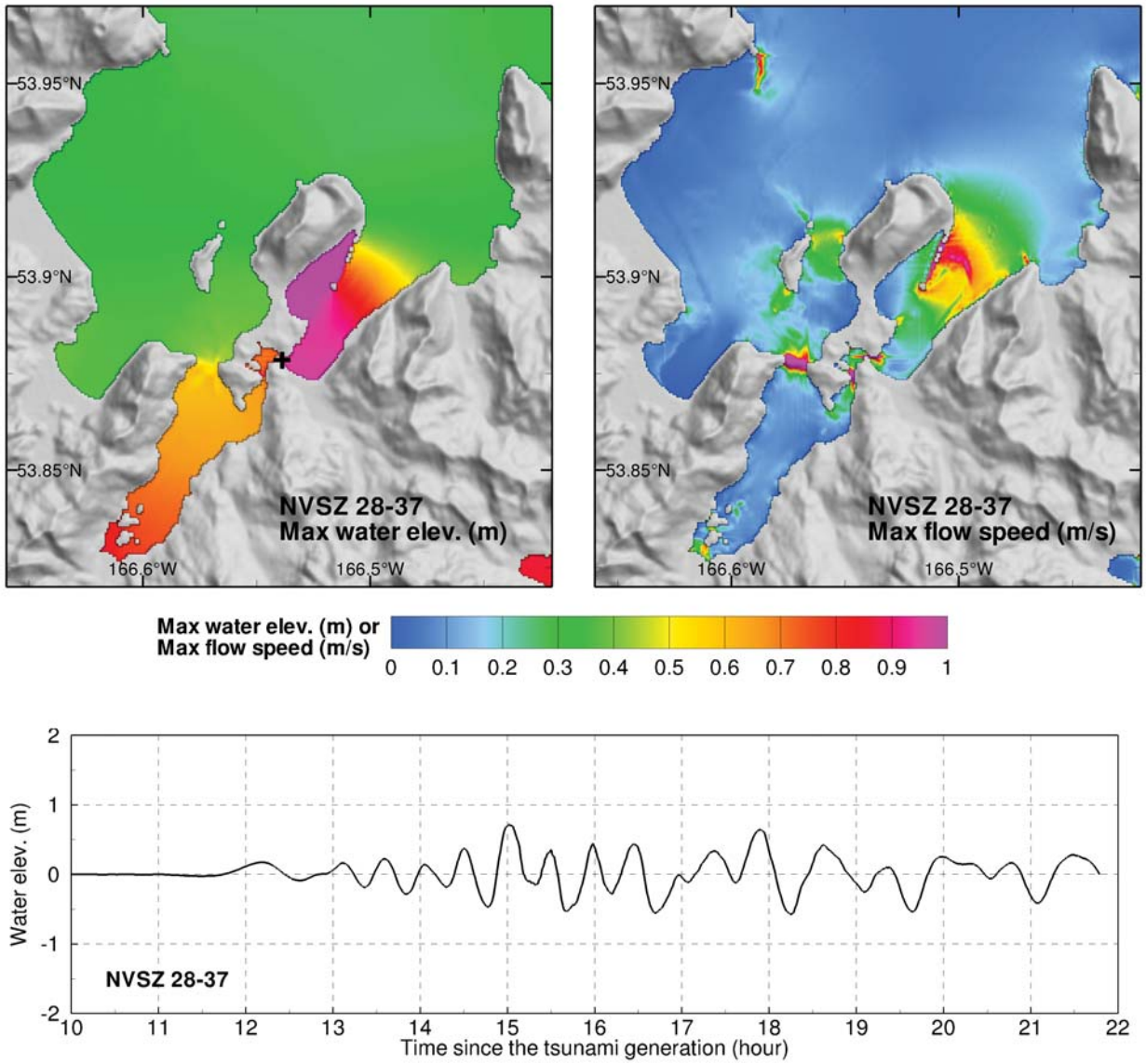

Figure 40: Maximum tsunami amplitude and maximum flow speed computed by the Unalaska forecast model for synthetic scenario NVSZ AB 28–37 (Scenario 15 in Table 7): computed maximum water elevation (upper left panel); computed maximum flow speed (upper right panel); and computed time series at tide gauge (lower panel).

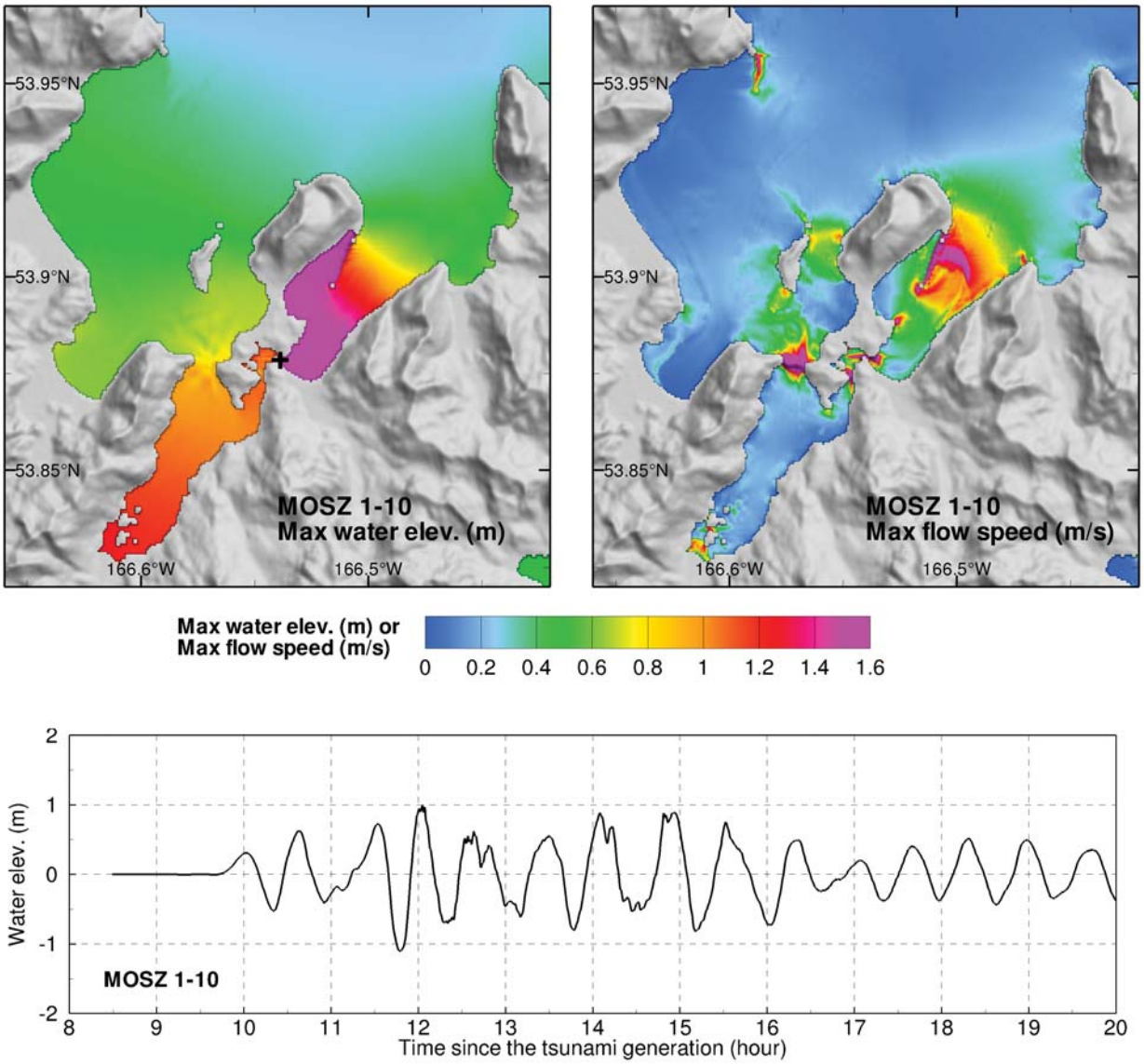

Figure 41: Maximum tsunami amplitude and maximum flow speed computed by the Unalaska forecast model for synthetic scenario MOSZ AB 1–10 (Scenario 16 in Table 7): computed maximum water elevation (upper left panel); computed maximum flow speed (upper right panel); and computed time series at tide gauge (lower panel).

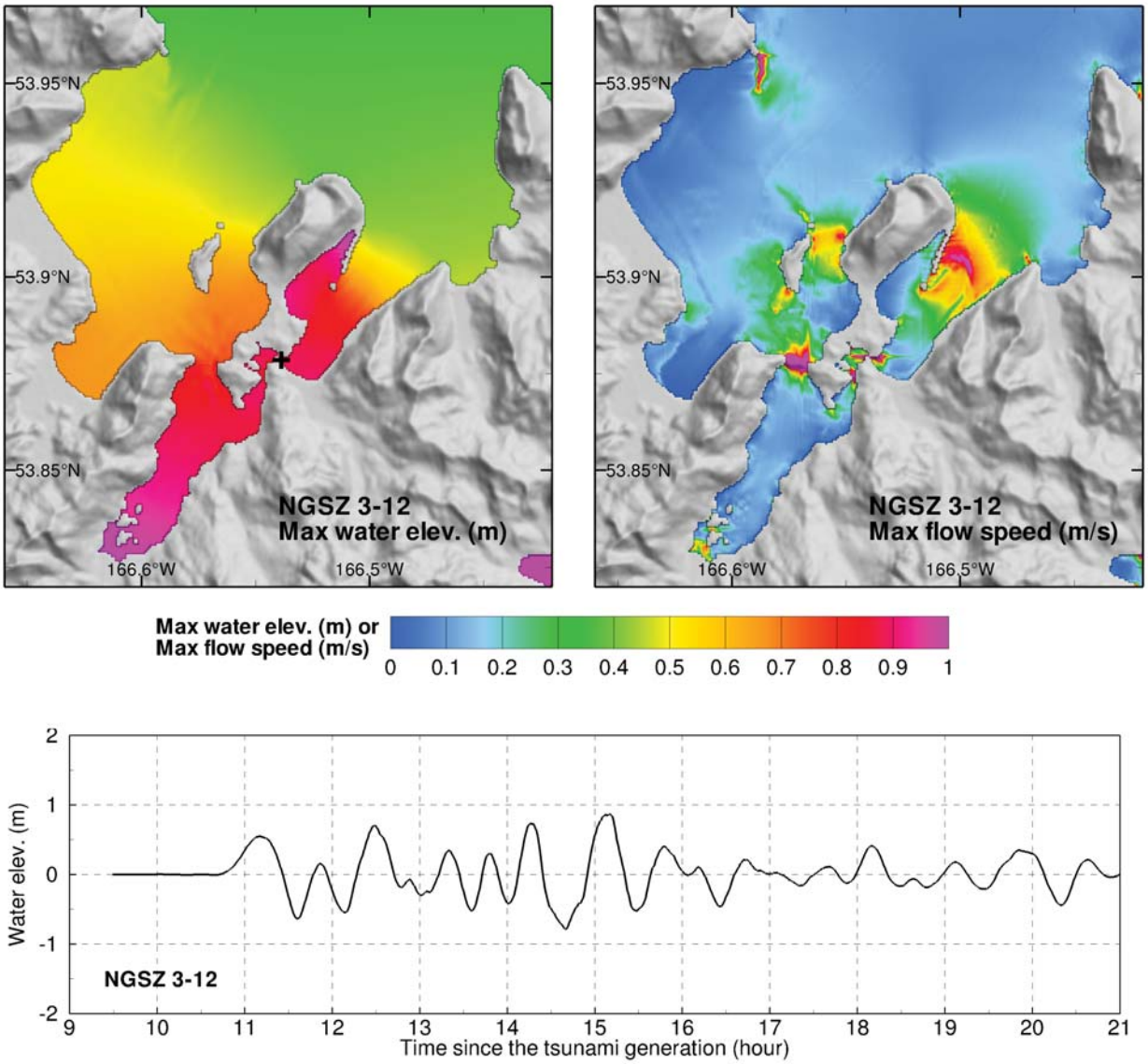

Figure 42: Maximum tsunami amplitude and maximum flow speed computed by the Unalaska forecast model for synthetic scenario NGSZ AB 3–12 (Scenario 17 in Table 7): computed maximum water elevation (upper left panel); computed maximum flow speed (upper right panel); and computed time series at tide gauge (lower panel).

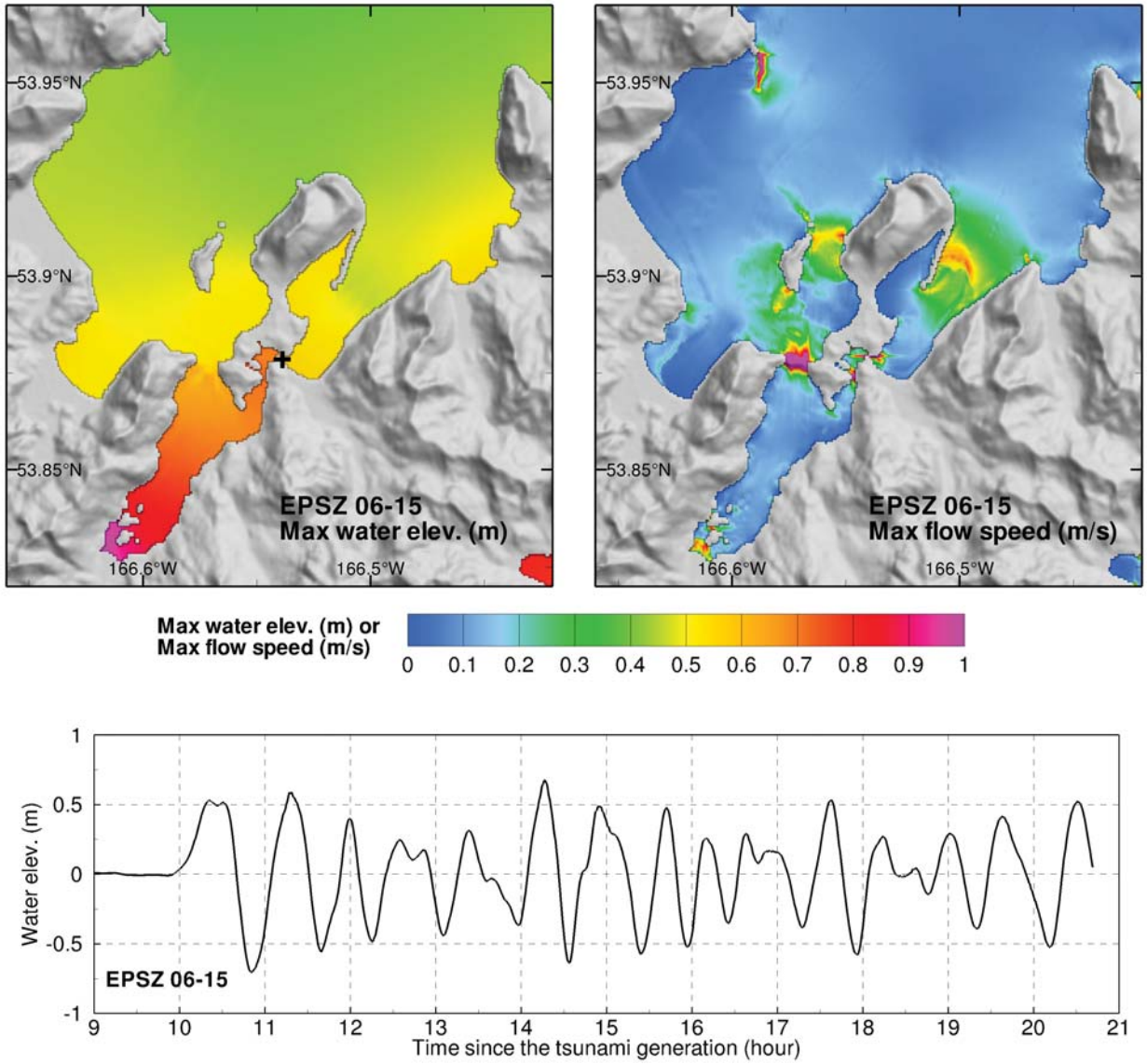

Figure 43: Maximum tsunami amplitude and maximum flow speed computed by the Unalaska forecast model for synthetic scenario EPSZ AB 6–15 (Scenario 18 in Table 7): computed maximum water elevation (upper left panel); computed maximum flow speed (upper right panel); and computed time series at tide gauge (lower panel).

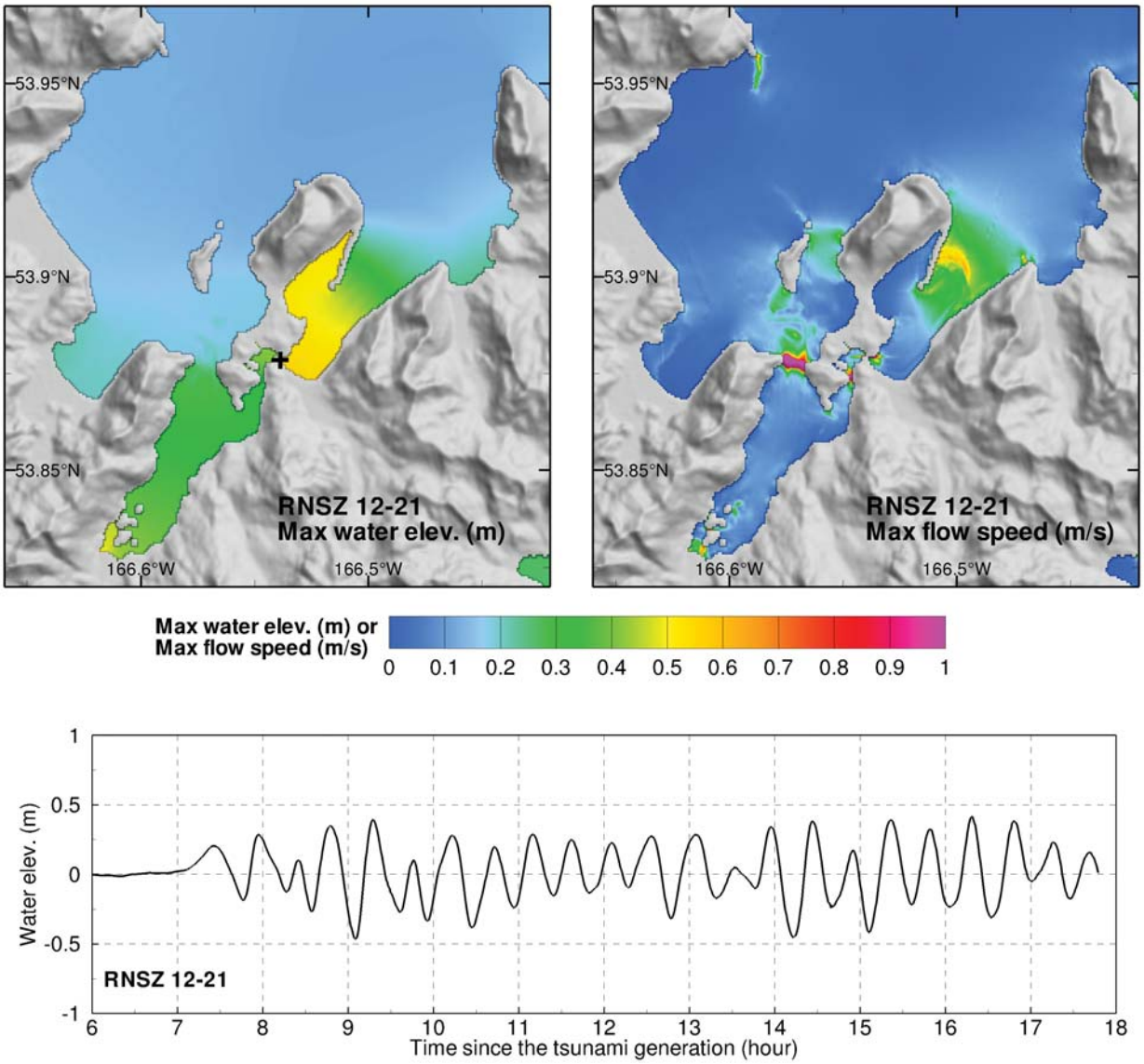

Figure 44: Maximum tsunami amplitude and maximum flow speed computed by the Unalaska forecast model for synthetic scenario RNSZ AB 12–21 (Scenario 19 in Table 7): computed maximum water elevation (upper left panel); computed maximum flow speed (upper right panel); and computed time series at tide gauge (lower panel).

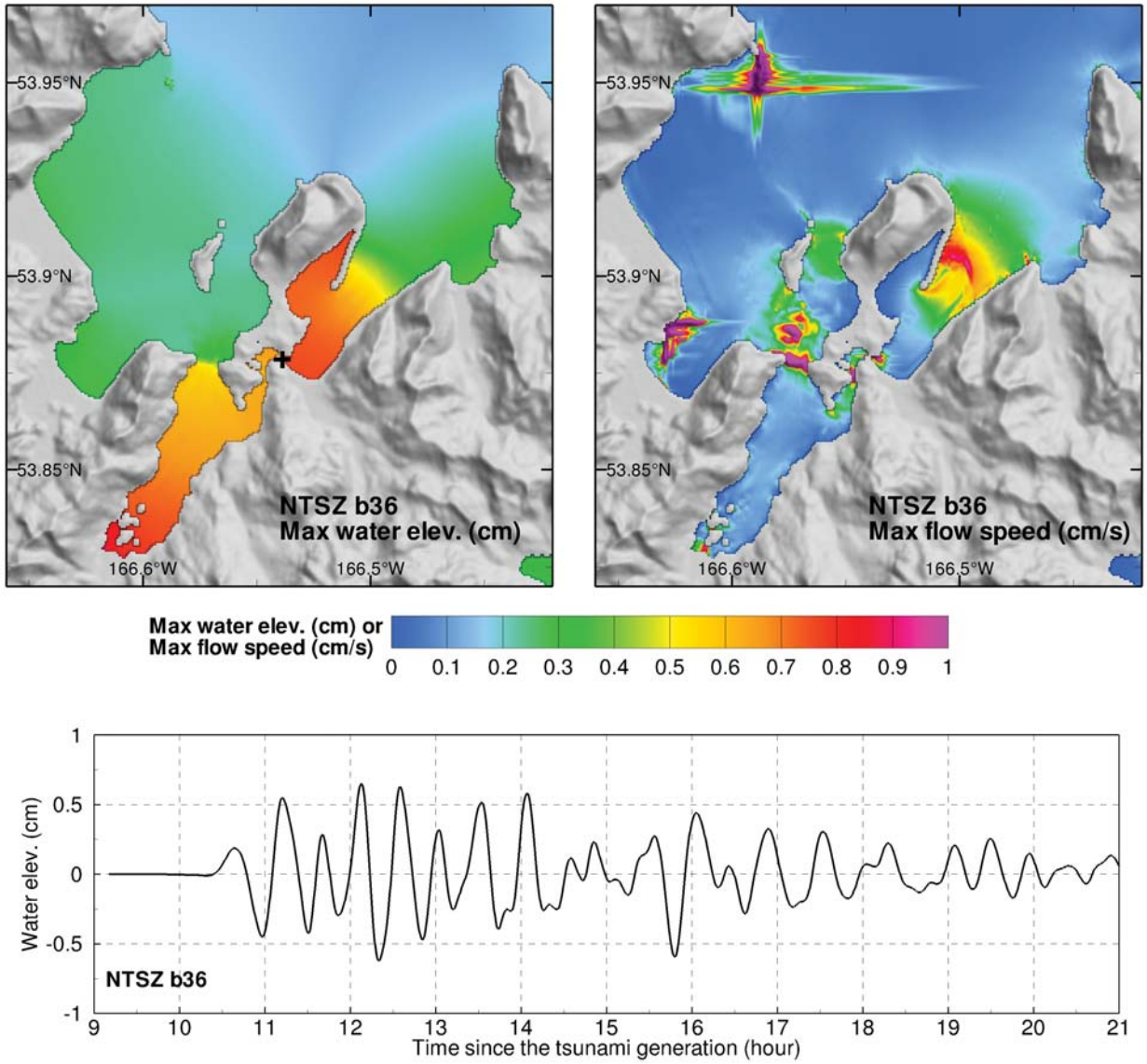

Figure 45: Maximum tsunami amplitude and maximum flow speed computed by the Unalaska forecast model for synthetic scenario NTSZ B 36 (Scenario 20 in Table 7): computed maximum water elevation (upper left panel); computed maximum flow speed (upper right panel); and computed time series at tide gauge (lower panel).

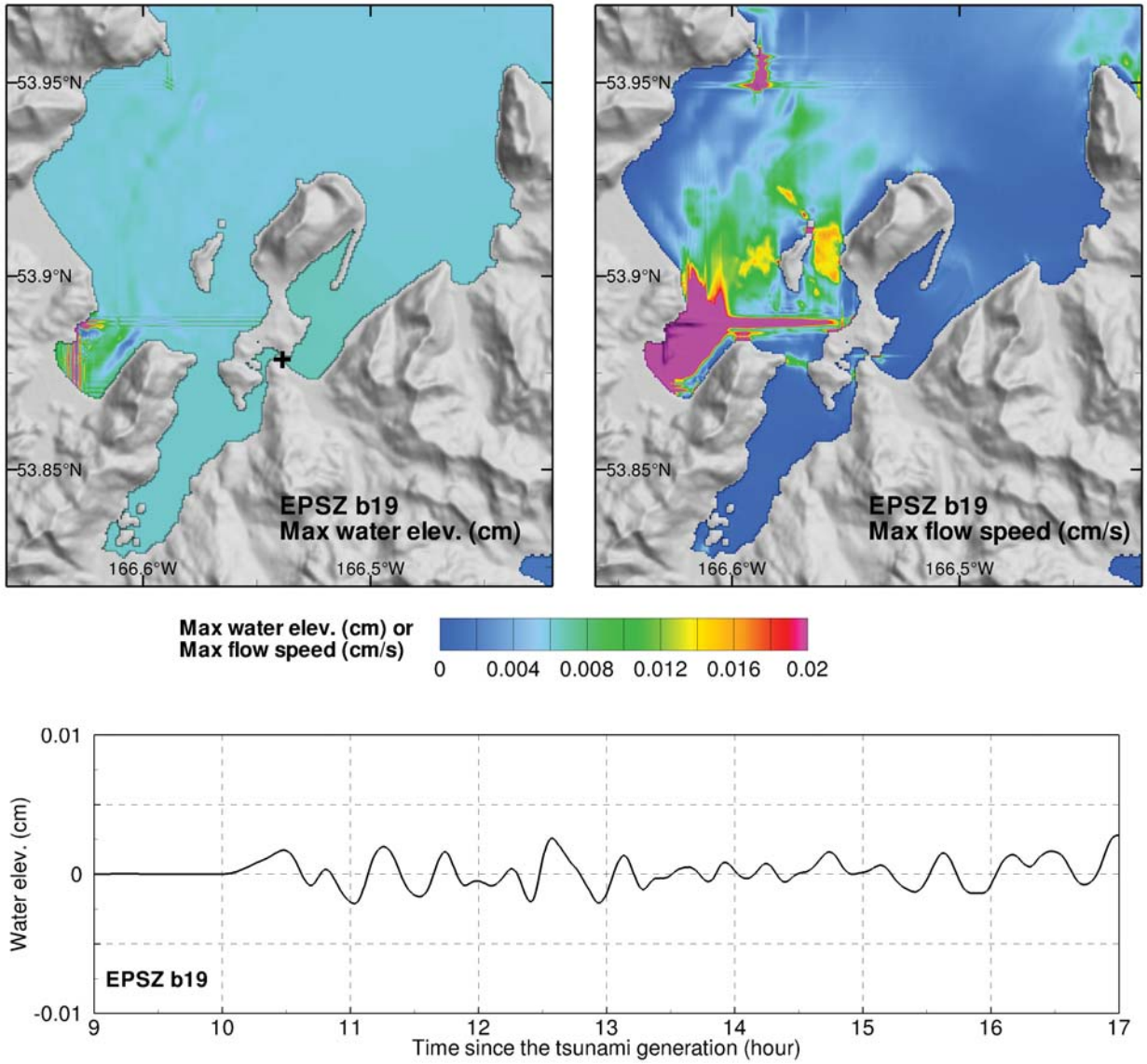

Figure 46: Maximum tsunami amplitude and maximum flow speed computed by the Unalaska forecast model for synthetic scenario EPSZ B 19 (Scenario 21 in Table 7): computed maximum water elevation (upper left panel); computed maximum flow speed (upper right panel); and computed time series at tide gauge (lower panel).

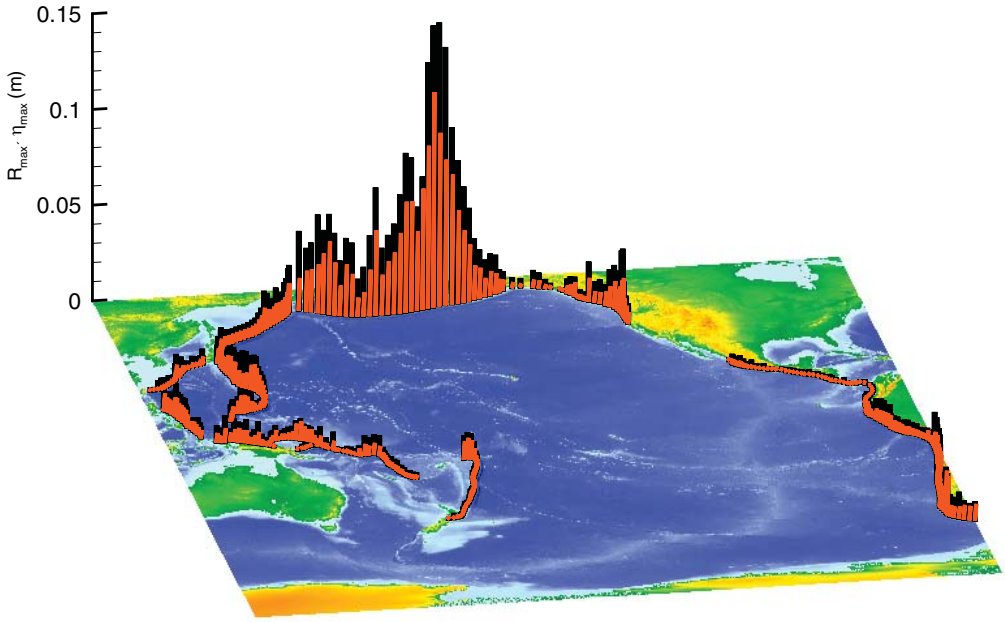

Figure 47: Computed tsunami impact on the Unalaska coastline due to potential tsunami scenarios of Mw 7.5 using the shore side (row A) unit sources. The black bar indicates the computed maximum runup height in Unalaska and the orange bar indicates the computed maximum wave amplitude at Unalaska tide gauge.

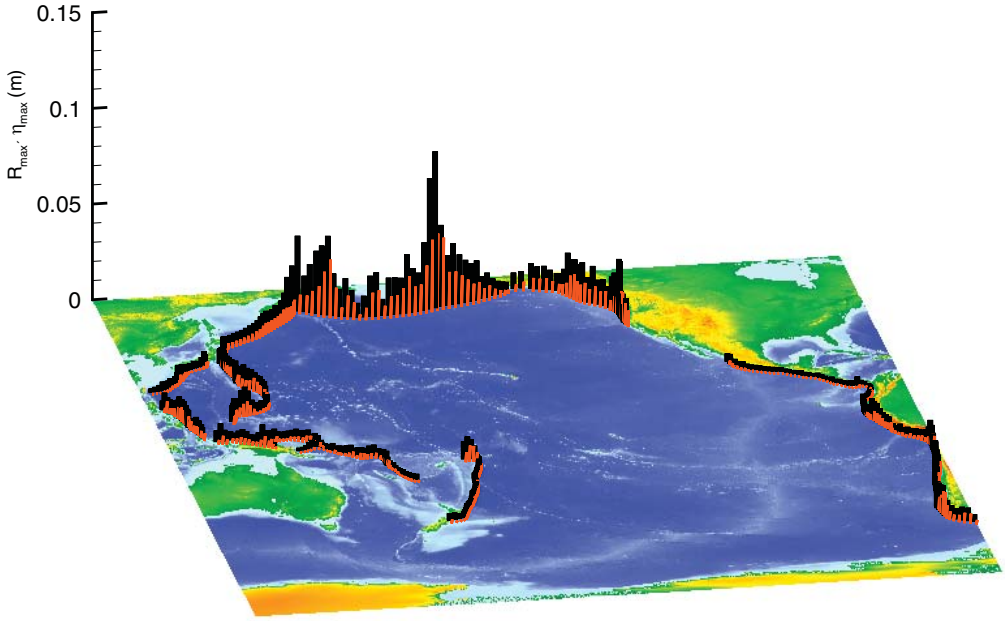

Figure 48: Computed tsunami impact on the Unalaska coastline due to potential tsunami scenarios of Mw 7.5 using the offshore (row B) unit sources. The black bar indicates the computed maximum runup height in Unalaska and the orange bar indicates the computed maximum wave amplitude at Unalaska tide gauge.

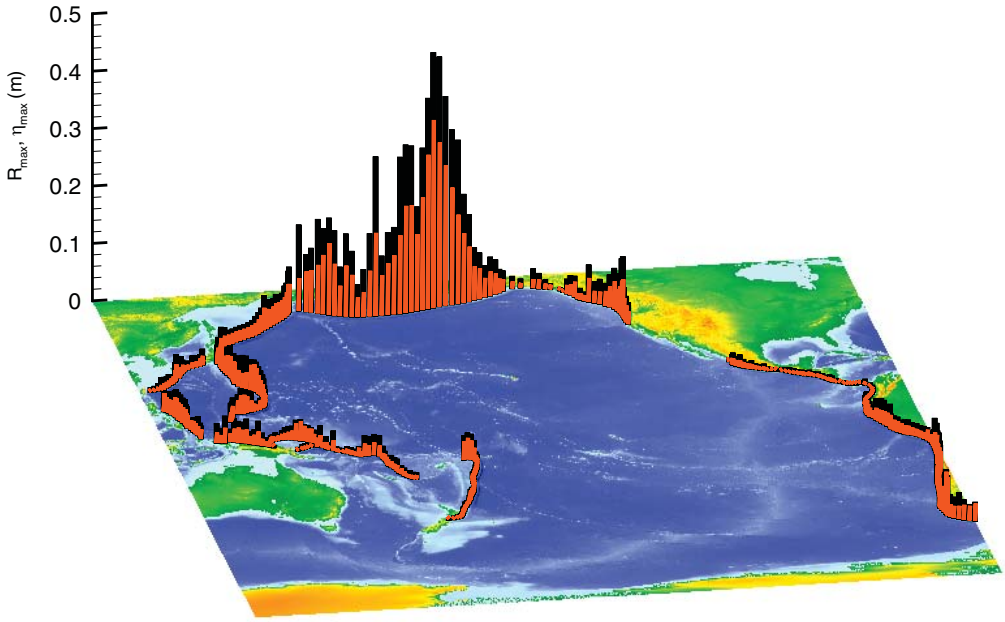

Figure 49: Computed tsunami impact on the Unalaska coastline due to potential tsunami scenarios of Mw 7.8 using the shore side (row A) unit sources. The black bar indicates the computed maximum runup height in Unalaska and the orange bar indicates the computed maximum wave amplitude at Unalaska tide gauge.

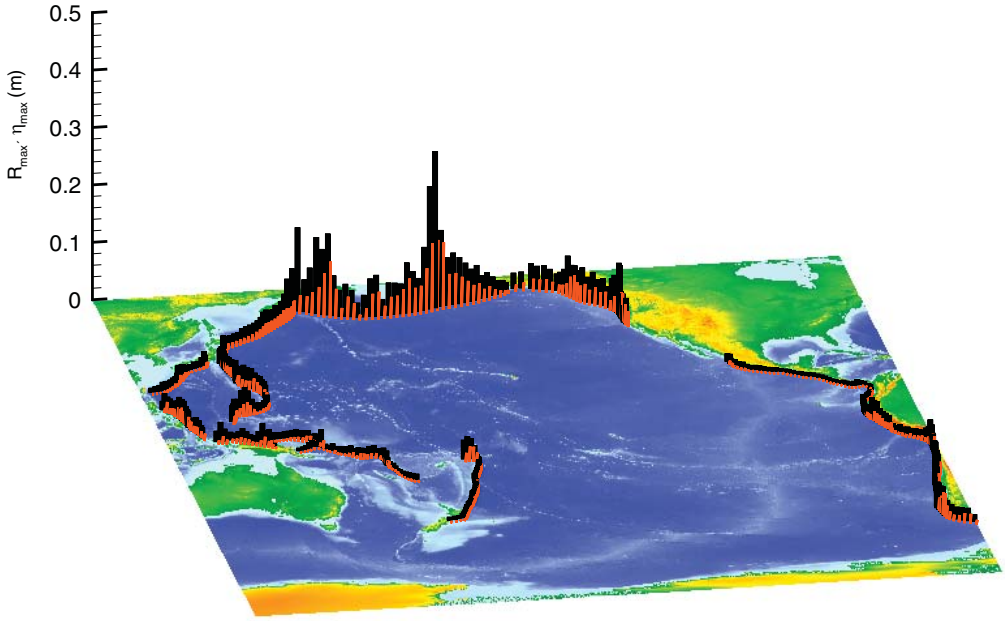

Figure 50: Computed tsunami impact on the Unalaska coastline due to potential tsunami scenarios of Mw 7.8 using the offshore (row B) unit sources. The black bar indicates the computed maximum runup height in Unalaska and the orange bar indicates the computed maximum wave amplitude at Unalaska tide gauge.

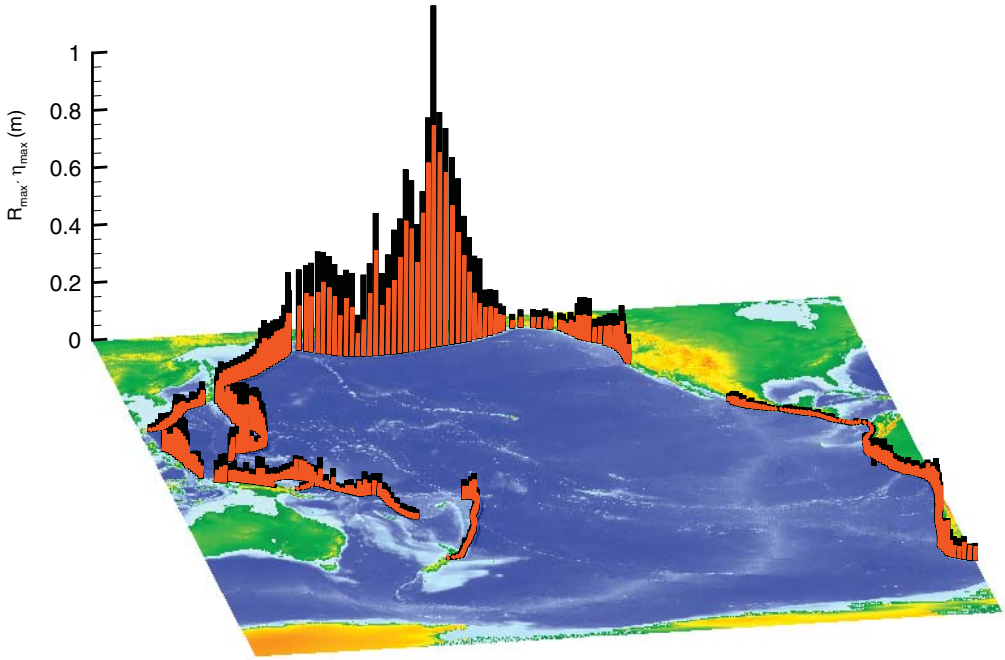

Figure 51: Computed tsunami impact on the Unalaska coastline due to potential tsunami scenarios of Mw 8.2. The black bar indicates the computed maximum runup height in Unalaska and the orange bar indicates the computed maximum wave amplitude at Unalaska tide gauge.

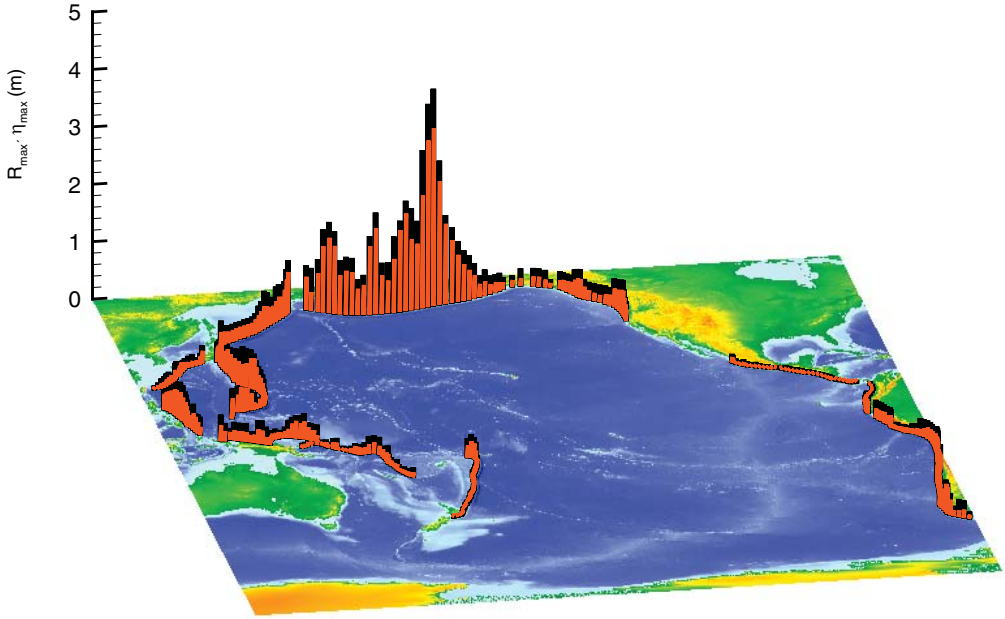

Figure 52: Computed tsunami impact on the Unalaska coastline due to potential tsunami scenarios of Mw 8.7. The black bar indicates the computed maximum runup height in Unalaska and the orange bar indicates the computed maximum wave amplitude at Unalaska tide gauge.

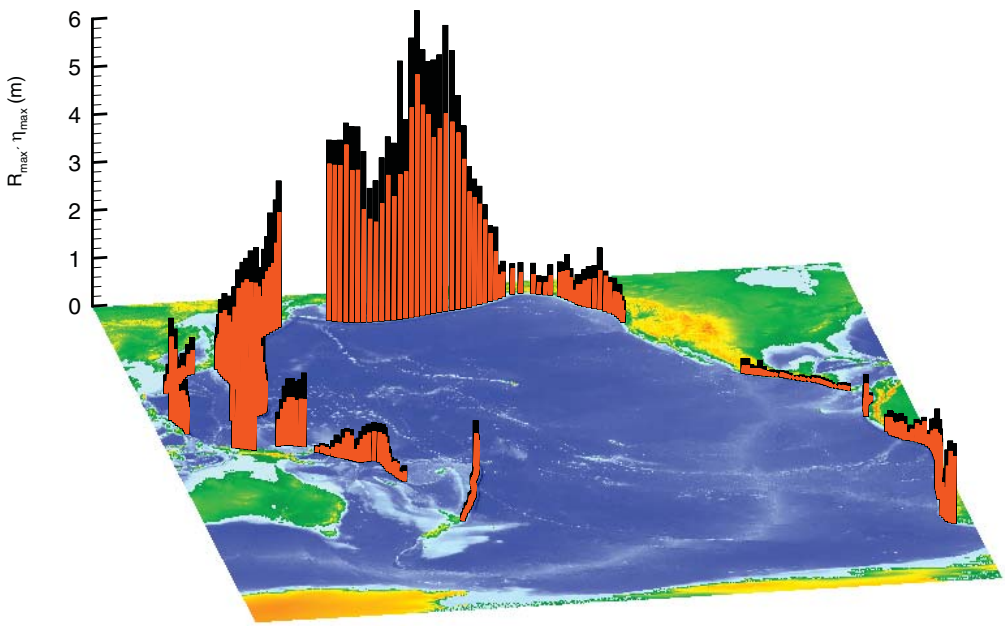

Figure 53: Computed tsunami impact on the Unalaska coastline due to potential tsunami scenarios of Mw 9.3. The black bar indicates the computed maximum runup height in Unalaska and the orange bar indicates the computed maximum wave amplitude at Unalaska tide gauge.

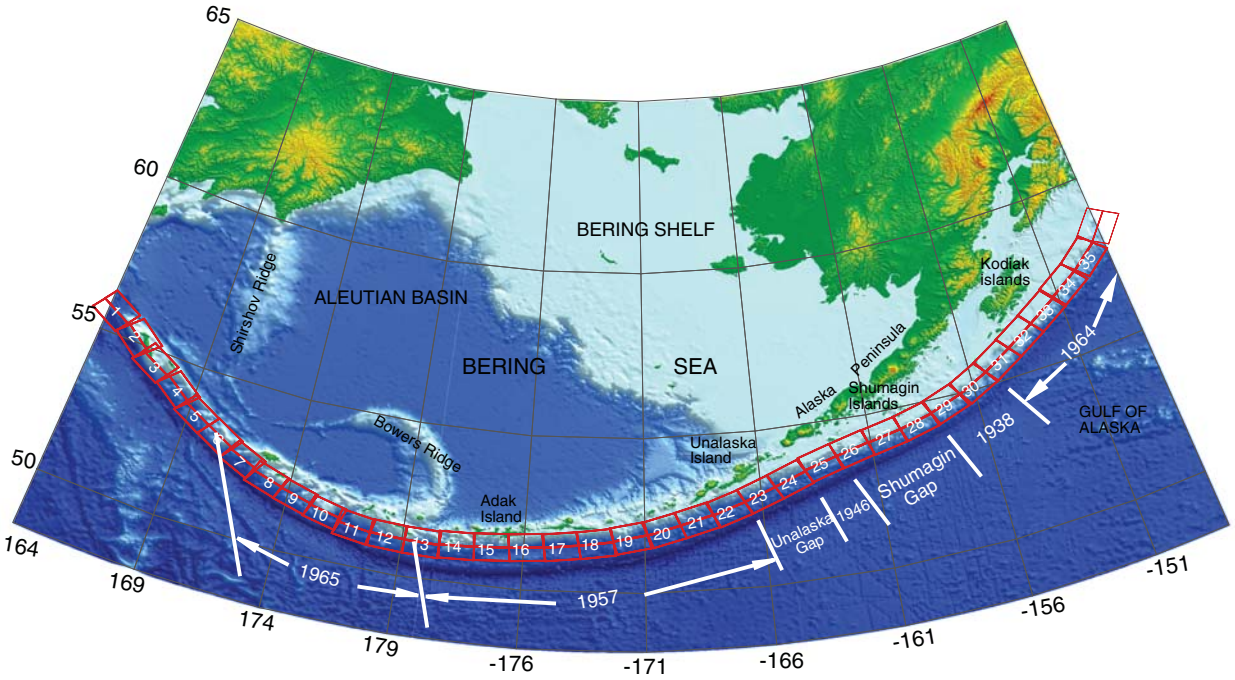

Figure 54: The Sumagin and Unalaska "gaps" along the Aleutian Island Chain in Alaska as noted by the absence of earthquake ruptures along these regions.

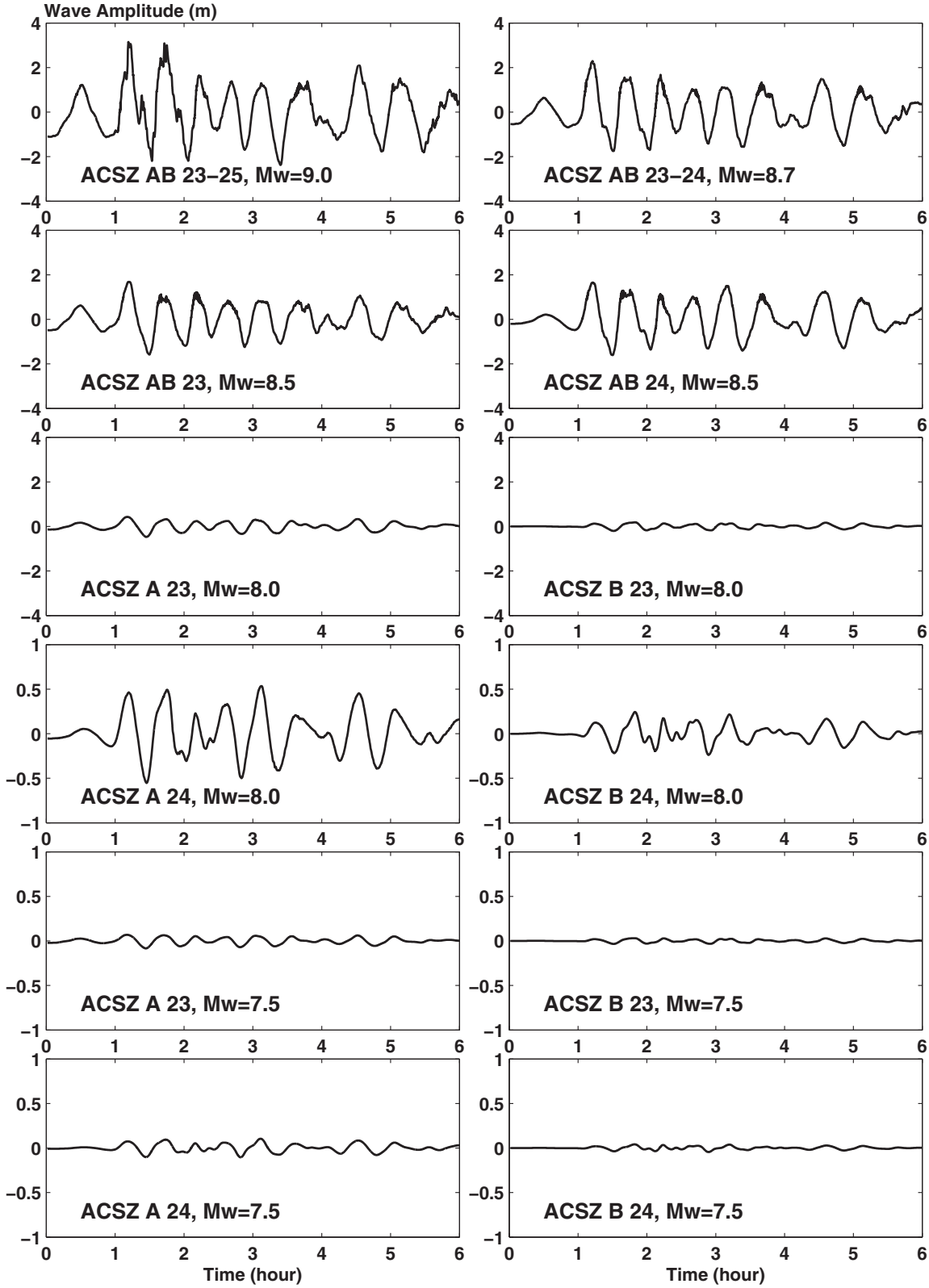

Figure 55: Computed time series at the Unalaska tide gauge for tsunami waves generated by synthetic earthquake scenarios in the Unalaska seismic gap.

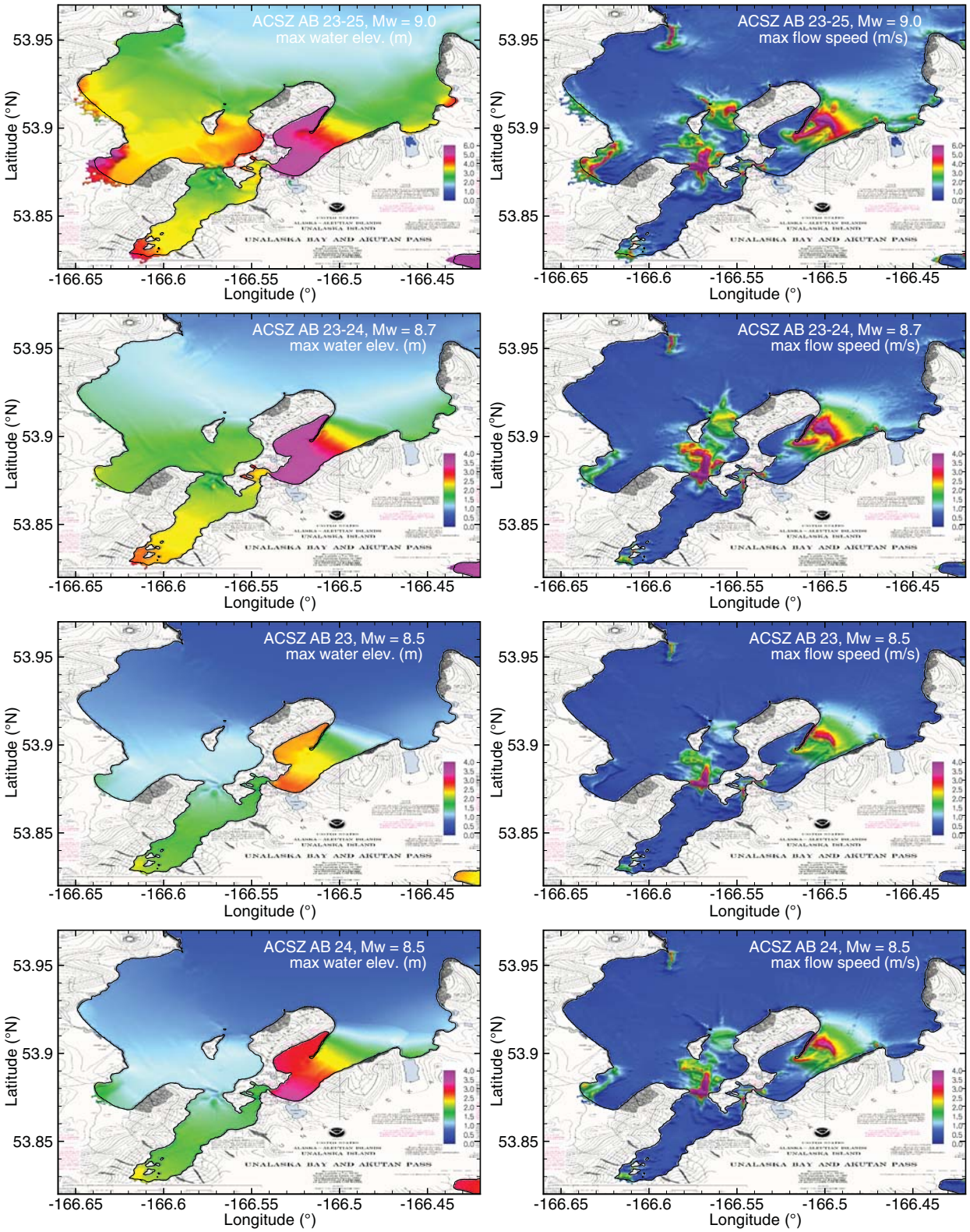

Figure 56: Computed maximum tsunami amplitude and maximum flow speed from the Unalaska forecast model: (1) ACSZ AB 23–25, Mw 9.0; (2) ACSZ AB 23–24, Mw 8.7; (3) ACSZ AB 23, Mw 8.5; (4) ACSZ AB 24, Mw 8.5.

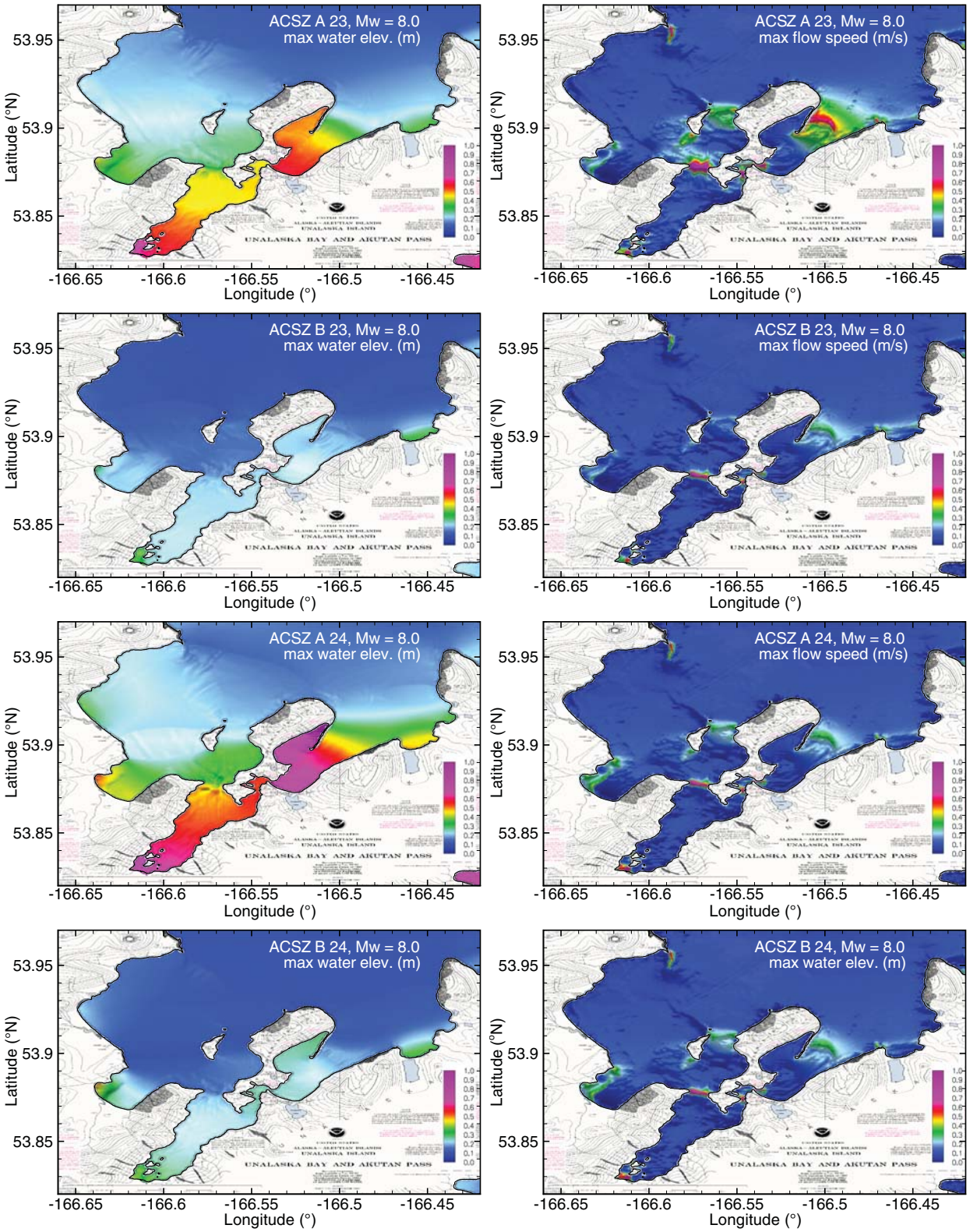

Figure 57: Computed maximum tsunami amplitude and maximum flow speed from the Unalaska forecast model: (1) ACSZ A 23, Mw 8.0; (2) ACSZ B 23, Mw 8.0; (3) ACSZ A 24, Mw 8.0; (4) ACSZ B 24, Mw 8.0.

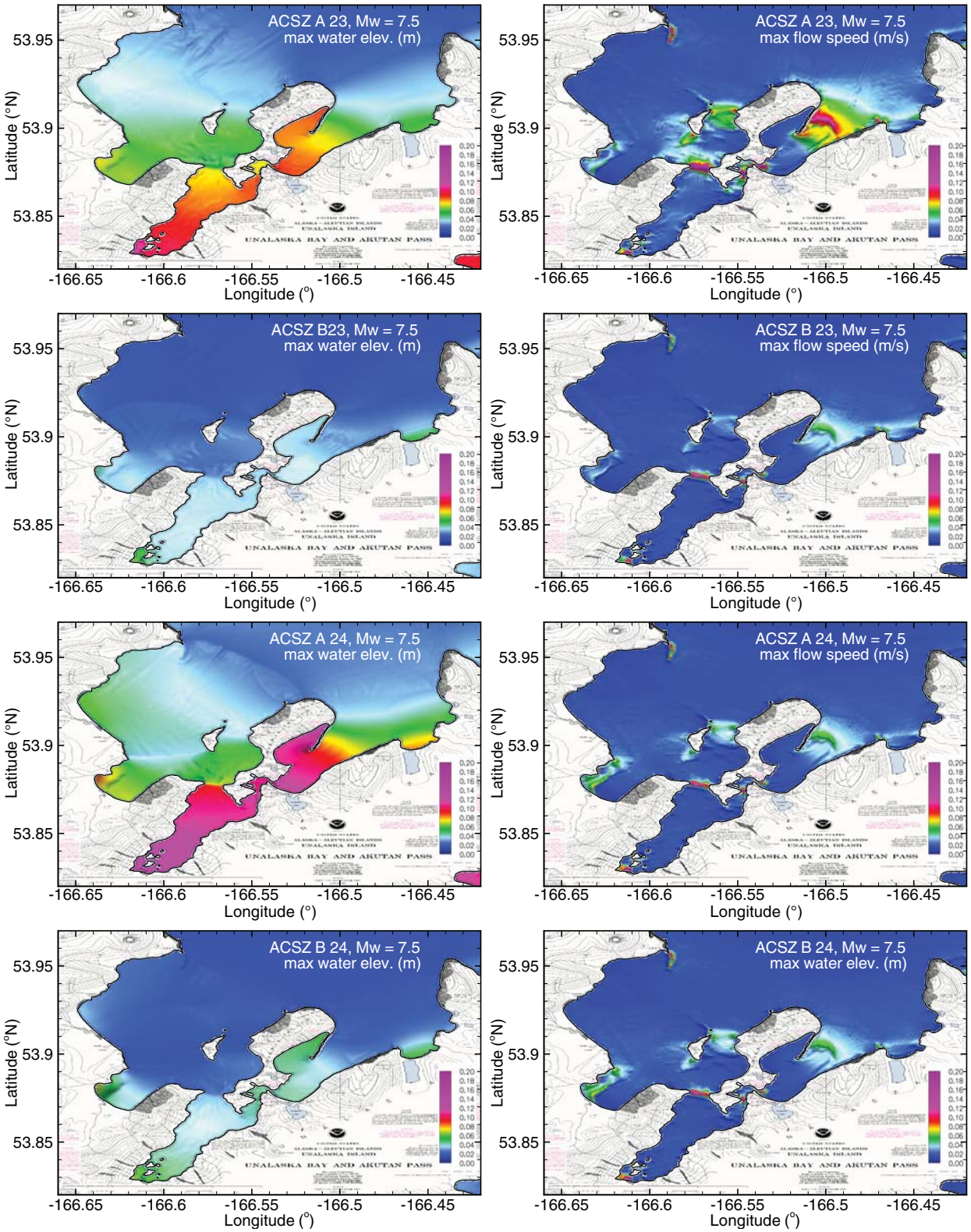

Figure 58: Computed maximum tsunami amplitude and maximum flow speed from the Unalaska forecast model: (1) ACSZ A 23, Mw 7.5; (2) ACSZ B 23, Mw 7.5; (3) ACSZ A 24, Mw 7.5; (4) ACSZ B 24, Mw 7.5.

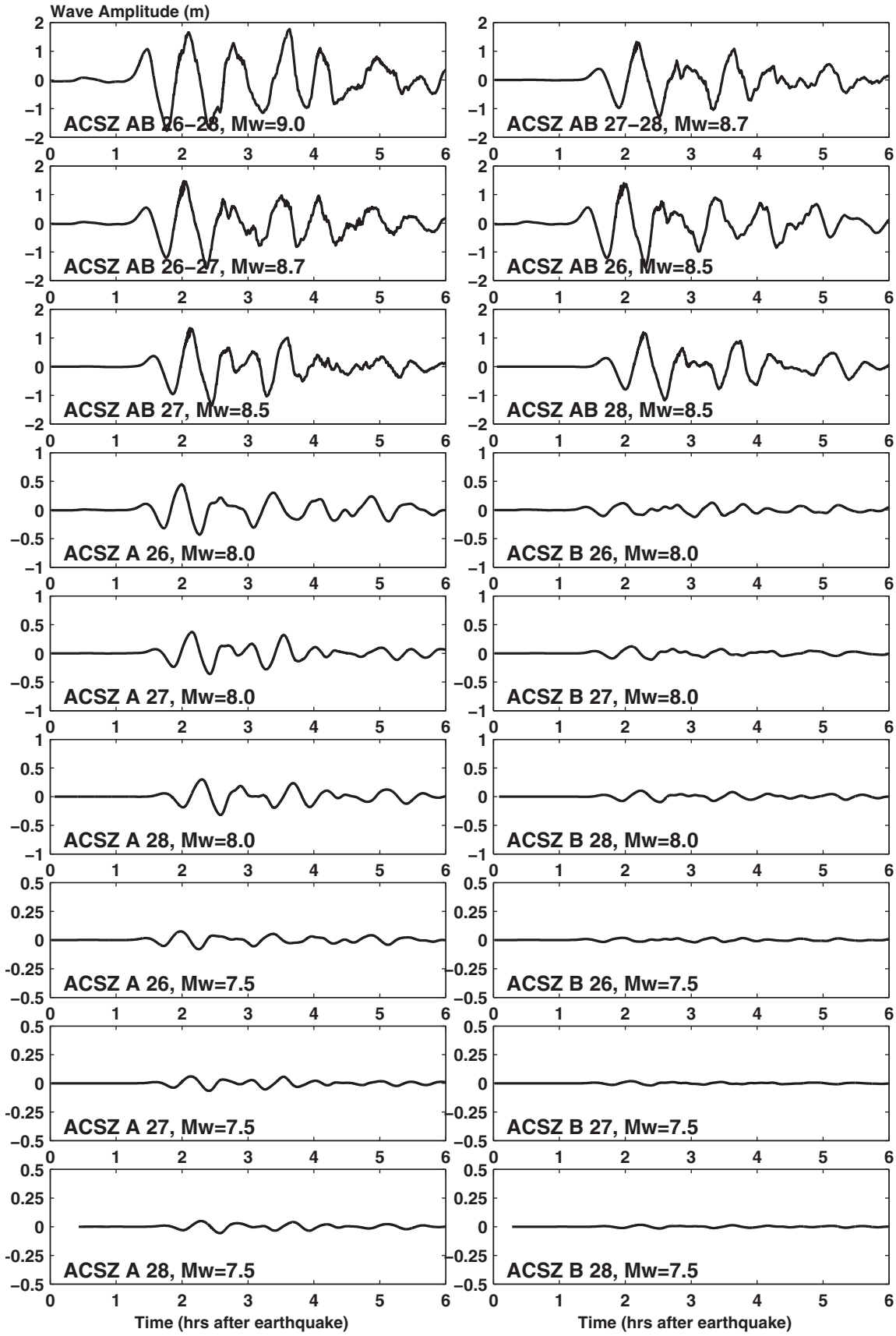

Figure 59: Computed time series at the Unalaska tide gauge for tsunami waves generated by synthetic earthquake scenarios in the Shumagin seismic gap.

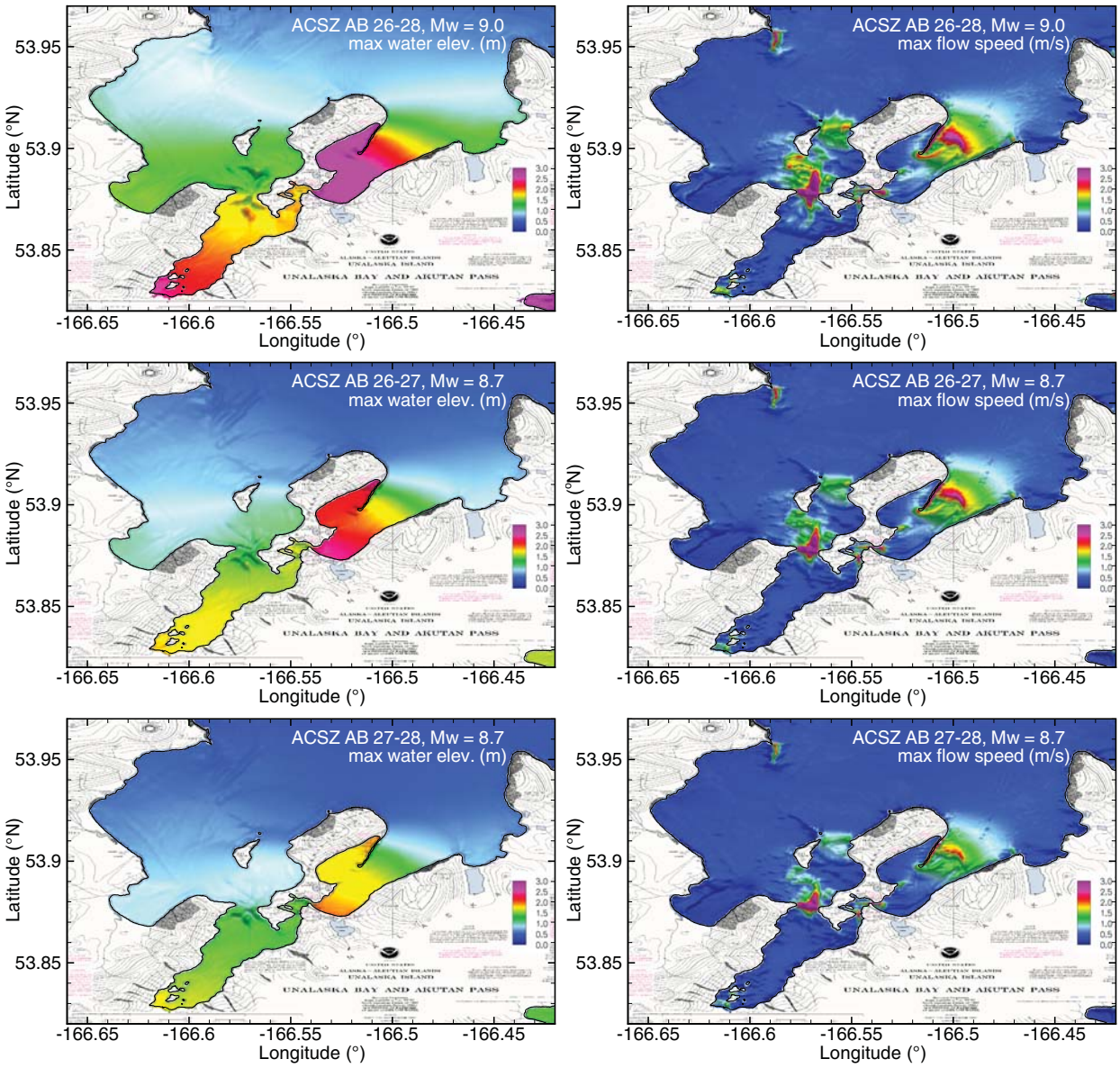

Figure 60: Computed maximum tsunami amplitude and maximum flow speed from the Unalaska forecast model: (1) ACSZ AB 26–28, Mw 9.0; (2) ACSZ AB 26–27, Mw 8.7; (3) ACSZ AB 27–28, Mw 8.7.

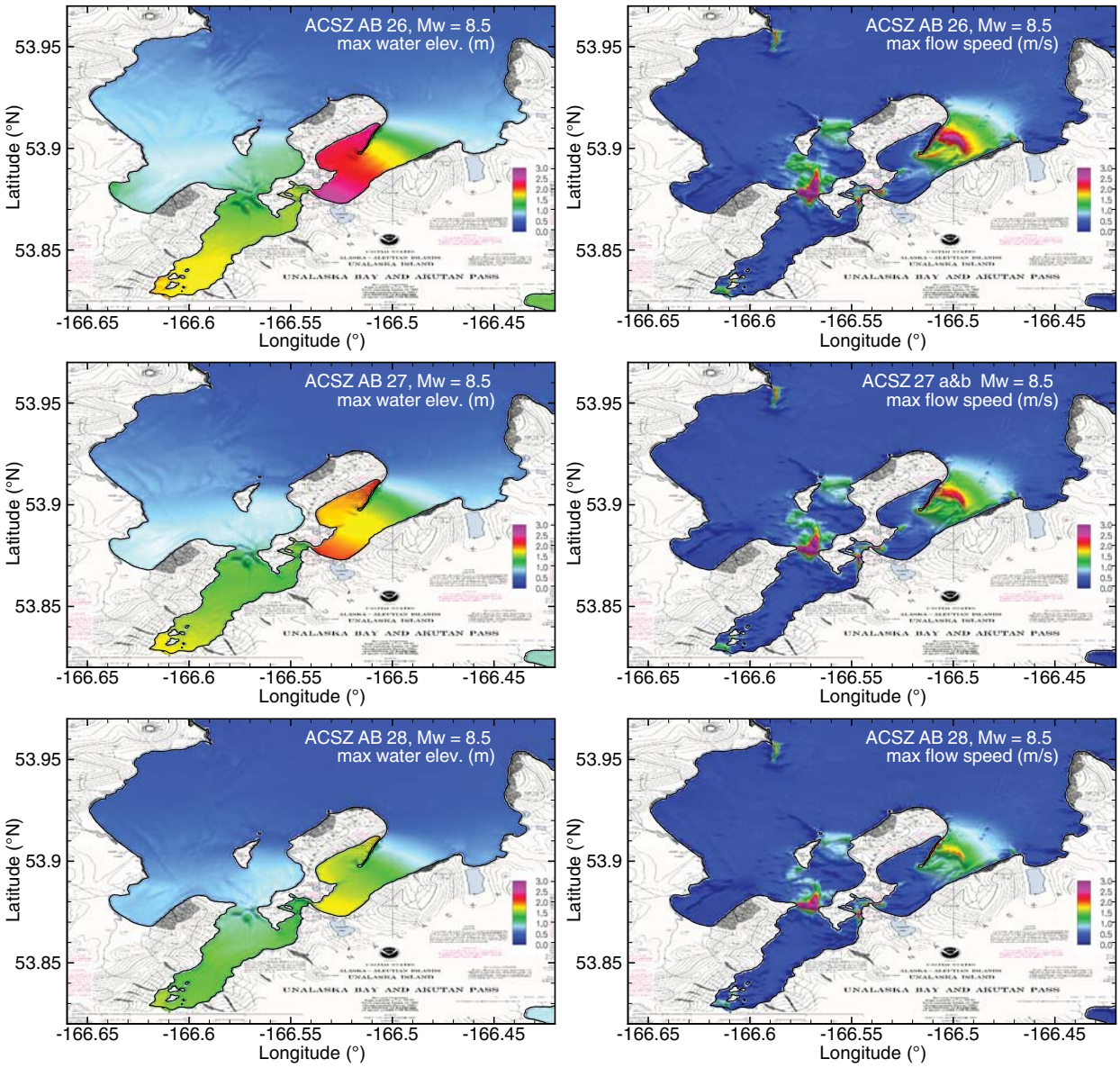

Figure 61: Computed maximum tsunami amplitude and maximum flow speed from the Unalaska forecast model: (1) ACSZ AB 26, Mw 8.5; (2) ACSZ AB 27, Mw 8.5; (3) ACSZ AB 28, Mw 8.5.

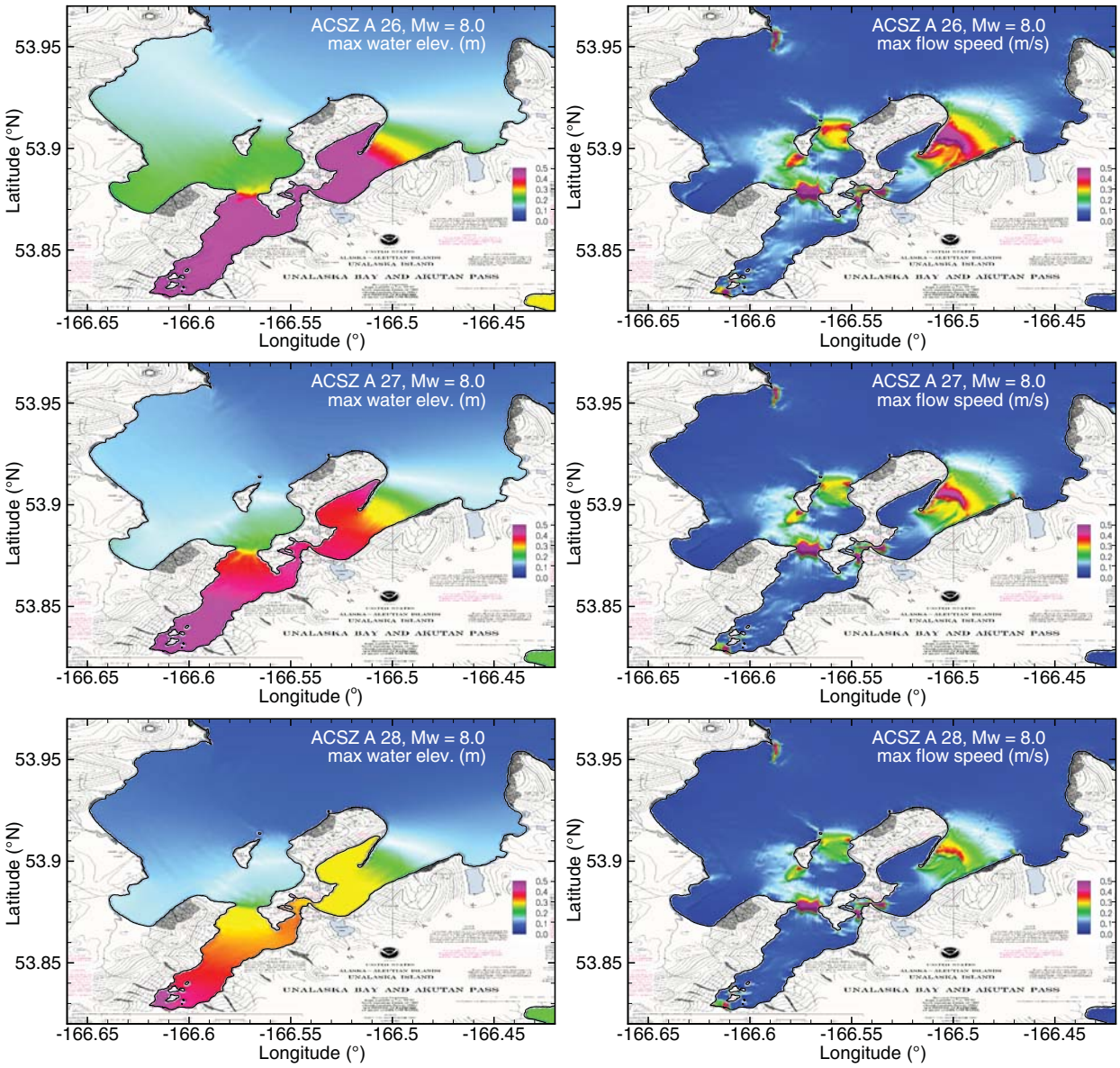

Figure 62: Computed maximum tsunami amplitude and maximum flow speed from the Unalaska forecast model: (1) ACSZ A 26, Mw 8.0; (2) ACSZ A 27, Mw 8.0; (3) ACSZ A 28, Mw 8.0.

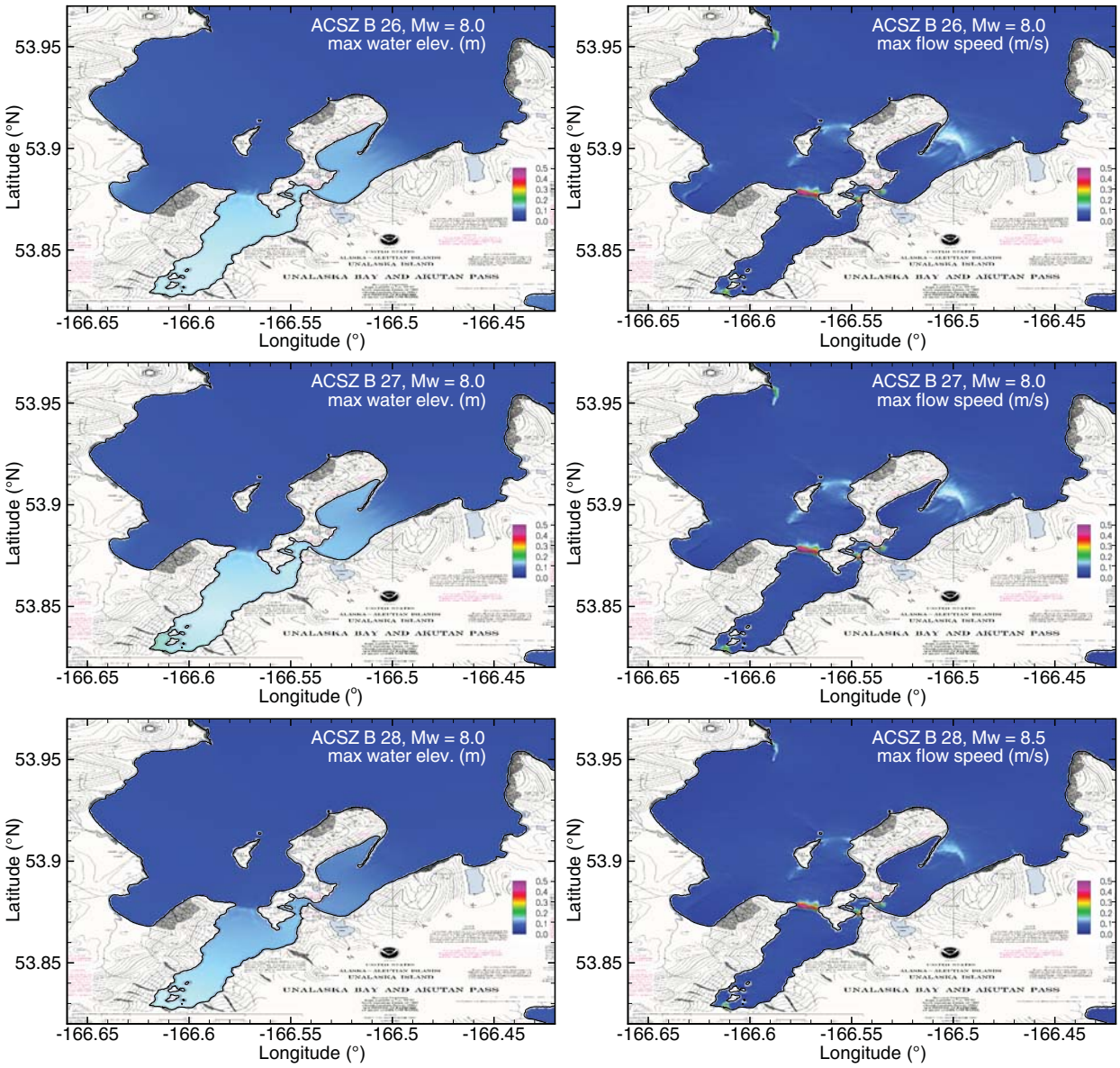

Figure 63: Computed maximum tsunami amplitude and maximum flow speed from the Unalaska forecast model: (1) ACSZ B 26, Mw 8.0; (2) ACSZ B 27, Mw 8.0; (3) ACSZ B 28, Mw 8.0.

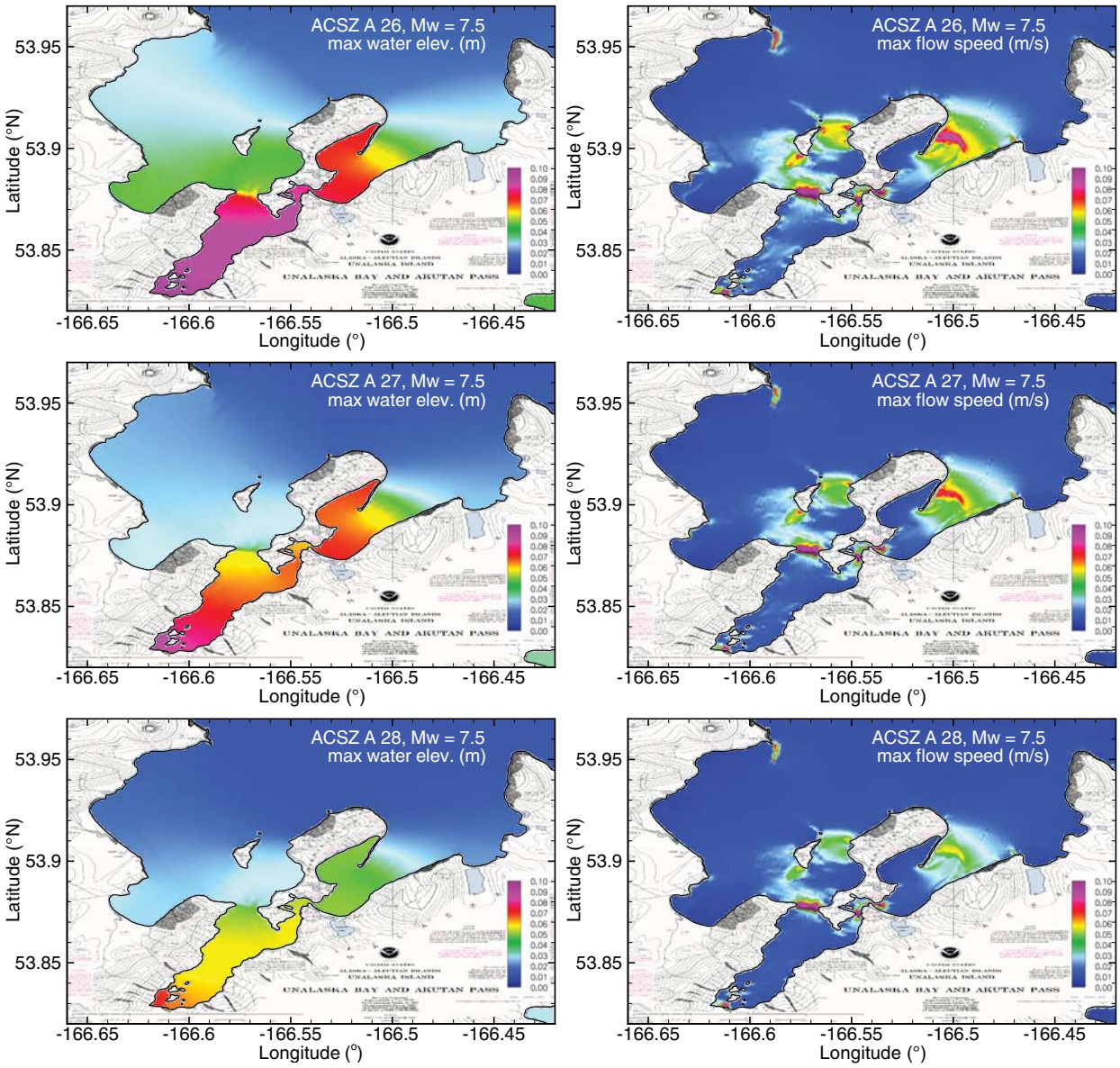

Figure 64: Computed maximum tsunami amplitude and maximum flow speed from the Unalaska forecast model: (1) ACSZ A 26, Mw 7.5; (2) ACSZ A 27, Mw 7.5; (3) ACSZ A 28, Mw 7.5.

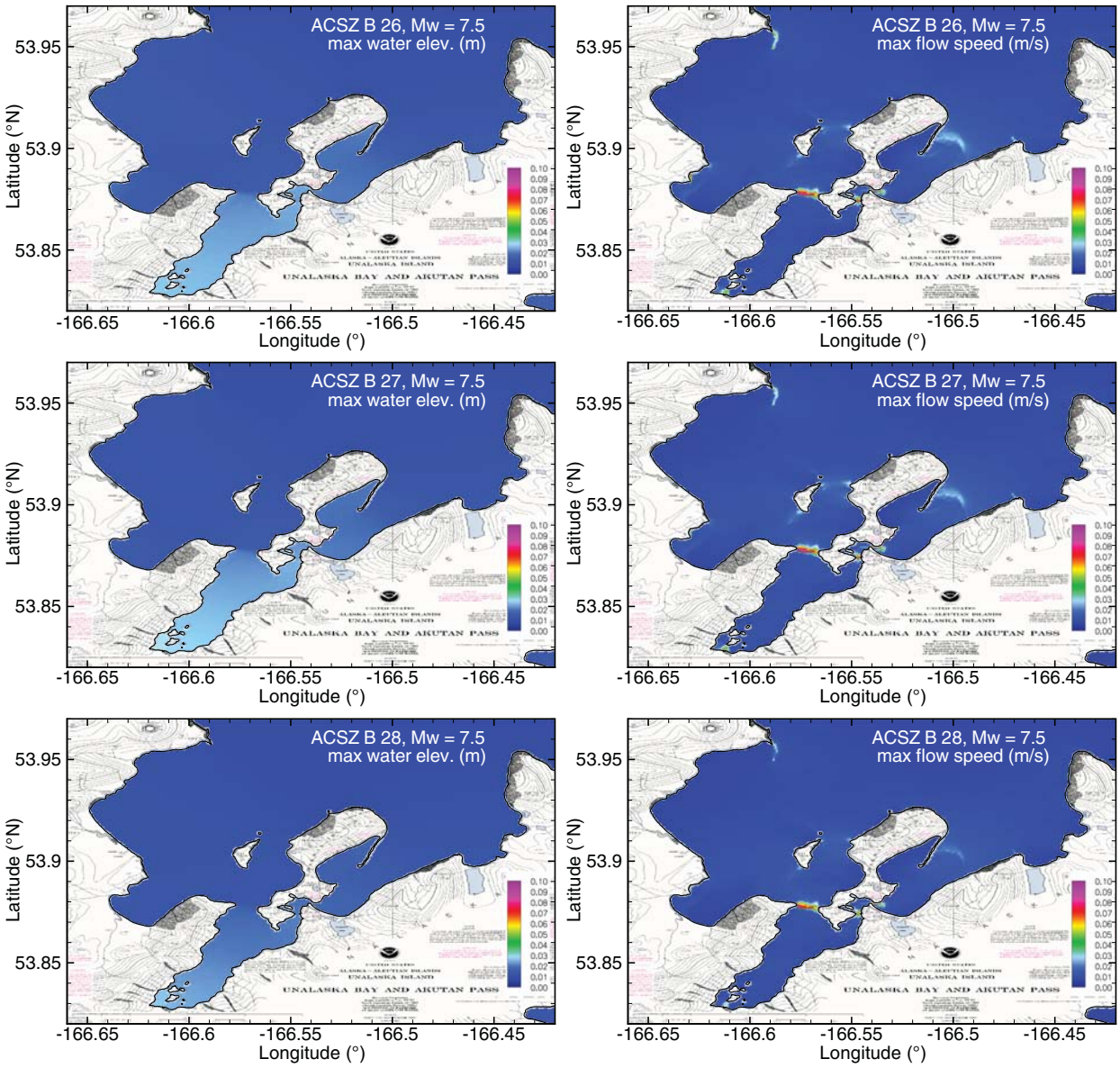

Figure 65: Computed maximum tsunami amplitude and maximum flow speed from the Unalaska forecast model: (1) ACSZ B 26, Mw 7.5; (2) ACSZ B 27, Mw 7.5; (3) ACSZ B 28, Mw 7.5.

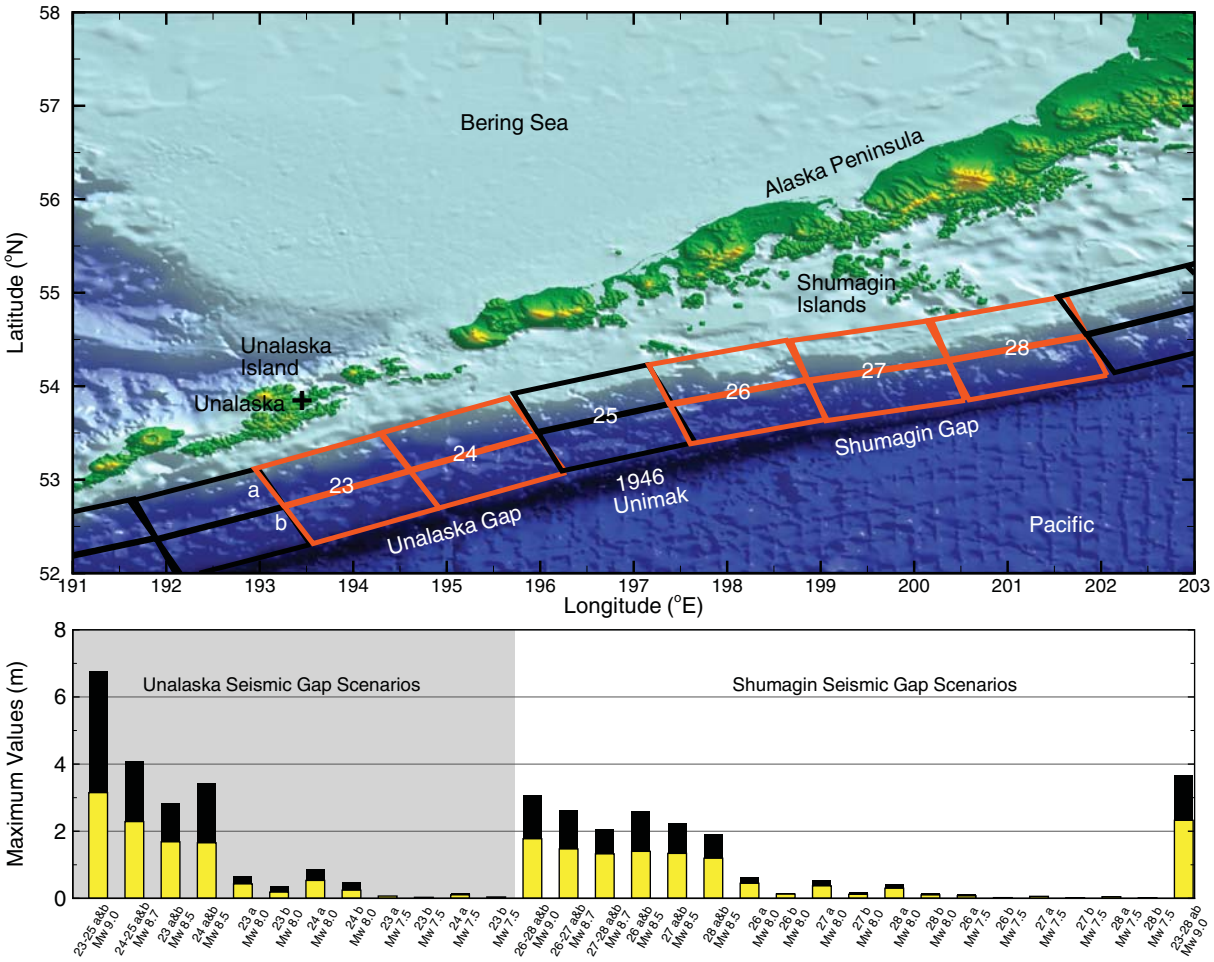

Figure 66: Computational maximum values in Unalaska for synthetic tsunami scenarios initiated in Unalaska and Shumagin seismic gaps. Top panel depicts the locations for the two seismic gaps vs. the source location of the 1946 Unimak tsunami, where the orange boxes represent the tsunami unit sources. In the bottom panel, the x axis (black and yellow bar) indicate the computed maximum tsunami runup in Unalaska and the computed maximum wave amplitude at the Unalaska tide gauge.

Appendix A.

Development of the Unalaska, Alaska, tsunami forecast model occurred prior to parameter changes that were made to reflect modifications to the MOST model code. As a result, the input file for running both the optimized tsunami forecast model and the high-resolution reference inundation model in MOST have been updated accordingly. Appendix A1 and A2 provide the updated files for Unalaska, Alaska.

A1. Reference model ∗.in file for Unalaska, Alaska

```
0.001    Minimum amplitude of input offshore wave (m)
1        Input minimum depth for offshore (m)
0.1      Input "dry land" depth for inundation (m)
0.01     Input friction coefficient (n**2)
1        A & B grid runup flag (1=allow runup, 0=disallow)
300.0    blowup limit (maximum eta before blowup)
0.2      Input time step (sec)
108000   Input number of steps
12       Compute "A" arrays every n-th time step, n=
4        Compute "B" arrays every n-th time step, n=
120      Input number of steps between snapshots
0        ...Starting from
1        ...Saving grid every n-th node, n=1
```

A2. Forecast model ∗.in file for Unalaska, Alaska

```
0.0001   Minimum amplitude of input offshore wave (m):
1        Input minimum depth for offshore (m)
0.1      Input "dry land" depth for inundation (m)
0.001225 Input friction coefficient (n**2)
1        A & B grid runup flag (1=allow runup, 0=disallow)
300.0    blowup limit (maximum eta before blowup)
1.0      Input time step (sec)
28800    Input number of steps
8        Compute "A" arrays every n-th time step, n=
2        Compute "B" arrays every n-th time step, n=
32       Input number of steps between snapshots
1        ...Starting from
1        ...Saving grid every n-th node, n=1
```

Appendix B. Propagation Database: Pacific Ocean Unit Sources

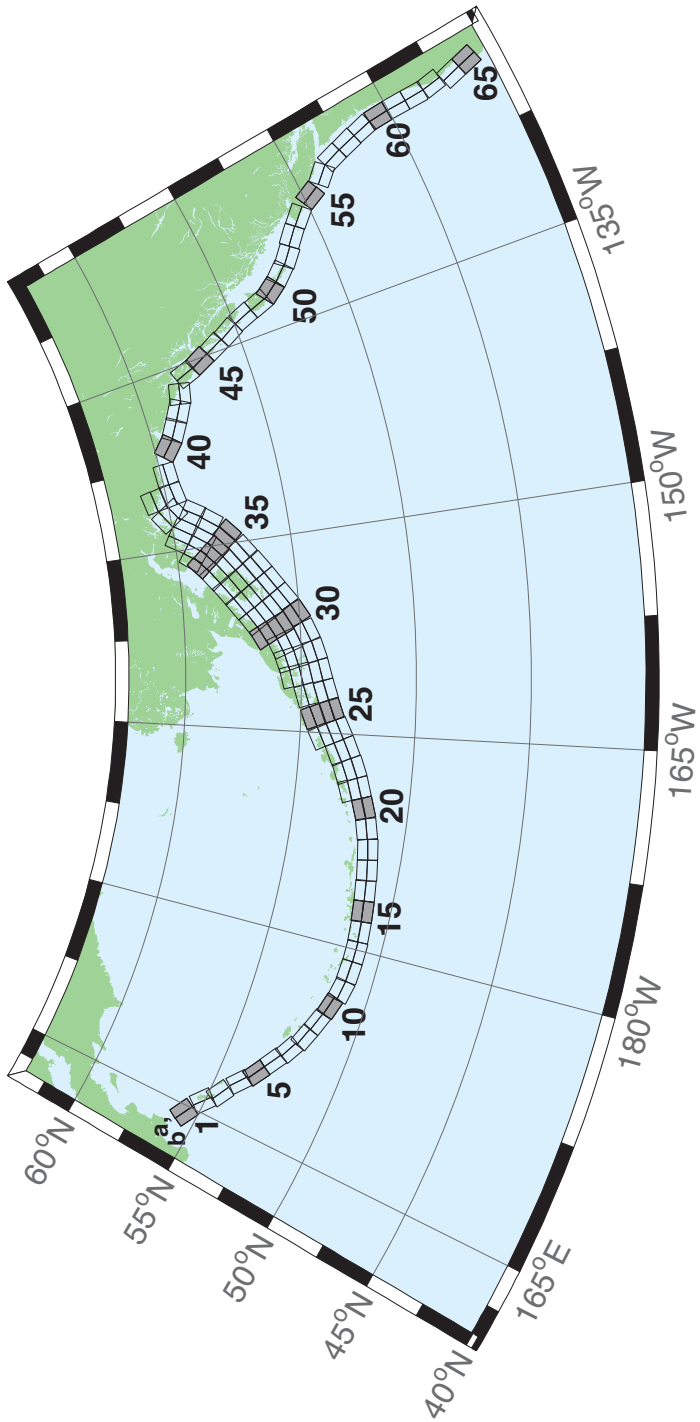

Figure B1: Aleutian-Alaska-Cascadia Subduction Zone unit sources.

Table B1: Earthquake parameters for Aleutian-Alaska-Cascadia Subduction Zone unit sources.

Segment	Description	Longitude (°E)	Latitude (°N)	Strike (°)	Dip (°)	Depth (km)
acsz–1a	Aleutian-Alaska-Cascadia	164.7994	55.9606	299	17	19.61
acsz–1b	Aleutian-Alaska-Cascadia	164.4310	55.5849	299	17	5
acsz–2a	Aleutian-Alaska-Cascadia	166.3418	55.4016	310.2	17	19.61
acsz–2b	Aleutian-Alaska-Cascadia	165.8578	55.0734	310.2	17	5
acsz–3a	Aleutian-Alaska-Cascadia	167.2939	54.8919	300.2	23.36	24.82
acsz–3b	Aleutian-Alaska-Cascadia	166.9362	54.5356	300.2	23.36	5
acsz–4a	Aleutian-Alaska-Cascadia	168.7131	54.2852	310.2	38.51	25.33
acsz–4b	Aleutian-Alaska-Cascadia	168.3269	54.0168	310.2	24	5
acsz–5a	Aleutian-Alaska-Cascadia	169.7447	53.7808	302.8	37.02	23.54
acsz–5b	Aleutian-Alaska-Cascadia	169.4185	53.4793	302.8	21.77	5
acsz–6a	Aleutian-Alaska-Cascadia	171.0144	53.3054	303.2	35.31	22.92
acsz–6b	Aleutian-Alaska-Cascadia	170.6813	52.9986	303.2	21	5
acsz–7a	Aleutian-Alaska-Cascadia	172.1500	52.8528	298.2	35.56	20.16
acsz–7b	Aleutian-Alaska-Cascadia	171.8665	52.5307	298.2	17.65	5
acsz–8a	Aleutian-Alaska-Cascadia	173.2726	52.4579	290.8	37.92	20.35
acsz–8b	Aleutian-Alaska-Cascadia	173.0681	52.1266	290.8	17.88	5
acsz–9a	Aleutian-Alaska-Cascadia	174.5866	52.1434	289	39.09	21.05
acsz–9b	Aleutian-Alaska-Cascadia	174.4027	51.8138	289	18.73	5
acsz–10a	Aleutian-Alaska-Cascadia	175.8784	51.8526	286.1	40.51	20.87
acsz–10b	Aleutian-Alaska-Cascadia	175.7265	51.5245	286.1	18.51	5
acsz–11a	Aleutian-Alaska-Cascadia	177.1140	51.6488	280	15	17.94
acsz–11b	Aleutian-Alaska-Cascadia	176.9937	51.2215	280	15	5
acsz–12a	Aleutian-Alaska-Cascadia	178.4500	51.5690	273	15	17.94
acsz–12b	Aleutian-Alaska-Cascadia	178.4130	51.1200	273	15	5
acsz–13a	Aleutian-Alaska-Cascadia	179.8550	51.5340	271	15	17.94
acsz–13b	Aleutian-Alaska-Cascadia	179.8420	51.0850	271	15	5
acsz–14a	Aleutian-Alaska-Cascadia	181.2340	51.5780	267	15	17.94
acsz–14b	Aleutian-Alaska-Cascadia	181.2720	51.1290	267	15	5
acsz–15a	Aleutian-Alaska-Cascadia	182.6380	51.6470	265	15	17.94
acsz–15b	Aleutian-Alaska-Cascadia	182.7000	51.2000	265	15	5
acsz–16a	Aleutian-Alaska-Cascadia	184.0550	51.7250	264	15	17.94
acsz–16b	Aleutian-Alaska-Cascadia	184.1280	51.2780	264	15	5
acsz–17a	Aleutian-Alaska-Cascadia	185.4560	51.8170	262	15	17.94
acsz–17b	Aleutian-Alaska-Cascadia	185.5560	51.3720	262	15	5
acsz–18a	Aleutian-Alaska-Cascadia	186.8680	51.9410	261	15	17.94
acsz–18b	Aleutian-Alaska-Cascadia	186.9810	51.4970	261	15	5
acsz–19a	Aleutian-Alaska-Cascadia	188.2430	52.1280	257	15	17.94
acsz–19b	Aleutian-Alaska-Cascadia	188.4060	51.6900	257	15	5
acsz–20a	Aleutian-Alaska-Cascadia	189.5810	52.3550	251	15	17.94
acsz–20b	Aleutian-Alaska-Cascadia	189.8180	51.9300	251	15	5
acsz–21a	Aleutian-Alaska-Cascadia	190.9570	52.6470	251	15	17.94
acsz–21b	Aleutian-Alaska-Cascadia	191.1960	52.2220	251	15	5
acsz–21z	Aleutian-Alaska-Cascadia	190.7399	53.0443	250.8	15	30.88
acsz–22a	Aleutian-Alaska-Cascadia	192.2940	52.9430	247	15	17.94
acsz–22b	Aleutian-Alaska-Cascadia	192.5820	52.5300	247	15	5
acsz–22z	Aleutian-Alaska-Cascadia	192.0074	53.3347	247.8	15	30.88
acsz–23a	Aleutian-Alaska-Cascadia	193.6270	53.3070	245	15	17.94
acsz–23b	Aleutian-Alaska-Cascadia	193.9410	52.9000	245	15	5
acsz–23z	Aleutian-Alaska-Cascadia	193.2991	53.6768	244.6	15	30.88
acsz–24a	Aleutian-Alaska-Cascadia	194.9740	53.6870	245	15	17.94
acsz–24b	Aleutian-Alaska-Cascadia	195.2910	53.2800	245	15	5
acsz–24y	Aleutian-Alaska-Cascadia	194.3645	54.4604	244.4	15	43.82
acsz–24z	Aleutian-Alaska-Cascadia	194.6793	54.0674	244.6	15	30.88
acsz–25a	Aleutian-Alaska-Cascadia	196.4340	54.0760	250	15	17.94
acsz–25b	Aleutian-Alaska-Cascadia	196.6930	53.6543	250	15	5

(continued on next page)

Table B1: (continued)

Segment	Description	Longitude (°E)	Latitude (°N)	Strike (°)	Dip (°)	Depth (km)
acsz–25y	Aleutian-Alaska-Cascadia	195.9009	54.8572	247.9	15	43.82
acsz–25z	Aleutian-Alaska-Cascadia	196.1761	54.4536	248.1	15	30.88
acsz–26a	Aleutian-Alaska-Cascadia	197.8970	54.3600	253	15	17.94
acsz–26b	Aleutian-Alaska-Cascadia	198.1200	53.9300	253	15	5
acsz–26y	Aleutian-Alaska-Cascadia	197.5498	55.1934	253.1	15	43.82
acsz–26z	Aleutian-Alaska-Cascadia	197.7620	54.7770	253.3	15	30.88
acsz–27a	Aleutian-Alaska-Cascadia	199.4340	54.5960	256	15	17.94
acsz–27b	Aleutian-Alaska-Cascadia	199.6200	54.1600	256	15	5
acsz–27x	Aleutian-Alaska-Cascadia	198.9736	55.8631	256.5	15	56.24
acsz–27y	Aleutian-Alaska-Cascadia	199.1454	55.4401	256.6	15	43.82
acsz–27z	Aleutian-Alaska-Cascadia	199.3135	55.0170	256.8	15	30.88
acsz–28a	Aleutian-Alaska-Cascadia	200.8820	54.8300	253	15	17.94
acsz–28b	Aleutian-Alaska-Cascadia	201.1080	54.4000	253	15	5
acsz–28x	Aleutian-Alaska-Cascadia	200.1929	56.0559	252.5	15	56.24
acsz–28y	Aleutian-Alaska-Cascadia	200.4167	55.6406	252.7	15	43.82
acsz–28z	Aleutian-Alaska-Cascadia	200.6360	55.2249	252.9	15	30.88
acsz–29a	Aleutian-Alaska-Cascadia	202.2610	55.1330	247	15	17.94
acsz–29b	Aleutian-Alaska-Cascadia	202.5650	54.7200	247	15	5
acsz–29x	Aleutian-Alaska-Cascadia	201.2606	56.2861	245.7	15	56.24
acsz–29y	Aleutian-Alaska-Cascadia	201.5733	55.8888	246	15	43.82
acsz–29z	Aleutian-Alaska-Cascadia	201.8797	55.4908	246.2	15	30.88
acsz–30a	Aleutian-Alaska-Cascadia	203.6040	55.5090	240	15	17.94
acsz–30b	Aleutian-Alaska-Cascadia	203.9970	55.1200	240	15	5
acsz–30w	Aleutian-Alaska-Cascadia	201.9901	56.9855	239.5	15	69.12
acsz–30x	Aleutian-Alaska-Cascadia	202.3851	56.6094	239.8	15	56.24
acsz–30y	Aleutian-Alaska-Cascadia	202.7724	56.2320	240.2	15	43.82
acsz–30z	Aleutian-Alaska-Cascadia	203.1521	55.8534	240.5	15	30.88
acsz–31a	Aleutian-Alaska-Cascadia	204.8950	55.9700	236	15	17.94
acsz–31b	Aleutian-Alaska-Cascadia	205.3400	55.5980	236	15	5
acsz–31w	Aleutian-Alaska-Cascadia	203.0825	57.3740	234.5	15	69.12
acsz–31x	Aleutian-Alaska-Cascadia	203.5408	57.0182	234.9	15	56.24
acsz–31y	Aleutian-Alaska-Cascadia	203.9904	56.6607	235.3	15	43.82
acsz–31z	Aleutian-Alaska-Cascadia	204.4315	56.3016	235.7	15	30.88
acsz–32a	Aleutian-Alaska-Cascadia	206.2080	56.4730	236	15	17.94
acsz–32b	Aleutian-Alaska-Cascadia	206.6580	56.1000	236	15	5
acsz–32w	Aleutian-Alaska-Cascadia	204.4129	57.8908	234.3	15	69.12
acsz–32x	Aleutian-Alaska-Cascadia	204.8802	57.5358	234.7	15	56.24
acsz–32y	Aleutian-Alaska-Cascadia	205.3385	57.1792	235.1	15	43.82
acsz–32z	Aleutian-Alaska-Cascadia	205.7880	56.8210	235.5	15	30.88
acsz–33a	Aleutian-Alaska-Cascadia	207.5370	56.9750	236	15	17.94
acsz–33b	Aleutian-Alaska-Cascadia	207.9930	56.6030	236	15	5
acsz–33w	Aleutian-Alaska-Cascadia	205.7126	58.3917	234.2	15	69.12
acsz–33x	Aleutian-Alaska-Cascadia	206.1873	58.0371	234.6	15	56.24
acsz–33y	Aleutian-Alaska-Cascadia	206.6527	57.6808	235	15	43.82
acsz–33z	Aleutian-Alaska-Cascadia	207.1091	57.3227	235.4	15	30.88
acsz–34a	Aleutian-Alaska-Cascadia	208.9371	57.5124	236	15	17.94
acsz–34b	Aleutian-Alaska-Cascadia	209.4000	57.1400	236	15	5
acsz–34w	Aleutian-Alaska-Cascadia	206.9772	58.8804	233.5	15	69.12
acsz–34x	Aleutian-Alaska-Cascadia	207.4677	58.5291	233.9	15	56.24
acsz–34y	Aleutian-Alaska-Cascadia	207.9485	58.1760	234.3	15	43.82
acsz–34z	Aleutian-Alaska-Cascadia	208.4198	57.8213	234.7	15	30.88
acsz–35a	Aleutian-Alaska-Cascadia	210.2597	58.0441	230	15	17.94
acsz–35b	Aleutian-Alaska-Cascadia	210.8000	57.7000	230	15	5
acsz–35w	Aleutian-Alaska-Cascadia	208.0204	59.3199	228.8	15	69.12
acsz–35x	Aleutian-Alaska-Cascadia	208.5715	58.9906	229.3	15	56.24

(continued on next page)

Table B1: (continued)

Segment	Description	Longitude (°E)	Latitude (°N)	Strike (°)	Dip (°)	Depth (km)
acsz–35y	Aleutian-Alaska-Cascadia	209.1122	58.6590	229.7	15	43.82
acsz–35z	Aleutian-Alaska-Cascadia	209.6425	58.3252	230.2	15	30.88
acsz–36a	Aleutian-Alaska-Cascadia	211.3249	58.6565	218	15	17.94
acsz–36b	Aleutian-Alaska-Cascadia	212.0000	58.3800	218	15	5
acsz–36w	Aleutian-Alaska-Cascadia	208.5003	59.5894	215.6	15	69.12
acsz–36x	Aleutian-Alaska-Cascadia	209.1909	59.3342	216.2	15	56.24
acsz–36y	Aleutian-Alaska-Cascadia	209.8711	59.0753	216.8	15	43.82
acsz–36z	Aleutian-Alaska-Cascadia	210.5412	58.8129	217.3	15	30.88
acsz–37a	Aleutian-Alaska-Cascadia	212.2505	59.2720	213.7	15	17.94
acsz–37b	Aleutian-Alaska-Cascadia	212.9519	59.0312	213.7	15	5
acsz–37x	Aleutian-Alaska-Cascadia	210.1726	60.0644	213	15	56.24
acsz–37y	Aleutian-Alaska-Cascadia	210.8955	59.8251	213.7	15	43.82
acsz–37z	Aleutian-Alaska-Cascadia	211.6079	59.5820	214.3	15	30.88
acsz–38a	Aleutian-Alaska-Cascadia	214.6555	60.1351	260.1	0	15
acsz–38b	Aleutian-Alaska-Cascadia	214.8088	59.6927	260.1	0	15
acsz–38y	Aleutian-Alaska-Cascadia	214.3737	60.9838	259	0	15
acsz–38z	Aleutian-Alaska-Cascadia	214.5362	60.5429	259	0	15
acsz–39a	Aleutian-Alaska-Cascadia	216.5607	60.2480	267	0	15
acsz–39b	Aleutian-Alaska-Cascadia	216.6068	59.7994	267	0	15
acsz–40a	Aleutian-Alaska-Cascadia	219.3069	59.7574	310.9	0	15
acsz–40b	Aleutian-Alaska-Cascadia	218.7288	59.4180	310.9	0	15
acsz–41a	Aleutian-Alaska-Cascadia	220.4832	59.3390	300.7	0	15
acsz–41b	Aleutian-Alaska-Cascadia	220.0382	58.9529	300.7	0	15
acsz–42a	Aleutian-Alaska-Cascadia	221.8835	58.9310	298.9	0	15
acsz–42b	Aleutian-Alaska-Cascadia	221.4671	58.5379	298.9	0	15
acsz–43a	Aleutian-Alaska-Cascadia	222.9711	58.6934	282.3	0	15
acsz–43b	Aleutian-Alaska-Cascadia	222.7887	58.2546	282.3	0	15
acsz–44a	Aleutian-Alaska-Cascadia	224.9379	57.9054	340.9	12	11.09
acsz–44b	Aleutian-Alaska-Cascadia	224.1596	57.7617	340.9	7	5
acsz–45a	Aleutian-Alaska-Cascadia	225.4994	57.1634	334.1	12	11.09
acsz–45b	Aleutian-Alaska-Cascadia	224.7740	56.9718	334.1	7	5
acsz–46a	Aleutian-Alaska-Cascadia	226.1459	56.3552	334.1	12	11.09
acsz–46b	Aleutian-Alaska-Cascadia	225.4358	56.1636	334.1	7	5
acsz–47a	Aleutian-Alaska-Cascadia	226.7731	55.5830	332.3	12	11.09
acsz–47b	Aleutian-Alaska-Cascadia	226.0887	55.3785	332.3	7	5
acsz–48a	Aleutian-Alaska-Cascadia	227.4799	54.6763	339.4	12	11.09
acsz–48b	Aleutian-Alaska-Cascadia	226.7713	54.5217	339.4	7	5
acsz–49a	Aleutian-Alaska-Cascadia	227.9482	53.8155	341.2	12	11.09
acsz–49b	Aleutian-Alaska-Cascadia	227.2462	53.6737	341.2	7	5
acsz–50a	Aleutian-Alaska-Cascadia	228.3970	53.2509	324.5	12	11.09
acsz–50b	Aleutian-Alaska-Cascadia	227.8027	52.9958	324.5	7	5
acsz–51a	Aleutian-Alaska-Cascadia	229.1844	52.6297	318.4	12	11.09
acsz–51b	Aleutian-Alaska-Cascadia	228.6470	52.3378	318.4	7	5
acsz–52a	Aleutian-Alaska-Cascadia	230.0306	52.0768	310.9	12	11.09
acsz–52b	Aleutian-Alaska-Cascadia	229.5665	51.7445	310.9	7	5
acsz–53a	Aleutian-Alaska-Cascadia	231.1735	51.5258	310.9	12	11.09
acsz–53b	Aleutian-Alaska-Cascadia	230.7150	51.1935	310.9	7	5
acsz–54a	Aleutian-Alaska-Cascadia	232.2453	50.8809	314.1	12	11.09
acsz–54b	Aleutian-Alaska-Cascadia	231.7639	50.5655	314.1	7	5
acsz–55a	Aleutian-Alaska-Cascadia	233.3066	49.9032	333.7	12	11.09
acsz–55b	Aleutian-Alaska-Cascadia	232.6975	49.7086	333.7	7	5
acsz–56a	Aleutian-Alaska-Cascadia	234.0588	49.1702	315	11	12.82
acsz–56b	Aleutian-Alaska-Cascadia	233.5849	48.8584	315	9	5
acsz–57a	Aleutian-Alaska-Cascadia	234.9041	48.2596	341	11	12.82
acsz–57b	Aleutian-Alaska-Cascadia	234.2797	48.1161	341	9	5

(continued on next page)

Table B1: (continued)

Segment	Description	Longitude (°E)	Latitude (°N)	Strike (°)	Dip (°)	Depth (km)
acsz–58a	Aleutian-Alaska-Cascadia	235.3021	47.3812	344	11	12.82
acsz–58b	Aleutian-Alaska-Cascadia	234.6776	47.2597	344	9	5
acsz–59a	Aleutian-Alaska-Cascadia	235.6432	46.5082	345	11	12.82
acsz–59b	Aleutian-Alaska-Cascadia	235.0257	46.3941	345	9	5
acsz–60a	Aleutian-Alaska-Cascadia	235.8640	45.5429	356	11	12.82
acsz–60b	Aleutian-Alaska-Cascadia	235.2363	45.5121	356	9	5
acsz–61a	Aleutian-Alaska-Cascadia	235.9106	44.6227	359	11	12.82
acsz–61b	Aleutian-Alaska-Cascadia	235.2913	44.6150	359	9	5
acsz–62a	Aleutian-Alaska-Cascadia	235.9229	43.7245	359	11	12.82
acsz–62b	Aleutian-Alaska-Cascadia	235.3130	43.7168	359	9	5
acsz–63a	Aleutian-Alaska-Cascadia	236.0220	42.9020	350	11	12.82
acsz–63b	Aleutian-Alaska-Cascadia	235.4300	42.8254	350	9	5
acsz–64a	Aleutian-Alaska-Cascadia	235.9638	41.9818	345	11	12.82
acsz–64b	Aleutian-Alaska-Cascadia	235.3919	41.8677	345	9	5
acsz–65a	Aleutian-Alaska-Cascadia	236.2643	41.1141	345	11	12.82
acsz–65b	Aleutian-Alaska-Cascadia	235.7000	41.0000	345	9	5
acsz–238a	Aleutian-Alaska-Cascadia	213.2878	59.8406	236.8	15	17.94
acsz–238y	Aleutian-Alaska-Cascadia	212.3424	60.5664	236.8	15	43.82
acsz–238z	Aleutian-Alaska-Cascadia	212.8119	60.2035	236.8	15	30.88

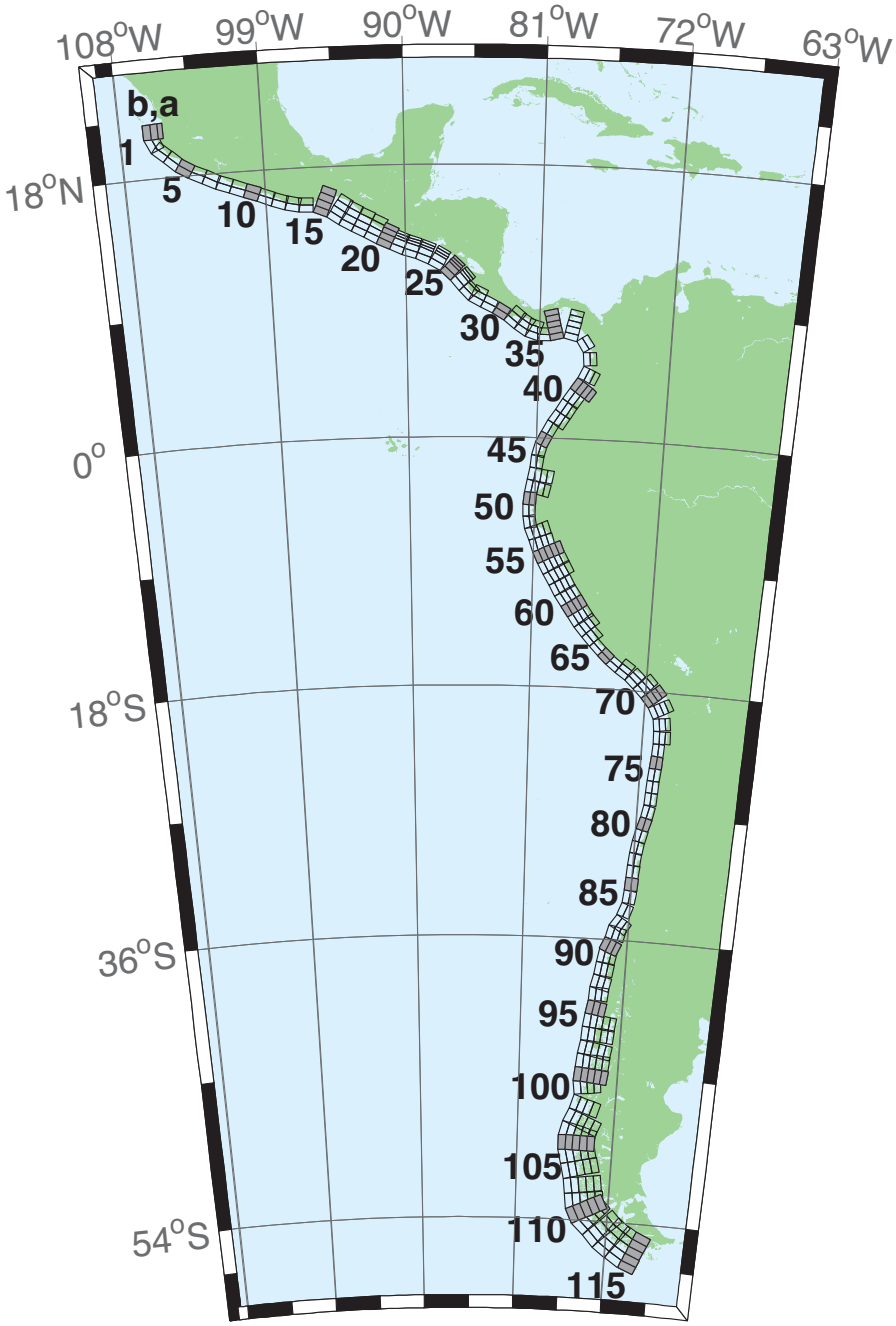

Figure B2: Central and South America Subduction Zone unit sources.

Table B2: Earthquake parameters for Central and South America Subduction Zone unit sources.

Segment	Description	Longitude (°E)	Latitude (°N)	Strike (°)	Dip (°)	Depth (km)
cssz–1a	Central and South America	254.4573	20.8170	359	19	15.4
cssz–1b	Central and South America	254.0035	20.8094	359	12	5
cssz–1z	Central and South America	254.7664	20.8222	359	50	31.67
cssz–2a	Central and South America	254.5765	20.2806	336.8	19	15.4
cssz–2b	Central and South America	254.1607	20.1130	336.8	12	5
cssz–3a	Central and South America	254.8789	19.8923	310.6	18.31	15.27
cssz–3b	Central and South America	254.5841	19.5685	310.6	11.85	5
cssz–4a	Central and South America	255.6167	19.2649	313.4	17.62	15.12
cssz–4b	Central and South America	255.3056	18.9537	313.4	11.68	5
cssz–5a	Central and South America	256.2240	18.8148	302.7	16.92	15
cssz–5b	Central and South America	255.9790	18.4532	302.7	11.54	5
cssz–6a	Central and South America	256.9425	18.4383	295.1	16.23	14.87
cssz–6b	Central and South America	256.7495	18.0479	295.1	11.38	5
cssz–7a	Central and South America	257.8137	18.0339	296.9	15.54	14.74
cssz–7b	Central and South America	257.6079	17.6480	296.9	11.23	5
cssz–8a	Central and South America	258.5779	17.7151	290.4	14.85	14.61
cssz–8b	Central and South America	258.4191	17.3082	290.4	11.08	5
cssz–9a	Central and South America	259.4578	17.4024	290.5	14.15	14.47
cssz–9b	Central and South America	259.2983	16.9944	290.5	10.92	5
cssz–10a	Central and South America	260.3385	17.0861	290.8	13.46	14.34
cssz–10b	Central and South America	260.1768	16.6776	290.8	10.77	5
cssz–11a	Central and South America	261.2255	16.7554	291.8	12.77	14.21
cssz–11b	Central and South America	261.0556	16.3487	291.8	10.62	5
cssz–12a	Central and South America	262.0561	16.4603	288.9	12.08	14.08
cssz–12b	Central and South America	261.9082	16.0447	288.9	10.46	5
cssz–13a	Central and South America	262.8638	16.2381	283.2	11.38	13.95
cssz–13b	Central and South America	262.7593	15.8094	283.2	10.31	5
cssz–14a	Central and South America	263.6066	16.1435	272.1	10.69	13.81
cssz–14b	Central and South America	263.5901	15.7024	272.1	10.15	5
cssz–15a	Central and South America	264.8259	15.8829	293	10	13.68
cssz–15b	Central and South America	264.6462	15.4758	293	10	5
cssz–15y	Central and South America	265.1865	16.6971	293	10	31.05
cssz–15z	Central and South America	265.0060	16.2900	293	10	22.36
cssz–16a	Central and South America	265.7928	15.3507	304.9	15	15.82
cssz–16b	Central and South America	265.5353	14.9951	304.9	12.5	5
cssz–16y	Central and South America	266.3092	16.0619	304.9	15	41.7
cssz–16z	Central and South America	266.0508	15.7063	304.9	15	28.76
cssz–17a	Central and South America	266.4947	14.9019	299.5	20	17.94
cssz–17b	Central and South America	266.2797	14.5346	299.5	15	5
cssz–17y	Central and South America	266.9259	15.6365	299.5	20	52.14
cssz–17z	Central and South America	266.7101	15.2692	299.5	20	35.04
cssz–18a	Central and South America	267.2827	14.4768	298	21.5	17.94
cssz–18b	Central and South America	267.0802	14.1078	298	15	5
cssz–18y	Central and South America	267.6888	15.2148	298	21.5	54.59
cssz–18z	Central and South America	267.4856	14.8458	298	21.5	36.27
cssz–19a	Central and South America	268.0919	14.0560	297.6	23	17.94
cssz–19b	Central and South America	267.8943	13.6897	297.6	15	5
cssz–19y	Central and South America	268.4880	14.7886	297.6	23	57.01
cssz–19z	Central and South America	268.2898	14.4223	297.6	23	37.48
cssz–20a	Central and South America	268.8929	13.6558	296.2	24	17.94
cssz–20b	Central and South America	268.7064	13.2877	296.2	15	5
cssz–20y	Central and South America	269.1796	14.2206	296.2	45.5	73.94
cssz–20z	Central and South America	269.0362	13.9382	296.2	45.5	38.28
cssz–21a	Central and South America	269.6797	13.3031	292.6	25	17.94
cssz–21b	Central and South America	269.5187	12.9274	292.6	15	5

(continued on next page)

Table B2: (continued)

Segment	Description	Longitude (°E)	Latitude (°N)	Strike (°)	Dip (°)	Depth (km)
cssz–21x	Central and South America	269.8797	13.7690	292.6	68	131.8
cssz–21y	Central and South America	269.8130	13.6137	292.6	68	85.43
cssz–21z	Central and South America	269.7463	13.4584	292.6	68	39.07
cssz–22a	Central and South America	270.4823	13.0079	288.6	25	17.94
cssz–22b	Central and South America	270.3492	12.6221	288.6	15	5
cssz–22x	Central and South America	270.6476	13.4864	288.6	68	131.8
cssz–22y	Central and South America	270.5925	13.3269	288.6	68	85.43
cssz–22z	Central and South America	270.5374	13.1674	288.6	68	39.07
cssz–23a	Central and South America	271.3961	12.6734	292.4	25	17.94
cssz–23b	Central and South America	271.2369	12.2972	292.4	15	5
cssz–23x	Central and South America	271.5938	13.1399	292.4	68	131.8
cssz–23y	Central and South America	271.5279	12.9844	292.4	68	85.43
cssz–23z	Central and South America	271.4620	12.8289	292.4	68	39.07
cssz–24a	Central and South America	272.3203	12.2251	300.2	25	17.94
cssz–24b	Central and South America	272.1107	11.8734	300.2	15	5
cssz–24x	Central and South America	272.5917	12.6799	300.2	67	131.1
cssz–24y	Central and South America	272.5012	12.5283	300.2	67	85.1
cssz–24z	Central and South America	272.4107	12.3767	300.2	67	39.07
cssz–25a	Central and South America	273.2075	11.5684	313.8	25	17.94
cssz–25b	Central and South America	272.9200	11.2746	313.8	15	5
cssz–25x	Central and South America	273.5950	11.9641	313.8	66	130.4
cssz–25y	Central and South America	273.4658	11.8322	313.8	66	84.75
cssz–25z	Central and South America	273.3366	11.7003	313.8	66	39.07
cssz–26a	Central and South America	273.8943	10.8402	320.4	25	17.94
cssz–26b	Central and South America	273.5750	10.5808	320.4	15	5
cssz–26x	Central and South America	274.3246	11.1894	320.4	66	130.4
cssz–26y	Central and South America	274.1811	11.0730	320.4	66	84.75
cssz–26z	Central and South America	274.0377	10.9566	320.4	66	39.07
cssz–27a	Central and South America	274.4569	10.2177	316.1	25	17.94
cssz–27b	Central and South America	274.1590	9.9354	316.1	15	5
cssz–27z	Central and South America	274.5907	10.3444	316.1	66	39.07
cssz–28a	Central and South America	274.9586	9.8695	297.1	22	14.54
cssz–28b	Central and South America	274.7661	9.4988	297.1	11	5
cssz–28z	Central and South America	275.1118	10.1643	297.1	42.5	33.27
cssz–29a	Central and South America	275.7686	9.4789	296.6	19	11.09
cssz–29b	Central and South America	275.5759	9.0992	296.6	7	5
cssz–30a	Central and South America	276.6346	8.9973	302.2	19	9.36
cssz–30b	Central and South America	276.4053	8.6381	302.2	5	5
cssz–31a	Central and South America	277.4554	8.4152	309.1	19	7.62
cssz–31b	Central and South America	277.1851	8.0854	309.1	3	5
cssz–31z	Central and South America	277.7260	8.7450	309.1	19	23.9
cssz–32a	Central and South America	278.1112	7.9425	303	18.67	8.49
cssz–32b	Central and South America	277.8775	7.5855	303	4	5
cssz–32z	Central and South America	278.3407	8.2927	303	21.67	24.49
cssz–33a	Central and South America	278.7082	7.6620	287.6	18.33	10.23
cssz–33b	Central and South America	278.5785	7.2555	287.6	6	5
cssz–33z	Central and South America	278.8328	8.0522	287.6	24.33	25.95
cssz–34a	Central and South America	279.3184	7.5592	269.5	18	17.94
cssz–34b	Central and South America	279.3223	7.1320	269.5	15	5
cssz–35a	Central and South America	280.0039	7.6543	255.9	17.67	14.54
cssz–35b	Central and South America	280.1090	7.2392	255.9	11	5
cssz–35x	Central and South America	279.7156	8.7898	255.9	29.67	79.22
cssz–35y	Central and South America	279.8118	8.4113	255.9	29.67	54.47
cssz–35z	Central and South America	279.9079	8.0328	255.9	29.67	29.72
cssz–36a	Central and South America	281.2882	7.6778	282.5	17.33	11.09

(continued on next page)

Table B2: (continued)

Segment	Description	Longitude (°E)	Latitude (°N)	Strike (°)	Dip (°)	Depth (km)
cssz–36b	Central and South America	281.1948	7.2592	282.5	7	5
cssz–36x	Central and South America	281.5368	8.7896	282.5	32.33	79.47
cssz–36y	Central and South America	281.4539	8.4190	282.5	32.33	52.73
cssz–36z	Central and South America	281.3710	8.0484	282.5	32.33	25.99
cssz–37a	Central and South America	282.5252	6.8289	326.9	17	10.23
cssz–37b	Central and South America	282.1629	6.5944	326.9	6	5
cssz–38a	Central and South America	282.9469	5.5973	355.4	17	10.23
cssz–38b	Central and South America	282.5167	5.5626	355.4	6	5
cssz–39a	Central and South America	282.7236	4.3108	24.13	17	10.23
cssz–39b	Central and South America	282.3305	4.4864	24.13	6	5
cssz–39z	Central and South America	283.0603	4.1604	24.13	35	24.85
cssz–40a	Central and South America	282.1940	3.3863	35.28	17	10.23
cssz–40b	Central and South America	281.8427	3.6344	35.28	6	5
cssz–40y	Central and South America	282.7956	2.9613	35.28	35	53.52
cssz–40z	Central and South America	282.4948	3.1738	35.28	35	24.85
cssz–41a	Central and South America	281.6890	2.6611	34.27	17	10.23
cssz–41b	Central and South America	281.3336	2.9030	34.27	6	5
cssz–41z	Central and South America	281.9933	2.4539	34.27	35	24.85
cssz–42a	Central and South America	281.2266	1.9444	31.29	17	10.23
cssz–42b	Central and South America	280.8593	2.1675	31.29	6	5
cssz–42z	Central and South America	281.5411	1.7533	31.29	35	24.85
cssz–43a	Central and South America	280.7297	1.1593	33.3	17	10.23
cssz–43b	Central and South America	280.3706	1.3951	33.3	6	5
cssz–43z	Central and South America	281.0373	0.9573	33.3	35	24.85
cssz–44a	Central and South America	280.3018	0.4491	28.8	17	10.23
cssz–44b	Central and South America	279.9254	0.6560	28.8	6	5
cssz–45a	Central and South America	279.9083	–0.3259	26.91	10	8.49
cssz–45b	Central and South America	279.5139	–0.1257	26.91	4	5
cssz–46a	Central and South America	279.6461	–0.9975	15.76	10	8.49
cssz–46b	Central and South America	279.2203	–0.8774	15.76	4	5
cssz–47a	Central and South America	279.4972	–1.7407	6.9	10	8.49
cssz–47b	Central and South America	279.0579	–1.6876	6.9	4	5
cssz–48a	Central and South America	279.3695	–2.6622	8.96	10	8.49
cssz–48b	Central and South America	278.9321	–2.5933	8.96	4	5
cssz–48y	Central and South America	280.2444	–2.8000	8.96	10	25.85
cssz–48z	Central and South America	279.8070	–2.7311	8.96	10	17.17
cssz–49a	Central and South America	279.1852	–3.6070	13.15	10	8.49
cssz–49b	Central and South America	278.7536	–3.5064	13.15	4	5
cssz–49y	Central and South America	280.0486	–3.8082	13.15	10	25.85
cssz–49z	Central and South America	279.6169	–3.7076	13.15	10	17.17
cssz–50a	Central and South America	279.0652	–4.3635	4.78	10.33	9.64
cssz–50b	Central and South America	278.6235	–4.3267	4.78	5.33	5
cssz–51a	Central and South America	279.0349	–5.1773	359.4	10.67	10.81
cssz–51b	Central and South America	278.5915	–5.1817	359.4	6.67	5
cssz–52a	Central and South America	279.1047	–5.9196	349.8	11	11.96
cssz–52b	Central and South America	278.6685	–5.9981	349.8	8	5
cssz–53a	Central and South America	279.3044	–6.6242	339.2	10.25	11.74
cssz–53b	Central and South America	278.8884	–6.7811	339.2	7.75	5
cssz–53y	Central and South America	280.1024	–6.3232	339.2	19.25	37.12
cssz–53z	Central and South America	279.7035	–6.4737	339.2	19.25	20.64
cssz–54a	Central and South America	279.6256	–7.4907	340.8	9.5	11.53
cssz–54b	Central and South America	279.2036	–7.6365	340.8	7.5	5
cssz–54y	Central and South America	280.4267	–7.2137	340.8	20.5	37.29
cssz–54z	Central and South America	280.0262	–7.3522	340.8	20.5	19.78
cssz–55a	Central and South America	279.9348	–8.2452	335.4	8.75	11.74

(continued on next page)

Table B2: (continued)

Segment	Description	Longitude (°E)	Latitude (°N)	Strike (°)	Dip (°)	Depth (km)
cssz–55b	Central and South America	279.5269	–8.4301	335.4	7.75	5
cssz–55x	Central and South America	281.0837	–7.7238	335.4	21.75	56.4
cssz–55y	Central and South America	280.7009	–7.8976	335.4	21.75	37.88
cssz–55z	Central and South America	280.3180	–8.0714	335.4	21.75	19.35
cssz–56a	Central and South America	280.3172	–8.9958	331.6	8	11.09
cssz–56b	Central and South America	279.9209	–9.2072	331.6	7	5
cssz–56x	Central and South America	281.4212	–8.4063	331.6	23	57.13
cssz–56y	Central and South America	281.0534	–8.6028	331.6	23	37.59
cssz–56z	Central and South America	280.6854	–8.7993	331.6	23	18.05
cssz–57a	Central and South America	280.7492	–9.7356	328.7	8.6	10.75
cssz–57b	Central and South America	280.3640	–9.9663	328.7	6.6	5
cssz–57x	Central and South America	281.8205	–9.0933	328.7	23.4	57.94
cssz–57y	Central and South America	281.4636	–9.3074	328.7	23.4	38.08
cssz–57z	Central and South America	281.1065	–9.5215	328.7	23.4	18.22
cssz–58a	Central and South America	281.2275	–10.5350	330.5	9.2	10.4
cssz–58b	Central and South America	280.8348	–10.7532	330.5	6.2	5
cssz–58y	Central and South America	281.9548	–10.1306	330.5	23.8	38.57
cssz–58z	Central and South America	281.5913	–10.3328	330.5	23.8	18.39
cssz–59a	Central and South America	281.6735	–11.2430	326.2	9.8	10.05
cssz–59b	Central and South America	281.2982	–11.4890	326.2	5.8	5
cssz–59y	Central and South America	282.3675	–10.7876	326.2	24.2	39.06
cssz–59z	Central and South America	282.0206	–11.0153	326.2	24.2	18.56
cssz–60a	Central and South America	282.1864	–11.9946	326.5	10.4	9.71
cssz–60b	Central and South America	281.8096	–12.2384	326.5	5.4	5
cssz–60y	Central and South America	282.8821	–11.5438	326.5	24.6	39.55
cssz–60z	Central and South America	282.5344	–11.7692	326.5	24.6	18.73
cssz–61a	Central and South America	282.6944	–12.7263	325.5	11	9.36
cssz–61b	Central and South America	282.3218	–12.9762	325.5	5	5
cssz–61y	Central and South America	283.3814	–12.2649	325.5	25	40.03
cssz–61z	Central and South America	283.0381	–12.4956	325.5	25	18.9
cssz–62a	Central and South America	283.1980	–13.3556	319	11	9.79
cssz–62b	Central and South America	282.8560	–13.6451	319	5.5	5
cssz–62y	Central and South America	283.8178	–12.8300	319	27	42.03
cssz–62z	Central and South America	283.5081	–13.0928	319	27	19.33
cssz–63a	Central and South America	283.8032	–14.0147	317.9	11	10.23
cssz–63b	Central and South America	283.4661	–14.3106	317.9	6	5
cssz–63z	Central and South America	284.1032	–13.7511	317.9	29	19.77
cssz–64a	Central and South America	284.4144	–14.6482	315.7	13	11.96
cssz–64b	Central and South America	284.0905	–14.9540	315.7	8	5
cssz–65a	Central and South America	285.0493	–15.2554	313.2	15	13.68
cssz–65b	Central and South America	284.7411	–15.5715	313.2	10	5
cssz–66a	Central and South America	285.6954	–15.7816	307.7	14.5	13.68
cssz–66b	Central and South America	285.4190	–16.1258	307.7	10	5
cssz–67a	Central and South America	286.4127	–16.2781	304.3	14	13.68
cssz–67b	Central and South America	286.1566	–16.6381	304.3	10	5
cssz–67z	Central and South America	286.6552	–15.9365	304.3	23	25.78
cssz–68a	Central and South America	287.2481	–16.9016	311.8	14	13.68
cssz–68b	Central and South America	286.9442	–17.2264	311.8	10	5
cssz–68z	Central and South America	287.5291	–16.6007	311.8	26	25.78
cssz–69a	Central and South America	287.9724	–17.5502	314.9	14	13.68
cssz–69b	Central and South America	287.6496	–17.8590	314.9	10	5
cssz–69y	Central and South America	288.5530	–16.9934	314.9	29	50.02
cssz–69z	Central and South America	288.2629	–17.2718	314.9	29	25.78
cssz–70a	Central and South America	288.6731	–18.2747	320.4	14	13.25
cssz–70b	Central and South America	288.3193	–18.5527	320.4	9.5	5

(continued on next page)

Table B2: (continued)

Segment	Description	Longitude (°E)	Latitude (°N)	Strike (°)	Dip (°)	Depth (km)
cssz–70y	Central and South America	289.3032	–17.7785	320.4	30	50.35
cssz–70z	Central and South America	288.9884	–18.0266	320.4	30	25.35
cssz–71a	Central and South America	289.3089	–19.1854	333.2	14	12.82
cssz–71b	Central and South America	288.8968	–19.3820	333.2	9	5
cssz–71y	Central and South America	290.0357	–18.8382	333.2	31	50.67
cssz–71z	Central and South America	289.6725	–19.0118	333.2	31	24.92
cssz–72a	Central and South America	289.6857	–20.3117	352.4	14	12.54
cssz–72b	Central and South America	289.2250	–20.3694	352.4	8.67	5
cssz–72z	Central and South America	290.0882	–20.2613	352.4	32	24.63
cssz–73a	Central and South America	289.7731	–21.3061	358.9	14	12.24
cssz–73b	Central and South America	289.3053	–21.3142	358.9	8.33	5
cssz–73z	Central and South America	290.1768	–21.2991	358.9	33	24.34
cssz–74a	Central and South America	289.7610	–22.2671	3.06	14	11.96
cssz–74b	Central and South America	289.2909	–22.2438	3.06	8	5
cssz–75a	Central and South America	289.6982	–23.1903	4.83	14.09	11.96
cssz–75b	Central and South America	289.2261	–23.1536	4.83	8	5
cssz–76a	Central and South America	289.6237	–24.0831	4.67	14.18	11.96
cssz–76b	Central and South America	289.1484	–24.0476	4.67	8	5
cssz–77a	Central and South America	289.5538	–24.9729	4.3	14.27	11.96
cssz–77b	Central and South America	289.0750	–24.9403	4.3	8	5
cssz–78a	Central and South America	289.4904	–25.8621	3.86	14.36	11.96
cssz–78b	Central and South America	289.0081	–25.8328	3.86	8	5
cssz–79a	Central and South America	289.3491	–26.8644	11.34	14.45	11.96
cssz–79b	Central and South America	288.8712	–26.7789	11.34	8	5
cssz–80a	Central and South America	289.1231	–27.7826	14.16	14.54	11.96
cssz–80b	Central and South America	288.6469	–27.6762	14.16	8	5
cssz–81a	Central and South America	288.8943	–28.6409	13.19	14.63	11.96
cssz–81b	Central and South America	288.4124	–28.5417	13.19	8	5
cssz–82a	Central and South America	288.7113	–29.4680	9.68	14.72	11.96
cssz–82b	Central and South America	288.2196	–29.3950	9.68	8	5
cssz–83a	Central and South America	288.5944	–30.2923	5.36	14.81	11.96
cssz–83b	Central and South America	288.0938	–30.2517	5.36	8	5
cssz–84a	Central and South America	288.5223	–31.1639	3.8	14.9	11.96
cssz–84b	Central and South America	288.0163	–31.1351	3.8	8	5
cssz–85a	Central and South America	288.4748	–32.0416	2.55	15	11.96
cssz–85b	Central and South America	287.9635	–32.0223	2.55	8	5
cssz–86a	Central and South America	288.3901	–33.0041	7.01	15	11.96
cssz–86b	Central and South America	287.8768	–32.9512	7.01	8	5
cssz–87a	Central and South America	288.1050	–34.0583	19.4	15	11.96
cssz–87b	Central and South America	287.6115	–33.9142	19.4	8	5
cssz–88a	Central and South America	287.5309	–35.0437	32.81	15	11.96
cssz–88b	Central and South America	287.0862	–34.8086	32.81	8	5
cssz–88z	Central and South America	287.9308	–35.2545	32.81	30	24.9
cssz–89a	Central and South America	287.2380	–35.5993	14.52	16.67	11.96
cssz–89b	Central and South America	286.7261	–35.4914	14.52	8	5
cssz–89z	Central and South America	287.7014	–35.6968	14.52	30	26.3
cssz–90a	Central and South America	286.8442	–36.5645	22.64	18.33	11.96
cssz–90b	Central and South America	286.3548	–36.4004	22.64	8	5
cssz–90z	Central and South America	287.2916	–36.7142	22.64	30	27.68
cssz–91a	Central and South America	286.5925	–37.2488	10.9	20	11.96
cssz–91b	Central and South America	286.0721	–37.1690	10.9	8	5
cssz–91z	Central and South America	287.0726	–37.3224	10.9	30	29.06
cssz–92a	Central and South America	286.4254	–38.0945	8.23	20	11.96
cssz–92b	Central and South America	285.8948	–38.0341	8.23	8	5
cssz–92z	Central and South America	286.9303	–38.1520	8.23	26.67	29.06

(continued on next page)

Table B2: (continued)

Segment	Description	Longitude (°E)	Latitude (°N)	Strike (°)	Dip (°)	Depth (km)
cssz–93a	Central and South America	286.2047	–39.0535	13.46	20	11.96
cssz–93b	Central and South America	285.6765	–38.9553	13.46	8	5
cssz–93z	Central and South America	286.7216	–39.1495	13.46	23.33	29.06
cssz–94a	Central and South America	286.0772	–39.7883	3.4	20	11.96
cssz–94b	Central and South America	285.5290	–39.7633	3.4	8	5
cssz–94z	Central and South America	286.6255	–39.8133	3.4	20	29.06
cssz–95a	Central and South America	285.9426	–40.7760	9.84	20	11.96
cssz–95b	Central and South America	285.3937	–40.7039	9.84	8	5
cssz–95z	Central and South America	286.4921	–40.8481	9.84	20	29.06
cssz–96a	Central and South America	285.7839	–41.6303	7.6	20	11.96
cssz–96b	Central and South America	285.2245	–41.5745	7.6	8	5
cssz–96x	Central and South America	287.4652	–41.7977	7.6	20	63.26
cssz–96y	Central and South America	286.9043	–41.7419	7.6	20	46.16
cssz–96z	Central and South America	286.3439	–41.6861	7.6	20	29.06
cssz–97a	Central and South America	285.6695	–42.4882	5.3	20	11.96
cssz–97b	Central and South America	285.0998	–42.4492	5.3	8	5
cssz–97x	Central and South America	287.3809	–42.6052	5.3	20	63.26
cssz–97y	Central and South America	286.8101	–42.5662	5.3	20	46.16
cssz–97z	Central and South America	286.2396	–42.5272	5.3	20	29.06
cssz–98a	Central and South America	285.5035	–43.4553	10.53	20	11.96
cssz–98b	Central and South America	284.9322	–43.3782	10.53	8	5
cssz–98x	Central and South America	287.2218	–43.6866	10.53	20	63.26
cssz–98y	Central and South America	286.6483	–43.6095	10.53	20	46.16
cssz–98z	Central and South America	286.0755	–43.5324	10.53	20	29.06
cssz–99a	Central and South America	285.3700	–44.2595	4.86	20	11.96
cssz–99b	Central and South America	284.7830	–44.2237	4.86	8	5
cssz–99x	Central and South America	287.1332	–44.3669	4.86	20	63.26
cssz–99y	Central and South America	286.5451	–44.3311	4.86	20	46.16
cssz–99z	Central and South America	285.9574	–44.2953	4.86	20	29.06
cssz–100a	Central and South America	285.2713	–45.1664	5.68	20	11.96
cssz–100b	Central and South America	284.6758	–45.1246	5.68	8	5
cssz–100x	Central and South America	287.0603	–45.2918	5.68	20	63.26
cssz–100y	Central and South America	286.4635	–45.2500	5.68	20	46.16
cssz–100z	Central and South America	285.8672	–45.2082	5.68	20	29.06
cssz–101a	Central and South America	285.3080	–45.8607	352.6	20	9.36
cssz–101b	Central and South America	284.7067	–45.9152	352.6	5	5
cssz–101y	Central and South America	286.5089	–45.7517	352.6	20	43.56
cssz–101z	Central and South America	285.9088	–45.8062	352.6	20	26.46
cssz–102a	Central and South America	285.2028	–47.1185	17.72	5	9.36
cssz–102b	Central and South America	284.5772	–46.9823	17.72	5	5
cssz–102y	Central and South America	286.4588	–47.3909	17.72	5	18.07
cssz–102z	Central and South America	285.8300	–47.2547	17.72	5	13.72
cssz–103a	Central and South America	284.7075	–48.0396	23.37	7.5	11.53
cssz–103b	Central and South America	284.0972	–47.8630	23.37	7.5	5
cssz–103x	Central and South America	286.5511	–48.5694	23.37	7.5	31.11
cssz–103y	Central and South America	285.9344	–48.3928	23.37	7.5	24.58
cssz–103z	Central and South America	285.3199	–48.2162	23.37	7.5	18.05
cssz–104a	Central and South America	284.3440	–48.7597	14.87	10	13.68
cssz–104b	Central and South America	283.6962	–48.6462	14.87	10	5
cssz–104x	Central and South America	286.2962	–49.1002	14.87	10	39.73
cssz–104y	Central and South America	285.6440	–48.9867	14.87	10	31.05
cssz–104z	Central and South America	284.9933	–48.8732	14.87	10	22.36
cssz–105a	Central and South America	284.2312	–49.4198	0.25	9.67	13.4
cssz–105b	Central and South America	283.5518	–49.4179	0.25	9.67	5
cssz–105x	Central and South America	286.2718	–49.4255	0.25	9.67	38.59

(continued on next page)

Table B2: (continued)

Segment	Description	Longitude (°E)	Latitude (°N)	Strike (°)	Dip (°)	Depth (km)
cssz–105y	Central and South America	285.5908	–49.4236	0.25	9.67	30.2
cssz–105z	Central and South America	284.9114	–49.4217	0.25	9.67	21.8
cssz–106a	Central and South America	284.3730	–50.1117	347.5	9.25	13.04
cssz–106b	Central and South America	283.6974	–50.2077	347.5	9.25	5
cssz–106x	Central and South America	286.3916	–49.8238	347.5	9.25	37.15
cssz–106y	Central and South America	285.7201	–49.9198	347.5	9.25	29.11
cssz–106z	Central and South America	285.0472	–50.0157	347.5	9.25	21.07
cssz–107a	Central and South America	284.7130	–50.9714	346.5	9	12.82
cssz–107b	Central and South America	284.0273	–51.0751	346.5	9	5
cssz–107x	Central and South America	286.7611	–50.6603	346.5	9	36.29
cssz–107y	Central and South America	286.0799	–50.7640	346.5	9	28.47
cssz–107z	Central and South America	285.3972	–50.8677	346.5	9	20.64
cssz–108a	Central and South America	285.0378	–51.9370	352	8.67	12.54
cssz–108b	Central and South America	284.3241	–51.9987	352	8.67	5
cssz–108x	Central and South America	287.1729	–51.7519	352	8.67	35.15
cssz–108y	Central and South America	286.4622	–51.8136	352	8.67	27.61
cssz–108z	Central and South America	285.7505	–51.8753	352	8.67	20.07
cssz–109a	Central and South America	285.2635	–52.8439	353.1	8.33	12.24
cssz–109b	Central and South America	284.5326	–52.8974	353.1	8.33	5
cssz–109x	Central and South America	287.4508	–52.6834	353.1	8.33	33.97
cssz–109y	Central and South America	286.7226	–52.7369	353.1	8.33	26.73
cssz–109z	Central and South America	285.9935	–52.7904	353.1	8.33	19.49
cssz–110a	Central and South America	285.5705	–53.4139	334.2	8	11.96
cssz–110b	Central and South America	284.8972	–53.6076	334.2	8	5
cssz–110x	Central and South America	287.5724	–52.8328	334.2	8	32.83
cssz–110y	Central and South America	286.9081	–53.0265	334.2	8	25.88
cssz–110z	Central and South America	286.2408	–53.2202	334.2	8	18.92
cssz–111a	Central and South America	286.1627	–53.8749	313.8	8	11.96
cssz–111b	Central and South America	285.6382	–54.1958	313.8	8	5
cssz–111x	Central and South America	287.7124	–52.9122	313.8	8	32.83
cssz–111y	Central and South America	287.1997	–53.2331	313.8	8	25.88
cssz–111z	Central and South America	286.6832	–53.5540	313.8	8	18.92
cssz–112a	Central and South America	287.3287	–54.5394	316.4	8	11.96
cssz–112b	Central and South America	286.7715	–54.8462	316.4	8	5
cssz–112x	Central and South America	288.9756	–53.6190	316.4	8	32.83
cssz–112y	Central and South America	288.4307	–53.9258	316.4	8	25.88
cssz–112z	Central and South America	287.8817	–54.2326	316.4	8	18.92
cssz–113a	Central and South America	288.3409	–55.0480	307.6	8	11.96
cssz–113b	Central and South America	287.8647	–55.4002	307.6	8	5
cssz–113x	Central and South America	289.7450	–53.9914	307.6	8	32.83
cssz–113y	Central and South America	289.2810	–54.3436	307.6	8	25.88
cssz–113z	Central and South America	288.8130	–54.6958	307.6	8	18.92
cssz–114a	Central and South America	289.5342	–55.5026	301.5	8	11.96
cssz–114b	Central and South America	289.1221	–55.8819	301.5	8	5
cssz–114x	Central and South America	290.7472	–54.3647	301.5	8	32.83
cssz–114y	Central and South America	290.3467	–54.7440	301.5	8	25.88
cssz–114z	Central and South America	289.9424	–55.1233	301.5	8	18.92
cssz–115a	Central and South America	290.7682	–55.8485	292.7	8	11.96
cssz–115b	Central and South America	290.4608	–56.2588	292.7	8	5
cssz–115x	Central and South America	291.6714	–54.6176	292.7	8	32.83
cssz–115y	Central and South America	291.3734	–55.0279	292.7	8	25.88
cssz–115z	Central and South America	291.0724	–55.4382	292.7	8	18.92

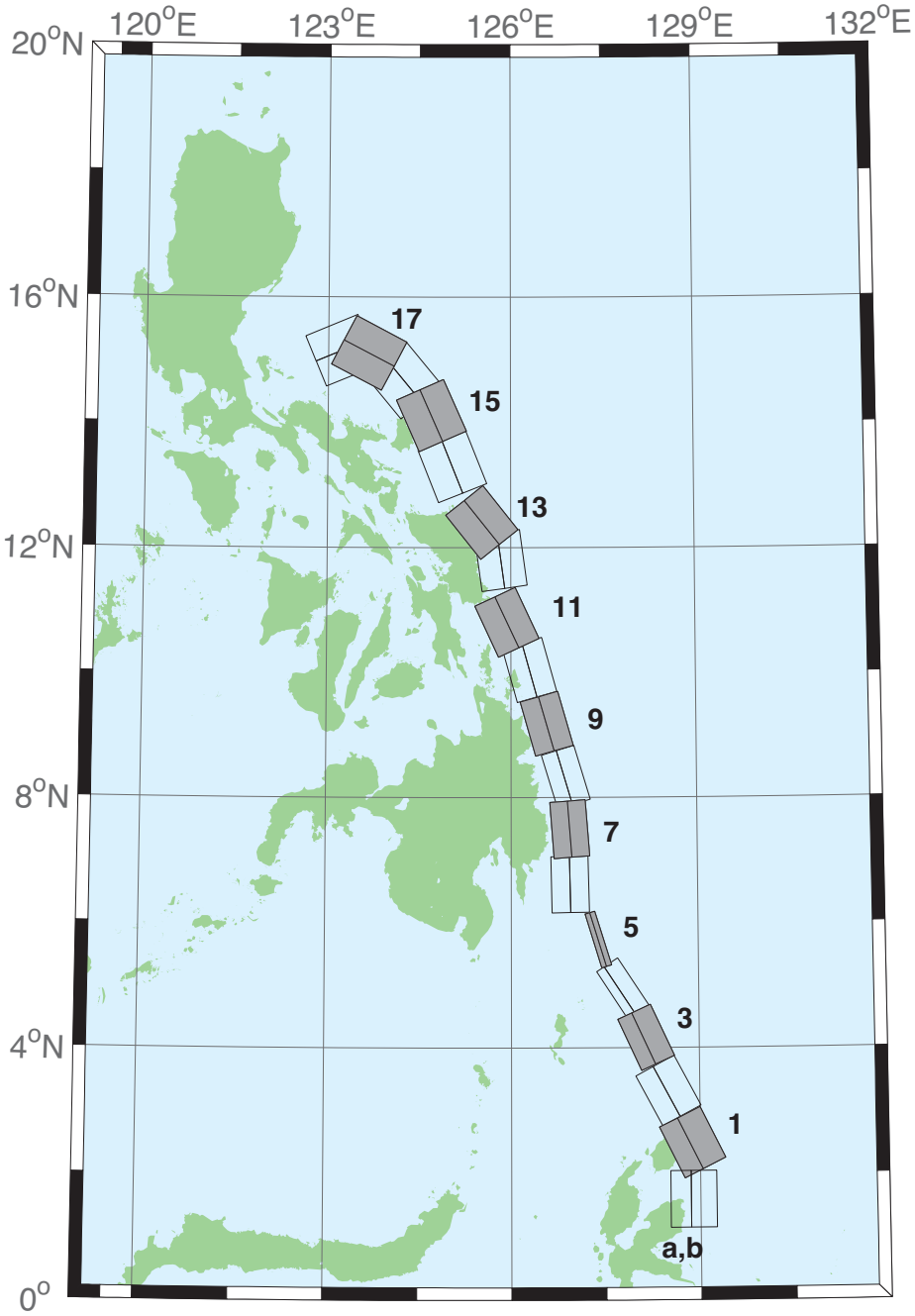

Figure B3: Eastern Philippines Subduction Zone unit sources.

Table B3: Earthquake parameters for Eastern Philippines Subduction Zone unit sources.

Segment	Description	Longitude (°E)	Latitude (°N)	Strike (°)	Dip (°)	Depth (km)
epsz–0a	Eastern Philippines	128.5264	1.5930	180	44	26.92
epsz–0b	Eastern Philippines	128.8496	1.5930	180	26	5
epsz–1a	Eastern Philippines	128.5521	2.3289	153.6	44.2	27.62
epsz–1b	Eastern Philippines	128.8408	2.4720	153.6	26.9	5
epsz–2a	Eastern Philippines	128.1943	3.1508	151.9	45.9	32.44
epsz–2b	Eastern Philippines	128.4706	3.2979	151.9	32.8	5.35
epsz–3a	Eastern Philippines	127.8899	4.0428	155.2	57.3	40.22
epsz–3b	Eastern Philippines	128.1108	4.1445	155.2	42.7	6.31
epsz–4a	Eastern Philippines	127.6120	4.8371	146.8	71.4	48.25
epsz–4b	Eastern Philippines	127.7324	4.9155	146.8	54.8	7.39
epsz–5a	Eastern Philippines	127.3173	5.7040	162.9	79.9	57.4
epsz–5b	Eastern Philippines	127.3930	5.7272	162.9	79.4	8.25
epsz–6a	Eastern Philippines	126.6488	6.6027	178.9	48.6	45.09
epsz–6b	Eastern Philippines	126.9478	6.6085	178.9	48.6	7.58
epsz–7a	Eastern Philippines	126.6578	7.4711	175.8	50.7	45.52
epsz–7b	Eastern Philippines	126.9439	7.4921	175.8	50.7	6.83
epsz–8a	Eastern Philippines	126.6227	8.2456	163.3	56.7	45.6
epsz–8b	Eastern Philippines	126.8614	8.3164	163.3	48.9	7.92
epsz–9a	Eastern Philippines	126.2751	9.0961	164.1	47	43.59
epsz–9b	Eastern Philippines	126.5735	9.1801	164.1	44.9	8.3
epsz–10a	Eastern Philippines	125.9798	9.9559	164.5	43.1	42.25
epsz–10b	Eastern Philippines	126.3007	10.0438	164.5	43.1	8.09
epsz–11a	Eastern Philippines	125.6079	10.6557	155	37.8	38.29
epsz–11b	Eastern Philippines	125.9353	10.8059	155	37.8	7.64
epsz–12a	Eastern Philippines	125.4697	11.7452	172.1	36	37.01
epsz–12b	Eastern Philippines	125.8374	11.7949	172.1	36	7.62
epsz–13a	Eastern Philippines	125.2238	12.1670	141.5	32.4	33.87
epsz–13b	Eastern Philippines	125.5278	12.4029	141.5	32.4	7.08
epsz–14a	Eastern Philippines	124.6476	13.1365	158.2	23	25.92
epsz–14b	Eastern Philippines	125.0421	13.2898	158.2	23	6.38
epsz–15a	Eastern Philippines	124.3107	13.9453	156.1	24.1	26.51
epsz–15b	Eastern Philippines	124.6973	14.1113	156.1	24.1	6.09
epsz–16a	Eastern Philippines	123.8998	14.4025	140.3	19.5	21.69
epsz–16b	Eastern Philippines	124.2366	14.6728	140.3	19.5	5
epsz–17a	Eastern Philippines	123.4604	14.7222	117.6	15.3	18.19
epsz–17b	Eastern Philippines	123.6682	15.1062	117.6	15.3	5
epsz–18a	Eastern Philippines	123.3946	14.7462	67.4	15	17.94
epsz–18b	Eastern Philippines	123.2219	15.1467	67.4	15	5

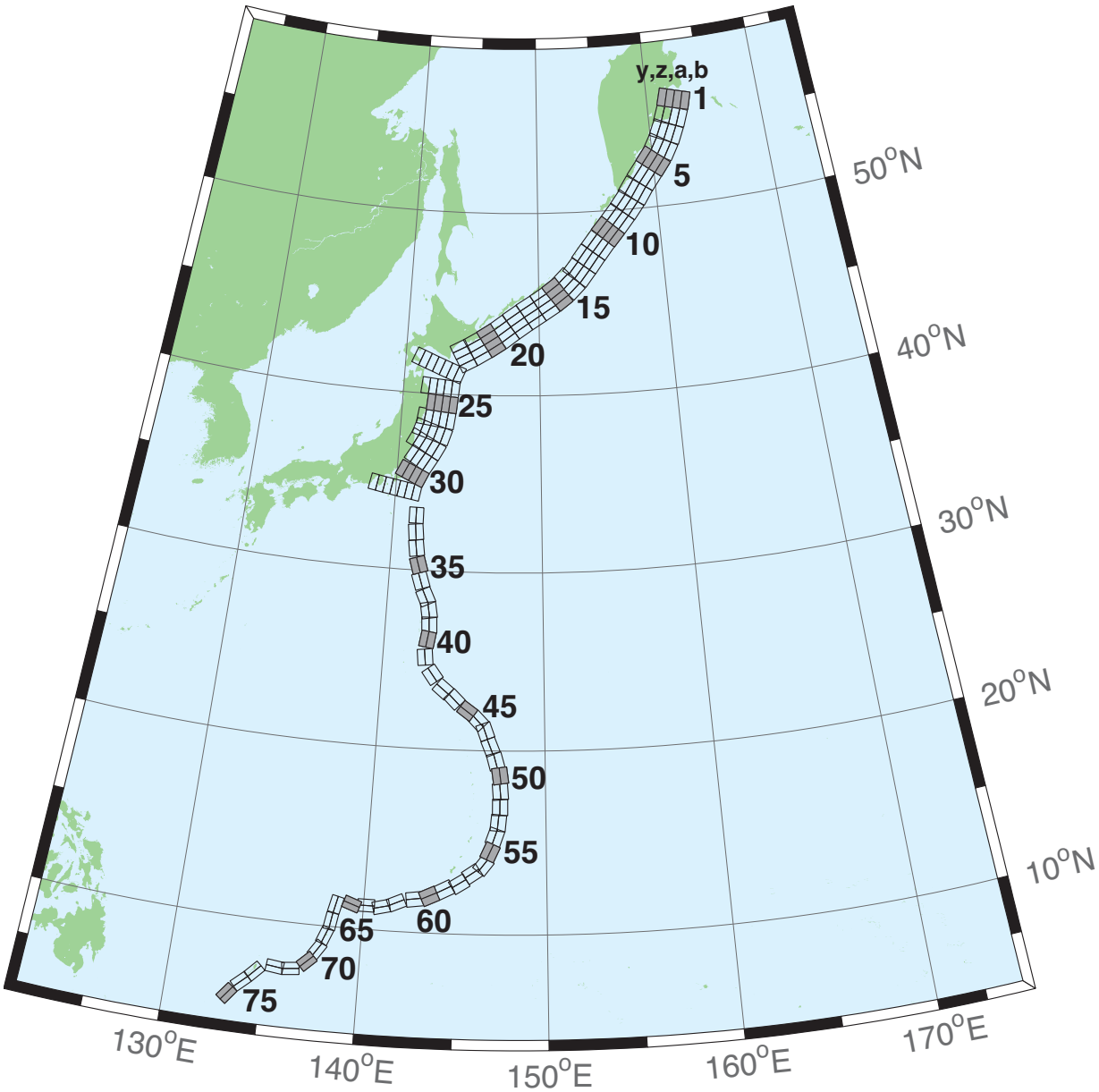

Figure B4: Kamchatka-Kuril-Japan-Izu-Mariana-Yap Subduction Zone unit sources.

Table B4: Earthquake parameters for Kamchatka-Kuril-Japan-Izu-Mariana-Yap Subduction Zone unit sources.

Segment	Description	Longitude (°E)	Latitude (°N)	Strike (°)	Dip (°)	Depth (km)
kisz–1a	Kamchatka-Kuril-Japan-Izu-Mariana-Yap	162.4318	55.5017	195	29	26.13
kisz–1b	Kamchatka-Kuril-Japan-Izu-Mariana-Yap	163.1000	55.4000	195	25	5
kisz–1y	Kamchatka-Kuril-Japan-Izu-Mariana-Yap	161.0884	55.7050	195	29	74.61
kisz–1z	Kamchatka-Kuril-Japan-Izu-Mariana-Yap	161.7610	55.6033	195	29	50.37
kisz–2a	Kamchatka-Kuril-Japan-Izu-Mariana-Yap	161.9883	54.6784	200	29	26.13
kisz–2b	Kamchatka-Kuril-Japan-Izu-Mariana-Yap	162.6247	54.5440	200	25	5
kisz–2y	Kamchatka-Kuril-Japan-Izu-Mariana-Yap	160.7072	54.9471	200	29	74.61
kisz–2z	Kamchatka-Kuril-Japan-Izu-Mariana-Yap	161.3488	54.8127	200	29	50.37
kisz–3a	Kamchatka-Kuril-Japan-Izu-Mariana-Yap	161.4385	53.8714	204	29	26.13
kisz–3b	Kamchatka-Kuril-Japan-Izu-Mariana-Yap	162.0449	53.7116	204	25	5
kisz–3y	Kamchatka-Kuril-Japan-Izu-Mariana-Yap	160.2164	54.1910	204	29	74.61
kisz–3z	Kamchatka-Kuril-Japan-Izu-Mariana-Yap	160.8286	54.0312	204	29	50.37
kisz–4a	Kamchatka-Kuril-Japan-Izu-Mariana-Yap	160.7926	53.1087	210	29	26.13
kisz–4b	Kamchatka-Kuril-Japan-Izu-Mariana-Yap	161.3568	52.9123	210	25	5
kisz–4y	Kamchatka-Kuril-Japan-Izu-Mariana-Yap	159.6539	53.5015	210	29	74.61
kisz–4z	Kamchatka-Kuril-Japan-Izu-Mariana-Yap	160.2246	53.3051	210	29	50.37
kisz–5a	Kamchatka-Kuril-Japan-Izu-Mariana-Yap	160.0211	52.4113	218	29	26.13
kisz–5b	Kamchatka-Kuril-Japan-Izu-Mariana-Yap	160.5258	52.1694	218	25	5
kisz–5y	Kamchatka-Kuril-Japan-Izu-Mariana-Yap	159.0005	52.8950	218	29	74.61
kisz–5z	Kamchatka-Kuril-Japan-Izu-Mariana-Yap	159.5122	52.6531	218	29	50.37
kisz–6a	Kamchatka-Kuril-Japan-Izu-Mariana-Yap	159.1272	51.7034	218	29	26.13
kisz–6b	Kamchatka-Kuril-Japan-Izu-Mariana-Yap	159.6241	51.4615	218	25	5
kisz–6y	Kamchatka-Kuril-Japan-Izu-Mariana-Yap	158.1228	52.1871	218	29	74.61
kisz–6z	Kamchatka-Kuril-Japan-Izu-Mariana-Yap	158.6263	51.9452	218	29	50.37
kisz–7a	Kamchatka-Kuril-Japan-Izu-Mariana-Yap	158.2625	50.9549	214	29	26.13
kisz–7b	Kamchatka-Kuril-Japan-Izu-Mariana-Yap	158.7771	50.7352	214	25	5
kisz–7y	Kamchatka-Kuril-Japan-Izu-Mariana-Yap	157.2236	51.3942	214	29	74.61
kisz–7z	Kamchatka-Kuril-Japan-Izu-Mariana-Yap	157.7443	51.1745	214	29	50.37
kisz–8a	Kamchatka-Kuril-Japan-Izu-Mariana-Yap	157.4712	50.2459	218	31	27.7
kisz–8b	Kamchatka-Kuril-Japan-Izu-Mariana-Yap	157.9433	50.0089	218	27	5
kisz–8y	Kamchatka-Kuril-Japan-Izu-Mariana-Yap	156.5176	50.7199	218	31	79.2
kisz–8z	Kamchatka-Kuril-Japan-Izu-Mariana-Yap	156.9956	50.4829	218	31	53.45
kisz–9a	Kamchatka-Kuril-Japan-Izu-Mariana-Yap	156.6114	49.5583	220	31	27.7
kisz–9b	Kamchatka-Kuril-Japan-Izu-Mariana-Yap	157.0638	49.3109	220	27	5
kisz–9y	Kamchatka-Kuril-Japan-Izu-Mariana-Yap	155.6974	50.0533	220	31	79.2
kisz–9z	Kamchatka-Kuril-Japan-Izu-Mariana-Yap	156.1556	49.8058	220	31	53.45
kisz–10a	Kamchatka-Kuril-Japan-Izu-Mariana-Yap	155.7294	48.8804	221	31	27.7
kisz–10b	Kamchatka-Kuril-Japan-Izu-Mariana-Yap	156.1690	48.6278	221	27	5
kisz–10y	Kamchatka-Kuril-Japan-Izu-Mariana-Yap	154.8413	49.3856	221	31	79.2
kisz–10z	Kamchatka-Kuril-Japan-Izu-Mariana-Yap	155.2865	49.1330	221	31	53.45
kisz–11a	Kamchatka-Kuril-Japan-Izu-Mariana-Yap	154.8489	48.1821	219	31	27.7
kisz–11b	Kamchatka-Kuril-Japan-Izu-Mariana-Yap	155.2955	47.9398	219	27	5
kisz–11y	Kamchatka-Kuril-Japan-Izu-Mariana-Yap	153.9472	48.6667	219	31	79.2
kisz–11z	Kamchatka-Kuril-Japan-Izu-Mariana-Yap	154.3991	48.4244	219	31	53.45
kisz–12a	Kamchatka-Kuril-Japan-Izu-Mariana-Yap	153.9994	47.4729	217	31	27.7
kisz–12b	Kamchatka-Kuril-Japan-Izu-Mariana-Yap	154.4701	47.2320	217	27	5
kisz–12y	Kamchatka-Kuril-Japan-Izu-Mariana-Yap	153.0856	47.9363	217	31	79.2
kisz–12z	Kamchatka-Kuril-Japan-Izu-Mariana-Yap	153.5435	47.7046	217	31	53.45
kisz–13a	Kamchatka-Kuril-Japan-Izu-Mariana-Yap	153.2239	46.7564	218	31	27.7
kisz–13b	Kamchatka-Kuril-Japan-Izu-Mariana-Yap	153.6648	46.5194	218	27	5
kisz–13y	Kamchatka-Kuril-Japan-Izu-Mariana-Yap	152.3343	47.2304	218	31	79.2
kisz–13z	Kamchatka-Kuril-Japan-Izu-Mariana-Yap	152.7801	46.9934	218	31	53.45
kisz–14a	Kamchatka-Kuril-Japan-Izu-Mariana-Yap	152.3657	46.1514	225	23	24.54
kisz–14b	Kamchatka-Kuril-Japan-Izu-Mariana-Yap	152.7855	45.8591	225	23	5

(continued on next page)

Table B4: (continued)

Segment	Description	Longitude (°E)	Latitude (°N)	Strike (°)	Dip (°)	Depth (km)
kisz–14y	Kamchatka-Kuril-Japan-Izu-Mariana-Yap	151.5172	46.7362	225	23	63.62
kisz–14z	Kamchatka-Kuril-Japan-Izu-Mariana-Yap	151.9426	46.4438	225	23	44.08
kisz–15a	Kamchatka-Kuril-Japan-Izu-Mariana-Yap	151.4663	45.5963	233	25	23.73
kisz–15b	Kamchatka-Kuril-Japan-Izu-Mariana-Yap	151.8144	45.2712	233	22	5
kisz–15y	Kamchatka-Kuril-Japan-Izu-Mariana-Yap	150.7619	46.2465	233	25	65.99
kisz–15z	Kamchatka-Kuril-Japan-Izu-Mariana-Yap	151.1151	45.9214	233	25	44.86
kisz–16a	Kamchatka-Kuril-Japan-Izu-Mariana-Yap	150.4572	45.0977	237	25	23.73
kisz–16b	Kamchatka-Kuril-Japan-Izu-Mariana-Yap	150.7694	44.7563	237	22	5
kisz–16y	Kamchatka-Kuril-Japan-Izu-Mariana-Yap	149.8253	45.7804	237	25	65.99
kisz–16z	Kamchatka-Kuril-Japan-Izu-Mariana-Yap	150.1422	45.4390	237	25	44.86
kisz–17a	Kamchatka-Kuril-Japan-Izu-Mariana-Yap	149.3989	44.6084	237	25	23.73
kisz–17b	Kamchatka-Kuril-Japan-Izu-Mariana-Yap	149.7085	44.2670	237	22	5
kisz–17y	Kamchatka-Kuril-Japan-Izu-Mariana-Yap	148.7723	45.2912	237	25	65.99
kisz–17z	Kamchatka-Kuril-Japan-Izu-Mariana-Yap	149.0865	44.9498	237	25	44.86
kisz–18a	Kamchatka-Kuril-Japan-Izu-Mariana-Yap	148.3454	44.0982	235	25	23.73
kisz–18b	Kamchatka-Kuril-Japan-Izu-Mariana-Yap	148.6687	43.7647	235	22	5
kisz–18y	Kamchatka-Kuril-Japan-Izu-Mariana-Yap	147.6915	44.7651	235	25	65.99
kisz–18z	Kamchatka-Kuril-Japan-Izu-Mariana-Yap	148.0194	44.4316	235	25	44.86
kisz–19a	Kamchatka-Kuril-Japan-Izu-Mariana-Yap	147.3262	43.5619	233	25	23.73
kisz–19b	Kamchatka-Kuril-Japan-Izu-Mariana-Yap	147.6625	43.2368	233	22	5
kisz–19y	Kamchatka-Kuril-Japan-Izu-Mariana-Yap	146.6463	44.2121	233	25	65.99
kisz–19z	Kamchatka-Kuril-Japan-Izu-Mariana-Yap	146.9872	43.8870	233	25	44.86
kisz–20a	Kamchatka-Kuril-Japan-Izu-Mariana-Yap	146.3513	43.0633	237	25	23.73
kisz–20b	Kamchatka-Kuril-Japan-Izu-Mariana-Yap	146.6531	42.7219	237	22	5
kisz–20y	Kamchatka-Kuril-Japan-Izu-Mariana-Yap	145.7410	43.7461	237	25	65.99
kisz–20z	Kamchatka-Kuril-Japan-Izu-Mariana-Yap	146.0470	43.4047	237	25	44.86
kisz–21a	Kamchatka-Kuril-Japan-Izu-Mariana-Yap	145.3331	42.5948	239	25	23.73
kisz–21b	Kamchatka-Kuril-Japan-Izu-Mariana-Yap	145.6163	42.2459	239	22	5
kisz–21y	Kamchatka-Kuril-Japan-Izu-Mariana-Yap	144.7603	43.2927	239	25	65.99
kisz–21z	Kamchatka-Kuril-Japan-Izu-Mariana-Yap	145.0475	42.9438	239	25	44.86
kisz–22a	Kamchatka-Kuril-Japan-Izu-Mariana-Yap	144.3041	42.1631	242	25	23.73
kisz–22b	Kamchatka-Kuril-Japan-Izu-Mariana-Yap	144.5605	41.8037	242	22	5
kisz–22y	Kamchatka-Kuril-Japan-Izu-Mariana-Yap	143.7854	42.8819	242	25	65.99
kisz–22z	Kamchatka-Kuril-Japan-Izu-Mariana-Yap	144.0455	42.5225	242	25	44.86
kisz–23a	Kamchatka-Kuril-Japan-Izu-Mariana-Yap	143.2863	41.3335	202	21	21.28
kisz–23b	Kamchatka-Kuril-Japan-Izu-Mariana-Yap	143.8028	41.1764	202	19	5
kisz–23v	Kamchatka-Kuril-Japan-Izu-Mariana-Yap	140.6816	42.1189	202	21	110.9
kisz–23w	Kamchatka-Kuril-Japan-Izu-Mariana-Yap	141.2050	41.9618	202	21	92.95
kisz–23x	Kamchatka-Kuril-Japan-Izu-Mariana-Yap	141.7273	41.8047	202	21	75.04
kisz–23y	Kamchatka-Kuril-Japan-Izu-Mariana-Yap	142.2482	41.6476	202	21	57.12
kisz–23z	Kamchatka-Kuril-Japan-Izu-Mariana-Yap	142.7679	41.4905	202	21	39.2
kisz–24a	Kamchatka-Kuril-Japan-Izu-Mariana-Yap	142.9795	40.3490	185	21	21.28
kisz–24b	Kamchatka-Kuril-Japan-Izu-Mariana-Yap	143.5273	40.3125	185	19	5
kisz–24x	Kamchatka-Kuril-Japan-Izu-Mariana-Yap	141.3339	40.4587	185	21	75.04
kisz–24y	Kamchatka-Kuril-Japan-Izu-Mariana-Yap	141.8827	40.4221	185	21	57.12
kisz–24z	Kamchatka-Kuril-Japan-Izu-Mariana-Yap	142.4312	40.3856	185	21	39.2
kisz–25a	Kamchatka-Kuril-Japan-Izu-Mariana-Yap	142.8839	39.4541	185	21	21.28
kisz–25b	Kamchatka-Kuril-Japan-Izu-Mariana-Yap	143.4246	39.4176	185	19	5
kisz–25y	Kamchatka-Kuril-Japan-Izu-Mariana-Yap	141.8012	39.5272	185	21	57.12
kisz–25z	Kamchatka-Kuril-Japan-Izu-Mariana-Yap	142.3426	39.4907	185	21	39.2
kisz–26a	Kamchatka-Kuril-Japan-Izu-Mariana-Yap	142.7622	38.5837	188	21	21.28
kisz–26b	Kamchatka-Kuril-Japan-Izu-Mariana-Yap	143.2930	38.5254	188	19	5
kisz–26x	Kamchatka-Kuril-Japan-Izu-Mariana-Yap	141.1667	38.7588	188	21	75.04
kisz–26y	Kamchatka-Kuril-Japan-Izu-Mariana-Yap	141.6990	38.7004	188	21	57.12
kisz–26z	Kamchatka-Kuril-Japan-Izu-Mariana-Yap	142.2308	38.6421	188	21	39.2

(continued on next page)

Table B4: (continued)

Segment	Description	Longitude (°E)	Latitude (°N)	Strike (°)	Dip (°)	Depth (km)
kisz–27a	Kamchatka-Kuril-Japan-Izu-Mariana-Yap	142.5320	37.7830	198	21	21.28
kisz–27b	Kamchatka-Kuril-Japan-Izu-Mariana-Yap	143.0357	37.6534	198	19	5
kisz–27x	Kamchatka-Kuril-Japan-Izu-Mariana-Yap	141.0142	38.1717	198	21	75.04
kisz–27y	Kamchatka-Kuril-Japan-Izu-Mariana-Yap	141.5210	38.0421	198	21	57.12
kisz–27z	Kamchatka-Kuril-Japan-Izu-Mariana-Yap	142.0269	37.9126	198	21	39.2
kisz–28a	Kamchatka-Kuril-Japan-Izu-Mariana-Yap	142.1315	37.0265	208	21	21.28
kisz–28b	Kamchatka-Kuril-Japan-Izu-Mariana-Yap	142.5941	36.8297	208	19	5
kisz–28x	Kamchatka-Kuril-Japan-Izu-Mariana-Yap	140.7348	37.6171	208	21	75.04
kisz–28y	Kamchatka-Kuril-Japan-Izu-Mariana-Yap	141.2016	37.4202	208	21	57.12
kisz–28z	Kamchatka-Kuril-Japan-Izu-Mariana-Yap	141.6671	37.2234	208	21	39.2
kisz–29a	Kamchatka-Kuril-Japan-Izu-Mariana-Yap	141.5970	36.2640	211	21	21.28
kisz–29b	Kamchatka-Kuril-Japan-Izu-Mariana-Yap	142.0416	36.0481	211	19	5
kisz–29y	Kamchatka-Kuril-Japan-Izu-Mariana-Yap	140.7029	36.6960	211	21	57.12
kisz–29z	Kamchatka-Kuril-Japan-Izu-Mariana-Yap	141.1506	36.4800	211	21	39.2
kisz–30a	Kamchatka-Kuril-Japan-Izu-Mariana-Yap	141.0553	35.4332	205	21	21.28
kisz–30b	Kamchatka-Kuril-Japan-Izu-Mariana-Yap	141.5207	35.2560	205	19	5
kisz–30y	Kamchatka-Kuril-Japan-Izu-Mariana-Yap	140.1204	35.7876	205	21	57.12
kisz–30z	Kamchatka-Kuril-Japan-Izu-Mariana-Yap	140.5883	35.6104	205	21	39.2
kisz–31a	Kamchatka-Kuril-Japan-Izu-Mariana-Yap	140.6956	34.4789	190	22	22.1
kisz–31b	Kamchatka-Kuril-Japan-Izu-Mariana-Yap	141.1927	34.4066	190	20	5
kisz–31v	Kamchatka-Kuril-Japan-Izu-Mariana-Yap	138.2025	34.8405	190	22	115.8
kisz–31w	Kamchatka-Kuril-Japan-Izu-Mariana-Yap	138.7021	34.7682	190	22	97.02
kisz–31x	Kamchatka-Kuril-Japan-Izu-Mariana-Yap	139.2012	34.6958	190	22	78.29
kisz–31y	Kamchatka-Kuril-Japan-Izu-Mariana-Yap	139.6997	34.6235	190	22	59.56
kisz–31z	Kamchatka-Kuril-Japan-Izu-Mariana-Yap	140.1979	34.5512	190	22	40.83
kisz–32a	Kamchatka-Kuril-Japan-Izu-Mariana-Yap	141.0551	33.0921	180	32	23.48
kisz–32b	Kamchatka-Kuril-Japan-Izu-Mariana-Yap	141.5098	33.0921	180	21.69	5
kisz–33a	Kamchatka-Kuril-Japan-Izu-Mariana-Yap	141.0924	32.1047	173.8	27.65	20.67
kisz–33b	Kamchatka-Kuril-Japan-Izu-Mariana-Yap	141.5596	32.1473	173.8	18.27	5
kisz–34a	Kamchatka-Kuril-Japan-Izu-Mariana-Yap	141.1869	31.1851	172.1	25	18.26
kisz–34b	Kamchatka-Kuril-Japan-Izu-Mariana-Yap	141.6585	31.2408	172.1	15.38	5
kisz–35a	Kamchatka-Kuril-Japan-Izu-Mariana-Yap	141.4154	30.1707	163	25	17.12
kisz–35b	Kamchatka-Kuril-Japan-Izu-Mariana-Yap	141.8662	30.2899	163	14.03	5
kisz–36a	Kamchatka-Kuril-Japan-Izu-Mariana-Yap	141.6261	29.2740	161.7	25.73	18.71
kisz–36b	Kamchatka-Kuril-Japan-Izu-Mariana-Yap	142.0670	29.4012	161.7	15.91	5
kisz–37a	Kamchatka-Kuril-Japan-Izu-Mariana-Yap	142.0120	28.3322	154.7	20	14.54
kisz–37b	Kamchatka-Kuril-Japan-Izu-Mariana-Yap	142.4463	28.5124	154.7	11	5
kisz–38a	Kamchatka-Kuril-Japan-Izu-Mariana-Yap	142.2254	27.6946	170.3	20	14.54
kisz–38b	Kamchatka-Kuril-Japan-Izu-Mariana-Yap	142.6955	27.7659	170.3	11	5
kisz–39a	Kamchatka-Kuril-Japan-Izu-Mariana-Yap	142.3085	26.9127	177.2	24.23	17.42
kisz–39b	Kamchatka-Kuril-Japan-Izu-Mariana-Yap	142.7674	26.9325	177.2	14.38	5
kisz–40a	Kamchatka-Kuril-Japan-Izu-Mariana-Yap	142.2673	26.1923	189.4	26.49	22.26
kisz–40b	Kamchatka-Kuril-Japan-Izu-Mariana-Yap	142.7090	26.1264	189.4	20.2	5
kisz–41a	Kamchatka-Kuril-Japan-Izu-Mariana-Yap	142.1595	25.0729	173.7	22.07	19.08
kisz–41b	Kamchatka-Kuril-Japan-Izu-Mariana-Yap	142.6165	25.1184	173.7	16.36	5
kisz–42a	Kamchatka-Kuril-Japan-Izu-Mariana-Yap	142.7641	23.8947	143.5	21.54	18.4
kisz–42b	Kamchatka-Kuril-Japan-Izu-Mariana-Yap	143.1321	24.1432	143.5	15.54	5
kisz–43a	Kamchatka-Kuril-Japan-Izu-Mariana-Yap	143.5281	23.0423	129.2	23.02	18.77
kisz–43b	Kamchatka-Kuril-Japan-Izu-Mariana-Yap	143.8128	23.3626	129.2	15.99	5
kisz–44a	Kamchatka-Kuril-Japan-Izu-Mariana-Yap	144.2230	22.5240	134.6	28.24	18.56
kisz–44b	Kamchatka-Kuril-Japan-Izu-Mariana-Yap	144.5246	22.8056	134.6	15.74	5
kisz–45a	Kamchatka-Kuril-Japan-Izu-Mariana-Yap	145.0895	21.8866	125.8	36.73	22.79
kisz–45b	Kamchatka-Kuril-Japan-Izu-Mariana-Yap	145.3171	22.1785	125.8	20.84	5
kisz–46a	Kamchatka-Kuril-Japan-Izu-Mariana-Yap	145.6972	21.3783	135.9	30.75	20.63
kisz–46b	Kamchatka-Kuril-Japan-Izu-Mariana-Yap	145.9954	21.6469	135.9	18.22	5

(continued on next page)

Table B4: (continued)

Segment	Description	Longitude (°E)	Latitude (°N)	Strike (°)	Dip (°)	Depth (km)
kisz–47a	Kamchatka-Kuril-Japan-Izu-Mariana-Yap	146.0406	20.9341	160.1	29.87	19.62
kisz–47b	Kamchatka-Kuril-Japan-Izu-Mariana-Yap	146.4330	21.0669	160.1	17	5
kisz–48a	Kamchatka-Kuril-Japan-Izu-Mariana-Yap	146.3836	20.0690	158	32.75	19.68
kisz–48b	Kamchatka-Kuril-Japan-Izu-Mariana-Yap	146.7567	20.2108	158	17.07	5
kisz–49a	Kamchatka-Kuril-Japan-Izu-Mariana-Yap	146.6689	19.3123	164.5	25.07	21.41
kisz–49b	Kamchatka-Kuril-Japan-Izu-Mariana-Yap	147.0846	19.4212	164.5	19.16	5
kisz–50a	Kamchatka-Kuril-Japan-Izu-Mariana-Yap	146.9297	18.5663	172.1	22	22.1
kisz–50b	Kamchatka-Kuril-Japan-Izu-Mariana-Yap	147.3650	18.6238	172.1	20	5
kisz–51a	Kamchatka-Kuril-Japan-Izu-Mariana-Yap	146.9495	17.7148	175.1	22.06	22.04
kisz–51b	Kamchatka-Kuril-Japan-Izu-Mariana-Yap	147.3850	17.7503	175.1	19.93	5
kisz–52a	Kamchatka-Kuril-Japan-Izu-Mariana-Yap	146.9447	16.8869	180	25.51	18.61
kisz–52b	Kamchatka-Kuril-Japan-Izu-Mariana-Yap	147.3683	16.8869	180	15.79	5
kisz–53a	Kamchatka-Kuril-Japan-Izu-Mariana-Yap	146.8626	16.0669	185.2	27.39	18.41
kisz–53b	Kamchatka-Kuril-Japan-Izu-Mariana-Yap	147.2758	16.0309	185.2	15.56	5
kisz–54a	Kamchatka-Kuril-Japan-Izu-Mariana-Yap	146.7068	15.3883	199.1	28.12	20.91
kisz–54b	Kamchatka-Kuril-Japan-Izu-Mariana-Yap	147.0949	15.2590	199.1	18.56	5
kisz–55a	Kamchatka-Kuril-Japan-Izu-Mariana-Yap	146.4717	14.6025	204.3	29.6	26.27
kisz–55b	Kamchatka-Kuril-Japan-Izu-Mariana-Yap	146.8391	14.4415	204.3	25.18	5
kisz–56a	Kamchatka-Kuril-Japan-Izu-Mariana-Yap	146.1678	13.9485	217.4	32.04	26.79
kisz–56b	Kamchatka-Kuril-Japan-Izu-Mariana-Yap	146.4789	13.7170	217.4	25.84	5
kisz–57a	Kamchatka-Kuril-Japan-Izu-Mariana-Yap	145.6515	13.5576	235.8	37	24.54
kisz–57b	Kamchatka-Kuril-Japan-Izu-Mariana-Yap	145.8586	13.2609	235.8	23	5
kisz–58a	Kamchatka-Kuril-Japan-Izu-Mariana-Yap	144.9648	12.9990	237.8	37.72	24.54
kisz–58b	Kamchatka-Kuril-Japan-Izu-Mariana-Yap	145.1589	12.6984	237.8	23	5
kisz–59a	Kamchatka-Kuril-Japan-Izu-Mariana-Yap	144.1799	12.6914	242.9	34.33	22.31
kisz–59b	Kamchatka-Kuril-Japan-Izu-Mariana-Yap	144.3531	12.3613	242.9	20.25	5
kisz–60a	Kamchatka-Kuril-Japan-Izu-Mariana-Yap	143.3687	12.3280	244.9	30.9	20.62
kisz–60b	Kamchatka-Kuril-Japan-Izu-Mariana-Yap	143.5355	11.9788	244.9	18.2	5
kisz–61a	Kamchatka-Kuril-Japan-Izu-Mariana-Yap	142.7051	12.1507	261.8	35.41	25.51
kisz–61b	Kamchatka-Kuril-Japan-Izu-Mariana-Yap	142.7582	11.7883	261.8	24.22	5
kisz–62a	Kamchatka-Kuril-Japan-Izu-Mariana-Yap	141.6301	11.8447	245.7	39.86	34.35
kisz–62b	Kamchatka-Kuril-Japan-Izu-Mariana-Yap	141.7750	11.5305	245.7	35.94	5
kisz–63a	Kamchatka-Kuril-Japan-Izu-Mariana-Yap	140.8923	11.5740	256.2	42	38.46
kisz–63b	Kamchatka-Kuril-Japan-Izu-Mariana-Yap	140.9735	11.2498	256.2	42	5
kisz–64a	Kamchatka-Kuril-Japan-Izu-Mariana-Yap	140.1387	11.6028	269.6	42.48	38.77
kisz–64b	Kamchatka-Kuril-Japan-Izu-Mariana-Yap	140.1410	11.2716	269.6	42.48	5
kisz–65a	Kamchatka-Kuril-Japan-Izu-Mariana-Yap	139.4595	11.5883	288.7	44.16	39.83
kisz–65b	Kamchatka-Kuril-Japan-Izu-Mariana-Yap	139.3541	11.2831	288.7	44.16	5
kisz–66a	Kamchatka-Kuril-Japan-Izu-Mariana-Yap	138.1823	11.2648	193.1	45	40.36
kisz–66b	Kamchatka-Kuril-Japan-Izu-Mariana-Yap	138.4977	11.1929	193.1	45	5
kisz–67a	Kamchatka-Kuril-Japan-Izu-Mariana-Yap	137.9923	10.3398	189.8	45	40.36
kisz–67b	Kamchatka-Kuril-Japan-Izu-Mariana-Yap	138.3104	10.2856	189.8	45	5
kisz–68a	Kamchatka-Kuril-Japan-Izu-Mariana-Yap	137.7607	9.6136	201.7	45	40.36
kisz–68b	Kamchatka-Kuril-Japan-Izu-Mariana-Yap	138.0599	9.4963	201.7	45	5
kisz–69a	Kamchatka-Kuril-Japan-Izu-Mariana-Yap	137.4537	8.8996	213.5	45	40.36
kisz–69b	Kamchatka-Kuril-Japan-Izu-Mariana-Yap	137.7215	8.7241	213.5	45	5
kisz–70a	Kamchatka-Kuril-Japan-Izu-Mariana-Yap	137.0191	8.2872	226.5	45	40.36
kisz–70b	Kamchatka-Kuril-Japan-Izu-Mariana-Yap	137.2400	8.0569	226.5	45	5
kisz–71a	Kamchatka-Kuril-Japan-Izu-Mariana-Yap	136.3863	7.9078	263.9	45	40.36
kisz–71b	Kamchatka-Kuril-Japan-Izu-Mariana-Yap	136.4202	7.5920	263.9	45	5
kisz–72a	Kamchatka-Kuril-Japan-Izu-Mariana-Yap	135.6310	7.9130	276.9	45	40.36
kisz–72b	Kamchatka-Kuril-Japan-Izu-Mariana-Yap	135.5926	7.5977	276.9	45	5
kisz–73a	Kamchatka-Kuril-Japan-Izu-Mariana-Yap	134.3296	7.4541	224	45	40.36
kisz–73b	Kamchatka-Kuril-Japan-Izu-Mariana-Yap	134.5600	7.2335	224	45	5
kisz–74a	Kamchatka-Kuril-Japan-Izu-Mariana-Yap	133.7125	6.8621	228.1	45	40.36

(continued on next page)

Table B4: (continued)

Segment	Description	Longitude (°E)	Latitude (°N)	Strike (°)	Dip (°)	Depth (km)
kisz–74b	Kamchatka-Kuril-Japan-Izu-Mariana-Yap	133.9263	6.6258	228.1	45	5
kisz–75a	Kamchatka-Kuril-Japan-Izu-Mariana-Yap	133.0224	6.1221	217.7	45	40.36
kisz–75b	Kamchatka-Kuril-Japan-Izu-Mariana-Yap	133.2751	5.9280	217.7	45	5

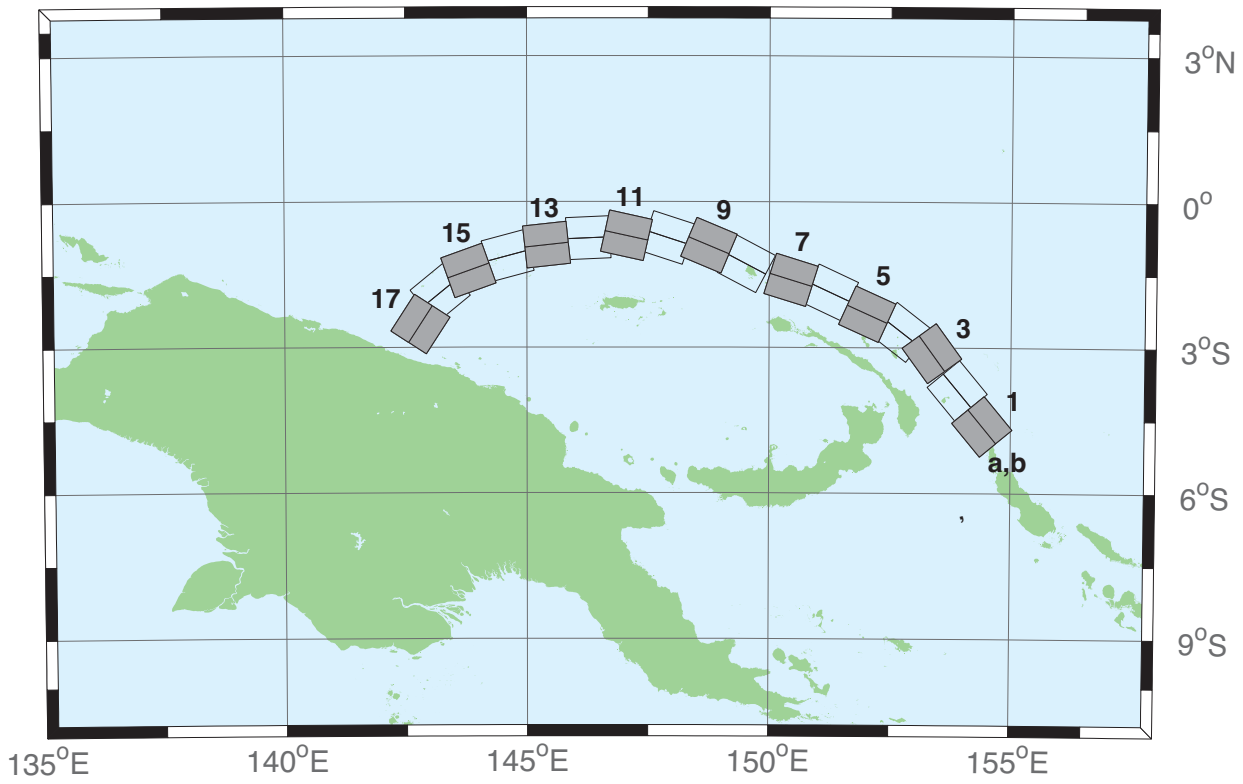

Figure B5: Manus-Oceanic Convergent Boundary Subduction Zone unit sources.

Table B5: Earthquake parameters for Manus-Oceanic Convergent Boundary Subduction Zone unit sources.

Segment	Description	Longitude (°E)	Latitude (°N)	Strike (°)	Dip (°)	Depth (km)
mosz–1a	Manus-Oceanic Convergent Boundary	154.0737	–4.8960	140.2	15	15.88
mosz–1b	Manus-Oceanic Convergent Boundary	154.4082	–4.6185	140.2	15	5
mosz–2a	Manus-Oceanic Convergent Boundary	153.5589	–4.1575	140.2	15	15.91
mosz–2b	Manus-Oceanic Convergent Boundary	153.8931	–3.8800	140.2	15	5.35
mosz–3a	Manus-Oceanic Convergent Boundary	153.0151	–3.3716	143.9	15	16.64
mosz–3b	Manus-Oceanic Convergent Boundary	153.3662	–3.1160	143.9	15	6.31
mosz–4a	Manus-Oceanic Convergent Boundary	152.4667	–3.0241	127.7	15	17.32
mosz–4b	Manus-Oceanic Convergent Boundary	152.7321	–2.6806	127.7	15	7.39
mosz–5a	Manus-Oceanic Convergent Boundary	151.8447	–2.7066	114.3	15	17.57
mosz–5b	Manus-Oceanic Convergent Boundary	152.0235	–2.3112	114.3	15	8.25
mosz–6a	Manus-Oceanic Convergent Boundary	151.0679	–2.2550	115	15	17.66
mosz–6b	Manus-Oceanic Convergent Boundary	151.2513	–1.8618	115	15	7.58
mosz–7a	Manus-Oceanic Convergent Boundary	150.3210	–2.0236	107.2	15	17.73
mosz–7b	Manus-Oceanic Convergent Boundary	150.4493	–1.6092	107.2	15	6.83
mosz–8a	Manus-Oceanic Convergent Boundary	149.3226	–1.6666	117.8	15	17.83
mosz–8b	Manus-Oceanic Convergent Boundary	149.5251	–1.2829	117.8	15	7.92
mosz–9a	Manus-Oceanic Convergent Boundary	148.5865	–1.3017	112.7	15	17.84
mosz–9b	Manus-Oceanic Convergent Boundary	148.7540	–0.9015	112.7	15	8.3
mosz–10a	Manus-Oceanic Convergent Boundary	147.7760	–1.1560	108	15	17.78
mosz–10b	Manus-Oceanic Convergent Boundary	147.9102	–0.7434	108	15	8.09
mosz–11a	Manus-Oceanic Convergent Boundary	146.9596	–1.1226	102.5	15	17.54
mosz–11b	Manus-Oceanic Convergent Boundary	147.0531	–0.6990	102.5	15	7.64
mosz–12a	Manus-Oceanic Convergent Boundary	146.2858	–1.1820	87.48	15	17.29
mosz–12b	Manus-Oceanic Convergent Boundary	146.2667	–0.7486	87.48	15	7.62
mosz–13a	Manus-Oceanic Convergent Boundary	145.4540	–1.3214	83.75	15	17.34
mosz–13b	Manus-Oceanic Convergent Boundary	145.4068	–0.8901	83.75	15	7.08
mosz–14a	Manus-Oceanic Convergent Boundary	144.7151	–1.5346	75.09	15	17.21
mosz–14b	Manus-Oceanic Convergent Boundary	144.6035	–1.1154	75.09	15	6.38
mosz–15a	Manus-Oceanic Convergent Boundary	143.9394	–1.8278	70.43	15	16.52
mosz–15b	Manus-Oceanic Convergent Boundary	143.7940	–1.4190	70.43	15	6.09
mosz–16a	Manus-Oceanic Convergent Boundary	143.4850	–2.2118	50.79	15	15.86
mosz–16b	Manus-Oceanic Convergent Boundary	143.2106	–1.8756	50.79	15	5
mosz–17a	Manus-Oceanic Convergent Boundary	143.1655	–2.7580	33	15	16.64
mosz–17b	Manus-Oceanic Convergent Boundary	142.8013	–2.5217	33	15	5

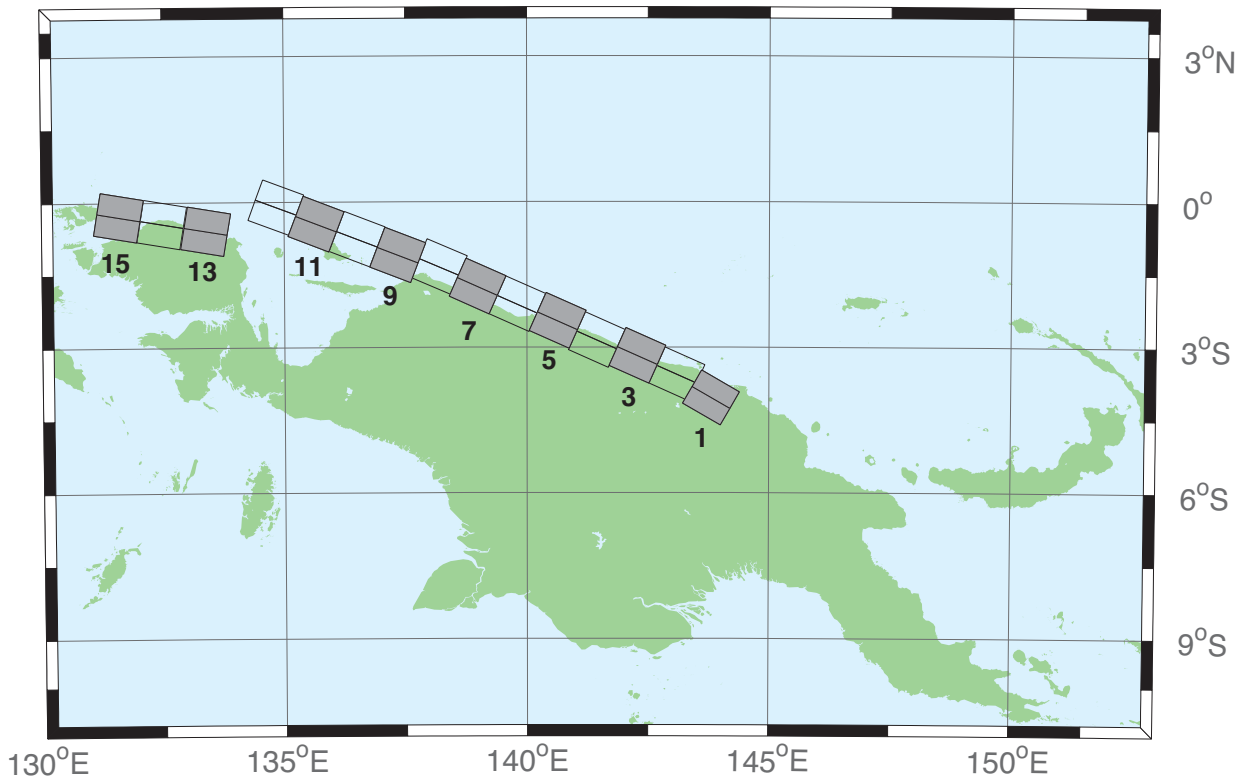

Figure B6: New Guinea Subduction Zone unit sources.

Table B6: Earthquake parameters for New Guinea Subduction Zone unit sources.

Segment	Description	Longitude (°E)	Latitude (°N)	Strike (°)	Dip (°)	Depth (km)
ngsz–1a	New Guinea	143.6063	–4.3804	120	29	25.64
ngsz–1b	New Guinea	143.8032	–4.0402	120	29	1.4
ngsz–2a	New Guinea	142.9310	–3.9263	114	27.63	20.1
ngsz–2b	New Guinea	143.0932	–3.5628	114	21.72	1.6
ngsz–3a	New Guinea	142.1076	–3.5632	114	20.06	18.73
ngsz–3b	New Guinea	142.2795	–3.1778	114	15.94	5
ngsz–4a	New Guinea	141.2681	–3.2376	114	21	17.76
ngsz–4b	New Guinea	141.4389	–2.8545	114	14.79	5
ngsz–5a	New Guinea	140.4592	–2.8429	114	21.26	16.14
ngsz–5b	New Guinea	140.6296	–2.4605	114	12.87	5
ngsz–6a	New Guinea	139.6288	–2.4960	114	22.72	15.4
ngsz–6b	New Guinea	139.7974	–2.1175	114	12	5
ngsz–7a	New Guinea	138.8074	–2.1312	114	21.39	15.4
ngsz–7b	New Guinea	138.9776	–1.7491	114	12	5
ngsz–8a	New Guinea	138.0185	–1.7353	113.1	18.79	15.14
ngsz–8b	New Guinea	138.1853	–1.3441	113.1	11.7	5
ngsz–9a	New Guinea	137.1805	–1.5037	111	15.24	13.23
ngsz–9b	New Guinea	137.3358	–1.0991	111	9.47	5
ngsz–10a	New Guinea	136.3418	–1.1774	111	13.51	11.09
ngsz–10b	New Guinea	136.4983	–0.7697	111	7	5
ngsz–11a	New Guinea	135.4984	–0.8641	111	11.38	12.49
ngsz–11b	New Guinea	135.6562	–0.4530	111	8.62	5
ngsz–12a	New Guinea	134.6759	–0.5216	110.5	10	13.68
ngsz–12b	New Guinea	134.8307	–0.1072	110.5	10	5
ngsz–13a	New Guinea	133.3065	–1.0298	99.5	10	13.68
ngsz–13b	New Guinea	133.3795	–0.5935	99.5	10	5
ngsz–14a	New Guinea	132.4048	–0.8816	99.5	10	13.68
ngsz–14b	New Guinea	132.4778	–0.4453	99.5	10	5
ngsz–15a	New Guinea	131.5141	–0.7353	99.5	10	13.68
ngsz–15b	New Guinea	131.5871	–0.2990	99.5	10	5

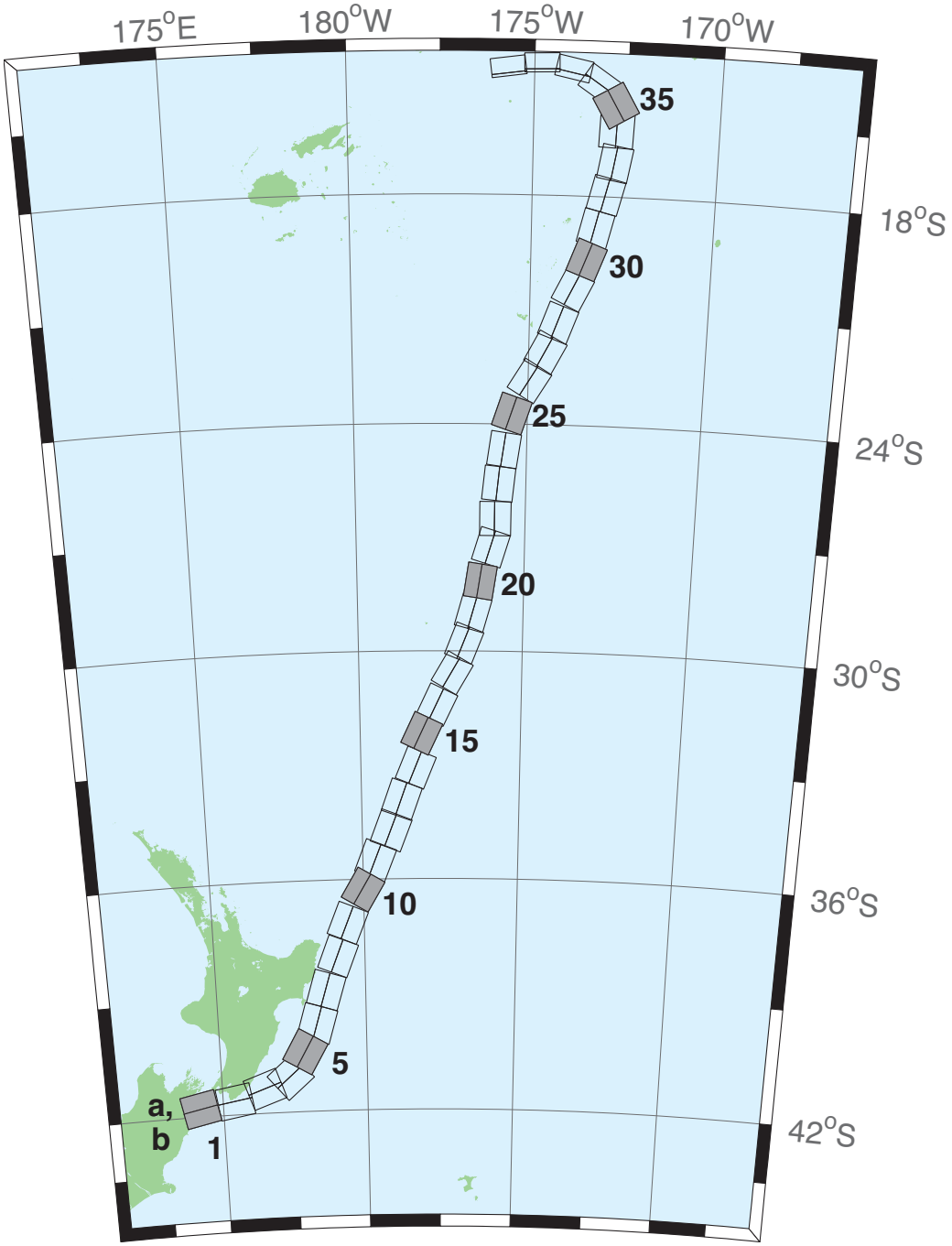

Figure B7: New Zealand-Kermadec-Tonga Subduction Zone unit sources.

Table B7: Earthquake parameters for New Zealand-Kermadec-Tonga Subduction Zone unit sources.

Segment	Description	Longitude (°E)	Latitude (°N)	Strike (°)	Dip (°)	Depth (km)
ntsz–1a	New Zealand-Kermadec-Tonga	174.0985	–41.3951	258.6	24	25.34
ntsz–1b	New Zealand-Kermadec-Tonga	174.2076	–41.7973	258.6	24	5
ntsz–2a	New Zealand-Kermadec-Tonga	175.3289	–41.2592	260.6	29.38	23.17
ntsz–2b	New Zealand-Kermadec-Tonga	175.4142	–41.6454	260.6	21.31	5
ntsz–3a	New Zealand-Kermadec-Tonga	176.2855	–40.9950	250.7	29.54	21.74
ntsz–3b	New Zealand-Kermadec-Tonga	176.4580	–41.3637	250.7	19.56	5
ntsz–4a	New Zealand-Kermadec-Tonga	177.0023	–40.7679	229.4	24.43	18.87
ntsz–4b	New Zealand-Kermadec-Tonga	177.3552	–41.0785	229.4	16.1	5
ntsz–5a	New Zealand-Kermadec-Tonga	177.4114	–40.2396	210	18.8	19.29
ntsz–5b	New Zealand-Kermadec-Tonga	177.8951	–40.4525	210	16.61	5
ntsz–6a	New Zealand-Kermadec-Tonga	177.8036	–39.6085	196.7	18.17	15.8
ntsz–6b	New Zealand-Kermadec-Tonga	178.3352	–39.7310	196.7	12.48	5
ntsz–7a	New Zealand-Kermadec-Tonga	178.1676	–38.7480	197	28.1	17.85
ntsz–7b	New Zealand-Kermadec-Tonga	178.6541	–38.8640	197	14.89	5
ntsz–8a	New Zealand-Kermadec-Tonga	178.6263	–37.8501	201.4	31.47	18.78
ntsz–8b	New Zealand-Kermadec-Tonga	179.0788	–37.9899	201.4	16	5
ntsz–9a	New Zealand-Kermadec-Tonga	178.9833	–36.9770	202.2	29.58	20.02
ntsz–9b	New Zealand-Kermadec-Tonga	179.4369	–37.1245	202.2	17.48	5
ntsz–10a	New Zealand-Kermadec-Tonga	179.5534	–36.0655	210.6	32.1	20.72
ntsz–10b	New Zealand-Kermadec-Tonga	179.9595	–36.2593	210.6	18.32	5
ntsz–11a	New Zealand-Kermadec-Tonga	179.9267	–35.3538	201.7	25	16.09
ntsz–11b	New Zealand-Kermadec-Tonga	180.3915	–35.5040	201.7	12.81	5
ntsz–12a	New Zealand-Kermadec-Tonga	180.4433	–34.5759	201.2	25	15.46
ntsz–12b	New Zealand-Kermadec-Tonga	180.9051	–34.7230	201.2	12.08	5
ntsz–13a	New Zealand-Kermadec-Tonga	180.7990	–33.7707	199.8	25.87	19.06
ntsz–13b	New Zealand-Kermadec-Tonga	181.2573	–33.9073	199.8	16.33	5
ntsz–14a	New Zealand-Kermadec-Tonga	181.2828	–32.9288	202.4	31.28	22.73
ntsz–14b	New Zealand-Kermadec-Tonga	181.7063	–33.0751	202.4	20.77	5
ntsz–15a	New Zealand-Kermadec-Tonga	181.4918	–32.0035	205.4	32.33	22.64
ntsz–15b	New Zealand-Kermadec-Tonga	181.8967	–32.1665	205.4	20.66	5
ntsz–16a	New Zealand-Kermadec-Tonga	181.9781	–31.2535	205.5	34.29	23.59
ntsz–16b	New Zealand-Kermadec-Tonga	182.3706	–31.4131	205.5	21.83	5
ntsz–17a	New Zealand-Kermadec-Tonga	182.4819	–30.3859	210.3	37.6	25.58
ntsz–17b	New Zealand-Kermadec-Tonga	182.8387	–30.5655	210.3	24.3	5
ntsz–18a	New Zealand-Kermadec-Tonga	182.8176	–29.6545	201.6	37.65	26.13
ntsz–18b	New Zealand-Kermadec-Tonga	183.1985	–29.7856	201.6	25	5
ntsz–19a	New Zealand-Kermadec-Tonga	183.0622	–28.8739	195.7	34.41	26.13
ntsz–19b	New Zealand-Kermadec-Tonga	183.4700	–28.9742	195.7	25	5
ntsz–20a	New Zealand-Kermadec-Tonga	183.2724	–28.0967	188.8	38	26.13
ntsz–20b	New Zealand-Kermadec-Tonga	183.6691	–28.1508	188.8	25	5
ntsz–21a	New Zealand-Kermadec-Tonga	183.5747	–27.1402	197.1	32.29	24.83
ntsz–21b	New Zealand-Kermadec-Tonga	183.9829	–27.2518	197.1	23.37	5
ntsz–22a	New Zealand-Kermadec-Tonga	183.6608	–26.4975	180	29.56	18.63
ntsz–22b	New Zealand-Kermadec-Tonga	184.0974	–26.4975	180	15.82	5
ntsz–23a	New Zealand-Kermadec-Tonga	183.7599	–25.5371	185.8	32.42	20.56
ntsz–23b	New Zealand-Kermadec-Tonga	184.1781	–25.5752	185.8	18.13	5
ntsz–24a	New Zealand-Kermadec-Tonga	183.9139	–24.6201	188.2	33.31	23.73
ntsz–24b	New Zealand-Kermadec-Tonga	184.3228	–24.6734	188.2	22	5
ntsz–25a	New Zealand-Kermadec-Tonga	184.1266	–23.5922	198.5	29.34	19.64
ntsz–25b	New Zealand-Kermadec-Tonga	184.5322	–23.7163	198.5	17.03	5
ntsz–26a	New Zealand-Kermadec-Tonga	184.6613	–22.6460	211.7	30.26	19.43
ntsz–26b	New Zealand-Kermadec-Tonga	185.0196	–22.8497	211.7	16.78	5
ntsz–27a	New Zealand-Kermadec-Tonga	185.0879	–21.9139	207.9	31.73	20.67
ntsz–27b	New Zealand-Kermadec-Tonga	185.4522	–22.0928	207.9	18.27	5
ntsz–28a	New Zealand-Kermadec-Tonga	185.4037	–21.1758	200.5	32.44	21.76

(continued on next page)

Table B7: (continued)

Segment	Description	Longitude (°E)	Latitude (°N)	Strike (°)	Dip (°)	Depth (km)
ntsz–28b	New Zealand-Kermadec-Tonga	185.7849	–21.3084	200.5	19.58	5
ntsz–29a	New Zealand-Kermadec-Tonga	185.8087	–20.2629	206.4	32.47	20.4
ntsz–29b	New Zealand-Kermadec-Tonga	186.1710	–20.4312	206.4	17.94	5
ntsz–30a	New Zealand-Kermadec-Tonga	186.1499	–19.5087	200.9	32.98	22.46
ntsz–30b	New Zealand-Kermadec-Tonga	186.5236	–19.6432	200.9	20.44	5
ntsz–31a	New Zealand-Kermadec-Tonga	186.3538	–18.7332	193.9	34.41	21.19
ntsz–31b	New Zealand-Kermadec-Tonga	186.7339	–18.8221	193.9	18.89	5
ntsz–32a	New Zealand-Kermadec-Tonga	186.5949	–17.8587	194.1	30	19.12
ntsz–32b	New Zealand-Kermadec-Tonga	186.9914	–17.9536	194.1	16.4	5
ntsz–33a	New Zealand-Kermadec-Tonga	186.8172	–17.0581	190	33.15	23.34
ntsz–33b	New Zealand-Kermadec-Tonga	187.2047	–17.1237	190	21.52	5
ntsz–34a	New Zealand-Kermadec-Tonga	186.7814	–16.2598	182.1	15	13.41
ntsz–34b	New Zealand-Kermadec-Tonga	187.2330	–16.2759	182.1	9.68	5
ntsz–35a	New Zealand-Kermadec-Tonga	186.8000	–15.8563	149.8	15	12.17
ntsz–35b	New Zealand-Kermadec-Tonga	187.1896	–15.6384	149.8	8.24	5
ntsz–36a	New Zealand-Kermadec-Tonga	186.5406	–15.3862	123.9	40.44	36.72
ntsz–36b	New Zealand-Kermadec-Tonga	186.7381	–15.1025	123.9	39.38	5
ntsz–37a	New Zealand-Kermadec-Tonga	185.9883	–14.9861	102	68.94	30.99
ntsz–37b	New Zealand-Kermadec-Tonga	186.0229	–14.8282	102	31.32	5
ntsz–38a	New Zealand-Kermadec-Tonga	185.2067	–14.8259	88.4	80	26.13
ntsz–38b	New Zealand-Kermadec-Tonga	185.2044	–14.7479	88.4	25	5
ntsz–39a	New Zealand-Kermadec-Tonga	184.3412	–14.9409	82.55	80	26.13
ntsz–39b	New Zealand-Kermadec-Tonga	184.3307	–14.8636	82.55	25	5

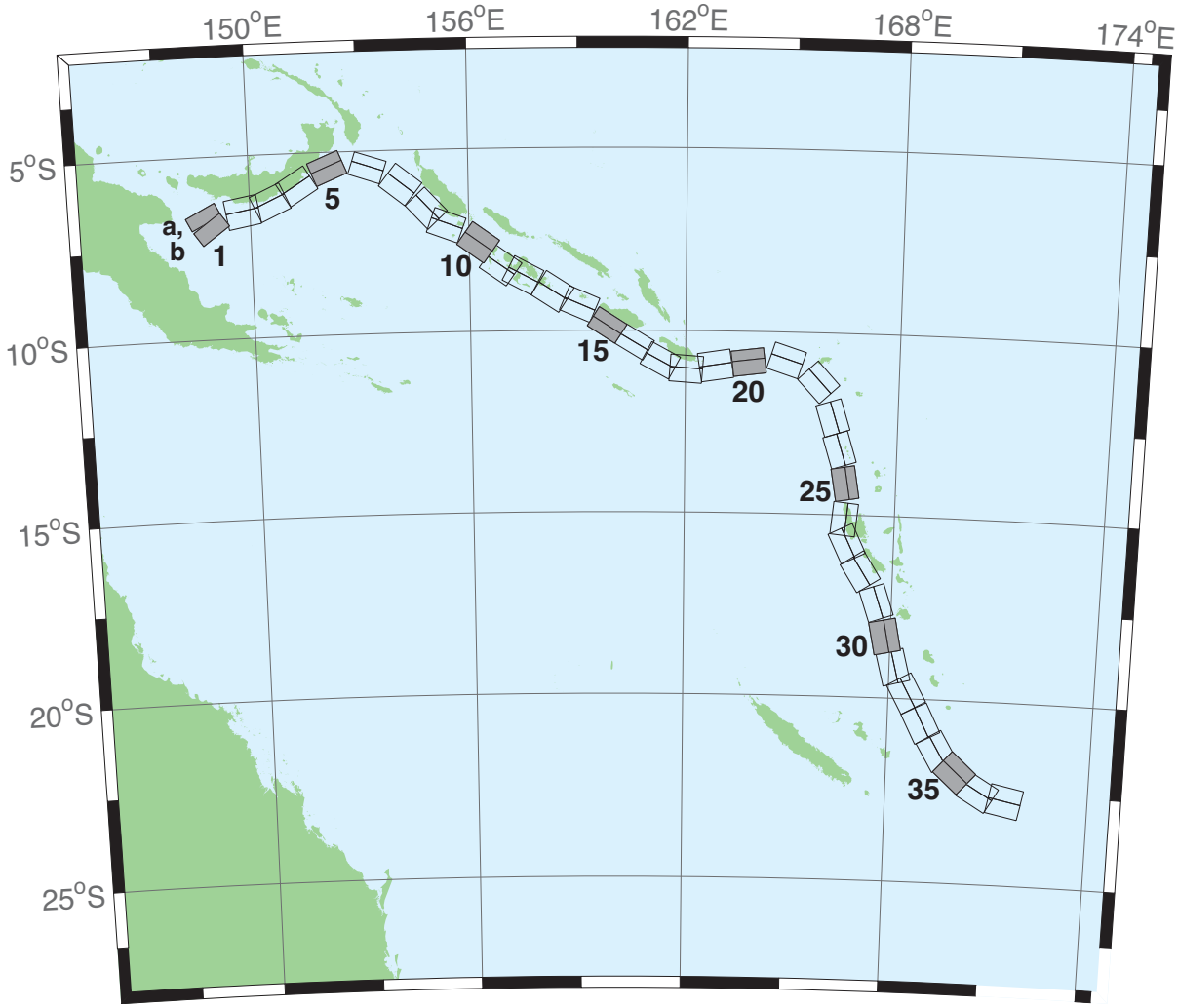

Figure B8: New Britain-Solomons-Vanuatu Subduction Zone unit sources.

Table B8: Earthquake parameters for New Britain-Solomons-Vanuatu Subduction Zone unit sources.

Segment	Description	Longitude (°E)	Latitude (°N)	Strike (°)	Dip (°)	Depth (km)
nvsz–1a	New Britain-Solomons-Vanuatu	148.6217	–6.4616	243.2	32.34	15.69
nvsz–1b	New Britain-Solomons-Vanuatu	148.7943	–6.8002	234.2	12.34	5
nvsz–2a	New Britain-Solomons-Vanuatu	149.7218	–6.1459	260.1	35.1	16.36
nvsz–2b	New Britain-Solomons-Vanuatu	149.7856	–6.5079	260.1	13.13	5
nvsz–3a	New Britain-Solomons-Vanuatu	150.4075	–5.9659	245.7	42.35	18.59
nvsz–3b	New Britain-Solomons-Vanuatu	150.5450	–6.2684	245.7	15.77	5
nvsz–4a	New Britain-Solomons-Vanuatu	151.1095	–5.5820	238.2	42.41	23.63
nvsz–4b	New Britain-Solomons-Vanuatu	151.2851	–5.8639	238.2	21.88	5
nvsz–5a	New Britain-Solomons-Vanuatu	152.0205	–5.1305	247.7	49.22	32.39
nvsz–5b	New Britain-Solomons-Vanuatu	152.1322	–5.4020	247.7	33.22	5
nvsz–6a	New Britain-Solomons-Vanuatu	153.3450	–5.1558	288.6	53.53	33.59
nvsz–6b	New Britain-Solomons-Vanuatu	153.2595	–5.4089	288.6	34.87	5
nvsz–7a	New Britain-Solomons-Vanuatu	154.3814	–5.6308	308.3	39.72	19.18
nvsz–7b	New Britain-Solomons-Vanuatu	154.1658	–5.9017	308.3	16.48	5
nvsz–8a	New Britain-Solomons-Vanuatu	155.1097	–6.3511	317.2	45.33	22.92
nvsz–8b	New Britain-Solomons-Vanuatu	154.8764	–6.5656	317.2	21	5
nvsz–9a	New Britain-Solomons-Vanuatu	155.5027	–6.7430	290.5	48.75	22.92
nvsz–9b	New Britain-Solomons-Vanuatu	155.3981	–7.0204	290.5	21	5
nvsz–10a	New Britain-Solomons-Vanuatu	156.4742	–7.2515	305.9	36.88	27.62
nvsz–10b	New Britain-Solomons-Vanuatu	156.2619	–7.5427	305.9	26.9	5
nvsz–11a	New Britain-Solomons-Vanuatu	157.0830	–7.8830	305.4	32.97	29.72
nvsz–11b	New Britain-Solomons-Vanuatu	156.8627	–8.1903	305.4	29.63	5
nvsz–12a	New Britain-Solomons-Vanuatu	157.6537	–8.1483	297.9	37.53	28.57
nvsz–12b	New Britain-Solomons-Vanuatu	157.4850	–8.4630	297.9	28.13	5
nvsz–13a	New Britain-Solomons-Vanuatu	158.5089	–8.5953	302.7	33.62	23.02
nvsz–13b	New Britain-Solomons-Vanuatu	158.3042	–8.9099	302.7	21.12	5
nvsz–14a	New Britain-Solomons-Vanuatu	159.1872	–8.9516	293.3	38.44	34.06
nvsz–14b	New Britain-Solomons-Vanuatu	159.0461	–9.2747	293.3	35.54	5
nvsz–15a	New Britain-Solomons-Vanuatu	159.9736	–9.5993	302.8	46.69	41.38
nvsz–15b	New Britain-Solomons-Vanuatu	159.8044	–9.8584	302.8	46.69	5
nvsz–16a	New Britain-Solomons-Vanuatu	160.7343	–10.0574	301	46.05	41
nvsz–16b	New Britain-Solomons-Vanuatu	160.5712	–10.3246	301	46.05	5
nvsz–17a	New Britain-Solomons-Vanuatu	161.4562	–10.5241	298.4	40.12	37.22
nvsz–17b	New Britain-Solomons-Vanuatu	161.2900	–10.8263	298.4	40.12	5
nvsz–18a	New Britain-Solomons-Vanuatu	162.0467	–10.6823	274.1	40.33	29.03
nvsz–18b	New Britain-Solomons-Vanuatu	162.0219	–11.0238	274.1	28.72	5
nvsz–19a	New Britain-Solomons-Vanuatu	162.7818	–10.5645	261.3	34.25	24.14
nvsz–19b	New Britain-Solomons-Vanuatu	162.8392	–10.9315	261.3	22.51	5
nvsz–20a	New Britain-Solomons-Vanuatu	163.7222	–10.5014	262.9	50.35	26.3
nvsz–20b	New Britain-Solomons-Vanuatu	163.7581	–10.7858	262.9	25.22	5
nvsz–21a	New Britain-Solomons-Vanuatu	164.9445	–10.4183	287.9	40.31	23.3
nvsz–21b	New Britain-Solomons-Vanuatu	164.8374	–10.7442	287.9	21.47	5
nvsz–22a	New Britain-Solomons-Vanuatu	166.0261	–11.1069	317.1	42.39	20.78
nvsz–22b	New Britain-Solomons-Vanuatu	165.7783	–11.3328	317.1	18.4	5
nvsz–23a	New Britain-Solomons-Vanuatu	166.5179	–12.2260	342.4	47.95	22.43
nvsz–23b	New Britain-Solomons-Vanuatu	166.2244	–12.3171	342.4	20.4	5
nvsz–24a	New Britain-Solomons-Vanuatu	166.7236	–13.1065	342.6	47.13	28.52
nvsz–24b	New Britain-Solomons-Vanuatu	166.4241	–13.1979	342.6	28.06	5
nvsz–25a	New Britain-Solomons-Vanuatu	166.8914	–14.0785	350.3	54.1	31.16
nvsz–25b	New Britain-Solomons-Vanuatu	166.6237	–14.1230	350.3	31.55	5
nvsz–26a	New Britain-Solomons-Vanuatu	166.9200	–15.1450	365.6	50.46	29.05
nvsz–26b	New Britain-Solomons-Vanuatu	166.6252	–15.1170	365.6	28.75	5
nvsz–27a	New Britain-Solomons-Vanuatu	167.0053	–15.6308	334.2	44.74	25.46
nvsz–27b	New Britain-Solomons-Vanuatu	166.7068	–15.7695	334.2	24.15	5
nvsz–28a	New Britain-Solomons-Vanuatu	167.4074	–16.3455	327.5	41.53	22.44

(continued on next page)

Table B8: (continued)

Segment	Description	Longitude (°E)	Latitude (°N)	Strike (°)	Dip (°)	Depth (km)
nvsz–28b	New Britain-Solomons-Vanuatu	167.1117	–16.5264	327.5	20.42	5
nvsz–29a	New Britain-Solomons-Vanuatu	167.9145	–17.2807	341.2	49.1	24.12
nvsz–29b	New Britain-Solomons-Vanuatu	167.6229	–17.3757	341.2	22.48	5
nvsz–30a	New Britain-Solomons-Vanuatu	168.2220	–18.2353	348.6	44.19	23.99
nvsz–30b	New Britain-Solomons-Vanuatu	167.8895	–18.2991	348.6	22.32	5
nvsz–31a	New Britain-Solomons-Vanuatu	168.5022	–19.0510	345.6	42.2	22.26
nvsz–31b	New Britain-Solomons-Vanuatu	168.1611	–19.1338	345.6	20.2	5
nvsz–32a	New Britain-Solomons-Vanuatu	168.8775	–19.6724	331.1	42.03	21.68
nvsz–32b	New Britain-Solomons-Vanuatu	168.5671	–19.8338	331.1	19.49	5
nvsz–33a	New Britain-Solomons-Vanuatu	169.3422	–20.4892	332.9	40.25	22.4
nvsz–33b	New Britain-Solomons-Vanuatu	169.0161	–20.6453	332.9	20.37	5
nvsz–34a	New Britain-Solomons-Vanuatu	169.8304	–21.2121	329.1	39	22.73
nvsz–34b	New Britain-Solomons-Vanuatu	169.5086	–21.3911	329.1	20.77	5
nvsz–35a	New Britain-Solomons-Vanuatu	170.3119	–21.6945	311.9	39	22.13
nvsz–35b	New Britain-Solomons-Vanuatu	170.0606	–21.9543	311.9	20.03	5
nvsz–36a	New Britain-Solomons-Vanuatu	170.9487	–22.1585	300.4	39.42	23.5
nvsz–36b	New Britain-Solomons-Vanuatu	170.7585	–22.4577	300.4	21.71	5
nvsz–37a	New Britain-Solomons-Vanuatu	171.6335	–22.3087	281.3	30	22.1
nvsz–37b	New Britain-Solomons-Vanuatu	171.5512	–22.6902	281.3	20	5

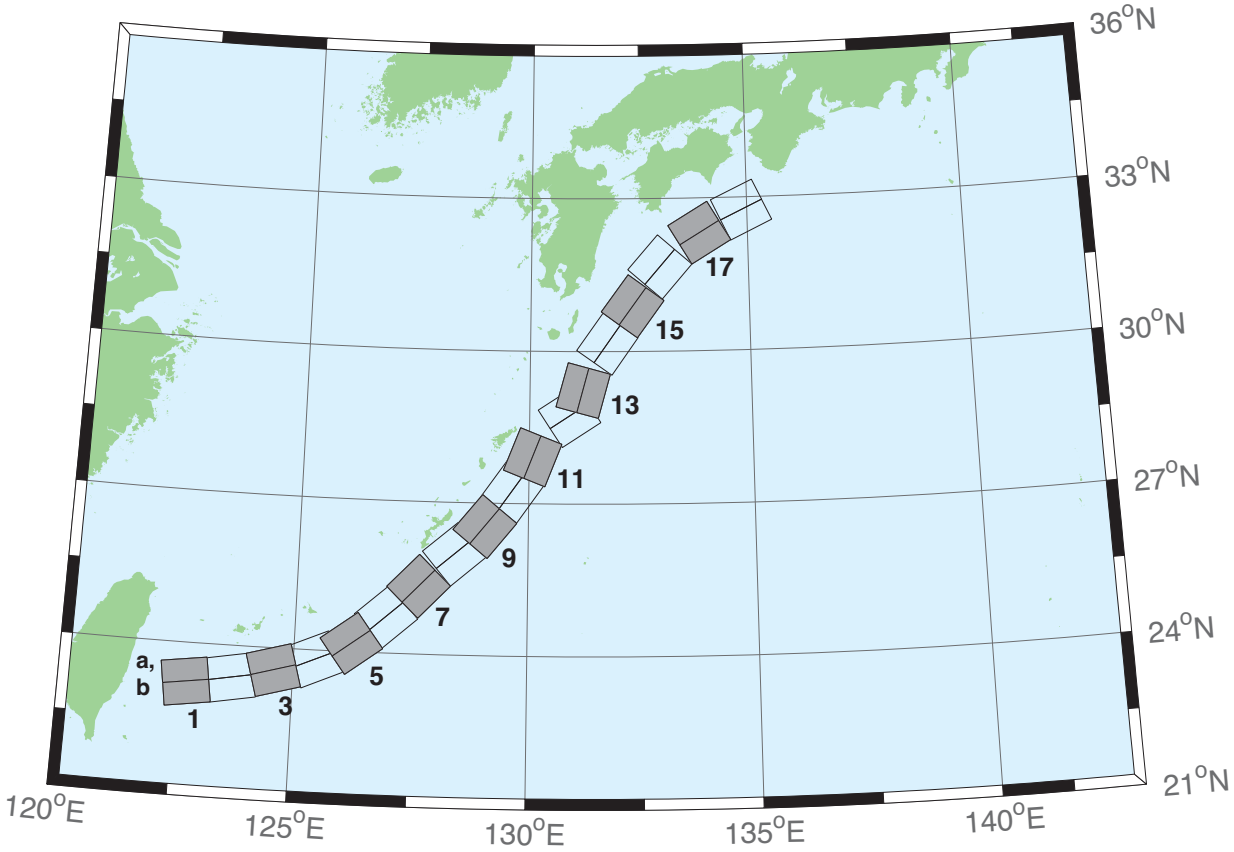

Figure B9: Ryukyu-Kyushu-Nankai Subduction Zone unit sources.

Table B9: Earthquake parameters for Ryukyu-Kyushu-Nankai Subduction Zone unit sources.

Segment	Description	Longitude (°E)	Latitude (°N)	Strike (°)	Dip (°)	Depth (km)
rnsz–1a	Ryukyu-Kyushu-Nankai	122.6672	23.6696	262	14	11.88
rnsz–1b	Ryukyu-Kyushu-Nankai	122.7332	23.2380	262	10	3.2
rnsz–2a	Ryukyu-Kyushu-Nankai	123.5939	23.7929	259.9	18.11	12.28
rnsz–2b	Ryukyu-Kyushu-Nankai	123.6751	23.3725	259.9	10	3.6
rnsz–3a	Ryukyu-Kyushu-Nankai	124.4604	23.9777	254.6	19.27	14.65
rnsz–3b	Ryukyu-Kyushu-Nankai	124.5830	23.5689	254.6	12.18	4.1
rnsz–4a	Ryukyu-Kyushu-Nankai	125.2720	24.2102	246.8	18	20.38
rnsz–4b	Ryukyu-Kyushu-Nankai	125.4563	23.8177	246.8	16	6.6
rnsz–5a	Ryukyu-Kyushu-Nankai	125.9465	24.5085	233.6	18	20.21
rnsz–5b	Ryukyu-Kyushu-Nankai	126.2241	24.1645	233.6	16	6.43
rnsz–6a	Ryukyu-Kyushu-Nankai	126.6349	25.0402	228.7	17.16	19.55
rnsz–6b	Ryukyu-Kyushu-Nankai	126.9465	24.7176	228.7	15.16	6.47
rnsz–7a	Ryukyu-Kyushu-Nankai	127.2867	25.6343	224	15.85	17.98
rnsz–7b	Ryukyu-Kyushu-Nankai	127.6303	25.3339	224	13.56	6.26
rnsz–8a	Ryukyu-Kyushu-Nankai	128.0725	26.3146	229.7	14.55	14.31
rnsz–8b	Ryukyu-Kyushu-Nankai	128.3854	25.9831	229.7	9.64	5.94
rnsz–9a	Ryukyu-Kyushu-Nankai	128.6642	26.8177	219.2	15.4	12.62
rnsz–9b	Ryukyu-Kyushu-Nankai	129.0391	26.5438	219.2	8	5.66
rnsz–10a	Ryukyu-Kyushu-Nankai	129.2286	27.4879	215.2	17	12.55
rnsz–10b	Ryukyu-Kyushu-Nankai	129.6233	27.2402	215.2	8.16	5.45
rnsz–11a	Ryukyu-Kyushu-Nankai	129.6169	28.0741	201.3	17	12.91
rnsz–11b	Ryukyu-Kyushu-Nankai	130.0698	27.9181	201.3	8.8	5.26
rnsz–12a	Ryukyu-Kyushu-Nankai	130.6175	29.0900	236.7	16.42	13.05
rnsz–12b	Ryukyu-Kyushu-Nankai	130.8873	28.7299	236.7	9.57	4.74
rnsz–13a	Ryukyu-Kyushu-Nankai	130.7223	29.3465	195.2	20.25	15.89
rnsz–13b	Ryukyu-Kyushu-Nankai	131.1884	29.2362	195.2	12.98	4.66
rnsz–14a	Ryukyu-Kyushu-Nankai	131.3467	30.3899	215.1	22.16	19.73
rnsz–14b	Ryukyu-Kyushu-Nankai	131.7402	30.1507	215.1	17.48	4.71
rnsz–15a	Ryukyu-Kyushu-Nankai	131.9149	31.1450	216	15.11	16.12
rnsz–15b	Ryukyu-Kyushu-Nankai	132.3235	30.8899	216	13.46	4.48
rnsz–16a	Ryukyu-Kyushu-Nankai	132.5628	31.9468	220.9	10.81	10.88
rnsz–16b	Ryukyu-Kyushu-Nankai	132.9546	31.6579	220.9	7.19	4.62
rnsz–17a	Ryukyu-Kyushu-Nankai	133.6125	32.6956	239	10.14	12.01
rnsz–17b	Ryukyu-Kyushu-Nankai	133.8823	32.3168	239	8.41	4.7
rnsz–18a	Ryukyu-Kyushu-Nankai	134.6416	33.1488	244.7	10.99	14.21
rnsz–18b	Ryukyu-Kyushu-Nankai	134.8656	32.7502	244.5	10.97	4.7

Appendix C. Synthetic Testing Report: Unalaska, Alaska

C1. Purpose

Forecast models are tested with synthetic tsunami events covering a range of tsunami source locations and magnitudes ranging from mega-events to micro-events. Testing is also done with a selected set of historical tsunami events when available.

The purpose of forecast model testing is three-fold. The first objective is to assure that the results obtained with the Short-term Inundation Forecasting of Tsunamis (SIFT) software, which has been released to the Tsunami Warning Centers for operational use, are identical to those obtained by the researcher during the development of the forecast model. The second objective is to test the forecast model for consistency, accuracy, time efficiency, and quality of results over a range of possible tsunami locations and magnitudes. The third objective is to identify bugs and issues in need of resolution by the researcher who developed the forecast model or by the SIFT software development team before the next version release to NOAA's two Tsunami Warning Centers.

Local hardware and software applications, and tools familiar to the researcher(s), are used to run the Method of Splitting Tsunamis (MOST) model during the forecast model development. The test results presented in this report lend confidence that the model performs as developed and produces the same results when initiated within the SIFT application in an operational setting as those produced by the researcher(s) during the forecast model development. The test results assure those who rely on the Unalaska tsunami forecast model that consistent results are produced irrespective of the system used.

C2. Testing Procedure

The general procedure for forecast model testing is to run a set of synthetic tsunami scenarios and a selected set of historical tsunami events through the SIFT application and compare the results with those obtained by the researcher during the forecast model development and presented in the tsunami forecast model report. Specific steps taken to test the model include:

- Identification of testing scenarios, including the standard set of synthetic events, appropriate historical events, and customized synthetic scenarios that may have been used by the researcher(s) in developing the forecast model.
- Creation of new SIFT events to represent customized synthetic scenarios used by the researcher(s) in developing the forecast model, if any.
- Submission of test model runs with SIFT, and export of the results from grids A, B, and C, along with time series.
- Recording applicable metadata, including the specific SIFT version used for testing.
- Examination of SIFT forecast model results for instabilities in both time series and plot results.
- Comparison of forecast model results obtained through SIFT with those obtained during the forecast model development.
- Summarization of results with specific mention of quality, consistency, and time efficiency.
- Reporting of issues identified to modeler and SIFT software development team.
- Retesting the forecast models in SIFT when reported issues have been addressed or explained.

Synthetic model runs were tested on a DELL PowerEdge R510 computer equipped with two Xeon E5670 processors at 2.93 GHz, each with 12 MB of cache and 32 GB memory. The processors are hex core and support hyper-threading, resulting in the computer performing as a 24 core processor machine. Additionally, the testing computer supports 10 Gigabit Ethernet for fast network connections. This computer configuration is similar or the same as the configurations of the computers installed at the Tsunami Warning Centers so the compute times should vary only slightly.

C3. Results

The Unalaska, Alaska, forecast model was tested with SIFT version 3.1, the current version installed at the NOAA Tsunami Warning Centers.

The Unalaska forecast model was tested with 23 synthetic scenario events and two historical events. Test results from the SIFT application and comparisons with the results obtained during the forecast model development are provided numerically in **Table C1** and graphically in **Figures C1 to 25**. The results show that the forecast model is stable and robust, with consistent and high quality results across geographically distributed tsunami sources and tsunami magnitudes from micro-events to mega-events. The model run time (wall-clock time) was 15.95 min for 7.99 hr of simulation time, and 7.96 min for 4.0 hr. This run time is within the 10 min run time for 4 hr of simulation time required by the warning centers, and satisfies the time efficiency requirements.

The standard suite of synthetic events was run on the Unalaska forecast model. The modeled scenarios were stable for all cases tested, with no instabilities or ringing. Results show that the largest modeled height was 3.9 m and originated in the Aleutian-Alaska-Cascadia (ACSZ 16–25) source. Additionally, large (2.8–3.1 m) amplitudes were recorded using the overlapping and adjacent Aleutian-Alaska-Cascadia (ACSZ 22–31 and 6–15) sources. Amplitudes greater than 1 m were recorded at the Kamchatka-Yap-Mariana-Izu-Bonin (KISZ 1–10), Manus OCB (MOSZ 1–10), and the New Zealand-Kermadec-Tonga (NTSZ 30–39) sources. The smallest signal of 0.13 m was recorded at the far-field Central and South America (CSSZ 1–10 and 37–46) sources. Small scale events (Mw = 7.5) and micro-events tested were also stable. Direct comparisons of SIFT output with development results of both the historical and synthetic events demonstrated that the wave pattern were similar in shape, pattern, and amplitude. However, in a few cases, the maximum amplitudes obtained during forecast model development of Unalaska were higher than the maximum amplitudes obtained using the SIFT software. This can be attributed to slight differences in the warning point location between Ferret, used by the modeler versus the SIFT output.

Table C1: Maximum and minimum amplitudes at the Unalaska, Alaska, warning point for synthetic and historical events tested using SIFT 3.1 and obtained during development.

			α	Max (cm)		Min (cm)	
Scenario	**Source Zone**	**Tsunami Source**	**(m)**	**SIFT**	**Devel.**	**SIFT**	**Devel.**
Mega-tsunami Scenario							
KISZ 1–10	Kamchatka-Yap-Mariana-Izu-Bonin	A1–A10, B1–B10	25	180.4	178.2	-145.0	-142.6
KISZ 22–31	Kamchatka-Yap-Mariana-Izu-Bonin	A22–A31, B22–B31	25	81.1	80.7	-79.1	-78.6
KISZ 32–41	Kamchatka-Yap-Mariana-Izu-Bonin	A32–A41, B32–B41	25	75.2	75.3	-83.1	-83.1
KISZ 56–65	Kamchatka-Yap-Mariana-Izu-Bonin	A56–A65, B56–B65	25	89.7	87.4	-95.8	-94.2
ACSZ 6–15	Aleutian-Alaska-Cascadia	A6–A15, B6–B15	25	282.2	279.8	-237.1	-238.0
ACSZ 16–25	Aleutian-Alaska-Cascadia	A16–A25, B16–B25	25	385.1	355.4	-204.8	-205.9
ACSZ 22–31	Aleutian-Alaska-Cascadia	A22–A31, B22–B31	25	306.1	298.4	-230.8	-234.0
ACSZ 50–59	Aleutian-Alaska-Cascadia	A50–A59, B50–B59	25	47.5	46.3	-47.2	-47.3
ACSZ 56–65	Aleutian-Alaska-Cascadia	A56–A65, B56–B65	25	57.8	58.5	-69.6	-70.2
CSSZ 1–10	Central and South America	A1–A10, B1–B10	25	13.5	14.8	-11.3	-14.5
CSSZ 37–46	Central and South America	A37–A46, B37–B46	25	12.8	12.7	-13.9	-13.7
CSSZ 89–98	Central and South America	A89–A98, B89–B98	25	99.8	97.6	-88.6	-88.7
CSSZ 102–111	Central and South America	A102–A111, B102–B111	25	95.3	95.9	-93.9	-93.1
NTSZ 30–39	New Zealand-Kermadec-Tonga	A30–A39, B30–B39	25	103.5	101.4	-95.3	-96.1
NVSZ 28–37	New Britain-Solomons-Vanuatu	A28–A37, B28–B37	25	72.2	71.3	-56.3	-57.1
MOSZ 1–10	Manus-OCB	A1–A10, B1–B10	25	106.8	100.0	-112.0	-111.0
NGSZ 3–12	North New Guinea	A3–A12, B3–B12	25	87.0	86.8	-77.8	-78.8
EPSZ 6–15	East Philippines	A6–A15, B6–B15	25	66.9	67.8	-71.2	-70.5
RNSZ 12–21	Ryukyu-Kyushu-Nankai	A12–A21, B12–B21	25	40.2	41.9	-47.0	-46.4
Mw 7.5 Scenario							
NTSZ B36	New Zealand-Kermadec-Tonga	B36	1	0.7	0.7	-0.6	-0.6
Micro-tsunami Scenario							
EPSZ B19	East Philippines	B19	0.04	0.01	0.01	-0.01	-0.01
RNSZ B14	Ryukyu-Kyushu-Nankai	B14	0.03	0.01	n/a	-0.01	n/a
ACSZ B6	Aleutian-Alaska-Cascadia	B6	0.02	0.06	n/a	-0.07	n/a
Historical Events							
2006 Kuril	n/a	n/a	n/a	8.2	n/a	-8.1	n/a
2007 Kuril	n/a	n/a	n/a	2.6	n/a	-3.5	n/a

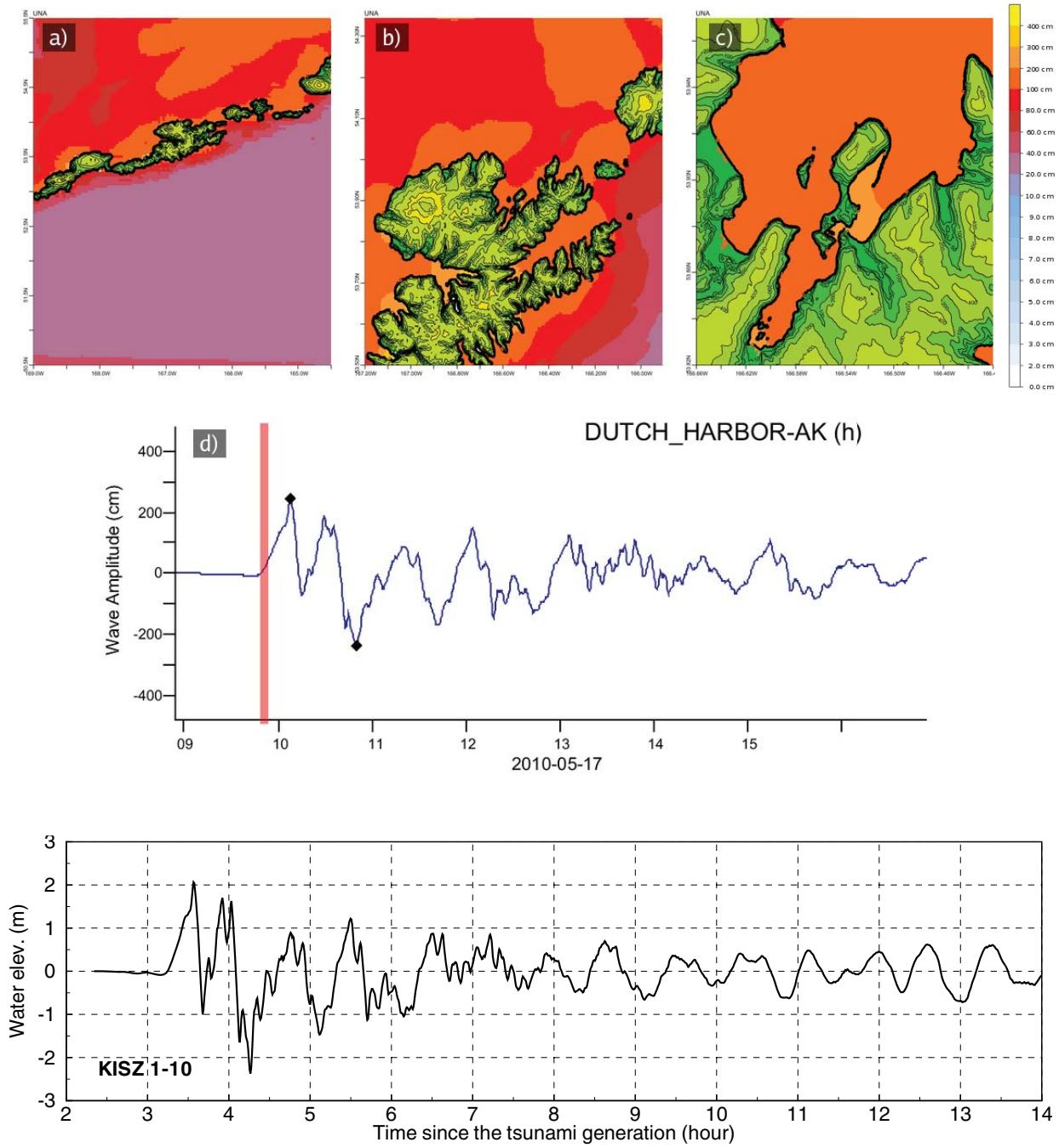

Figure C1: Response of the Unalaska forecast model to synthetic scenario KISZ 1–10 (alpha=25). Maximum sea surface elevation for (a) A grid, b) B grid, c) C grid. Sea surface elevation time series at the C-grid warning point (d). The lower time series plot is the result obtained during model development and is shown for comparison with test results.

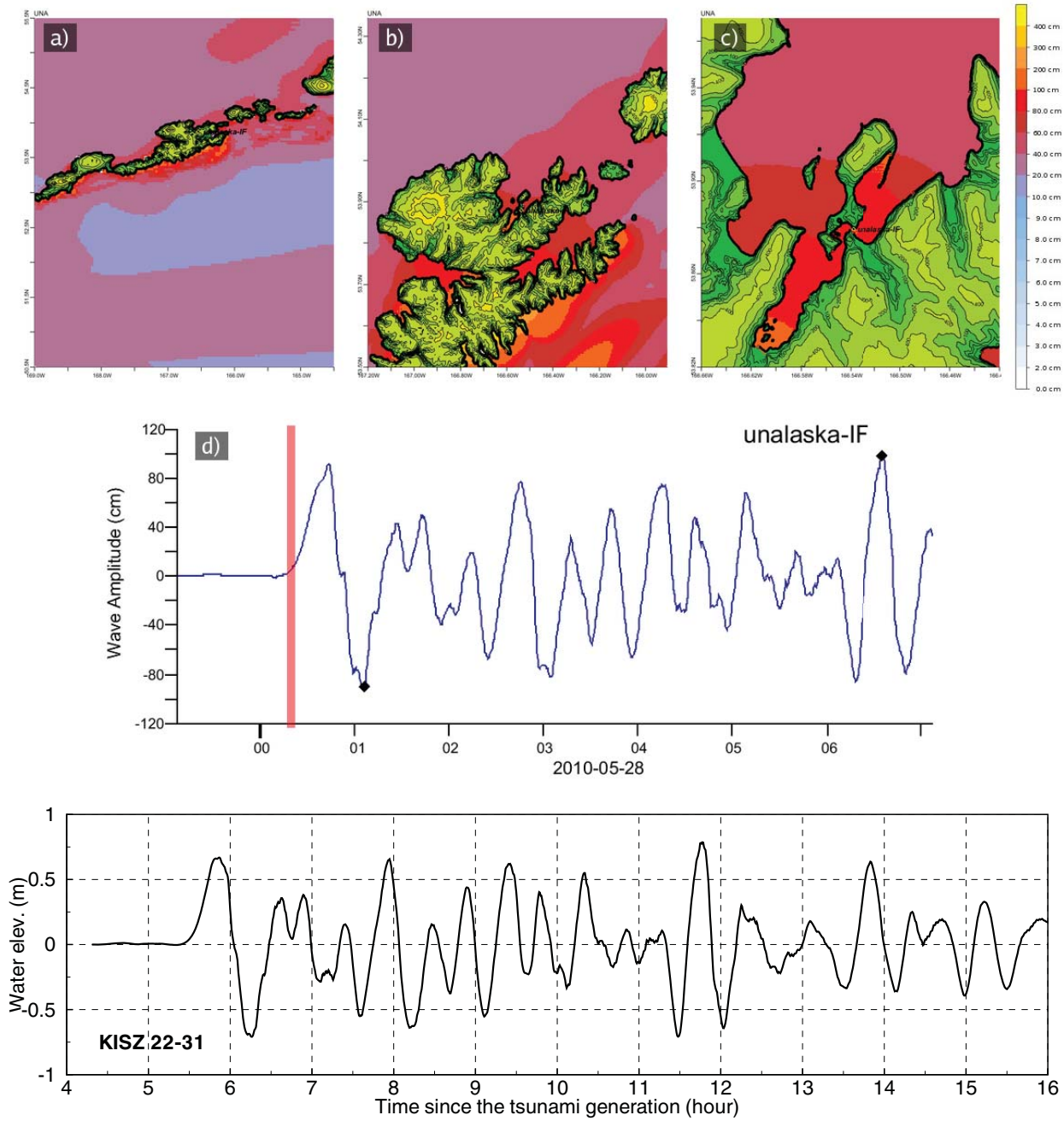

Figure C2: Response of the Unalaska forecast model to synthetic scenario KISZ 22–31 (alpha=25). Maximum sea surface elevation for (a) A grid, b) B grid, c) C grid. Sea surface elevation time series at the C-grid warning point (d). The lower time series plot is the result obtained during model development and is shown for comparison with test results.

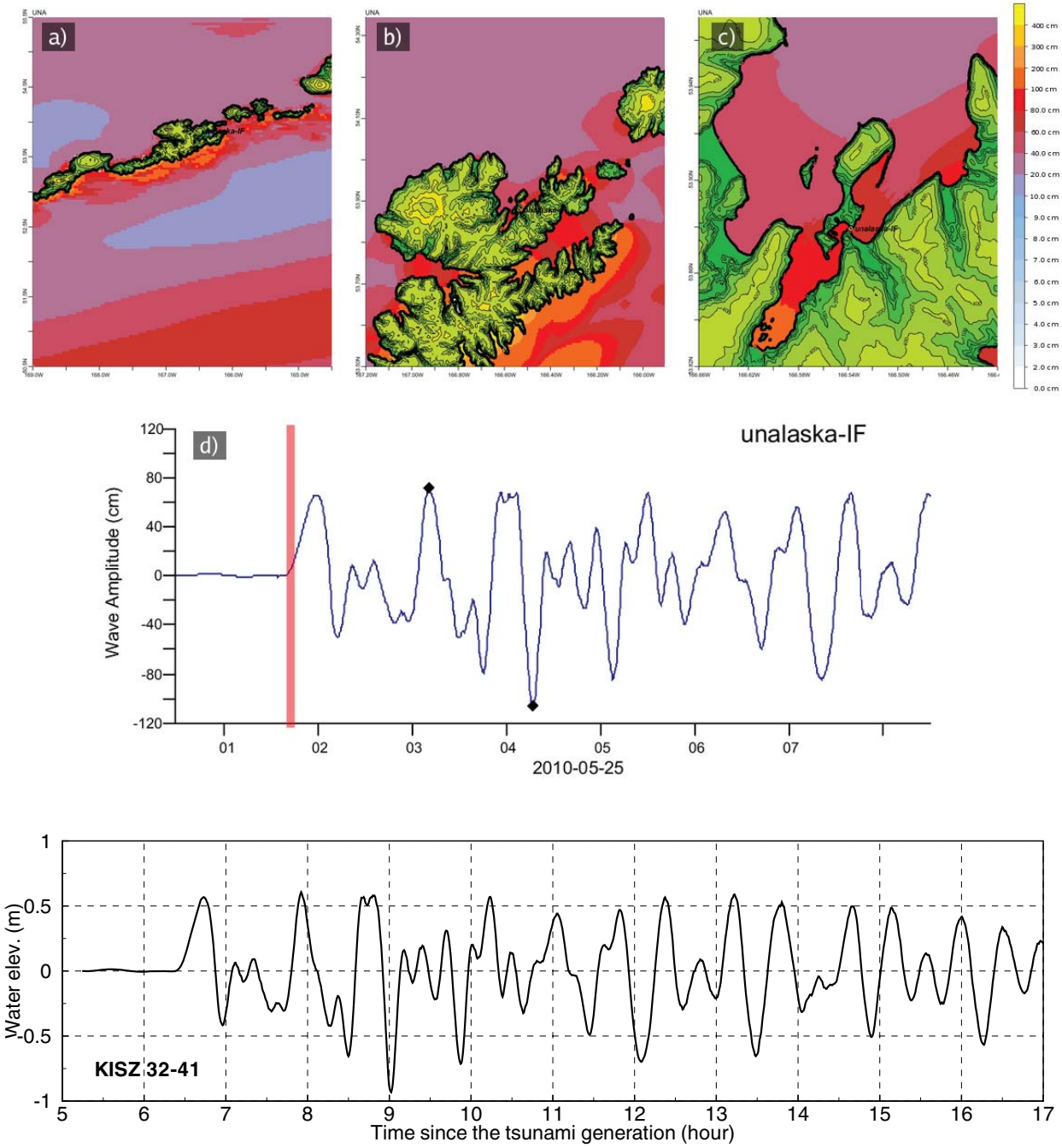

Figure C3: Response of the Unalaska forecast model to synthetic scenario KISZ 32–41 (alpha=25). Maximum sea surface elevation for (a) A grid, b) B grid, c) C grid. Sea surface elevation time series at the C-grid warning point (d). The lower time series plot is the result obtained during model development and is shown for comparison with test results.

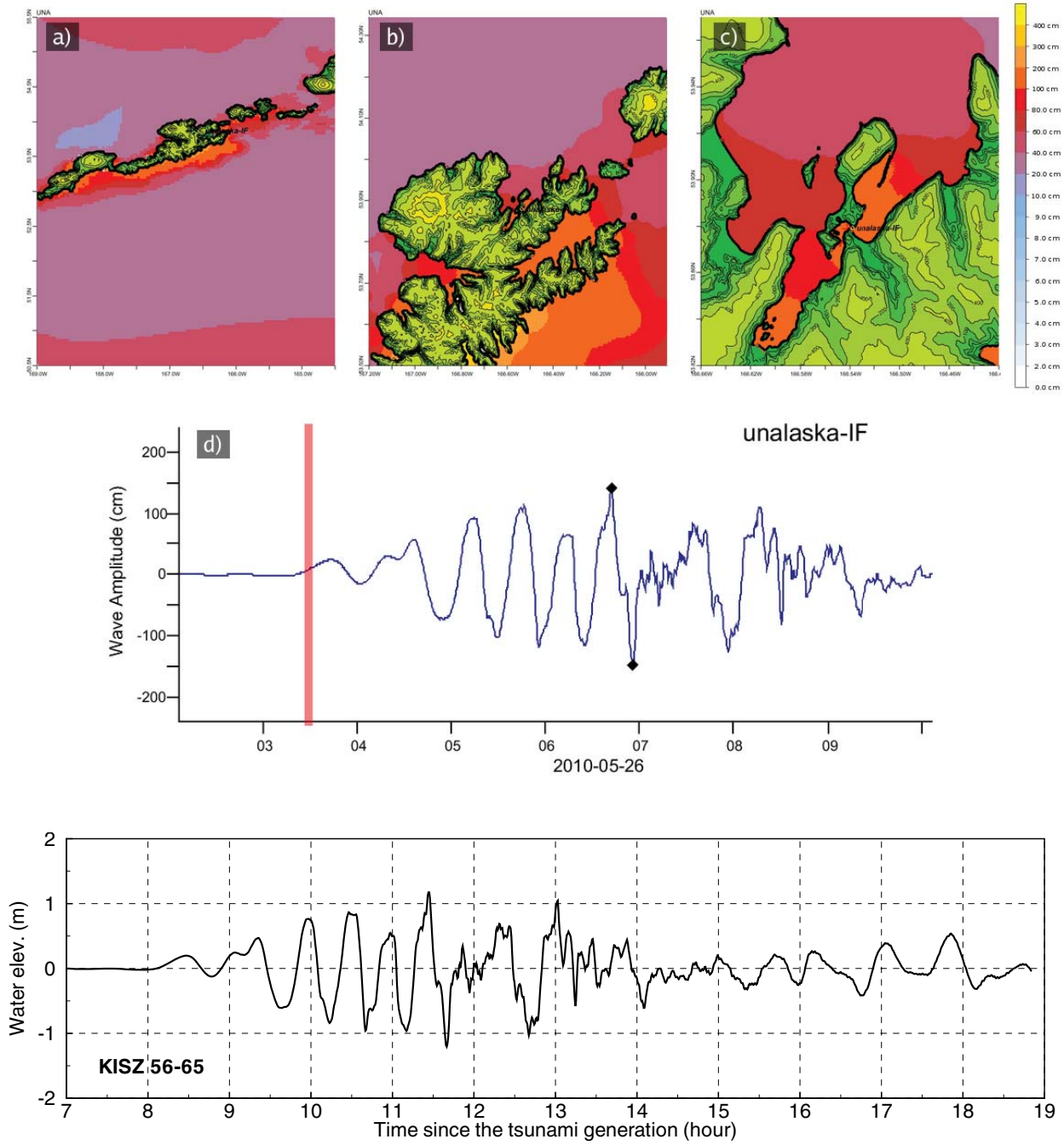

Figure C4: Response of the Unalaska forecast model to synthetic scenario KISZ 56–65 (alpha=25). Maximum sea surface elevation for (a) A grid, b) B grid, c) C grid. Sea surface elevation time series at the C-grid warning point (d). The lower time series plot is the result obtained during model development and is shown for comparison with test results.

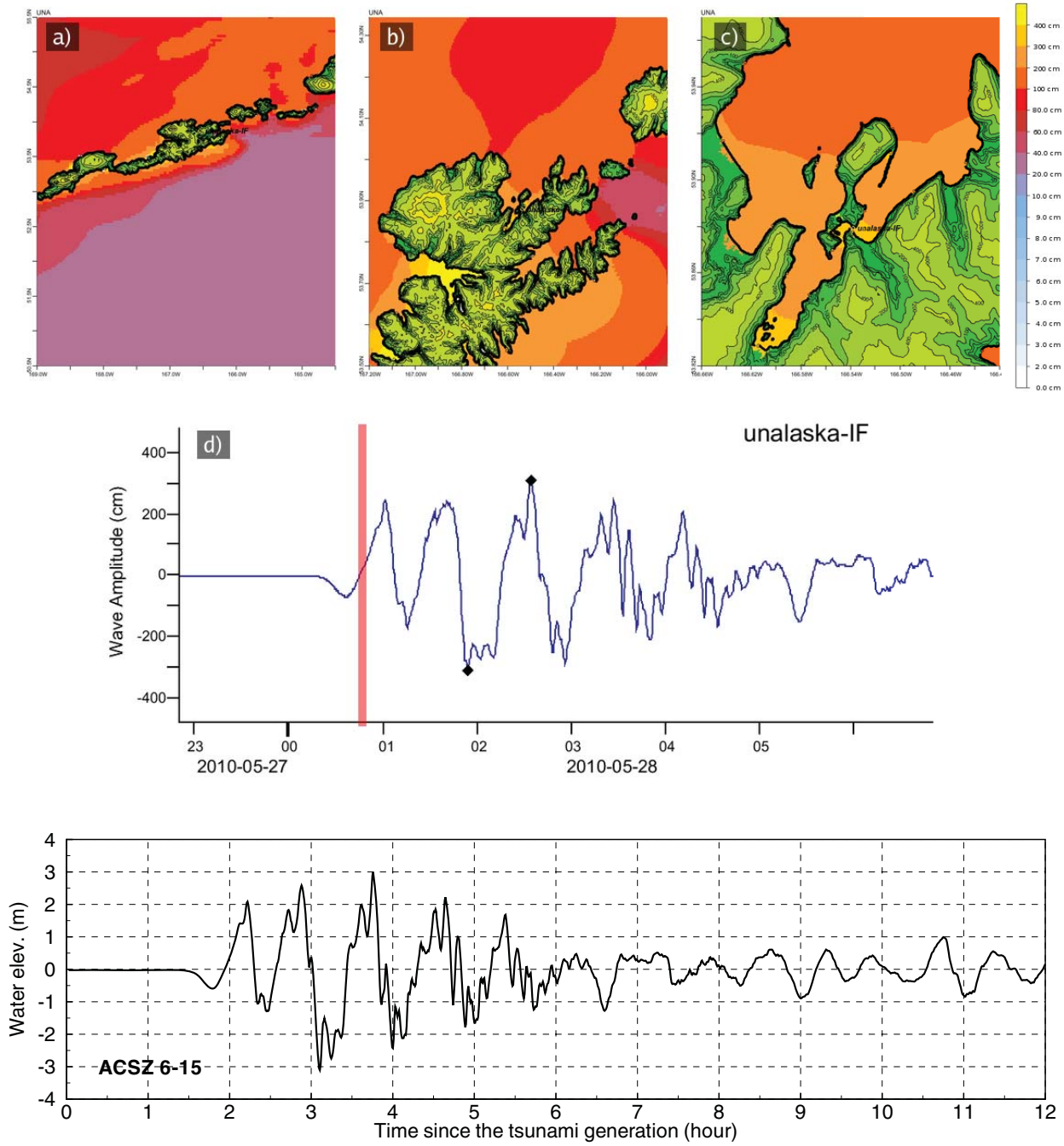

Figure C5: Response of the Unalaska forecast model to synthetic scenario ACSZ 6–15 (alpha=25). Maximum sea surface elevation for (a) A grid, b) B grid, c) C grid. Sea surface elevation time series at the C-grid warning point (d). The lower time series plot is the result obtained during model development and is shown for comparison with test results.

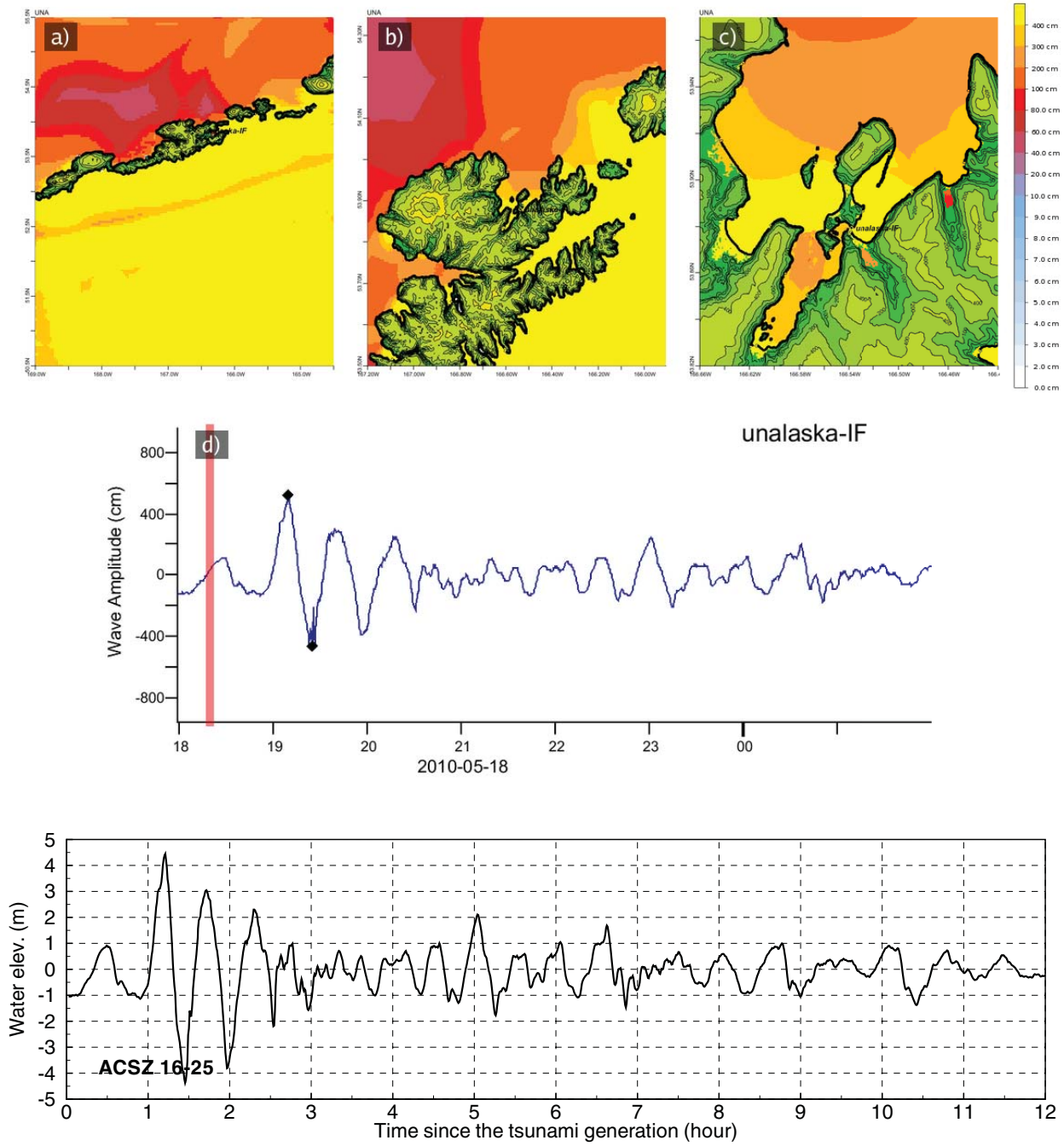

Figure C6: Response of the Unalaska forecast model to synthetic scenario ACSZ 16–25 (alpha=25). Maximum sea surface elevation for (a) A grid, b) B grid, c) C grid. Sea surface elevation time series at the C-grid warning point (d). The lower time series plot is the result obtained during model development and is shown for comparison with test results.

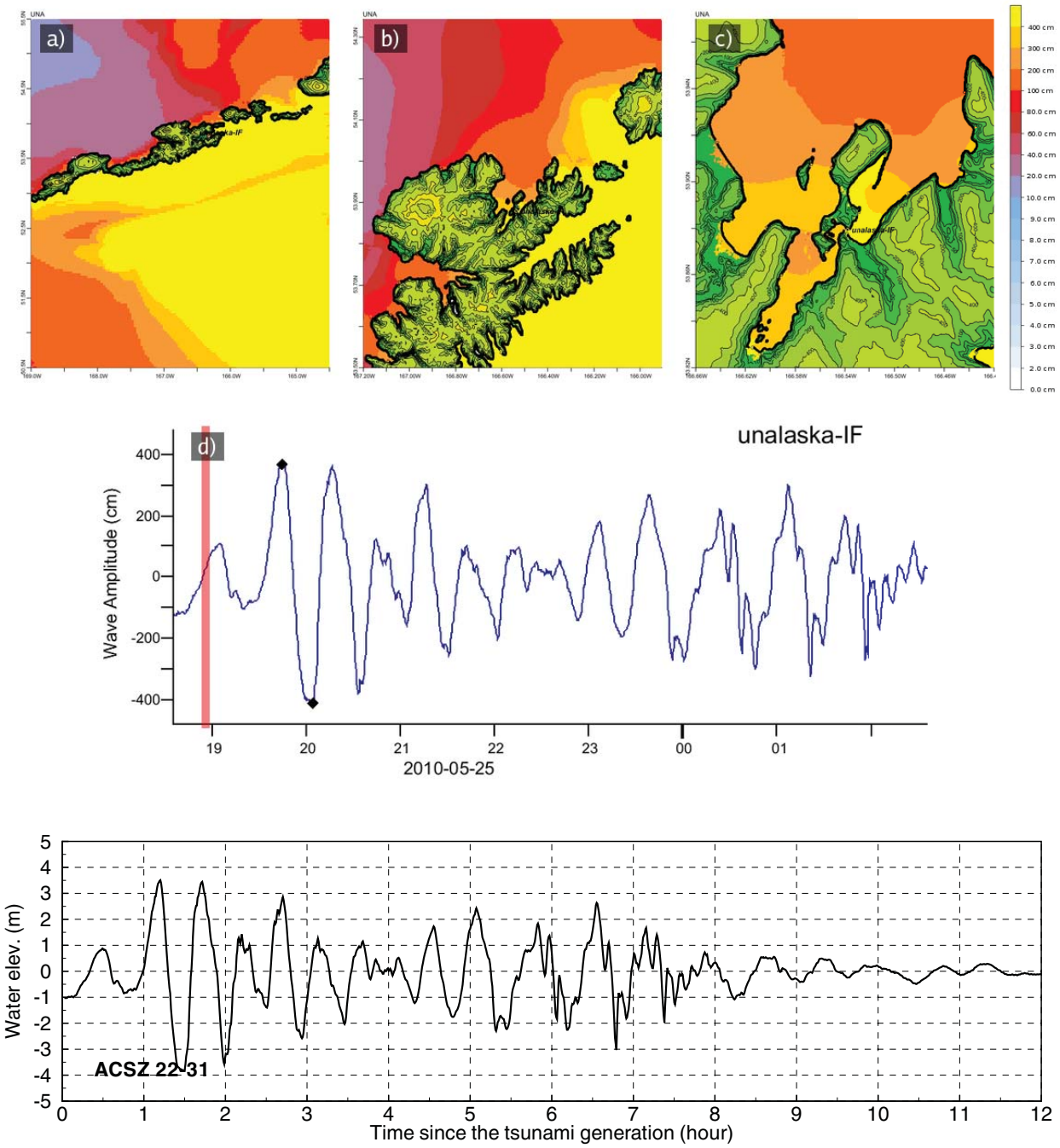

Figure C7: Response of the Unalaska forecast model to synthetic scenario ACSZ 22–31 (alpha=25). Maximum sea surface elevation for (a) A grid, b) B grid, c) C grid. Sea surface elevation time series at the C-grid warning point (d). The lower time series plot is the result obtained during model development and is shown for comparison with test results.

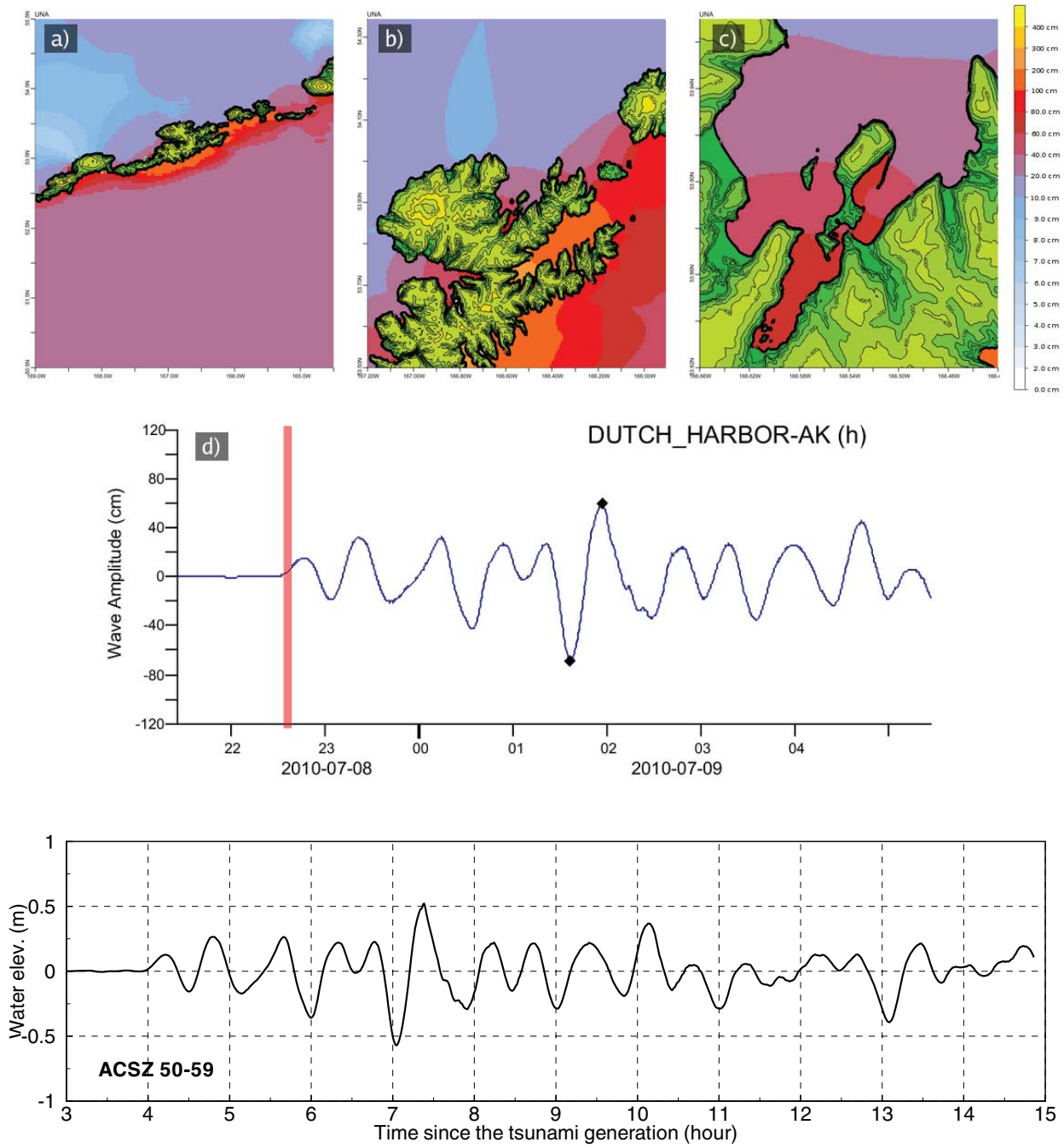

Figure C8: Response of the Unalaska forecast model to synthetic scenario ACSZ 50–59 (alpha=25). Maximum sea surface elevation for (a) A grid, b) B grid, c) C grid. Sea surface elevation time series at the C-grid warning point (d). The lower time series plot is the result obtained during model development and is shown for comparison with test results.

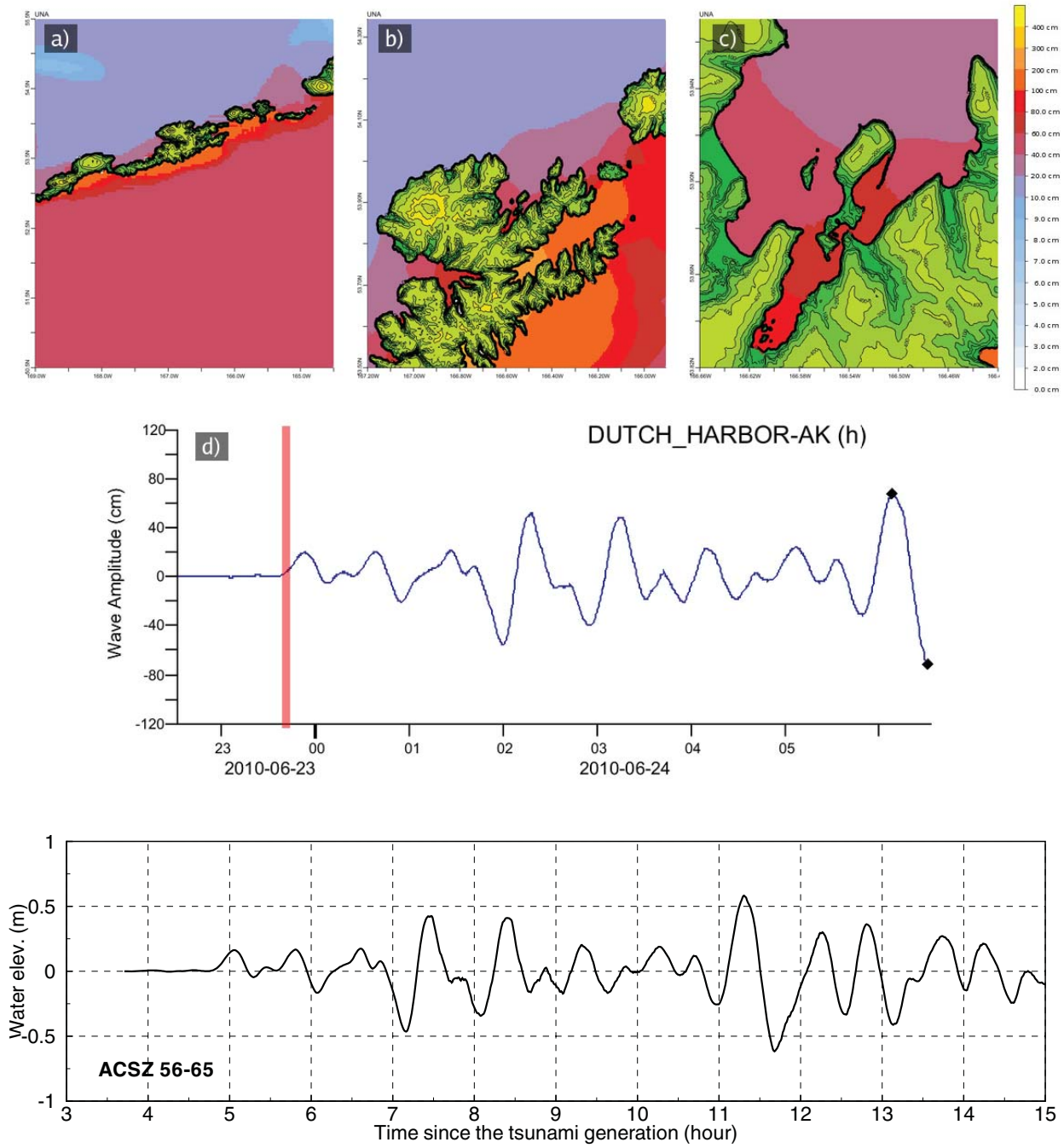

Figure C9: Response of the Unalaska forecast model to synthetic scenario ACSZ 56–65 (alpha=25). Maximum sea surface elevation for (a) A grid, b) B grid, c) C grid. Sea surface elevation time series at the C-grid warning point (d). The lower time series plot is the result obtained during model development and is shown for comparison with test results.

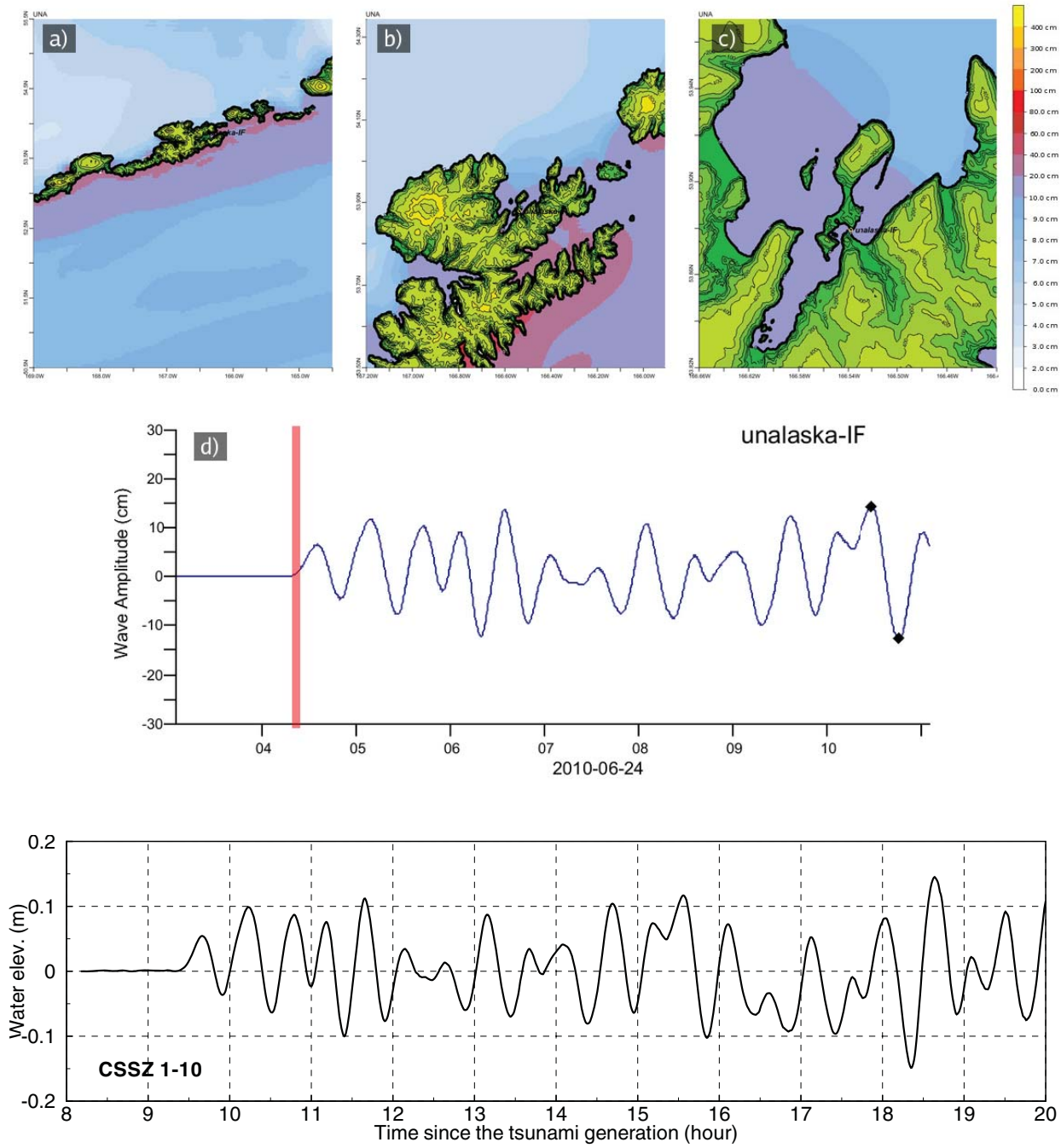

Figure C10: Response of the Unalaska forecast model to synthetic scenario CSSZ 1–10 (alpha=25). Maximum sea surface elevation for (a) A grid, b) B grid, c) C grid. Sea surface elevation time series at the C-grid warning point (d). The lower time series plot is the result obtained during model development and is shown for comparison with test results.

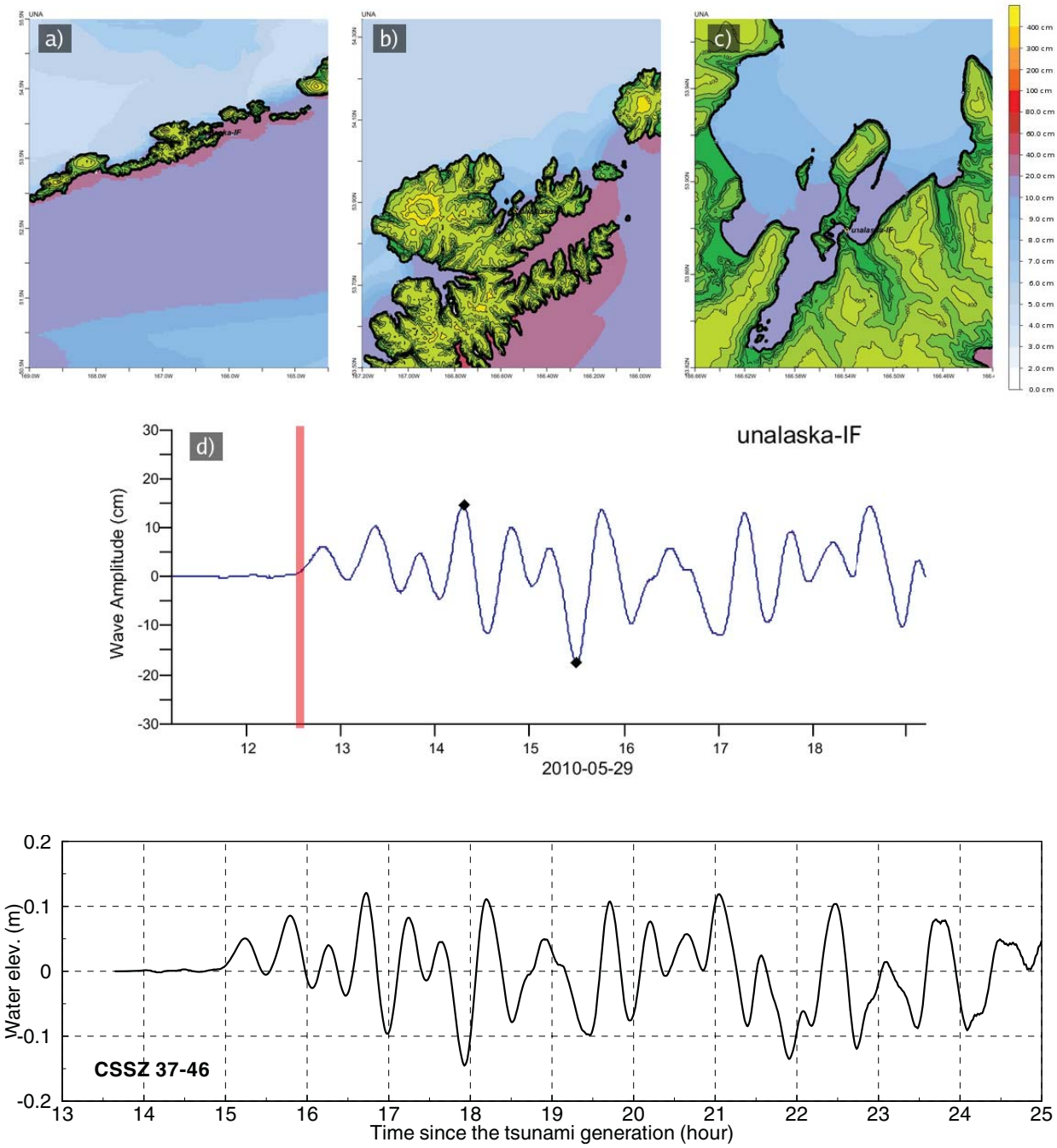

Figure C11: Response of the Unalaska forecast model to synthetic scenario CSSZ 37–46 (alpha=25). Maximum sea surface elevation for (a) A grid, b) B grid, c) C grid. Sea surface elevation time series at the C-grid warning point (d). The lower time series plot is the result obtained during model development and is shown for comparison with test results.

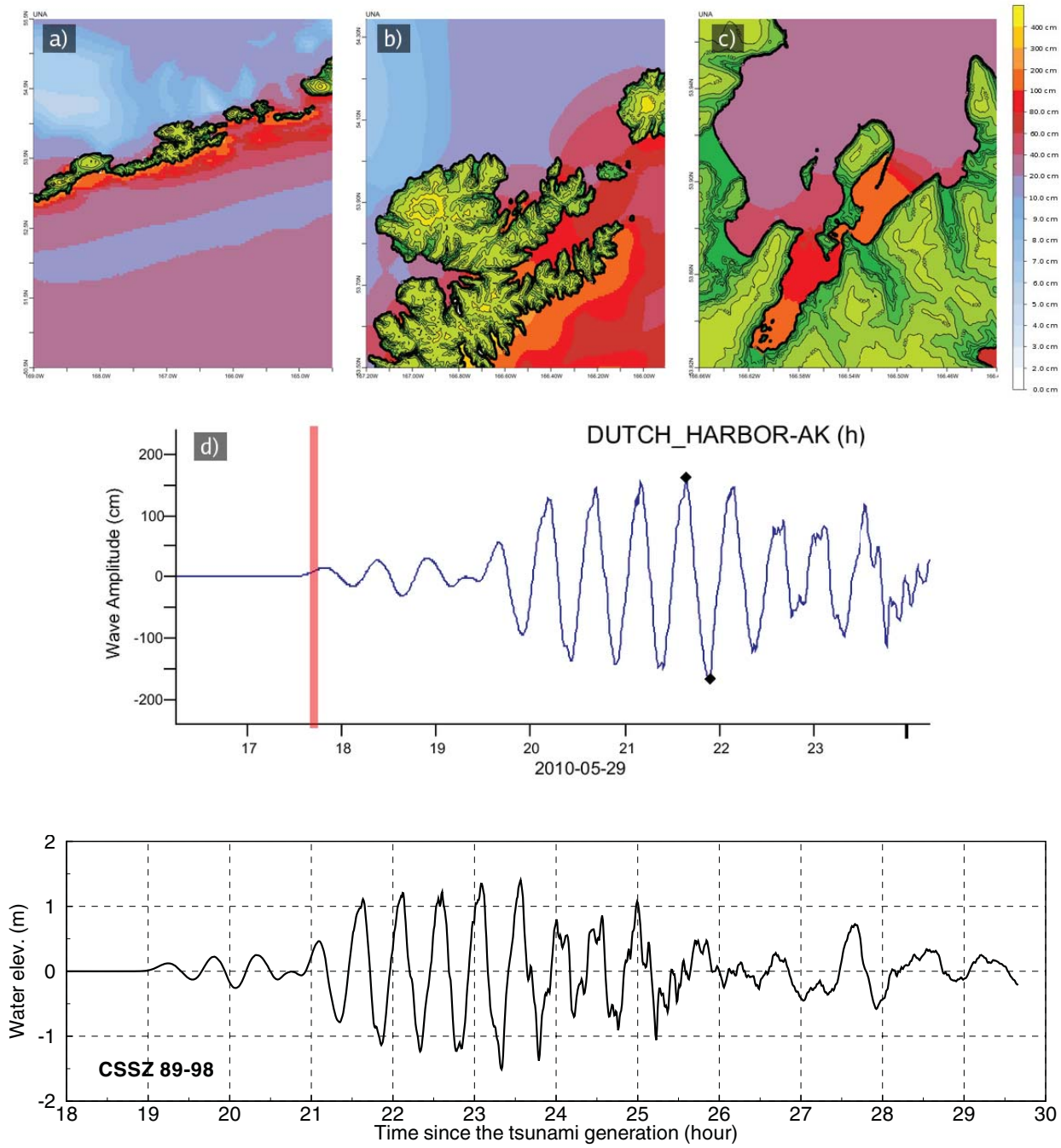

Figure C12: Response of the Unalaska forecast model to synthetic scenario CSSZ 89–98 (alpha=25). Maximum sea surface elevation for (a) A grid, b) B grid, c) C grid. Sea surface elevation time series at the C-grid warning point (d). The lower time series plot is the result obtained during model development and is shown for comparison with test results.

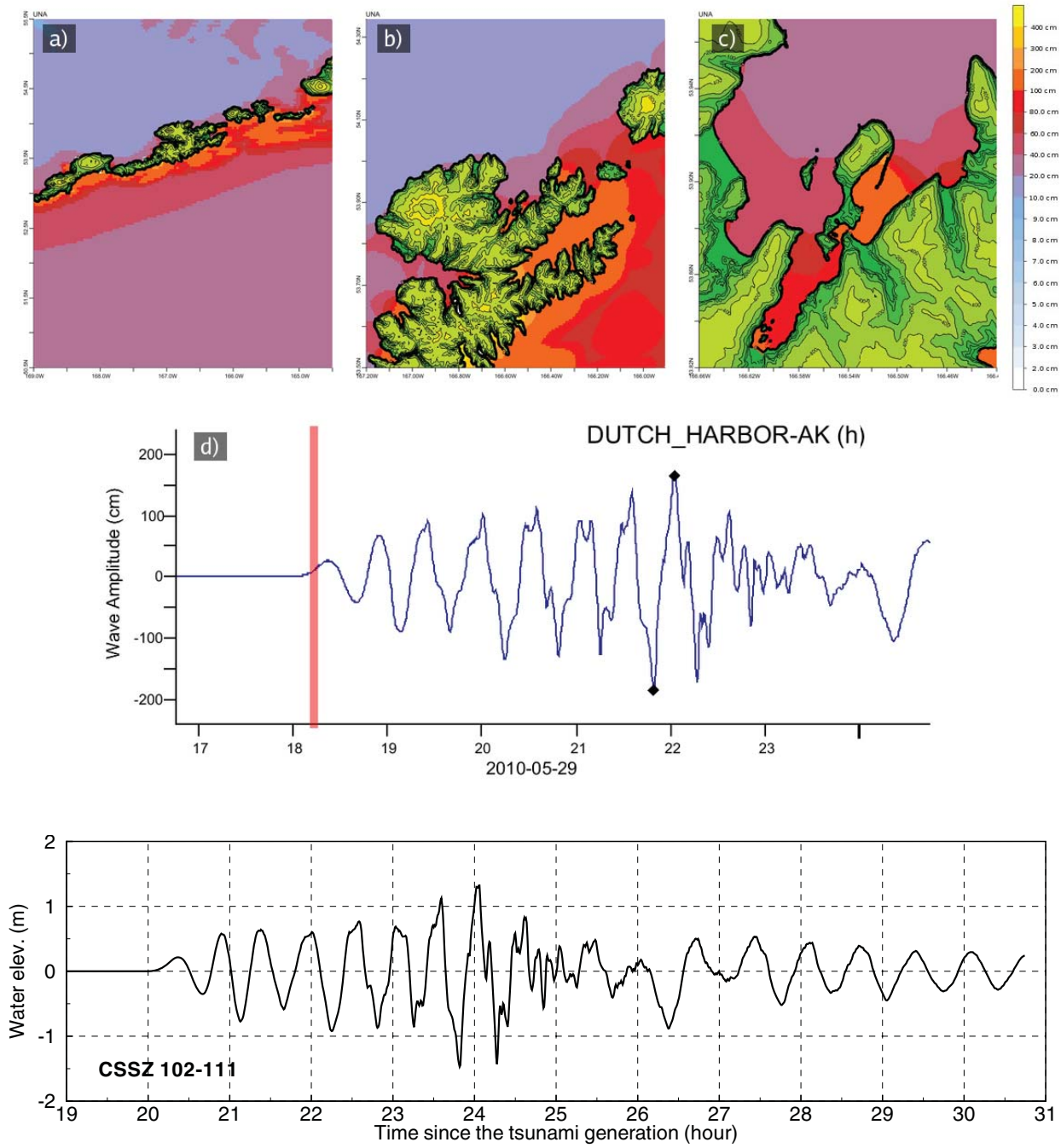

Figure C13: Response of the Unalaska forecast model to synthetic scenario CSSZ 102–111 (alpha=25). Maximum sea surface elevation for (a) A grid, b) B grid, c) C grid. Sea surface elevation time series at the C-grid warning point (d). The lower time series plot is the result obtained during model development and is shown for comparison with test results.

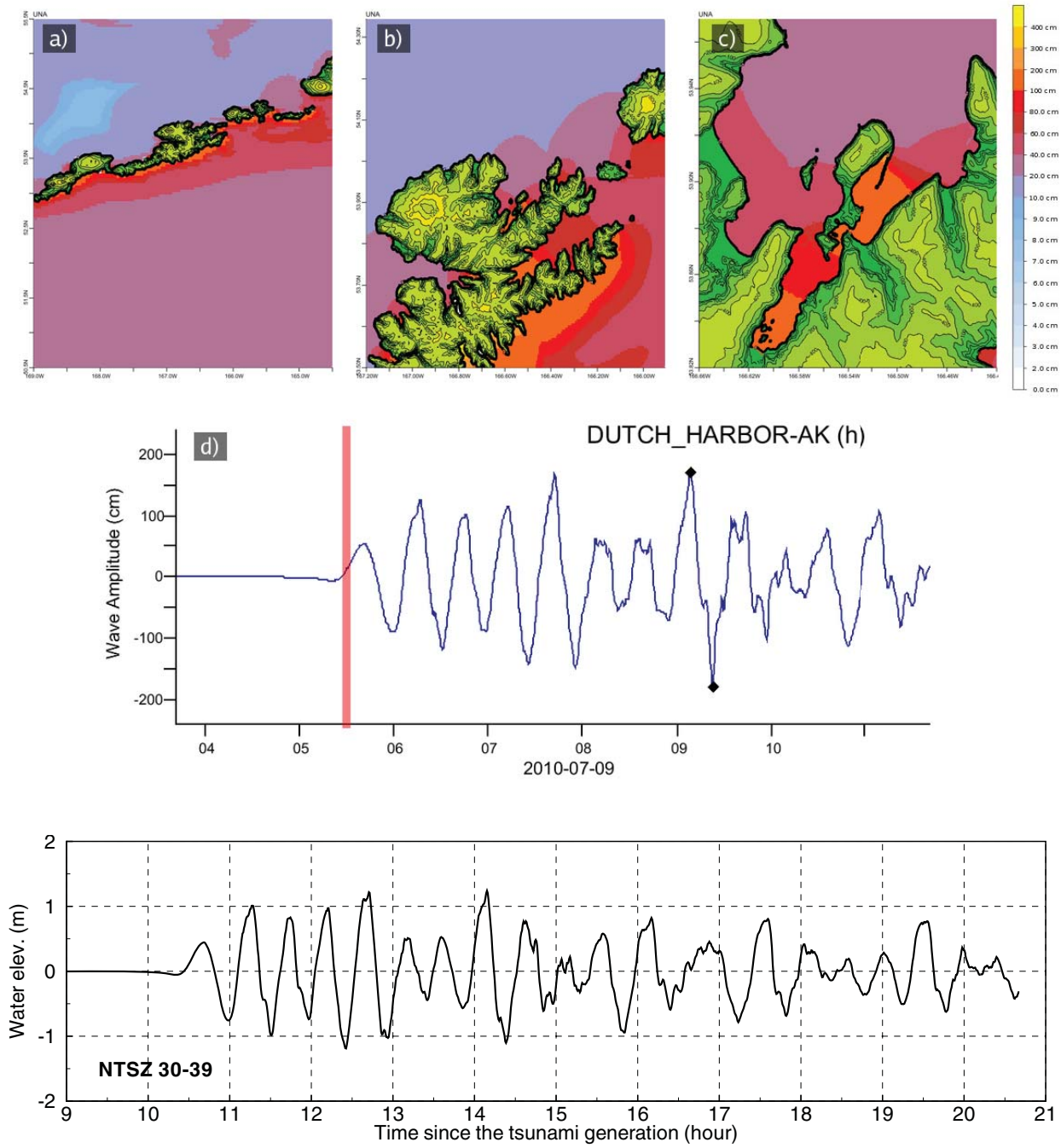

Figure C14: Response of the Unalaska forecast model to synthetic scenario NTSZ 30–39 (alpha=25). Maximum sea surface elevation for (a) A grid, b) B grid, c) C grid. Sea surface elevation time series at the C-grid warning point (d). The lower time series plot is the result obtained during model development and is shown for comparison with test results.

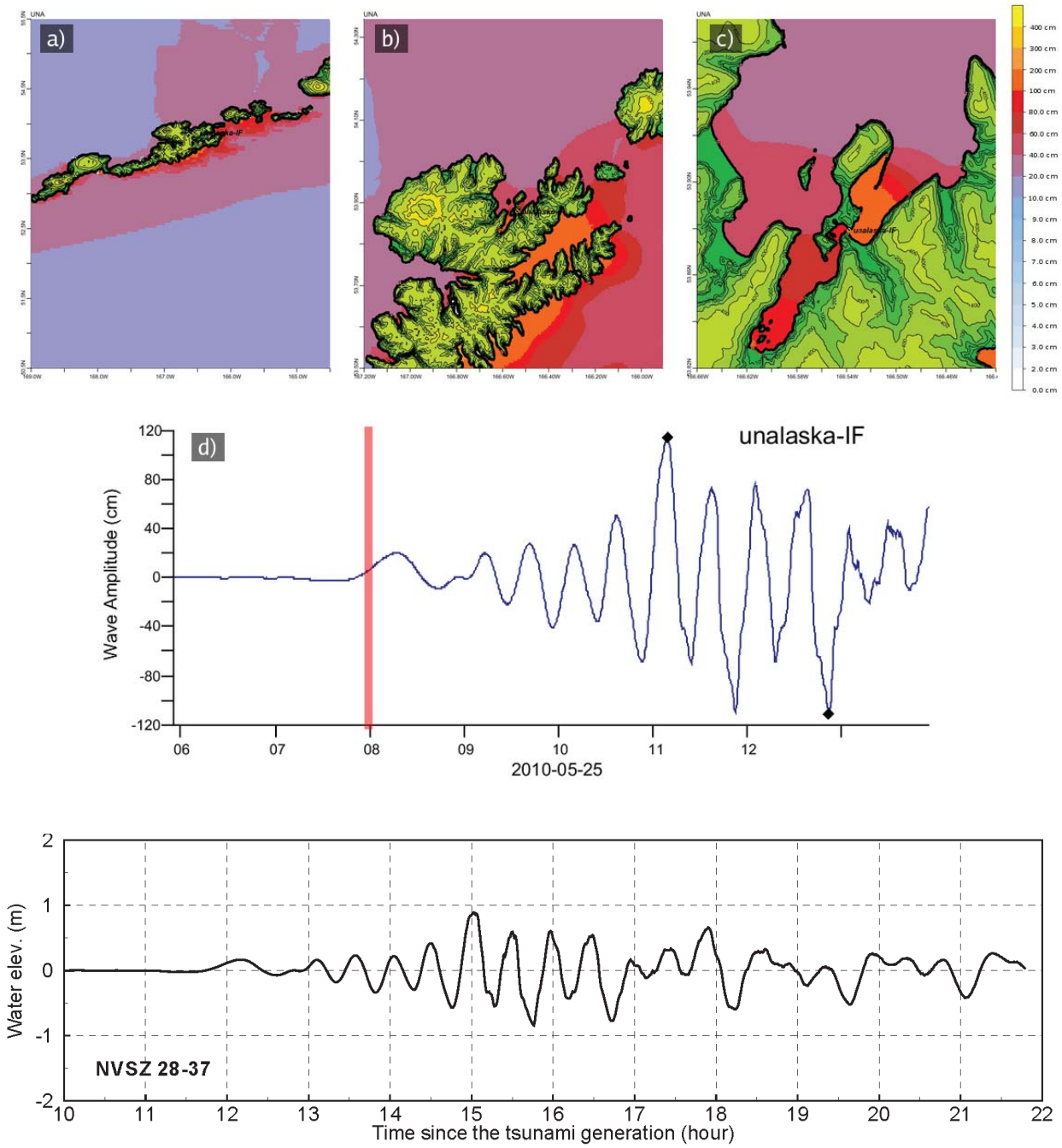

Figure C15: Response of the Unalaska forecast model to synthetic scenario NVSZ 28–37 (alpha=25). Maximum sea surface elevation for (a) A grid, b) B grid, c) C grid. Sea surface elevation time series at the C-grid warning point (d). The lower time series plot is the result obtained during model development and is shown for comparison with test results.

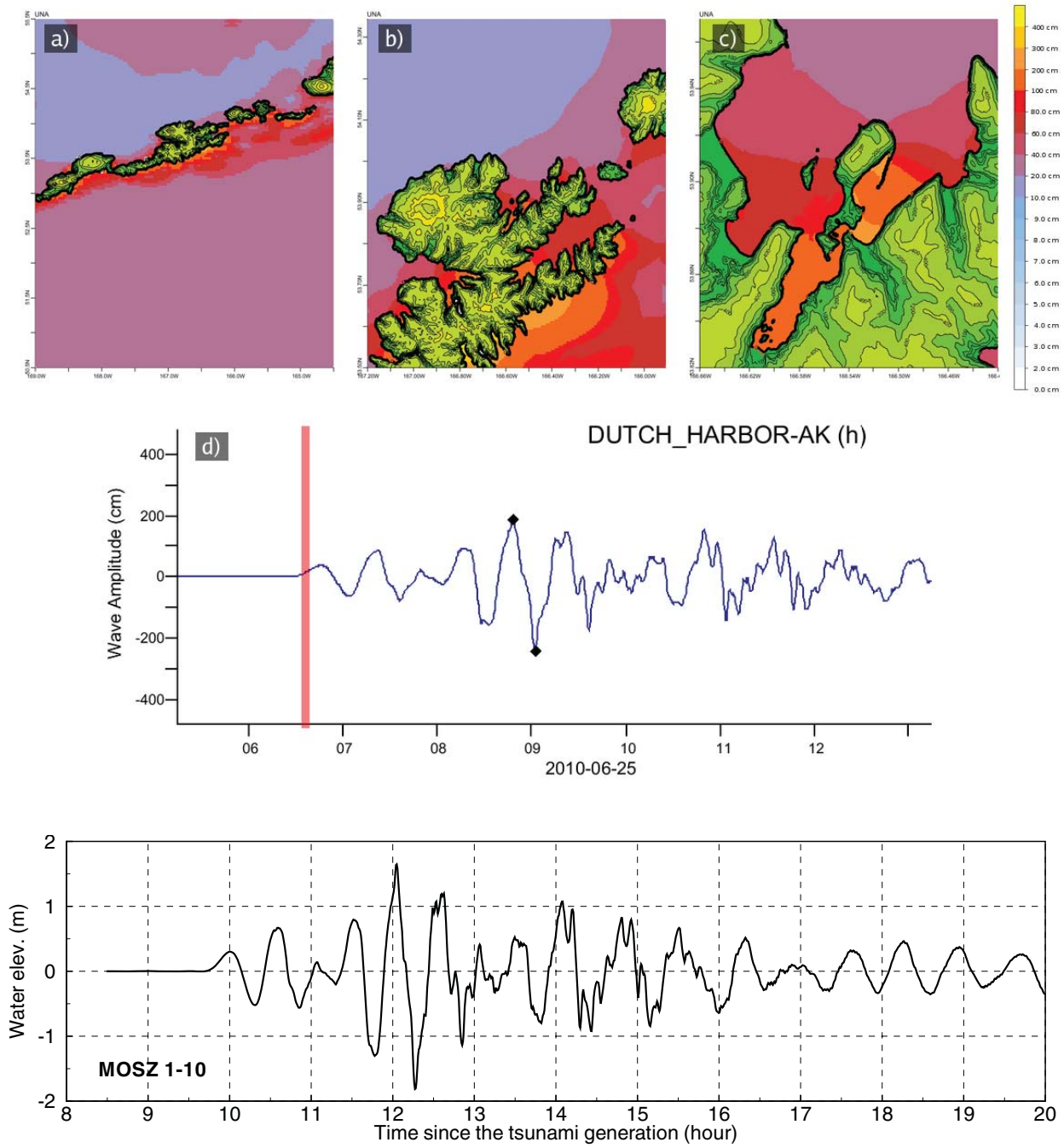

Figure C16: Response of the Unalaska forecast model to synthetic scenario MOSZ 1–10 (alpha=25). Maximum sea surface elevation for (a) A grid, b) B grid, c) C grid. Sea surface elevation time series at the C-grid warning point (d). The lower time series plot is the result obtained during model development and is shown for comparison with test results.

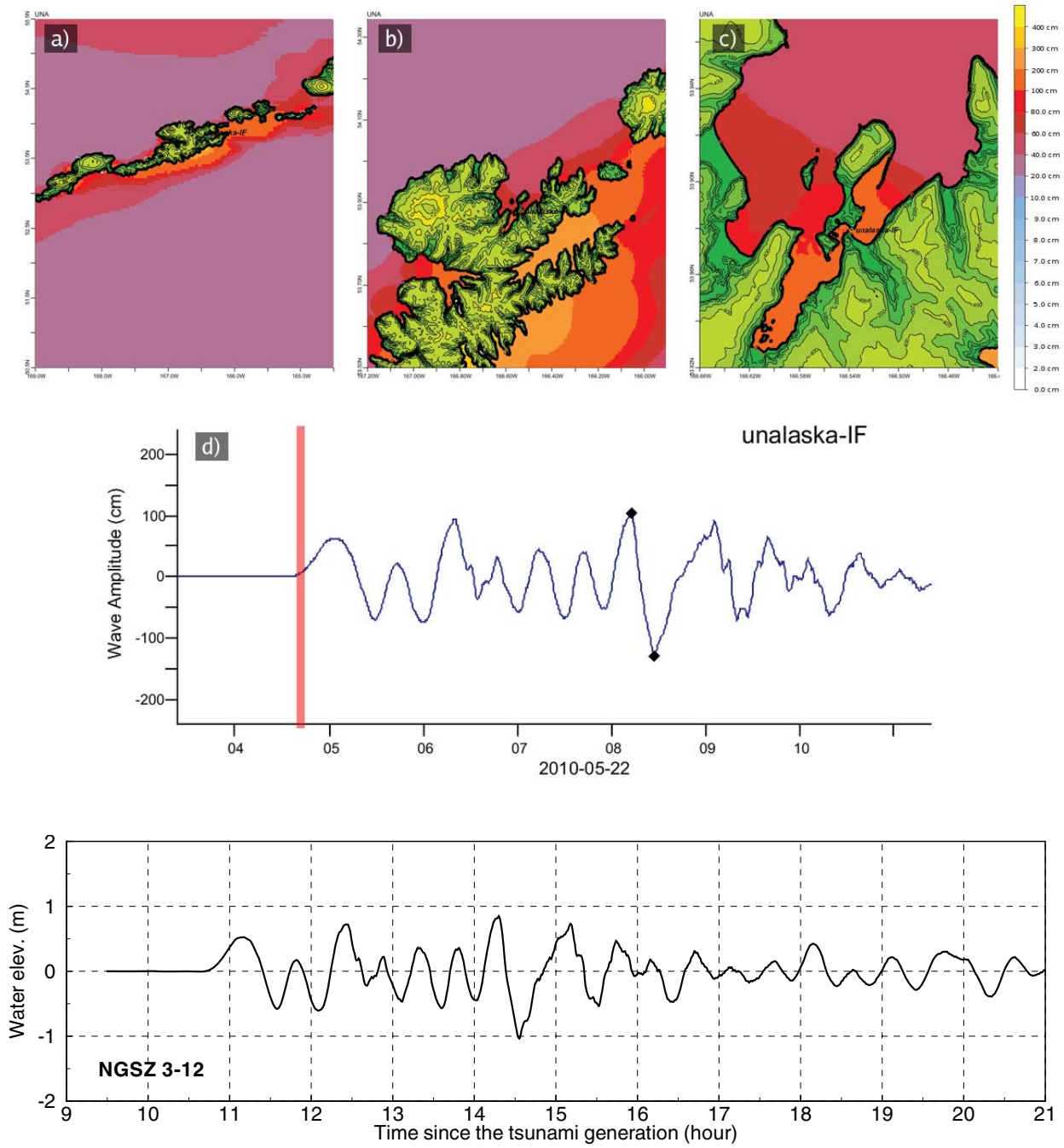

Figure C17: Response of the Unalaska forecast model to synthetic scenario NGSZ 3–12 (alpha=25). Maximum sea surface elevation for (a) A grid, b) B grid, c) C grid. Sea surface elevation time series at the C-grid warning point (d). The lower time series plot is the result obtained during model development and is shown for comparison with test results.

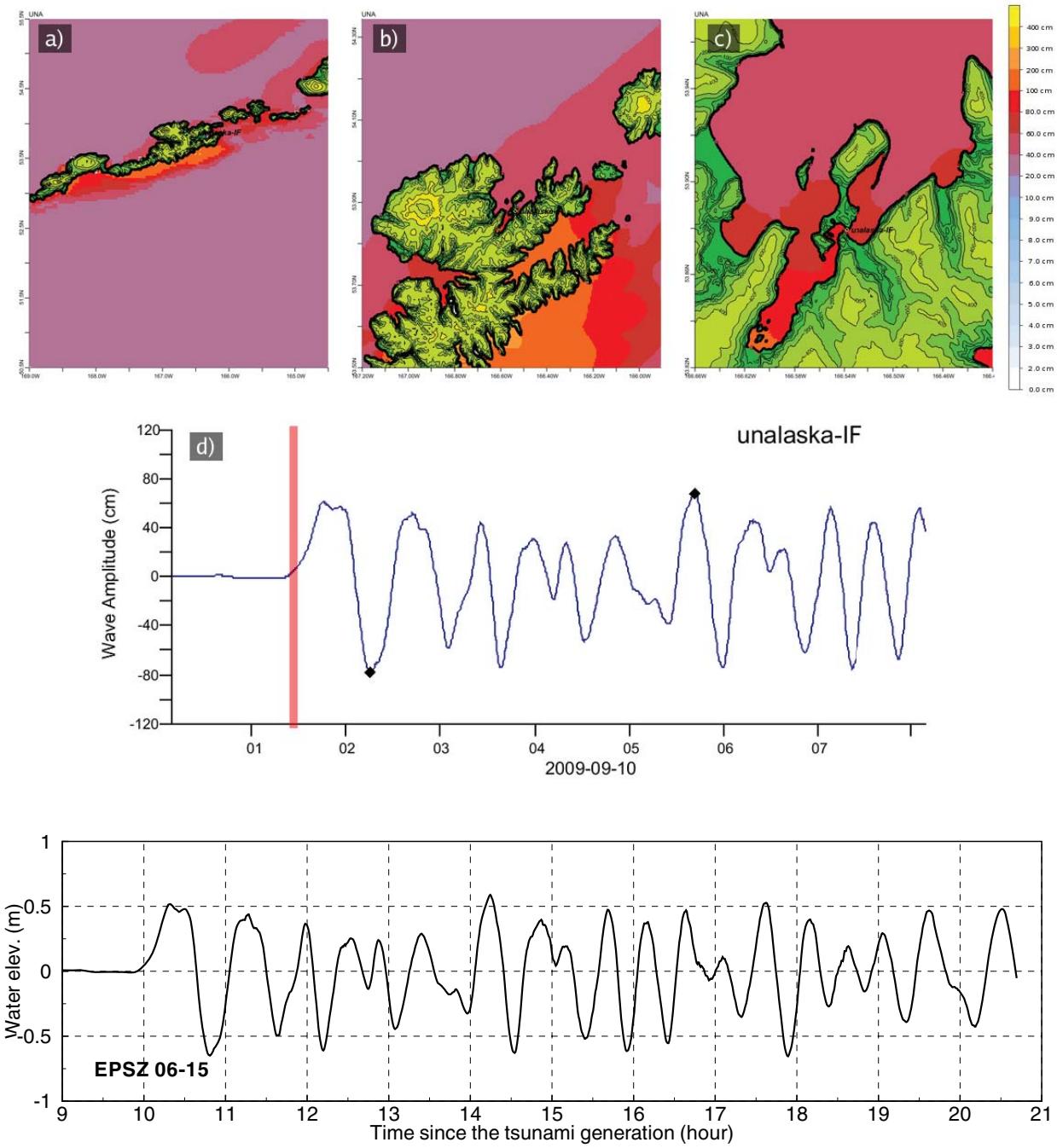

Figure C18: Response of the Unalaska forecast model to synthetic scenario EPSZ 6–15 (alpha=25). Maximum sea surface elevation for (a) A grid, b) B grid, c) C grid. Sea surface elevation time series at the C-grid warning point (d). The lower time series plot is the result obtained during model development and is shown for comparison with test results.

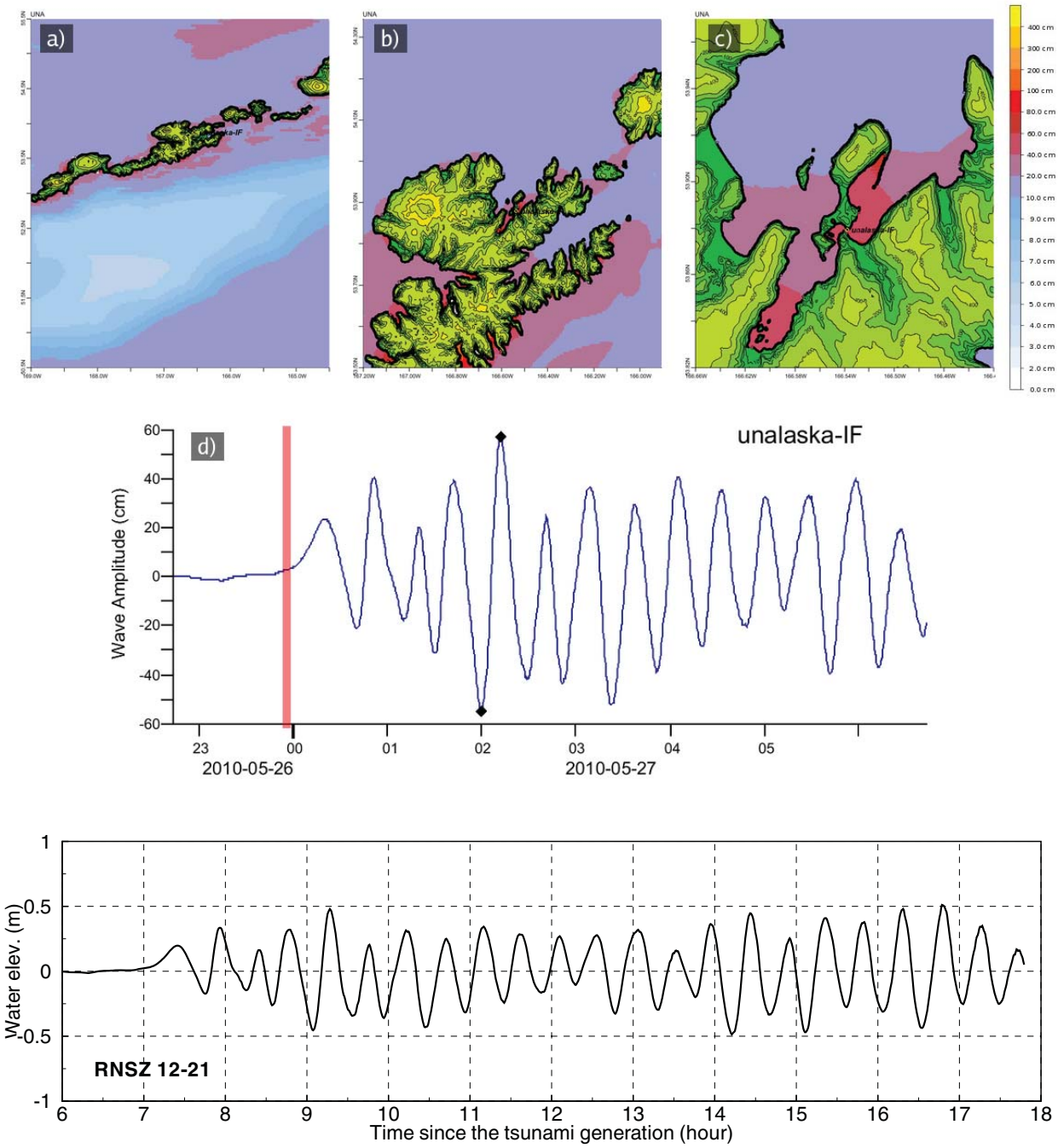

Figure C19: Response of the Unalaska forecast model to synthetic scenario RNSZ 12–21 (alpha=25). Maximum sea surface elevation for (a) A grid, b) B grid, c) C grid. Sea surface elevation time series at the C-grid warning point (d). The lower time series plot is the result obtained during model development and is shown for comparison with test results.

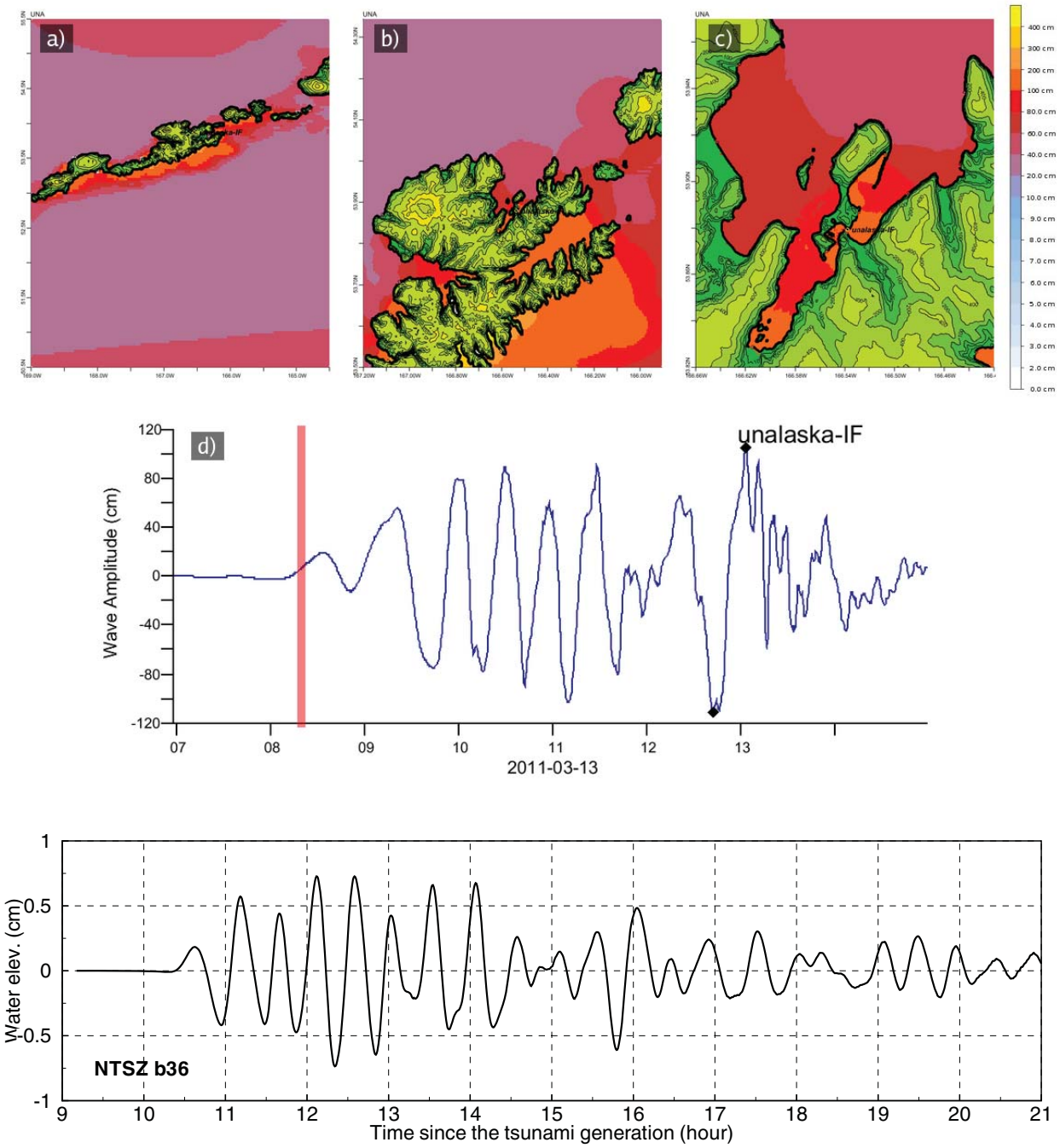

Figure C20: Response of the Unalaska forecast model to Mw 7.5 synthetic scenario NTSZ B36 (alpha=1). Maximum sea surface elevation for (a) A grid, b) B grid, c) C grid. Sea surface elevation time series at the C-grid warning point (d). The lower time series plot is the result obtained during model development and is shown for comparison with test results.

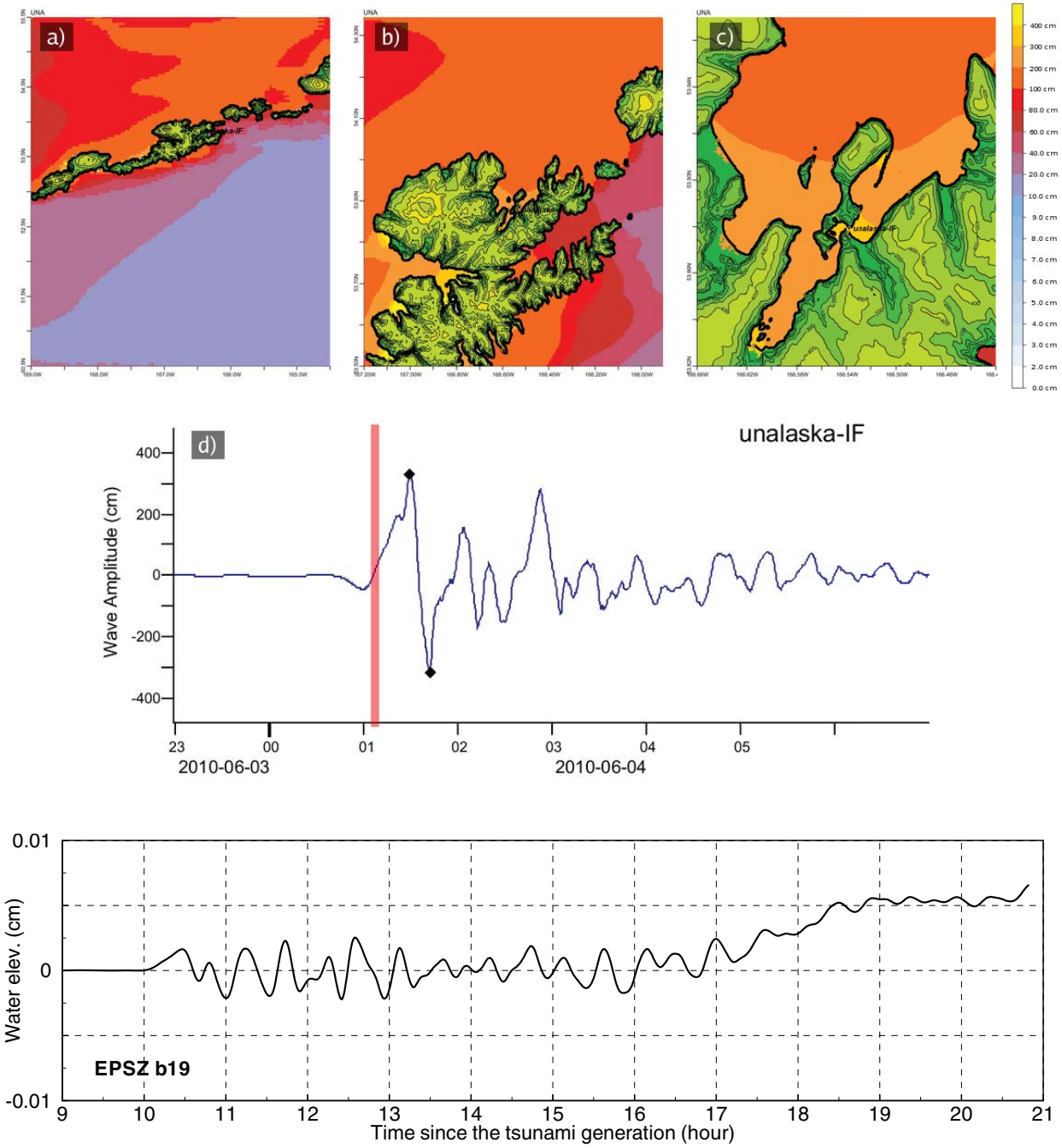

Figure C21: Response of the Unalaska forecast model to a microtsunami synthetic scenario EPSZ B19 (alpha=0.04). Maximum sea surface elevation for (a) A grid, b) B grid, c) C grid. Sea surface elevation time series at the C-grid warning point (d). The lower time series plot is the result obtained during model development and is shown for comparison with test results.

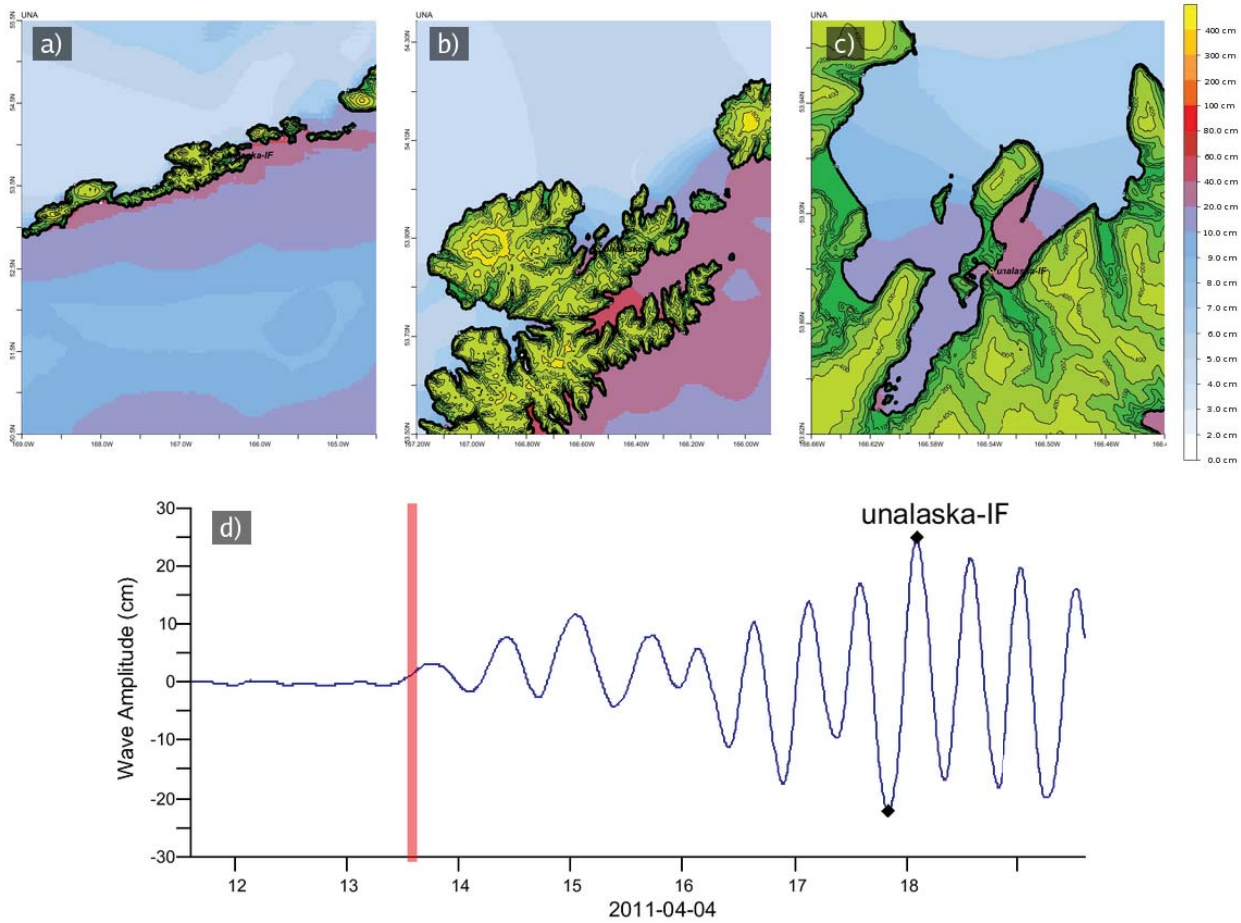

Figure C22: Response of the Unalaska forecast model to a microtsunami synthetic scenario RNSZ B14 (alpha=0.03). Maximum sea surface elevation for (a) A grid, b) B grid, c) C grid. Sea surface elevation time series at the C-grid warning point (d).

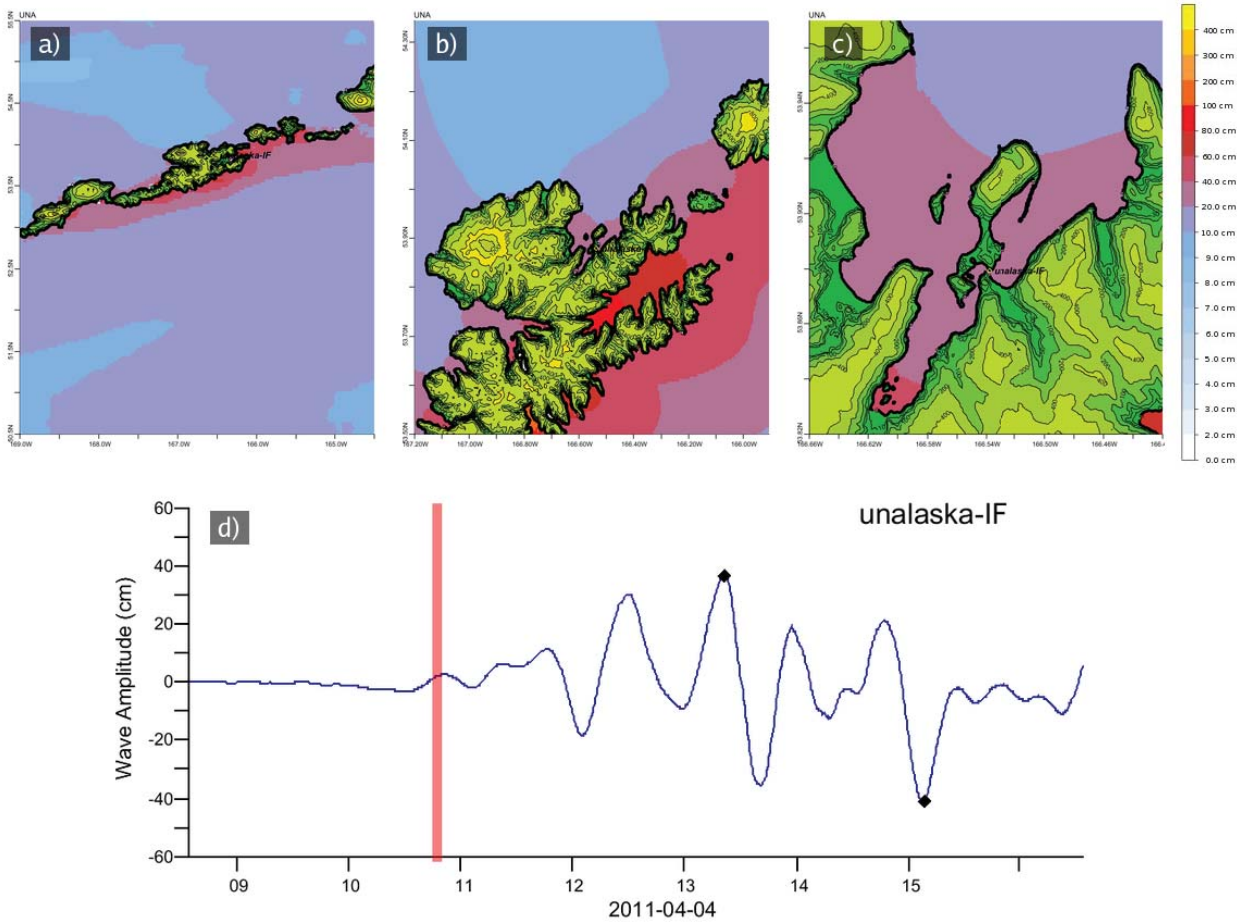

Figure C23: Response of the Unalaska forecast model to a microtsunami synthetic scenario ACSZ B6 (alpha=0.02). Maximum sea surface elevation for (a) A grid, b) B grid, c) C grid. Sea surface elevation time series at the C-grid warning point (d).

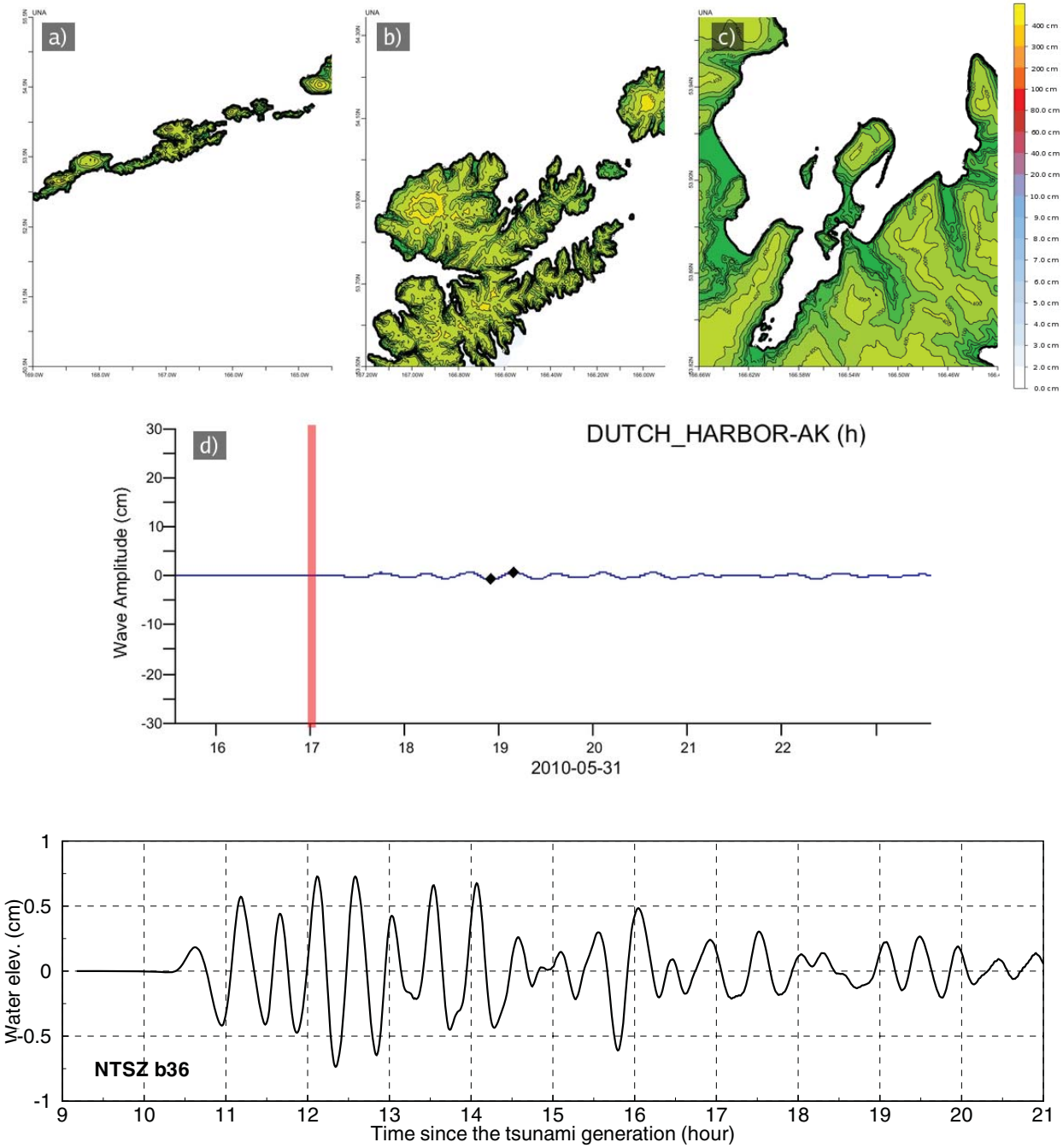

Figure C24: Response of the Unalaska forecast model to the 2006 Kuril tsunami. Maximum sea surface elevation for (a) A grid, b) B grid, c) C grid. Sea surface elevation time series at the C-grid warning point (d). The lower time series plot is the result obtained during model development and is shown for comparison with test results.

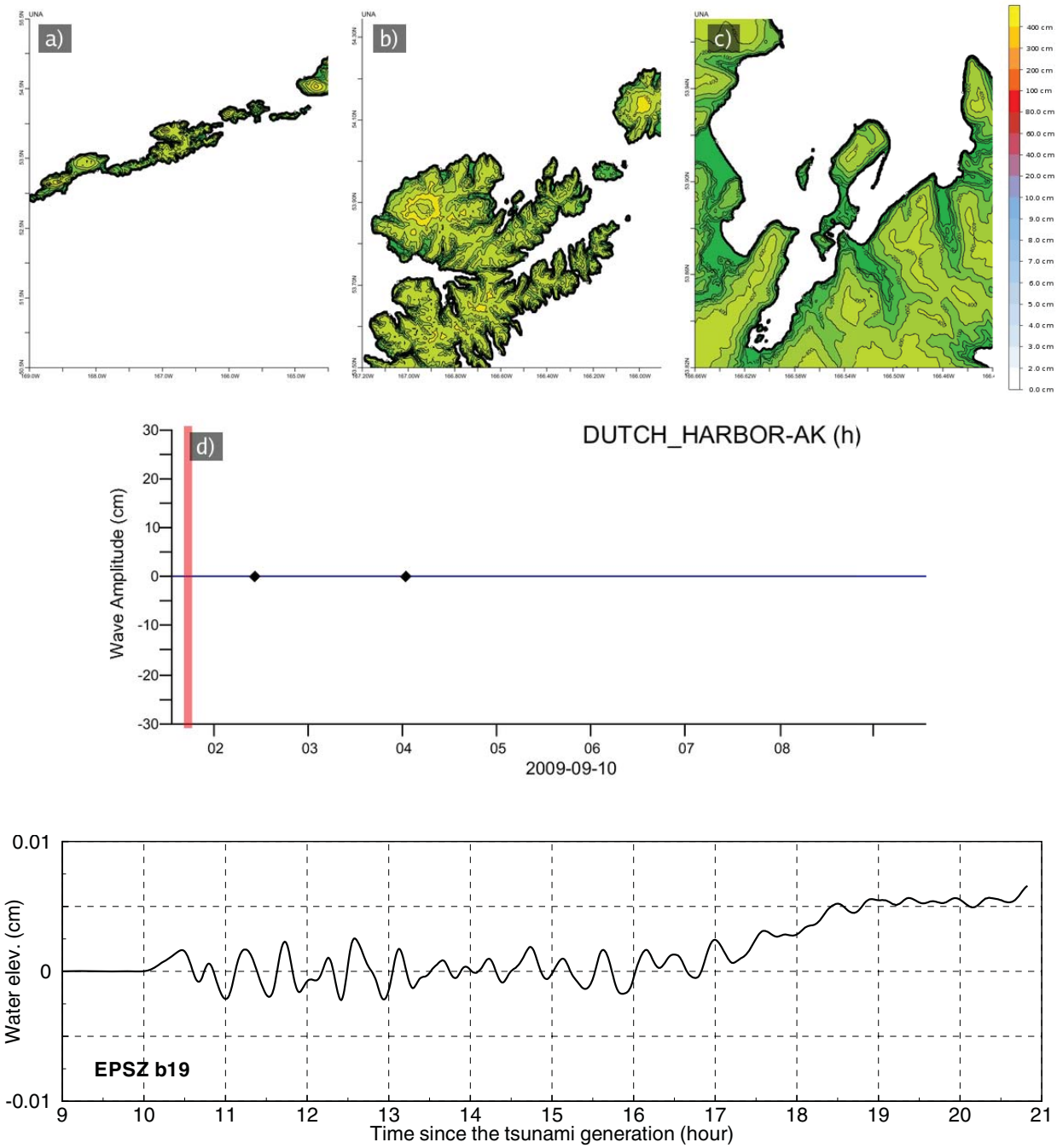

Figure C25: Response of the Unalaska forecast model to the 2007 Kuril tsunami. Maximum sea surface elevation for (a) A grid, b) B grid, c) C grid. Sea surface elevation time series at the C-grid warning point (d). The lower time series plot is the result obtained during model development and is shown for comparison with test results.

Glossary

Arrival time — The time when the first tsunami wave is observed at a particular location, typically given in local and/or universal time but also commonly noted in minutes or hours relative to time of earthquake.

Bathymetry — The measurement of water depth of an undisturbed body of water.

Cascadia Subduction Zone — Fault that extends from Cape Mendocino in Northern California northward to mid-Vancouver Island Canada. The fault marks the convergence boundary where the Juan de Fuca tectonic plate is being subducted under the margin of the North America plate.

Current speed — The scalar rate of water motion measured as distance/time.

Current velocity — Movement of water expressed as a vector quantity. Velocity is the distance of movement per time coupled with direction of motion.

Deep-ocean Assessment and Reporting of Tsunamis — (DART®) Tsunami detection and transmission system that measures the pressure of an overlying column of water and detects the passage of a tsunami.

Digital Elevation Model (DEM) — A digital representation of bathymetry or topography based on regional survey data or satellite imagery. Data are arrays of regularly spaced elevations referenced to a map projection of the geographic coordinate system.

Epicenter — The point on the surface of the earth that is directly above the focus of an earthquake.

Far-field — Region outside of the source of a tsunami where no direct observations of the tsunami-generating event are evident, except for the tsunami waves themselves.

Focus — The point beneath the surface of the earth where a rupture or energy release occurs due to a build up of stress or the movement of earth's tectonic plates relative to one another.

Inundation — The horizontal inland extent of land that a tsunami penetrates, generally measured perpendicularly to a shoreline.

Marigram — Tide gauge recording of wave level as a function of time at a particular location. The instrument used for recording is termed marigraph.

Method of Splitting Tsunamis (MOST) — A suite of numerical simulation codes used to provide estimates of the three processes of tsunami evolution: tsunami generation, propagation, and inundation.

Moment magnitude (Mw) — The magnitude of an earthquake on a logarithmic scale in terms of the energy released. Moment magnitude is based on the size and characteristics of a fault rupture as determined from long-period seismic waves.

Near-field — Region of primary tsunami impact near the source of the tsunami. The near-field is defined as the region where non-tsunami effects of the tsunami-generating event have been observed, such as earth shaking from the earthquake, visible or measured ground deformation, or other direct (non-tsunami) evidences of the source of the tsunami wave.

Propagation database — A basin-wide database of pre-computed water elevations and flow velocities at uniformly spaced grid points throughout the world oceans. Values are computed from tsunamis generated by earthquakes with a fault rupture at any one of discrete 100 × 50 km unit sources along worldwide subduction zones.

Runup or run-up — Vertical difference between the elevation of tsunami inundation and the sea level at the time of a tsunami. Runup is the elevation of the highest point of land inundated by a tsunami as measured relative to a stated datum, such as mean sea level.

Short-term Inundation Forecasting for Tsunamis (SIFT) — A tsunami forecast system that integrates tsunami observations in the deep ocean with numerical models to provide an estimate of tsunami wave arrival and amplitude at specific coastal locations while a tsunami propagates across an ocean basin.

Subduction zone — A submarine region of the earth's crust at which two or more tectonic plates converge to cause one plate to sink under another, overriding plate. Subduction zones are regions of high seismic activity.

Synthetic event — Hypothetical events based on computer simulations or theory of possible or even likely future scenarios.

Tidal wave — Term frequently used incorrectly as a synonym for tsunami. A tsunami is unrelated to the predictable periodic rise and fall of sea level due to the gravitational attractions of the moon and sun: the tide.

Tide — The predictable rise and fall of a body of water (ocean, sea, bay, etc.) due to the gravitational attractions of the moon and sun.

Tide gauge — An instrument for measuring the rise and fall of a column of water over time at a particular location.

Tele-tsunami or distant tsunami — Most commonly, a tsunami originating from a source greater than 1000 km away from a particular location. In some contexts, a tele-tsunami is one that propagates through deep ocean before reaching a particular location without regard to distance separation.

Travel time — The time it takes for a tsunami to travel from the generating source to a particular location.

Tsunameter — An oceanographic instrument used to detect and measure tsunamis in the deep ocean. Tsunami measurements are typically transmitted acoustically to a surface buoy that in turn relays them in real time to ground stations via satellite.

Tsunami — A Japanese term that literally translates to "harbor wave." Tsunamis are a series of long-period shallow-water waves that are generated by the sudden displacement of water due to subsea disturbances such as earthquakes, submarine landslides, or volcanic eruptions. Less commonly, meteoric impact to the ocean or meteorological forcing can generate a tsunami.

Tsunami hazard assessment — A systematic investigation of seismically active regions of the world oceans to determine their potential tsunami impact at a particular location. Numerical models are typically used to characterize tsunami generation, propagation, and inundation and to quantify the risk posed to a particular community from tsunamis generated in each source region investigated.

Tsunami magnitude — A number that characterizes the strength of a tsunami based on the tsunami wave amplitudes. Several different tsunami magnitude determination methods have been proposed.

Tsunami propagation — The directional movement of a tsunami wave outward from the source of generation. The speed at which a tsunami propagates depends on the depth of the water column in which the wave is traveling. Tsunamis travel at a speed of 700 km/hr (450 mi/hr) over the average depth of 4000 m in the open deep Pacific Ocean.

Tsunami source — Abrupt deformation of the ocean surface that generates series of long gravity waves propagating outward from the source area. The deformation is typically produced by underwater earthquakes, landslides, volcano eruptions, or other catastrophic geophysical processes.

Wall-clock time — The time that passes on a common clock or watch between the start and end of a model run, as distinguished from the time needed by a CPU or computer processor to complete the run, typically less than wall-clock time.

Wave amplitude — The maximum vertical rise or drop of a column of water as measured from wave crest (peak) or trough to a defined mean water level state.

Wave crest or peak — The highest part of a wave or maximum rise above a defined mean water level state, such as mean lower low water.

Wave height — The vertical difference between the highest part of a specific wave (crest) and its corresponding lowest point (trough).

Wavelength — The horizontal distance between two successive wave crests or troughs.

Wave period — The length of time between the passage of two successive wave crests or troughs as measured at a fixed location.

Wave trough — The lowest part of a wave or the maximum drop below a defined mean water level state, such as mean lower low water.